UNIVERSITY OF CALIFORNIA
RIVERSIDE

Regulation of Gene Expression in the *Drosophila* Olfactory System Varies Widely With Stimulus, Duration, Age, and Development

A Dissertation submitted in partial satisfaction
of the requirements for the degree of

Doctor of Philosophy

in

Cell, Molecular, and Developmental Biology

by

Christi Ann Scott

March 2019

Dissertation Committee:

- Dr. Anandasankar Ray, Chairperson
- Dr. Anupama Dahanukar
- Dr. Karine Le Roch
- Dr. Patricia Springer

The Dissertation of Christi Ann Scott is approved:

_____

_____

_____

_____

Committee Chairperson

University of California, Riverside

Acknowledgements

Scientific contributions:

The text of this dissertation is in part reproduced with permission of the Liscensor through PLSclear as is appears in:

Scott, Christi A., and Anupama Dahanukar. 2014. “Sensory Coding of Olfaction and Taste.” *Behavioral Genetics of the Fly (Drosophila Melanogaster)* 2: 49.

Dr. Anupama Dahanukar planned and co-wrote the chapter. This publication is in copyright. Subject to statutory exception and to the provisions of relevant collective licensing agreements, no reproduction of any part may take place without the written permission of Cambridge University Press.

I am grateful to the following collaborators who contributed to work in this dissertation:

Dr. Anandasankar Ray supervised and directed the research that forms the basis for this dissertation. Dr. Crystal Pontrello contributed equally to the design and library preparations for the brain activity regulated gene (ARG) experiments and performed the memory experiments. Dr. Anupama Dahanukar contributed to the planning and funding of the brain ARG project. For the diacetyl experiments, Dr. Sachiko Haga-Yamanaka performed the biochemical assays, cell culture assays, neurodegeneration assays. Dr. Sarah Perry prepared some of the transcriptome libraries. Dr. Crystal Pontrello performed some of the mouse experiments. Dr. Meera Goh Nair helped to plan and assisted with the mouse exposure experiments. For the axon guidance work, Dr. Christine Pham prepared the RNA for the *pdm3* mutant experiments.

I would like to thank Dr. Thomas Girke for guidance in bioinformatics analysis used in all RNA-seq experiments.

Personal acknowledgements:

I would first like to thank my advisor, Dr. Anandasankar Ray for his unwavering support during my graduate school tenure. Anand, your enthusiasm for science is both unparalleled and infectious. Every time I struggled with any aspect of my research, one meeting in your office left me feeling like I was on my way to a Nobel prize. I will forever be grateful to you for your wild ideas and your guidance.

My dissertation committee has been very supportive throughout graduate school. Thank you to Dr. Anupama Dahanukar for your continued support of my research. I value all of our regular conversations both science and non-science alike. Thank you to Dr. Karine Le Roch and Dr. Patricia Springer. I appreciate all of the time you have committed and the clear feedback you always provided.

Thank you Dr. Crystal Pontrello, my bench mate for so many years. When we first started our project, I don't think either of us quite knew how it would turn out. After all of these years and all of our reanalysis, I am so glad that I had a teammate that never gave up. Though I could go on, I'll end it here because I don't want this to be an agarose situation.

I am grateful to the members of the Ray and Dahanukar labs for all of our scientific discussions and the non-stop entertainment. Tom "Good" Guda, I am thankful for all of the work you put in to keep our lab running and your daily positive attitude. And a special shout-out to my lunch buddies over the years: Adriana, Arun, Greg, Mikkal, Perry, Sean Michael Boyle, and Zev. My midday break wouldn't have been the same without each of you.

I'd also like to thank my new-age pen pals, MamaD and Bear. I hope to reunite with you in person one day, but getting to know you was a definite highlight. Thank you

also to Taylor Swift. These projects began with *Speak Now* and continued through the *Reputation* era. Much of the work presented here was done to the tune of “Enchanted” and “Style” ,among others and “Don’t Blame Me” has fueled much of the writing process.

To my family, thank you for putting up with my never-ending college career. Mom, thank you for always supporting my education, starting with walking me to school everyday in kindergarten. I’m pretty sure this solidifies my spot as your favorite child. Thank you to my brothers and sisters: Jimmy, Jill, Mrrto, Brian, Melissa, Michelle, Andy, Lindsey, Ashley, and Billy and my 22 (and counting) nieces and nephews, with a special shout-out to Jessica and Aiden for coming to my defense. Thank you to the Rowden/Alexander family especially Tommy, Cyndi and Glenn for always making me feel like part of the family over the holidays.

Thank you to my additional extended family, the Medina/Lomeli/Dillon/Franco group. Again, you guys never fail to make me feel as though I’m part of the family and I look forward to many more parties and trips to Mexico. Thank you to Irma Medina for always welcoming me into your home. Tu comida y tu amor ayudarme a todo, muchas gracias.

I have been lucky to have two lifelong best friends, who I love more than I can say. Adriana Lomeli, I am so grateful I had someone to share this experience with. Whether you were supporting my work or with me swatching eyeshadows in Sephora, being your best friend is rewarding every day. And finally to my original ride-or-die, Leah Timme. From BC to PhD, I couldn’t have asked for a better partner to see me through it. It’s been a great 20 (!) years, I can’t wait for the next 20.

For my father

Pop, I'd like to think you'd place this 2nd among

your proudest moments. We both know my

first tuna takes the top spot.

I miss you every day.

ABSTRACT OF THE DISSERTATION

Regulation of Gene Expression in the *Drosophila* Olfactory System Varies Widely With Stimulus, Duration, Age, and Development

by

Christi Ann Scott

Doctor of Philosophy, Graduate Program in
Cell, Molecular, and Developmental Biology
University of California, Riverside, March 2019
Dr. Anandasankar Ray, Chairperson

The *Drosophila* olfactory system is an ideal model for the investigation of principles of gene regulation in the nervous system. Within this system, we characterize gene expression changes in response to short-term and long-term exposure to odorants. Additionally, we examine the contributions of two transcription factors to the development of this chemosensory system. Short-term exposure to odorants and light leads to neural activation and induction of activity regulated genes (ARGs). ARG induction in neurons in can lead to long-term changes at the level of the synapse. Such alterations in synaptic structure/function are thought to underlie important cellular processes such as synaptic plasticity and long-term memory formation. We have conducted a genome-wide study of genes in the *Drosophila* central nervous system induced after brief periods of sensory stimulation and have identified 352 genes whose

expression increases in response to neural activity. The regulation of these genes is altered with increasing age. Furthermore, we demonstrate that loss of a histone deacetylase alters neuronal response to sensory stimuli, suggesting a mechanism of epigenetic regulation. We extended our transcriptome analysis to the fly antenna and found that the genes increased in response to fruit odorants differ significantly from the genes induced by the repellent DEET. In response to long-term exposure to the odorant diacetyl, we find that dramatic changes in gene expression can, in part, be attributed to inhibition of histone deacetylases. This non-traditional action of diacetyl slows neurodegeneration in the fly model for Huntington's Disease. We conclude with an analysis of two transcription factors *acj6* and *pdm3* and find they regulated proper chemosensory receptor and axon guidance gene expression in the developing *Drosophila* olfactory system.

TABLE OF CONTENTS

LIST OF TABLES

LIST OF FIGURES

Chapter 1

An introduction to the organization and development of the *Drosophila* olfactory system

Overview

Insect chemosensory systems are tasked with the challenge of detecting and discriminating thousands of chemicals in the environment. Chemical stimulus quality and intensity impart key information to drive essential behaviors including location and selection of food, mates, and oviposition sites. The olfactory system harbors the capacity to encode properties of distant chemical stimuli by way of large, highly divergent chemoreceptor gene families. The identification of *Drosophila* chemoreceptor genes hailed a new era of molecular and neurophysiological research in this model organism. The past decade or so has been witness to remarkable progress in our understanding of the principles by which odorants are encoded by the olfactory system: the manner in which olfactory sensory neurons (OSNs) are molecularly and functionally organized, and the anatomical and physiological mechanisms governing the transmission of their activity to higher brain centers.

Here I review the organization and function of peripheral olfactory neurons in the fly, and summarize the current understanding of chemosensory processing in the central nervous system. I include a synopsis of recent advances that have brought new perspectives to the idea of how such an ordered system is generated during development. I conclude with findings that have demonstrated that genetic pathways involved in several elements of development, including olfactory receptor (*Or*) gene choice, have profound roles in wiring the *Drosophila* olfactory system. The field is now poised to unravel the mechanisms that govern genetic responses to sensory cues that are generated at the periphery in response to both short- and long-term stimuli.

Chemosensory neurons and receptors

The peripheral olfactory system

Olfactory sensory neurons (OSNs) are housed in stereotypical combinations in porous cuticular structures called sensilla that cover the surfaces of the third antennal segments and the maxillary palps on the *Drosophila* head (Stocker 1994). Antennal sensilla are sub-divided into three morphological types – basiconics, coeloconics, and trichoids – that are distributed in distinct, overlapping zones (Venkatesh and Naresh Singh 1984). Only basiconic sensilla are present on the maxillary palps (Naresh Singh and Nayak 1985). OSNs are also located in other sub-structures of the antennae – the three-chambered sacculus compartment, and a bristle-like projection called the arista (Stocker 1994).

Olfactory sensilla, which can house up to four OSNs, are further sub-divided into 23 functional classes – 12 antennal basiconics (ab1 – ab12), 4 coeloconics (ac1 – ac4), 4 trichoids (at1 – at4), and 3 maxillary palp basiconics (pb1 – pb3) – based on their unique response profiles to large panels of volatile odorants and their molecular identities (Table 1.1). At least three different features of odorant responses can be used to distinguish individual OSNs: the level of spontaneous activity, the excitatory or inhibitory response to individual odorants, and the temporal dynamics of the response. Although not absolute, there appears to be some degree of functional specialization among the three morphological types – basiconic OSNs are tuned to general fruit and plant volatiles, trichoid OSNs to pheromones, and coeloconic OSNs to volatile products of microbial degradation and fermentation. Furthermore, the grouping of OSNs within a given sensillum is constant from fly to fly. This stereotypic compartmentalization carries functional significance as activation of one OSN can lead to lateral inhibition of

neighboring OSNs (Su et al. 2012). Thus, in addition to the generation of the initial response, the peripheral olfactory system also marks the sites of integration of olfactory information from multiple neurons.

The functional identity of each OSN is determined by the membrane-bound receptor(s) it expresses (Dobritsa et al. 2003). Those mapped to OSNs belong to one of three large families of chemoreceptor genes: *Odor receptor* (*Or*)*, Ionotropic receptor* (*Ir*), or *Gustatory receptor* (*Gr*) genes.

Odor receptors

Or genes belong to an insect-specific superfamily that encodes proteins unrelated in sequence or membrane topology to olfactory receptors in other organisms, and were discovered independently by bioinformatic and differential expression screens (Peter J. Clyne et al. 1999; Leslie B. Vosshall et al. 1999; Gao and Chess 1999). OSNs of basiconic and trichoid sensilla typically express a single *Or* gene along with an obligate co-receptor, *Or83b* or *Orco*, which is required for proper dendritic localization and function of the odor receptor protein (Larsson et al. 2004; Leslie B. Vosshall et al. 1999; L. B. Vosshall, Wong, and Axel 2000; Neuhaus et al. 2005). Epitope-tagging studies of Or and Orco proteins revealed a membrane topology with an intracellular N-terminal domain, which is inverted to that of canonical G-protein coupled receptors (Benton et al. 2006; Wistrand, Käll, and Sonnhammer 2006; Lundin et al. 2007). In keeping with the structural dissimilarity, Or/Orco complexes were found to be novel ligand-gated ionotropic receptors capable of rapid signal transduction in the absence of G-protein second messenger signaling when expressed in human cell lines and *Xenopus* oocytes (Sato et al. 2008; Wicher et al. 2008). However, one study reported an additional, slower metabotropic response that is also ligand-dependent (Wicher et al.

2008). Disruption of key genes involved in metabotropic signaling pathways reduced odor sensitivity, but did not abolish it completely, consistent with some, although not exclusive, role for G proteins (Smart et al. 2008; Kain et al. 2008; Chatterjee, Roman, and Hardin 2009). Detailed studies concerning the topology and signaling of Or/Orco complexes in endogenous neurons are now needed to fully understand the mechanistic properties of this receptor complex.

In each OSN, the specific or “tuning” Or is the determinant of its odor coding features. Expression of any Or in an “empty” basiconic OSN lacking its endogenous tuning receptors, but retaining Orco, resulted in the host neuron adopting the odorant response properties of the OSN that the exogenous Or was derived from (Dobritsa et al. 2003). This so-called “empty neuron” strategy became instrumental in decoding individual tuning Ors (Hallem, Ho, and Carlson 2004; Hallem and Carlson 2006), which in concert with comprehensive molecular and transgenic expression analyses (Couto, Alenius, and Dickson 2005; Fishilevich and Vosshall 2005) led to a detailed Or-to-OSN-to-function map of the peripheral olfactory system. The molecular organization of fly OSNs revealed remarkable parallels to olfactory systems of vertebrate animals, in which an individual OSN selects only one from among ~1000 odorant receptor genes to express (Vassar, Ngai, and Axel 1993).

The interaction of an odorant with a select Or/Orco receptor, and thereby its corresponding OSN, is typified by a response of a characteristic type (excitatory or inhibitory), strength, and temporal decay. Or/Orco receptors are unique not only with respect to which odorants they respond to but also in their breadth of tuning. Some Or receptors such as Or35a are broadly tuned and respond to several structurally diverse odorants; by comparison, others such as Or85a are far more selective in their responses

(Hallem and Carlson 2006). Similarly, odorants themselves vary in the number and degree to which they activate various receptors. For example, 1-hexanol activates a number of different Ors from several different sensillar classes across both olfactory organs (Hallem and Carlson 2006); by contrast only *Or67d*- and *Or65a*-expressing OSNs in trichoid sensilla are activated by the sex pheromone 11-*cis*-vaccenyl acetate (cVA) (Ha and Smith 2006; van der Goes van Naters and Carlson 2007). The identity and intensity for most general odors is thus largely represented at the periphery via differential activity across ensembles of OSNs.

Ionotropic receptors

Neurons that express *Or*/*Orco* genes accounted for ~70% of the OSNs in the antennae, positing that the remaining OSNs, mainly housed in coeloconic sensilla, are likely to express other classes of receptors (Couto, Alenius, and Dickson 2005; Yao and Carlson 2010; Yao, Ignell, and Carlson 2005). The recent identification of variant ionotropic glutamate receptor genes (*Irs*) that represent an ancient family shared throughout protostomes, revealed exclusive expression of *Irs* in all but one of the coeloconic OSNs (Benton et al. 2009), ac3B, which expresses *Or35a/Orco* in addition to *Ir76b*. Reporter analysis suggests that *Ir* genes are also expressed in olfactory neurons of the sacculus and the arista (Benton et al. 2009; Ai et al. 2010; Silbering et al. 2011) . Two members of the *Ir* gene family, *Ir8a* and *Ir25a,* are broadly expressed in multiple OSN classes and are thought to function as co-receptors. Similar to *Orco,* co-expression of *Ir8a* or *Ir25a* with ligand specific *Ir(*s) is required for proper shuttling to the dendritic membrane and function of Ir complexes (Abuin et al. 2011).

Unlike the general one-receptor-per-neuron rule for *Or* genes, OSNs express combinations of up to 4 *Ir*s in addition to either *Ir8a* or *Ir25a (Abuin et al. 2011)*. Co-

expression of *Ir8a* and *Ir84a* was sufficient to generate a response to phenalacetaldehyde in *Xenopus* oocytes, suggesting a tuning subunit/co-receptor complex reminiscent of Or/Orco receptors (Abuin et al. 2011). In the *in vivo* "empty neuron" system, however, at least three different Irs, *Ir25a, Ir76a,* and *Ir76b*, were required to reconstitute the phenylethyl amine response of the *Ir*-expressing coeloconic OSN of their origin (Abuin et al. 2011). Although other combinations of Irs have not been matched with ligands in this manner, systematic analysis of coeloconic responses to a variety of odorants revealed that several *Ir*-expressing OSNs are more narrowly tuned than their *Or*-expressing counterparts, with $Ir8a^{+}$ OSNs responding to a variety of acids and $Ir25^{+}$ OSNs responding to amines (Silbering et al. 2011).

Canonical ionotropic glutamate receptors (iGluRs) in mammalian nervous systems are ion channels gated by the neurotransmitter glutamate, which is recognized by an extracellular ligand-binding domain (Mayer 2006; Sobolevsky, Rosconi, and Gouaux 2009). This ligand- binding domain is conserved in many classes of iGluRs described thus far: AMPA, kainite, and NMDA receptors. The divergent *Ir* family found in *Drosophila* functions instead to detect odorants and bears significant differences in the ligand-binding region (Mayer 2006; Benton et al. 2009), leading to the model that Irs also serve as ion channels, gated by various odorants instead of glutamate.

Further investigations are required to understand the exact mechanisms of heteromeric Ir complex function, including the role of individual Irs within such complexes and their means of ligand-activated signal transduction.

Gustatory receptors

A family of 60 *Gr* genes encoding 68 divergent receptor proteins was identified soon after the *Or* gene family (P. J. Clyne 2000; Scott et al. 2001). Although *Gr* genes

are primarily expressed in taste neurons and are discussed in more detail below, two prominent members that are highly conserved between flies and mosquitoes, Gr21a and Gr63a, were mapped to a single basiconic OSN that is tuned to carbon dioxide (Jones et al. 2007; Kwon et al. 2007) . Co-expression of the two receptors in the empty neuron system conferred a response to CO_2, providing evidence for a heteromeric Gr receptor (Jones et al. 2007; Kwon et al. 2007). The strength of the CO_2 response was significantly enhanced by the inclusion of the Gq protein (Yao and Carlson 2010), suggesting a role for second messenger signaling mechanisms in Gr function. Correspondingly, a knockdown of Gq affects the level of CO_2 response, but not general odorant responses of other OSNs (Yao and Carlson 2010). Gr21a/Gr63a remains the sole illustration of Gr function in OSNs; at least one other *Gr*, *Gr10a*, has been mapped to an OSN (Scott et al. 2001; Fishilevich and Vosshall 2005), but its functional relevance is not yet clear.

Odorant binding proteins

Insect odorant-binding proteins (OBPs) are a large, conserved family of proteins, many of which are concentrated in the sensillar lymph of olfactory and gustatory sensilla and are thought to facilitate interactions of odorants with membrane-bound olfactory receptors (Pelosi and Maida 1995). In *Drosophila* there are as many as 51 predicted members of the OBP family, several of which are expressed in specific regions of the antenna (Heimbeck et al. 2001; McKenna et al. 1994; Galindo and Smith 2001; Pikielny et al. 1994). The protein LUSH is expressed in trichoid sensilla and evidence suggests that it binds the male aggression and anti-aphrodisiac pheromone cVA (Kim, Repp, and Smith 1998; Shanbhag and Hekmat-Scafe 2001; Xu et al. 2005). LUSH has been shown to be required for odor-evoked responses in trichoid sensilla and behavioral responses to cVA (Xu et al. 2005). A prevailing model for *Drosophila* pheromone detection involves

a conformational change in LUSH when bound to cVA which in turn acts as a ligand to activate Or67d/Orco complexes (Laughlin et al. 2008). A recent study, however, challenges this model directly and instead proposes a more supportive rather than direct role for the OBP LUSH in pheromone detection (Gomez-Diaz et al. 2013).

The role(s) for many of the additional OBP members in olfactory coding is largely unknown. Evidence suggests that a family of 12-14 sensory neuron membrane proteins (SNMPs) may also be involved in odor detection (Benton, Vannice, and Vosshall 2007; Rothenfluh et al. 2006). One member, encoded by *Snmp*, is necessary for activation of Or67d/Orco by cVA (Benton, Vannice, and Vosshall 2007; Gomez-Diaz et al. 2013). However, the precise role of Snmp, as well as other members of this family, is not yet known.

Central representation of chemosensory activity

Glomerular maps of odor responses

The axons of both antennal and maxillary palp OSNs terminate in an ordered fashion in a pair of antennal lobes (AL) in the fly brain (Table 1.1)(Stensmyr et al. 2012; Muench and Giovanni Galizia 2015; Enjin et al. 2016), which is the site where olfactory processing begins. Each antennal lobe is comprised of approximately 50 discrete spheroidal units or glomeruli (Stocker et al. 1990; Laissue et al. 1999). The axons of all OSNs of the same functional class fasciculate and converge on one, or in few instances two, glomeruli (Couto, Alenius, and Dickson 2005; Fishilevich and Vosshall 2005; Gao, Yuan, and Chess 2000). In the AL, invariant synaptic connections are made between the axon termini of OSNs and the dendrites of projection neurons (PNs) (Stocker et al. 1990). Most OSN classes have axons that send bilateral projections to the AL (Stocker et al. 1990; Couto, Alenius, and Dickson 2005). Despite the redundancy, the fly can still

determine the direction from which an olfactory cue originated via an increase in neurotransmitter release on the side of the brain that corresponds with the activated antenna (left or right) (Gaudry et al. 2013).

Patterns of odor-evoked activity were monitored across the whole system by assaying changes in calcium in the AL, either from axons of OSNs or dendrites of PNs (J. W. Wang et al. 2003). Each odor recognized at the periphery elicits a stereotypic pattern of glomerular activity reflecting the specificity of Or/Orco responses of the corresponding OSNs. Furthermore, low odorant concentrations evoked sparse activation of glomeruli, which was more dispersed at higher odorant concentrations suggesting one possible mechanism by which odor intensity is encoded (J. W. Wang et al. 2003). From the glomerular activity map it also became clear that neurons responding to similar classes of chemicals converge onto glomeruli that are scattered throughout the AL. This suggests that rather than a chemotopic map in the central nervous system, it is more likely that the topographic map created at the periphery is maintained at the AL.

Interglomerular integration of olfactory input

The one-to-one connectivity between OSNs and PNs suggested the existence of a discrete, parallel channel for processing information from each OSN class. However, this idea was brought into question by two observations. First, the AL contains a complex network of interglomerular connections via lateral interneurons (LNs) (Stocker et al. 1990). Second, a systematic comparison of OSN and PN responses found that odor-receptive fields of PNs are generally stronger and broader than those of their cognate OSNs (Bhandawat et al. 2007). The latter observation suggested that PNs could receive excitatory input from LNs making presynaptic connections with other glomeruli, which was corroborated by measurements of “silent” PN activity from

glomeruli that lacked their own functional presynaptic OSNs (Olsen, Bhandawat, and Wilson 2007; Shang et al. 2007). Interestingly, the tuning of each “silent” PN varied across PN classes, indicating a role for ensemble activity patterns of OSNs as signatures of odor identity (Olsen, Bhandawat, and Wilson 2007). Although initial studies failed to find evidence for inhibitory interactions between glomeruli, surgical and genetic manipulations to removal lateral input to PNs led to an increase in the tuning breadth of some individual PNs, suggesting a role for lateral inhibition in olfactory coding (Olsen and Wilson 2008). The inhibition was shown to occur via GABAergic interneurons that directly blocked OSN to PN transmission (Root et al. 2011; Olsen and Wilson 2008). Overall, the current view is that the various channels influencing OSN-to-PN transmission allow for superior division of odorant representation across PN activity by boosting the signal-to-noise ratios of glomerular activity patterns.

Propagation of olfactory input to higher brain centers

PNs in the AL relay olfactory information gathered at the periphery to higher processing centers in the *Drosophila* brain. The organization of the PN network is similar to that of the OSNs in that the dendrite of a single PN typically innervates a single glomerulus, effectively maintaining the peripheral one-to-one topographic map. On average, a single glomerulus is innervated by three PNs that make synaptic connections with approximately 30 OSN axons (Wong, Wang, and Axel 2002; Marin et al. 2002). PNs belong to one of three broad classes named on the basis of the relative positions of their cell bodies in the AL: anterodorsal, lateral, and ventral PNs (Marin et al. 2002). PNs within a given class are all derived from a single progenitor and make stereotypic connections in the AL (G. S. Jefferis et al. 2001). Thus, the architecture of this second-order signaling network is also genetically prespecified. Activity in PNs is relayed to two

olfactory processing centers in the *Drosophila* protocerebrum: the mushroom body (MB) and the lateral horn (LH). The MB is involved in olfactory learning (de Belle and Heisenberg 1994; Davis 2005). The role of the LH is less clear and has been implicated in a variety of functions including innate olfactory behavior (Heimbeck et al. 2001; Kido and Ito 2002) and both bilateral and multimodal integration of sensory information (N. Gupta and Stopfer 2012).

Single-cell labeling experiments allowed for identification of PN glomerular targets as well as characterization of their axon branching and terminal arborization patterns. Interestingly, PNs that innervate the same glomerulus have stereotypic projection patterns in the LH (Marin et al. 2002). Although there is some overlap, the cognate OSN class of a PN can be reliably predicted on the basis of the pattern of axon branching and arborization in the LH alone. Thus, the spatial map of olfactory activity appears to be conveyed to the LH, with some degree of overlap that may allow for convergence of olfactory input from multiple OSN classes in third order neurons. The PN axons that extend to the MB are simpler in terms of numbers of arborizations, and initial studies were unable to demonstrate clear topographic stereotypy as seen in the LH (Marin et al. 2002).

Subsequent high-resolution mapping of PN processes confirmed the class-specific stereotypic arborizations in the LH and demonstrated a previously unreported degree of stereotypy in the MB. In-depth analysis of PN projection patterns established five groups in the LH and four in the MB (G. S. X. E. Jefferis et al. 2007). Superimposition of this spatial organization of the higher olfactory centers with the established Or-OSN-PN map and Or/OSN responses at the periphery exposed a spatial separation of PN classes that respond to general fruit odors from those that respond to

specific pheromones, offering the first evidence that anatomical segregation in the LH is linked to biologically distinct functions (G. S. X. E. Jefferis et al. 2007).

In the MB, PNs converge on to the dendrites of Kenyon cells (KCs) in a seemingly random manner (Caron et al. 2013). Although there is no apparent organization of glomerular inputs to individual KC cells, KC axons make connections with spatially segregated extrinsic output neurons in the various lobes of the MB which are involved in different forms of learned behavior (Tanaka, Tanimoto, and Ito 2008; Séjourné et al. 2011). Additionally, the KC cells that innervate a given lobe have similar glomerular inputs (Lin et al. 2007), which may represent acquired connections for the appropriate behavioral ouput. Taken together, these studies implicate a mechanism by which the fly can respond to complex stimuli and can acquire a behavioral valence through experience.

Glomerular activity and behavioral output

Studies of individual receptor function and glomerular activation patterns have given insight into how odorant identity and intensity are represented in the AL. How the complex glomerular activity patterns are translated to behavioral output is less clear. A behavioral screen with 110 single odorants to determine innate positive or negative valence for each found that a majority were classified as either attractive or neutral whereas only 6 of the tested compounds bore repellent properties (Knaden et al. 2012). Surprisingly, there was no obvious correlation between odorant valence and its chemical category, or its activation pattern in the peripheral olfactory system. However, the patterns of PN activation were separated by valence. In particular, 6 glomeruli that are clustered in the lateral region of the AL were strongly activated by the aversive odorants,

raising the possibility that they may be components of hard-wired repellent circuits (Knaden et al. 2012).

Results of another study support the idea that one or more “aversive” glomeruli recruited at higher concentrations can be responsible for concentration-dependent switches in valence that are observed for many odorants (Semmelhack and Wang 2009). The study examined behavior of *Drosophila* to apple cider vinegar, a low concentration of which activated six glomeruli in the AL and was behaviorally attractive. Selective silencing and activation of individual OSN classes, and thus individual glomeruli, revealed that two of the engaged glomeruli, DM1 (Or42b) and VA2 (Or92a), mediated the attraction. On the other hand, wild-type flies showed a robust aversion to apple cider vinegar at high concentrations. Analysis of the glomerular activity map revealed that an additional glomerulus, DM5 (Or85a), was activated at the increased concentration (Semmelhack and Wang 2009). Genetic manipulation of glomerular activity showed that this single glomerulus could account for the valence reversal at high concentrations of apple cider vinegar, suggesting that the DM5 glomerulus is hard-wired to generate avoidance behavior.

While most general odorants are represented in combinatorial glomerular activity, the peripheral and AL representations of carbon dioxide and strong acids are distinct exceptions (de Bruyne, Foster, and Carlson 2001; Suh et al. 2004; Ai et al. 2010). Each of these compounds activates one or two OSN/glomeruli and is perceived as aversive, suggesting a “labeled-line” avoidance circuit for its detection. Carbon dioxide, for example, activates the Gr21a/Gr63a receptor in ab1C OSNs (de Bruyne, Foster, and Carlson 2001; Jones et al. 2007; Kwon et al. 2007), the axons of which terminate in the

V glomerulus in the AL (Suh et al. 2004). Similarly, strong acids activate *Ir64a*$^{+}$ OSNs in the sacculus that target the DC4 glomerulus (Ai et al. 2010).

To date, the most significant advances in linking olfactory system wiring to behavior have come through studies of pheromone detection and courtship behavior. Courtship by the *Drosophila* male comprises a complex set of innate behavioral sequences (Hall 1994) set in place by the male-specific isoform of the *fruitless* gene, Fru^{M} (Manoli et al. 2005; Stockinger et al. 2005). Courtship is influenced, in part, by the detection of the male-emitted pheromone cVA. In both sexes, one of two OSN classes that detect cVA expresses *Or67d* and projects to the DA1 glomerulus in the AL (Kurtovic, Widmer, and Dickson 2007). Despite identical first order projections, cVA elicits disparate behavioral responses in males and females. In males, cVA promotes aggression towards other males (L. Wang and Anderson 2010) and suppresses courtship towards both males and females (Ejima et al. 2007). By contrast, cVA detection in females stimulates an increase in receptivity to courting males (Kurtovic, Widmer, and Dickson 2007). Exposure to cVA generates similar responses in OSNs and PNs in both sexes (Datta et al. 2008), suggesting that the differences in behavior are generated in higher brain centers. Tracing the axons of PNs that innervate the Or67d/DA1 glomerulus revealed a high density of arborizations in the ventral region of the LH in males, but not in females (Datta et al. 2008). Given that the narrowly tuned *Or67d* olfactory channel expresses *fru* in the OSN and the cognate PN, the sexually dimorphic arborizations in the LH were examined in *fru* mutant males. The arborizations in the ventral region of the LH were significantly reduced in *fru* mutant males, showing instead arborization resembling that present in wild-type females (Datta et al. 2008). *fru* mutant males court other males with an increased frequency, which suggests that the

fru-regulated axon topography in the LH contributes to the sexually dimorphic behavioral responses to cVA.

Sexual dimorphism of the specialized cVA pathway continued in higher order neurons (Ruta et al. 2010). Four clusters of cell bodies are in close proximity to the DA1 PN terminal arborizations. Among these putative third order neurons, one dorsal cluster (DC1), which showed responses following stimulation of the DA1 glomerulus but not other glomeruli, was specific to males. DC1 axons were traced to the lateral triangle and the superior medial protocerebrum (SMP tract), neuropil structures that are only present in males. Further tracing of this circuit revealed male-specific DN1 neurons, which extend dendrites into the lateral triangle and the SMP tract, and send long axons down to the ventral nerve cord. These DN1 axons terminate in the thoracic and abdominal ganglia and intermingle with motor neurons. DN1 neurons receive excitatory signals in response to cVA and DA1 activation, and this excitation requires input from the third order DC1 neurons (Ruta et al. 2010). The specificity of the cVA circuit has been key in following a neural pathway from olfactory detection to motor output.

Sophisticated processing by chemosensory neurons

Olfactory coding of odor blends

Thus far, properties of OSNs have been described in terms of response profiles to monomolecular odorants. In nature, however, many odors encountered are mixtures and can be perceived, at least by humans, as unique fragrances (Laing and Francis 1989). This unique perception has been thought to be the product of sophisticated central processing. There is mounting evidence, however, that OSN activity itself can reflect information about the context in which an odorant is received. For example, the presence of odorants that inhibit the Gr21a/Gr63a CO_2 receptor can disrupt the innate

avoidance behavior to CO_2 in *Drosophila* (Turner and Ray 2009). Other work that examined mixtures containing both excitatory and inhibitory components for a given Or/Orco receptor demonstrated that individual OSNs have the capacity to generate responses to mixtures that differ from the mere sum of its components. Recordings to such binary mixtures showed a change not only in the firing frequency of the OSN but also in the timing of the response (Su et al. 2011). Thus, odorant mixtures can generate unique signatures in the periphery that afford the freedom to discriminate blends from individual components alone, even across a range of concentrations.

Each component of an odor mixture has unique physicochemical properties that likely affect the rates in which their vapors reach the fly's olfactory organs. In a mixture of a "fast" excitatory odorant with a "slow" inhibitory odorant, the presence of the inhibitory odorant sharpened the activation response (Su et al. 2011). The reverse experiment ("slow" activator paired with a "fast" inhibitor) was carried out in a *Drosophila* OSN that ectopically expressed a mosquito olfactory receptor (Su et al. 2011). In this case, a biphasic response was observed where spontaneous activity was reduced upon initial exposure to the binary mixture and activation was marked by a slower response profile. Taken together, these experiments suggest that a given OSN has the power to generate unique responses to blends of odorants due to varying response dynamics of the constituents.

Starvation-induced changes in olfactory neurons

A change in an organism's internal physiological state often leads to distinct changes in behavior. The stereotypic nature of chemoreceptor expression and first-order connectivity would suggest that such plasticity relies largely on modulation of central processing. However, circadian changes in responses and spontaneous spike

amplitudes of OSNs (B. Krishnan, Dryer, and Hardin 1999; P. Krishnan et al. 2008) suggested that OSN responses are not rigid. Also, a recent study demonstrated that flies show a robust increase in food-search behavior that is largely dependent on modulation of olfactory processing at the periphery. Food odor-evoked changes in calcium-influx in PNs showed that some neurons in the AL were subject to modulation in response to starvation (Root et al. 2011). Specifically, three glomeruli (DM1, DM4, and DM2) showed enhanced odor-evoked responses and two (VM2 and VA3) showed decreased responses following starvation (Root et al. 2011). This modulation was specific to the glomerulus and not to the odor tested. Thus, a change in internal state appears to cause specific changes in olfactory representation in the brain along with changes in behavior.

Analysis of food odor-evoked activity in OSNs and PNs revealed that this glomerular-specific change in olfactory representation occurred at the level of transmission of OSN signal to PNs (Root et al. 2011). The *Drosophila* neuropeptide sNPF, known to promote feeding behavior (Lee et al. 2004), is expressed in a subset of OSNs along with its receptor sNPFR1 (Carlsson et al. 2010). Knockdown of sNPF in OSNs, using *Orco-Gal4* and *UAS-RNAi* transgenes, abolished the starvation-mediated increase in OSN signaling and the corresponding enhancement in food-search behavior. This loss of starvation-induced modulation was absent if either sNPF or sNPFR were knocked down in PNs. Further knockdown experiments with OSN-specific drivers refined the starvation-dependent requirement of sNPF/sNPFR to Or42b OSNs that project to the DM1 glomerulus. Moreover, overexpression of sNPFR1, but not sNPF, in Or42b OSNs in fed flies was sufficient to induce a starved phenotype (Root et al. 2011). Together, the results suggest that a starvation-regulated increase in sNPFR expression in Or42b

neurons brings about changes in DM1 activity, leading to an increase in food-search behavior.

There is also conclusive evidence to link the regulation of sNPFR1 expression in OSNs to insulin signaling. A combination of genetic and pharmacological manipulation was used to show that insulin receptor-mediated signalling was both necessary and sufficient for the up-regulation of sNPFR1 and the subsequent enhancement of odor-evoked activity in Or42b OSNs (Root et al. 2011). The study thus uncovered a simple yet credible mechanism for how a change in internal state is translated to a change in sensory input via insulin signaling, and in so doing brings about an appropriate behavioral modification to meet the physiological needs of the fly.

Development of the olfactory system

During metamorphosis, the axons of class-specific odor receptor neurons (OSNs) must all converge onto the same discrete region of the AL. This axon patterning in an OSN-specific manner underlies faithful representation of olfactory information in the adult *Drosophila* nervous system. The mechanisms by which such a precise circuit develops is largely unknown. Recent findings have demonstrated that key developmental genetic programs, including those within olfactory receptor (*Or*) gene choice, have dual roles in wiring the *Drosophila* olfactory system. These studies suggest that the genetic programs that dictate OSN identity are employed to specify proper axon guidance of these same OSNs

Genetic specification of axon guidance in the olfactory system

While there are several organizational similarities shared between mammalian and insect olfactory systems (Hildebrand and Shepherd 1997; Mombaerts et al. 1996; Vassar et al. 1994), there are fundamental differences in the developmental programs

employed by these animals to specify the formation of such precise neural circuits. In the olfactory sensory neurons of mice, for example, *Or* gene choice occurs in a stochastic manner, where the expression of a single *Or* provides negative feedback to inhibit the expression of all other *Or* genes (Vassar et al. 1994; Serizawa et al. 2003). Also, the specific Or that is expressed in the OSN can be detected in the developing axon and plays a role in the proper axon guidance of the OSN (Feinstein et al. 2004). In *Drosophila*, however, the selection of a single *Or* gene is much more deterministic, and displays no evidence of a negative feedback mechanism (Ray et al. 2007; Ray, van der Goes van Naters, and Carlson 2008). Additionally, the Or itself does not play a role in guiding the OSN axons to the AL, as *Or* gene expression occurs after the OSN axons have formed their specific connections in their stereotypic glomeruli (G. S. X. E. Jefferis et al. 2004).

Olfactory sensilla originate from undifferentiated cells of the antennal disc and their identity is initially determined by the actions of two proneural genes, *atonal* and *amos*. Atonal is required for the development of coeloconic sensilla (Jhaveri et al. 2000; B. P. Gupta and Rodrigues 1997), and amos specifies both basiconics and trichoids (zur Lage et al. 2003). Further differentiation between basiconics and trichoids depends on the levels of the Lozenge transcription factor in combination with Amos (Goulding, zur Lage, and Jarman 2000). Given that the OSN class that is expressed in each sensilla type is stereotyped and restricted to specific regions of the antenna, this genetically programmed differentiation through the action of proneural genes also limits possible glomerular targets in the AL.

Positioning within the antennal disc also corresponds to varying levels of Hedgehog (Hh) protein. High levels of Hh in the posterior compartment generates cells

with high levels of the Patched (Ptc) receptor in the posterior and low levels of Ptc in the anterior compartment (Hooper and Scott 2005). In a coupled two-step model of Hh signaling proposed by Luo and colleagues, this initial specification of Ptc levels determines the responsiveness of OSNs to brain-derived Hh source in a second round of Hh signaling (Chou et al. 2010). OSNs that express low levels of the Ptc receptor are responsive to the Hh expressed near the AL, and this group of OSNs shows axon guidance defects when Hh signaling is disrupted (Chou et al. 2010). Once again, spatial positioning, which will ultimately restrict OSN class that can be expressed, also plays a role in the guidance of the OSN axon to the AL.

Links between Or gene choice and glomerular targeting

Another recent cell lineage study provides strong evidence that specific genetic programs of differentiation are responsible for both Or gene choice and faithful axon guidance. Endo et al. demonstrate that the OSNs of a single sensillum are divided into two classes based on asymmetric Notch signaling (Endo et al. 2007). This Notch-On or Notch-Off identity of the OSN not only specified which Or gene was expressed but also which glomerulus was targeted. If Notch function is disrupted, all of the OSNs will express the Or that is specified in the Notch-Off class for that sensillum, and all OSN axons will project to the corresponding Notch-Off glomerulus (Endo et al. 2007). These results strongly suggest that the changes in early cell fate programs have a coupled effect on Or gene choice and axon targeting.

Many recent studies strongly suggest that the cell lineage and positional information in the antennal disc initiate specific transcriptional programs that first lead to OSN axon targeting to their proper AL regions and later leads to the expression of the corresponding *Or* gene (Figure 1.1). Interestingly, the cis-regulatory elements in *Or*

promoters that have been found to specify *Or* gene expression are also found in the upstream regions of many axon guidance molecules (Ray et al. 2007; Ray, van der Goes van Naters, and Carlson 2008; Miller and Carlson 2010).

These defined patterns of gene expression generate a program of cell differentiation where a unique collection of transcription factors lead to precise mapping of OSN axons that is consistent with the *Or* gene expressed, thus conferring unique OSN-class identity (Figure 1.2A). Presumably, the array of cell surface molecules are used to instruct neuronal processes along different axes, both in long and short-range axonal targeting (Figure 1.2B). Through a combination of spatial location of OSNs, genetic programming and local and long range interactions of axons, *Drosophila* are able to generate a sophisticated internal representation of the chemical world.

POU-domain transcription factors *acj6* and *pdm3* also have dual roles in *Or* gene choice and axon guidance of neurons within the olfactory system. Their role in such developmental processes will be explored in the final chapter.

Concluding remarks

It is within this highly organized olfactory system of *Drosophila melanogaster* that I explore various mechanisms of gene expression in response to odorants. First, I characterize the landscape of genetic changes in the central nervous system immediately following exposure to a fruit odor blend. I explore how regulation of these genes is altered with aging and loss of the histone deacetylase HDAC6. This analysis is followed by identification of activity-regulated genes in the antenna and exploring the contribution of olfactory sensory neuron activity to regulation of these genes. Moving in to the genetic effects of long-term odor exposure, I characterize the special odorant diacetyl and its non-canonical pathway of olfactory signaling in the *Drosophila* antenna.

This long-term effect is also observed in cell culture, mice and even plants. Finally, I conclude with an examination of gene expression in mutants for two POU-domain transcription factors with important roles in development and wiring of the *Drosophila* olfactory system: *acj6* and *pdm3.*

References

Abuin, Liliane, Benoîte Bargeton, Maximilian H. Ulbrich, Ehud Y. Isacoff, Stephan Kellenberger, and Richard Benton. 2011. “Functional Architecture of Olfactory Ionotropic Glutamate Receptors.” *Neuron* 69 (1): 44–60.

Ai, Minrong, Soohong Min, Yael Grosjean, Charlotte Leblanc, Rati Bell, Richard Benton, and Greg S. B. Suh. 2010. “Acid Sensing by the Drosophila Olfactory System.” *Nature* 468 (7324): 691–95.

Belle, J. S. de, and M. Heisenberg. 1994. “Associative Odor Learning in Drosophila Abolished by Chemical Ablation of Mushroom Bodies.” *Science* 263 (5147): 692–95.

Benton, Richard, Silke Sachse, Stephen W. Michnick, and Leslie B. Vosshall. 2006. “Atypical Membrane Topology and Heteromeric Function of Drosophila Odorant Receptors in Vivo.” *PLoS Biology* 4 (2): e20.

Benton, Richard, Kirsten S. Vannice, Carolina Gomez-Diaz, and Leslie B. Vosshall. 2009. “Variant Ionotropic Glutamate Receptors as Chemosensory Receptors in Drosophila.” *Cell* 136 (1): 149–62.

Benton, Richard, Kirsten S. Vannice, and Leslie B. Vosshall. 2007. “An Essential Role for a CD36-Related Receptor in Pheromone Detection in Drosophila.” *Nature* 450 (7167): 289–93.

Bhandawat, Vikas, Shawn R. Olsen, Nathan W. Gouwens, Michelle L. Schlief, and Rachel I. Wilson. 2007. “Sensory Processing in the Drosophila Antennal Lobe Increases Reliability and Separability of Ensemble Odor Representations.” *Nature Neuroscience* 10 (11): 1474–82.

Bruyne, M. de, K. Foster, and J. R. Carlson. 2001. “Odor Coding in the Drosophila Antenna.” *Neuron* 30 (2): 537–52.

Carlsson, Mikael A., Max Diesner, Joachim Schachtner, and Dick R. Nässel. 2010. “Multiple Neuropeptides in the Drosophila Antennal Lobe Suggest Complex Modulatory Circuits.” *The Journal of Comparative Neurology* 518 (16): 3359–80.

Caron, Sophie J. C., Vanessa Ruta, L. F. Abbott, and Richard Axel. 2013. “Random Convergence of Olfactory Inputs in the Drosophila Mushroom Body.” *Nature* 497 (7447): 113–17.

Chatterjee, Abhishek, Gregg Roman, and Paul E. Hardin. 2009. “Go Contributes to Olfactory Reception in Drosophila Melanogaster.” *BMC Physiology* 9 (November): 22.

Chou, Ya-Hui, Xiaoyan Zheng, Philip A. Beachy, and Liqun Luo. 2010. “Patterning Axon Targeting of Olfactory Receptor Neurons by Coupled Hedgehog Signaling at Two Distinct Steps.” *Cell* 142 (6): 954–66.

Clyne, Peter J., Coral G. Warr, Marc R. Freeman, Derek Lessing, Junhyong Kim, and John R. Carlson. 1999. “A Novel Family of Divergent Seven-Transmembrane Proteins: Candidate Odorant Receptors in Drosophila.” *Neuron* 22 (2): 327–38.

Clyne, P. J. 2000. “Candidate Taste Receptors in Drosophila.” *Science* 287 (5459): 1830–34.

Couto, Africa, Mattias Alenius, and Barry J. Dickson. 2005. “Molecular, Anatomical, and Functional Organization of the Drosophila Olfactory System.” *Current Biology: CB* 15 (17): 1535–47.

Datta, Sandeep Robert, Maria Luisa Vasconcelos, Vanessa Ruta, Sean Luo, Allan Wong, Ebru Demir, Jorge Flores, Karen Balonze, Barry J. Dickson, and Richard Axel. 2008. “The Drosophila Pheromone cVA Activates a Sexually Dimorphic Neural Circuit.” *Nature* 452 (7186): 473–77.

Davis, Ronald L. 2005. “Olfactory Memory Formation in Drosophila: From Molecular to Systems Neuroscience.” *Annual Review of Neuroscience* 28: 275–302.

Dobritsa, Anna A., Wynand van der Goes van Naters, Coral G. Warr, R. Alexander Steinbrecht, and John R. Carlson. 2003. “Integrating the Molecular and Cellular Basis of Odor Coding in the Drosophila Antenna.” *Neuron* 37 (5): 827–41.

Ejima, Aki, Benjamin P. C. Smith, Christophe Lucas, Wynand van der Goes van Naters, Carson J. Miller, John R. Carlson, Joel D. Levine, and Leslie C. Griffith. 2007. “Generalization of Courtship Learning in Drosophila Is Mediated by Cis-Vaccenyl Acetate.” *Current Biology: CB* 17 (7): 599–605.

Endo, Keita, Tomoko Aoki, Yuka Yoda, Ken-Ichi Kimura, and Chihiro Hama. 2007. “Notch Signal Organizes the Drosophila Olfactory Circuitry by Diversifying the Sensory Neuronal Lineages.” *Nature Neuroscience* 10 (2): 153–60.

Enjin, Anders, Emanuela E. Zaharieva, Dominic D. Frank, Suzan Mansourian, Greg S. B. Suh, Marco Gallio, and Marcus C. Stensmyr. 2016. “Humidity Sensing in Drosophila.” *Current Biology: CB* 26 (10): 1352–58.

Feinstein, Paul, Thomas Bozza, Ivan Rodriguez, Anne Vassalli, and Peter Mombaerts. 2004. “Axon Guidance of Mouse Olfactory Sensory Neurons by Odorant Receptors and the beta2 Adrenergic Receptor.” *Cell* 117 (6): 833–46.

Fishilevich, Elane, and Leslie B. Vosshall. 2005. “Genetic and Functional Subdivision of the Drosophila Antennal Lobe.” *Current Biology: CB* 15 (17): 1548–53.

Galindo, K., and D. P. Smith. 2001. “A Large Family of Divergent Drosophila Odorant-Binding Proteins Expressed in Gustatory and Olfactory Sensilla.” *Genetics* 159 (3): 1059–72.

Gao, Q., and A. Chess. 1999. “Identification of Candidate Drosophila Olfactory Receptors from Genomic DNA Sequence.” *Genomics* 60 (1): 31–39.

Gao, Q., B. Yuan, and A. Chess. 2000. “Convergent Projections of Drosophila Olfactory Neurons to Specific Glomeruli in the Antennal Lobe.” *Nature Neuroscience* 3 (8): 780–85.

Gaudry, Quentin, Elizabeth J. Hong, Jamey Kain, Benjamin L. de Bivort, and Rachel I. Wilson. 2013. “Asymmetric Neurotransmitter Release Enables Rapid Odour Lateralization in Drosophila.” *Nature* 493 (7432): 424–28.

Goes van Naters, Wynand van der, and John R. Carlson. 2007. “Receptors and Neurons for Fly Odors in Drosophila.” *Current Biology: CB* 17 (7): 606–12.

Gomez-Diaz, Carolina, Jaime H. Reina, Christian Cambillau, and Richard Benton. 2013.

"Ligands for Pheromone-Sensing Neurons Are Not Conformationally Activated Odorant Binding Proteins." *PLoS Biology* 11 (4): e1001546.

Goulding, Sarah E., Petra zur Lage, and Andrew P. Jarman. 2000. "Amos, a Proneural Gene for Drosophila Olfactory Sense Organs That Is Regulated by Lozenge." *Neuron* 25 (1): 69–78.

Gupta, Bhagwati Prasad, and Veronica Rodrigues. 1997. "Atonal Is a Proneural Gene for a Subset of Olfactory Sense Organs in Drosophila." *Genes to Cells: Devoted to Molecular & Cellular Mechanisms* 2 (3): 225–33.

Gupta, Nitin, and Mark Stopfer. 2012. "Functional Analysis of a Higher Olfactory Center, the Lateral Horn." *The Journal of Neuroscience: The Official Journal of the Society for Neuroscience* 32 (24): 8138–48.

Hallem, Elissa A., and John R. Carlson. 2006. "Coding of Odors by a Receptor Repertoire." *Cell* 125 (1): 143–60.

Hallem, Elissa A., Michael G. Ho, and John R. Carlson. 2004. "The Molecular Basis of Odor Coding in the Drosophila Antenna." *Cell* 117 (7): 965–79.

Hall, Jeffrey C. 1994. "The Mating of a Fly." *Science* 264 (5166): 1702–14.

Ha, Tal Soo, and Dean P. Smith. 2006. "A Pheromone Receptor Mediates 11-Cis-Vaccenyl Acetate-Induced Responses in Drosophila." *The Journal of Neuroscience: The Official Journal of the Society for Neuroscience* 26 (34): 8727–33.

Heimbeck, G., V. Bugnon, N. Gendre, A. Keller, and R. F. Stocker. 2001. "A Central Neural Circuit for Experience-Independent Olfactory and Courtship Behavior in Drosophila Melanogaster." *Proceedings of the National Academy of Sciences of the United States of America* 98 (26): 15336–41.

Hildebrand, J. G., and G. M. Shepherd. 1997. "Mechanisms of Olfactory Discrimination: Converging Evidence for Common Principles across Phyla." *Annual Review of Neuroscience* 20: 595–631.

Hooper, Joan E., and Matthew P. Scott. 2005. "Communicating with Hedgehogs." *Nature Reviews. Molecular Cell Biology* 6 (4): 306–17.

Jefferis, Gregory S. X. E., Christopher J. Potter, Alexander M. Chan, Elizabeth C. Marin, Torsten Rohlfing, Calvin R. Maurer Jr, and Liqun Luo. 2007. "Comprehensive Maps of Drosophila Higher Olfactory Centers: Spatially Segregated Fruit and Pheromone Representation." *Cell* 128 (6): 1187–1203.

Jefferis, Gregory S. X. E., Raj M. Vyas, Daniela Berdnik, Ariane Ramaekers, Reinhard F. Stocker, Nobuaki K. Tanaka, Kei Ito, and Liqun Luo. 2004. "Developmental Origin of Wiring Specificity in the Olfactory System of Drosophila." *Development* 131 (1): 117–30.

Jefferis, G. S., E. C. Marin, R. F. Stocker, and L. Luo. 2001. "Target Neuron Prespecification in the Olfactory Map of Drosophila." *Nature* 414 (6860): 204–8.

Jhaveri, Dhanisha, Anindya Sen, G. Venugopala Reddy, and Veronica Rodrigues. 2000. "Sense Organ Identity in the Drosophila Antenna Is Specified by the Expression of the Proneural Gene Atonal." *Mechanisms of Development* 99 (1): 101–11.

Jones, Walton D., Pelin Cayirlioglu, Ilona Grunwald Kadow, and Leslie B. Vosshall. 2007. “Two Chemosensory Receptors Together Mediate Carbon Dioxide Detection in Drosophila.” *Nature* 445 (7123): 86–90.

Kain, P., T. S. Chakraborty, S. Sundaram, O. Siddiqi, V. Rodrigues, and G. Hasan. 2008. “Reduced Odor Responses from Antennal Neurons of Gq , Phospholipase C , and rdgA Mutants in Drosophila Support a Role for a Phospholipid Intermediate in Insect Olfactory Transduction.” *Journal of Neuroscience* 28 (18): 4745–55.

Kido, Asami, and Kei Ito. 2002. “Mushroom Bodies Are Not Required for Courtship Behavior by Normal and Sexually Mosaic Drosophila.” *Journal of Neurobiology* 52 (4): 302–11.

Kim, M. S., A. Repp, and D. P. Smith. 1998. “LUSH Odorant-Binding Protein Mediates Chemosensory Responses to Alcohols in Drosophila Melanogaster.” *Genetics* 150 (2): 711–21.

Knaden, Markus, Antonia Strutz, Jawaid Ahsan, Silke Sachse, and Bill S. Hansson. 2012. “Spatial Representation of Odorant Valence in an Insect Brain.” *Cell Reports* 1 (4): 392–99.

Krishnan, B., S. E. Dryer, and P. E. Hardin. 1999. “Circadian Rhythms in Olfactory Responses of Drosophila Melanogaster.” *Nature* 400 (6742): 375–78.

Krishnan, Parthasarathy, Abhishek Chatterjee, Shintaro Tanoue, and Paul E. Hardin. 2008. “Spike Amplitude of Single-Unit Responses in Antennal Sensillae Is Controlled by the Drosophila Circadian Clock.” *Current Biology: CB* 18 (11): 803–7.

Kurtovic, Amina, Alexandre Widmer, and Barry J. Dickson. 2007. “A Single Class of Olfactory Neurons Mediates Behavioural Responses to a Drosophila Sex Pheromone.” *Nature* 446 (7135): 542–46.

Kwon, Jae Young, Anupama Dahanukar, Linnea A. Weiss, and John R. Carlson. 2007. “The Molecular Basis of CO2 Reception in Drosophila.” *Proceedings of the National Academy of Sciences of the United States of America* 104 (9): 3574–78.

Lage, Petra I. zur, David R. A. Prentice, Eimear E. Holohan, and Andrew P. Jarman. 2003. “The Drosophila Proneural Gene Amos Promotes Olfactory Sensillum Formation and Suppresses Bristle Formation.” *Development* 130 (19): 4683–93.

Laing, D. G., and G. W. Francis. 1989. “The Capacity of Humans to Identify Odors in Mixtures.” *Physiology & Behavior* 46 (5): 809–14.

Laissue, P. P., C. H. Reiter, P. R. Hiesinger, S. Halter, K. F. Fischbach, and R. F. Stocker. 1999. “Three-Dimensional Reconstruction of the Antennal Lobe in Drosophila Melanogaster.” *The Journal of Comparative Neurology* 405 (4): 543–52.

Larsson, Mattias C., Ana I. Domingos, Walton D. Jones, M. Eugenia Chiappe, Hubert Amrein, and Leslie B. Vosshall. 2004. “Or83b Encodes a Broadly Expressed Odorant Receptor Essential for Drosophila Olfaction.” *Neuron* 43 (5): 703–14.

Laughlin, John D., Tal Soo Ha, David N. M. Jones, and Dean P. Smith. 2008. “Activation of Pheromone-Sensitive Neurons Is Mediated by Conformational Activation of Pheromone-Binding Protein.” *Cell* 133 (7): 1255–65.

Lee, Kyu-Sun, Kwan-Hee You, Jong-Kil Choo, Yong-Mahn Han, and Kweon Yu. 2004. “Drosophila Short Neuropeptide F Regulates Food Intake and Body Size.” *The Journal of Biological Chemistry* 279 (49): 50781–89.

Lin, Hui-Hao, Jason Sih-Yu Lai, An-Lun Chin, Yung-Chang Chen, and Ann-Shyn Chiang. 2007. “A Map of Olfactory Representation in the Drosophila Mushroom Body.” *Cell* 128 (6): 1205–17.

Lundin, Carolina, Lukas Käll, Scott A. Kreher, Katja Kapp, Erik L. Sonnhammer, John R. Carlson, Gunnar von Heijne, and Ingmarie Nilsson. 2007. “Membrane Topology of theDrosophilaOR83b Odorant Receptor.” *FEBS Letters* 581 (29): 5601–4.

Manoli, Devanand S., Margit Foss, Adriana Villella, Barbara J. Taylor, Jeffrey C. Hall, and Bruce S. Baker. 2005. “Male-Specific Fruitless Specifies the Neural Substrates of Drosophila Courtship Behaviour.” *Nature* 436 (7049): 395–400.

Marin, Elizabeth C., Gregory S. X. E. Jefferis, Takaki Komiyama, Haitao Zhu, and Liqun Luo. 2002. “Representation of the Glomerular Olfactory Map in the Drosophila Brain.” *Cell* 109 (2): 243–55.

Mayer, Mark L. 2006. “Glutamate Receptors at Atomic Resolution.” *Nature* 440 (7083): 456–62.

McKenna, M. P., D. S. Hekmat-Scafe, P. Gaines, and J. R. Carlson. 1994. “Putative Drosophila Pheromone-Binding Proteins Expressed in a Subregion of the Olfactory System.” *The Journal of Biological Chemistry* 269 (23): 16340–47.

Miller, Carson J., and John R. Carlson. 2010. “Regulation of Odor Receptor Genes in Trichoid Sensilla of the Drosophila Antenna.” *Genetics* 186 (1): 79–95.

Mombaerts, P., F. Wang, C. Dulac, S. K. Chao, A. Nemes, M. Mendelsohn, J. Edmondson, and R. Axel. 1996. “Visualizing an Olfactory Sensory Map.” *Cell* 87 (4): 675–86.

Muench, Daniel, and C. Giovanni Galizia. 2015. “DoOR 2.0 - Comprehensive Mapping ofDrosophila melanogasterOdorant Responses.” https://doi.org/10.1101/027920.

Naresh Singh, R., and Shubha V. Nayak. 1985. “Fine Structure and Primary Sensory Projections of Sensilla on the Maxillary Palp of Drosophila Melanogaster Meigen (Diptera : Drosophilidae).” *International Journal of Insect Morphology and Embryology* 14 (5): 291–306.

Neuhaus, Eva M., Günter Gisselmann, Weiyi Zhang, Ruth Dooley, Klemens Störtkuhl, and Hanns Hatt. 2005. “Odorant Receptor Heterodimerization in the Olfactory System of Drosophila Melanogaster.” *Nature Neuroscience* 8 (1): 15–17.

Olsen, Shawn R., Vikas Bhandawat, and Rachel I. Wilson. 2007. “Excitatory Interactions between Olfactory Processing Channels in the Drosophila Antennal Lobe.” *Neuron* 54 (1): 89–103.

Olsen, Shawn R., and Rachel I. Wilson. 2008. “Lateral Presynaptic Inhibition Mediates Gain Control in an Olfactory Circuit.” *Nature* 452 (7190): 956–60.

Pelosi, P., and R. Maida. 1995. “Odorant-Binding Proteins in Insects.” *Comparative Biochemistry and Physiology. Part B, Biochemistry & Molecular Biology* 111 (3):

503–14.

Pikielny, C. W., G. Hasan, F. Rouyer, and M. Rosbash. 1994. “Members of a Family of Drosophila Putative Odorant-Binding Proteins Are Expressed in Different Subsets of Olfactory Hairs.” *Neuron* 12 (1): 35–49.

Ray, Anandasankar, Wynand van der Goes van Naters, and John R. Carlson. 2008. “A Regulatory Code for Neuron-Specific Odor Receptor Expression.” *PLoS Biology* 6 (5): e125.

Ray, Anandasankar, Wynand van der Goes van Naters, Takashi Shiraiwa, and John R. Carlson. 2007. “Mechanisms of Odor Receptor Gene Choice in Drosophila.” *Neuron* 53 (3): 353–69.

Root, Cory M., Kang I. Ko, Amir Jafari, and Jing W. Wang. 2011. “Presynaptic Facilitation by Neuropeptide Signaling Mediates Odor-Driven Food Search.” *Cell* 145 (1): 133–44.

Rothenfluh, Adrian, Robert J. Threlkeld, Roland J. Bainton, Linus T-Y Tsai, Amy W. Lasek, and Ulrike Heberlein. 2006. “Distinct Behavioral Responses to Ethanol Are Regulated by Alternate RhoGAP18B Isoforms.” *Cell* 127 (1): 199–211.

Ruta, Vanessa, Sandeep Robert Datta, Maria Luisa Vasconcelos, Jessica Freeland, Loren L. Looger, and Richard Axel. 2010. “A Dimorphic Pheromone Circuit in Drosophila from Sensory Input to Descending Output.” *Nature* 468 (7324): 686–90.

Sato, Koji, Maurizio Pellegrino, Takao Nakagawa, Tatsuro Nakagawa, Leslie B. Vosshall, and Kazushige Touhara. 2008. “Insect Olfactory Receptors Are Heteromeric Ligand-Gated Ion Channels.” *Nature* 452 (7190): 1002–6.

Scott, K., R. Brady Jr, A. Cravchik, P. Morozov, A. Rzhetsky, C. Zuker, and R. Axel. 2001. “A Chemosensory Gene Family Encoding Candidate Gustatory and Olfactory Receptors in Drosophila.” *Cell* 104 (5): 661–73.

Séjourné, Julien, Pierre-Yves Plaçais, Yoshinori Aso, Igor Siwanowicz, Séverine Trannoy, Vladimiros Thoma, Stevanus R. Tedjakumala, et al. 2011. “Mushroom Body Efferent Neurons Responsible for Aversive Olfactory Memory Retrieval in Drosophila.” *Nature Neuroscience* 14 (7): 903–10.

Semmelhack, Julia L., and Jing W. Wang. 2009. “Select Drosophila Glomeruli Mediate Innate Olfactory Attraction and Aversion.” *Nature* 459 (7244): 218–23.

Serizawa, Shou, Kazunari Miyamichi, Hiroko Nakatani, Misao Suzuki, Michiko Saito, Yoshihiro Yoshihara, and Hitoshi Sakano. 2003. “Negative Feedback Regulation Ensures the One Receptor-One Olfactory Neuron Rule in Mouse.” *Science* 302 (5653): 2088–94.

Shanbhag, S. R., and D. Hekmat-Scafe. 2001. “Expression Mosaic of Odorant-binding Proteins in Drosophila Olfactory Organs.” *Microscopy Research and Technique*. https://onlinelibrary.wiley.com/doi/abs/10.1002/jemt.1179.

Shang, Yuhua, Adam Claridge-Chang, Lucas Sjulson, Marc Pypaert, and Gero Miesenböck. 2007. “Excitatory Local Circuits and Their Implications for Olfactory Processing in the Fly Antennal Lobe.” *Cell* 128 (3): 601–12.

Silbering, Ana F., Raphael Rytz, Yael Grosjean, Liliane Abuin, Pavan Ramdya, Gregory S. X. E. Jefferis, and Richard Benton. 2011. “Complementary Function and Integrated Wiring of the Evolutionarily Distinct Drosophila Olfactory Subsystems.” *The Journal of Neuroscience: The Official Journal of the Society for Neuroscience* 31 (38): 13357–75.

Smart, Renee, Aidan Kiely, Morgan Beale, Ernesto Vargas, Colm Carraher, Andrew V. Kralicek, David L. Christie, Chen Chen, Richard D. Newcomb, and Coral G. Warr. 2008. “Drosophila Odorant Receptors Are Novel Seven Transmembrane Domain Proteins That Can Signal Independently of Heterotrimeric G Proteins.” *Insect Biochemistry and Molecular Biology* 38 (8): 770–80.

Sobolevsky, Alexander I., Michael P. Rosconi, and Eric Gouaux. 2009. “X-Ray Structure, Symmetry and Mechanism of an AMPA-Subtype Glutamate Receptor.” *Nature* 462 (7274): 745–56.

Stensmyr, Marcus C., Hany K. M. Dweck, Abu Farhan, Irene Ibba, Antonia Strutz, Latha Mukunda, Jeanine Linz, et al. 2012. “A Conserved Dedicated Olfactory Circuit for Detecting Harmful Microbes in Drosophila.” *Cell* 151 (6): 1345–57.

Stocker, R. F. 1994. “The Organization of the Chemosensory System in Drosophila Melanogaster: A Review.” *Cell and Tissue Research* 275 (1): 3–26.

Stocker, R. F., M. C. Lienhard, A. Borst, and K. F. Fischbach. 1990. “Neuronal Architecture of the Antennal Lobe in Drosophila Melanogaster.” *Cell and Tissue Research* 262 (1): 9–34.

Stockinger, Petra, Duda Kvitsiani, Shay Rotkopf, László Tirián, and Barry J. Dickson. 2005. “Neural Circuitry That Governs Drosophila Male Courtship Behavior.” *Cell* 121 (5): 795–807.

Su, Chih-Ying, Carlotta Martelli, Thierry Emonet, and John R. Carlson. 2011. “Temporal Coding of Odor Mixtures in an Olfactory Receptor Neuron.” *Proceedings of the National Academy of Sciences of the United States of America* 108 (12): 5075–80.

Su, Chih-Ying, Karen Menuz, Johannes Reisert, and John R. Carlson. 2012. “Non-Synaptic Inhibition between Grouped Neurons in an Olfactory Circuit.” *Nature* 492 (7427): 66–71.

Suh, Greg S. B., Allan M. Wong, Anne C. Hergarden, Jing W. Wang, Anne F. Simon, Seymour Benzer, Richard Axel, and David J. Anderson. 2004. “A Single Population of Olfactory Sensory Neurons Mediates an Innate Avoidance Behaviour in Drosophila.” *Nature* 431 (7010): 854–59.

Tanaka, Nobuaki K., Hiromu Tanimoto, and Kei Ito. 2008. “Neuronal Assemblies of the Drosophila Mushroom Body.” *The Journal of Comparative Neurology* 508 (5): 711–55.

Turner, Stephanie Lynn, and Anandasankar Ray. 2009. “Modification of CO2 Avoidance Behaviour in Drosophila by Inhibitory Odorants.” *Nature* 461 (7261): 277–81.

Vassar, R., S. K. Chao, R. Sitcheran, J. M. Nuñez, L. B. Vosshall, and R. Axel. 1994. “Topographic Organization of Sensory Projections to the Olfactory Bulb.” *Cell* 79 (6): 981–91.

Vassar, R., J. Ngai, and R. Axel. 1993. “Spatial Segregation of Odorant Receptor Expression in the Mammalian Olfactory Epithelium.” *Cell* 74 (2): 309–18.

Venkatesh, Sunita, and R. Naresh Singh. 1984. “Sensilla on the Third Antennal Segment of Drosophila Melanogaster Meigen (Diptera : Drosophilidae).” *International Journal of Insect Morphology and Embryology* 13 (1): 51–63.

Vosshall, L. B., A. M. Wong, and R. Axel. 2000. “An Olfactory Sensory Map in the Fly Brain.” *Cell* 102 (2): 147–59.

Vosshall, Leslie B., Hubert Amrein, Pavel S. Morozov, Andrey Rzhetsky, and Richard Axel. 1999. “A Spatial Map of Olfactory Receptor Expression in the Drosophila Antenna.” *Cell* 96 (5): 725–36.

Wang, Jing W., Allan M. Wong, Jorge Flores, Leslie B. Vosshall, and Richard Axel. 2003. “Two-Photon Calcium Imaging Reveals an Odor-Evoked Map of Activity in the Fly Brain.” *Cell* 112 (2): 271–82.

Wang, Liming, and David J. Anderson. 2010. “Identification of an Aggression-Promoting Pheromone and Its Receptor Neurons in Drosophila.” *Nature* 463 (7278): 227–31.

Wicher, Dieter, Ronny Schäfer, René Bauernfeind, Marcus C. Stensmyr, Regine Heller, Stefan H. Heinemann, and Bill S. Hansson. 2008. “Drosophila Odorant Receptors Are Both Ligand-Gated and Cyclic-Nucleotide-Activated Cation Channels.” *Nature* 452 (7190): 1007–11.

Wistrand, Markus, Lukas Käll, and Erik L. L. Sonnhammer. 2006. “A General Model of G Protein-Coupled Receptor Sequences and Its Application to Detect Remote Homologs.” *Protein Science: A Publication of the Protein Society* 15 (3): 509–21.

Wong, Allan M., Jing W. Wang, and Richard Axel. 2002. “Spatial Representation of the Glomerular Map in the Drosophila Protocerebrum.” *Cell* 109 (2): 229–41.

Xu, Pingxi, Rachel Atkinson, David N. M. Jones, and Dean P. Smith. 2005. “Drosophila OBP LUSH Is Required for Activity of Pheromone-Sensitive Neurons.” *Neuron* 45 (2): 193–200.

Yao, C. Andrea, and John R. Carlson. 2010. “Role of G-Proteins in Odor-Sensing and CO2-Sensing Neurons in Drosophila.” *The Journal of Neuroscience: The Official Journal of the Society for Neuroscience* 30 (13): 4562–72.

Yao, C. Andrea, Rickard Ignell, and John R. Carlson. 2005. “Chemosensory Coding by Neurons in the Coeloconic Sensilla of the Drosophila Antenna.” *The Journal of Neuroscience: The Official Journal of the Society for Neuroscience* 25 (37): 8359–67.

Figure 1.1. Genetic programming patterns both *Or* gene choice and axon guidance

A

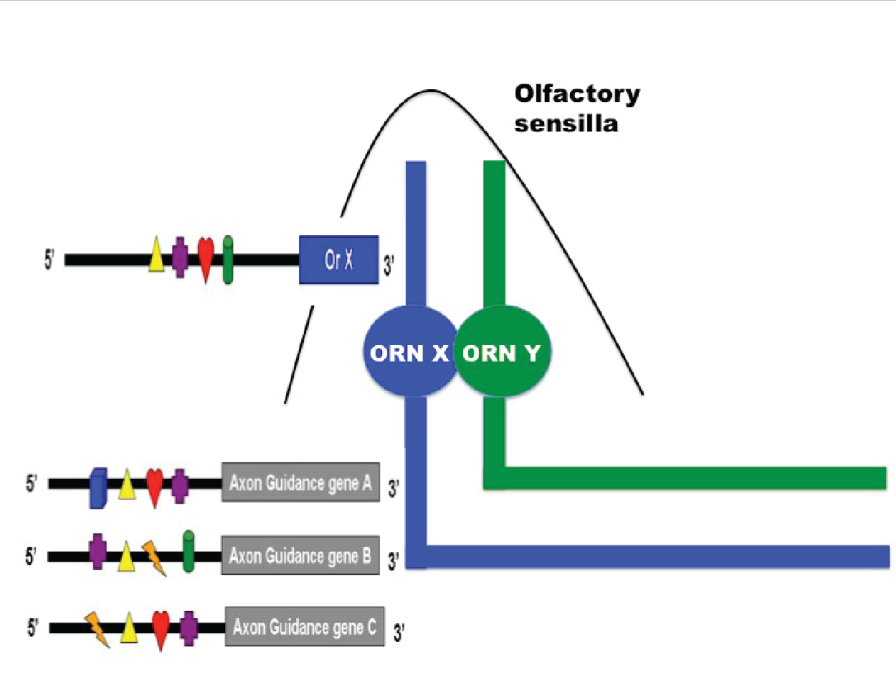

B

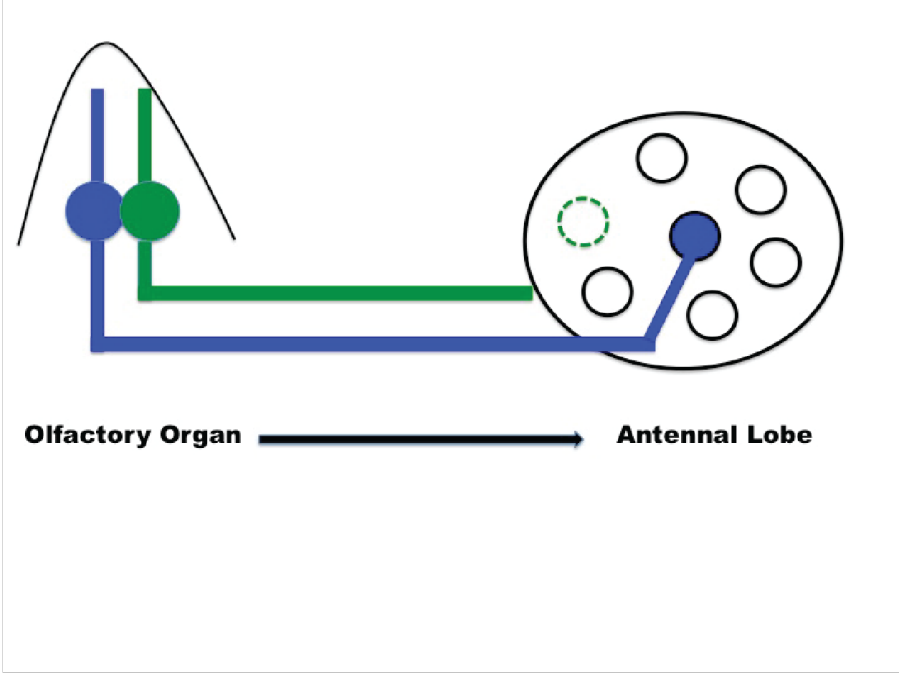

Figure 1.1. Genetic programming patterns both *Or* gene choice and axon guidance.

(A) The promoter region of the *OrX* gene contains a collection of regulatory elements that specify its expression within its endogenous sensillum. In this model, similar sets of regulatory elements regulate the *OrX*-specific expression of group of axon guidance genes (A,B,and C). The *OrY* promoter would have its own unique set of regulatory elements that direct its expression in the same sensillum. Many of these *OrY* regulatory elements would also be present upstream of a different, possibly overlapping, set of axon guidance molecules.

(B) The combination of axon guidance molecules expressed by ORN X can mediate axon-axon, axon-dendrite, and axon-signaling molecule interactions that direct axon targeting to its stereotypic glomerulus in the AL. The unique repertoire of axon guidance molecules expressed by ORN Y will eventually target its axons to a stereotypic region of the AL (green-dashed circle). This combinatorial code of genetic regulation is presumably set up by the initial genetic programs that lead to differentiation of the antennal disc (atonal, amos, Hh/Ptc, asymmetric Notch activity), and in several instances requires the POU-domain transcription factors Acj6 and Pdm3.

Figure 1.2. Diagram of olfactory connections in the adult *Drosophila* nervous system

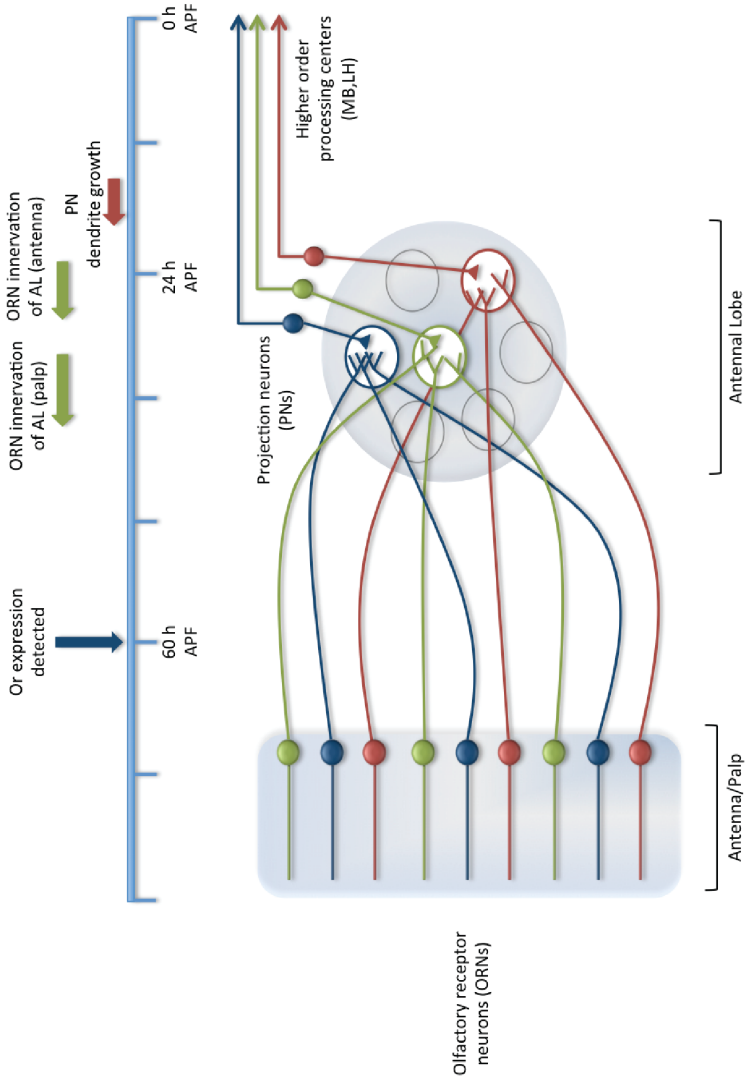

Figure 1.2. Diagram of olfactory connections in the adult *Drosophila* nervous system.

This diagram depicts the wiring organization of the olfactory system. A single ORN class is labeled with a unique color in the two olfactory organs, the antennae and the maxillary palps. All axons from ORNs of the same class terminate in the same region of the antennal lobe (AL). At the AL, ORNs connect to projection neurons (PNs) in a similar stereotypic manner.

Table 1.1 Organization of the *Drosophila* olfactory system

Neuron	Receptor(s)	Glomerulus	PN Class	Strongest ligand(s)	Behavior valence
antennal large basiconic sensilla					
ab1A	Or42b	DM1	l	propyl acetate	attractive
ab1B	Or92a	VA2	ad	2,3-butanedione	attractive
ab1C	Gr21a/Gr63a	V		carbon dioxide	aversive
ab1D	Or10a	DL1	ad	methyl salicylate	aversive
ab2A	Or59b	DM4		methyl acetate	attractive
ab2B	Or85a	DM5	l	ethyl-3-hydroxybutyrate	attractive
ab3A	Or22a/b	DM2	l	ethyl hexanoate	attractive
ab3B	Or85b	VM5d		2-heptanone	
antennal small basiconic sensilla					
ab4A	Or7a	DL5	ad	E2-hexenal	aversive
ab4B	Or56a			geosmin	aversive
ab5A	Or82a	VA6	ad	geranyl acetate	
ab5B	Or47a	DM3	ad	pentyl acetate	
ab6A	Or98b	VM5d			
ab6B	Or49b	VA5		2-methylphenol	
ab7A	Or98a	VM5v		ethyl benzoate	

Table 1.1 (cont'd)

Neuron	Receptor(s)	Glomerulus	PN Class	Strongest ligand(s)	Behavior valence
antennal small basiconic sensilla (cont'd)					
ab7B	Or67c	VC4		ethyl lactate	
ab8A	Or43b	VM2	ad	ethyl butyrate	
ab8B	Or9a	VM3	ad	2-pentanol	
ab9A	Or69aA/B	D	ad	ethyl-3-hydroxy hexanoate	aversive
ab9B	Or67b	VA3	ad	acetophenone	
ab10A	Or49a/Or85f	DL4			aversive at high conc.
ab10B	Or67a	DM6	ad	ethyl benzoate	
ab11A				citronellal	
ab11B					
ab12A				citronellal	
ab12B				benzaldehyde	
Antennal coeloconic sensilla					
ac1A	Ir31a/Ir8a	VL2p		2-oxopentanoic acid	
ac1B	Ir75d/Ir25a	VL1		pyrrolidine	
ac1C	Ir92a/Ir76b	VM1		ammonia	
ac2A	Ir75a/Ir8a	DP1l		Propionic acid, acetic acid	

Table 1.1 (cont'd)

Neuron	Receptor(s)	Glomerulus	PN Class	Strongest ligand(s)	Behavior valence
antennal coeloconic sensilla (cont'd)					
ac2A	Ir75a/Ir8a	DP1l		Propionic acid, acetic acid	
ac2B	Ir75d/Ir25a	VL1		pyrrolidine	
ac2C	Ir76b				
ac3A	Ir75a/b/c/ Ir8a	DL2?		butyric acid	
ac3B	Or35a/ Ir76b	VC3			
ac4A	Ir76a/b/ Ir25a	VM4	ad	phenylethylamine	
ac4B	Ir75d/Ir25a	VL1		pyrrolidine	
ac4C	Ir84a/ Ir8a	VL2a		phenylacetaldehyde	
anennal trichoid sensilla					
at1A	Or67d	DA1	l,v	11-*cis*-vaccenyl acetate	
at2A	Or23a	DA3	ad		
at2B	Or83c	DC3	ad		aversive at high conc.
at3A	Or2a	DA4m			
at3B	Or19a/b	DC1	ad	1-octen-3-ol	
at3C	Or43a	DA4l		1-hexanol	
at4A	Or47b	VA1lm	ad,v	male extract	

Table 1.1 (cont'd)

Neuron	Receptor(s)	Glomerulus	PN Class	Strongest ligand(s)	Behavior valence
anennal trichoid sensilla (cont'd)					
at4B	Or65a/b/c	DL3	l		
at4C	Or88a	VA1d	ad	male and female extract	
sacculus I					
	Ir25a				
	Ir40a	VP1?		Humidity and temperature	
	Ir93a	VP1?			
sacculus II					
	Ir25a				
	Ir40a	VP1?		Humidity and temperature	
	Ir93a	VP1?			
sacculus III					
	Ir8a				
	Ir21a?				
	Ir64a	DP1m	ad	strong acids	
arista					
	Ir21a	VP3?			
	Ir25a				

Table 1.1 (cont'd)

Neuron	Receptor(s)	Glomerulus	PN Class	Strongest ligand(s)	Behavior valence
palp basiconic sensilla					
pb1A	Or42a	VM7	ad	propyl acetate	
pb1B	Or71a	VC2	l	4-methylphenol	
pb2A	Or33c/ Or85e	VC1		(-) fenchone	
pb2B	Or46a	VA7l	ad	4-methylphenol	
pb3A	Or59c	l	ad		
pb3B	Or85d	VA4			

Chapter 2

Dysregulation of the sensory activity-regulated transcriptome in the brain with aging or HDAC6 knockout

Overview

Activated neurons rapidly induce expression of several immediate early genes (IEGs) or activity-regulated genes (ARGs) that are thought to mark them with long-term cellular changes, which are likely the hallmarks of memory. Surprisingly, ARGs induced by synthetic stimuli that were previously identified in *Drosophila* were found to be cell-type and stimulus-type specific (Chen et al. 2016a). To assess whether natural sensory stimuli can also induce ARGs, we stimulated *Drosophila* with odorants and light and identified ARGs induced in the adult brain. ARGs showed changes in abundance (up and down) in multiple waves across 10, 20, 30 and 45-minute time points. We found evidence that some of these ARGs, including a down-regulated one, could mark activated neural circuits and contribute to learning and memory. This raises an interesting question as to whether neuronal plasticity and learning is driven in part by the numerous ARGs. Since testing the contributions of these genes simultaneously is not tractable, we instead checked for alterations in patterns of ARG abundance in two conditions that are known to produce memory deficits: aged flies and flies lacking HDAC6. Most of the ARGs found in juvenile adult flies (4-5 days) were not properly modulated in middle-aged (10 days) or old (25 days) flies. Levels of most ARGs were also not modulated in brains of HDAC6 mutants, suggesting a possible mechanism of epigenetic regulation.

Introduction

Immediate early genes (IEGs) are a select group of genes whose expression can be rapidly induced by extracellular stimuli. This phenomenon of transcriptional modulation of specific genes in a rapid and transient manner is common to many cell types that must respond quickly to a changing external environment (Cochran, Reffel, and Stiles 1983; Almendral et al. 1988; Lau and Nathans 1985). Of particular interest is IEG induction in neurons in response to being activated (from here on referred to as activity-regulated genes, ARGs), which can lead to long-term changes at the level of the synapse (Brakeman et al. 1997; Nedivi et al. 1993). Such alterations in activated neurons and their synaptic structure and function are thought to underlie important cellular processes such as synaptic plasticity and long-term memory formation (Bailey et al. 1992; Abraham et al. 1993; Worley et al. 1993)

Many ARGs have been characterized in the nervous system of organisms ranging from *Aplysia* to mammals. Expression of these genes can be detected within minutes in active neurons, typically reaching a peak in mRNA expression levels around 30 minutes after stimulation (reviewed in (Clayton 2000)). ARG expression usually returns to basal levels within 180 minutes of activity (Morgan et al. 1987; Cullinan et al. 1995). The fast and short-lived nature of ARG expression has made these genes valuable tools for tracing neuronal circuits that are active within specific time windows (Barth 2004; French et al. 2001; Guthrie et al. 1993; Lin et al. 2011). These ARGs include transcription factors, such as *egr-1* and *c-fos* (Saffen et al. 1988*),* which are thought to control in turn the transcription of multiple target genes that lead to long-term neuronal changes. Other ARGs encode effector proteins, including *Arc* (activity-regulated cytoskeleton-associated protein) *(Lyford et al. 1995)*.

Most of the *Drosophila* homologs of canonical mammalian ARGs, however, do not appear to be specifically induced in active neurons (Chen et al. 2016a; Guan et al. 2005). In fact, the most comprehensive study of ARGs to date in the *Drosophila* model shows a high level of complexity such that ARG regulation differs depending on the type of activating stimulus as well as cell type (Chen et al. 2016a). Identification of ARG regulation in different contexts would thus offer the prospect of mapping neuronal circuits that give rise to specific behaviors in response to sensory input.

Results

Sensory stimulation leads to waves of ARGs in the brain

In order to identify changes in mRNA abundance in response to neural activation from a natural sensory stimulus, rather than pan-neuronal activation of all neurons, we isolated brains following light and odor stimulation (Figure 2.1). We sensory-deprived flies and then exposed them simultaneously to room lighting and a broadly-activating fruit odor blend. Transcriptome analyses revealed that gene expression changes in response to sensory stimulation began within 10 minutes of exposure (Figure 2.2). In total, we found 352 genes that were up-regulated at any time point relative to control (Fold change>2, FDR<0.05) (Figures 2.2, 2.3). We also found a smaller group of 48 ARGs whose mRNA shows reduced abundance following stimulation (Fold change<-2, FDR<0.05) (Figures 2.2, 2.3). Only 4 out of the 12 common ARGs found in the previous study (Chen et al. 2016a) were found to be significantly up-regulated in our data sets (FDR<0.05) (Figure 2.4).

We sorted the differentially expressed ARGs into 4 clusters based on their diverse temporal dynamics (Figure 2.5A-D). The up-regulated genes were further

divided into 3 clusters based on similarities in the direction and duration of gene expression changes. The first cluster, UP1, contains 72 genes that rose steadily across each time point, peaking at the last time point assayed (Figure 2.5A). We found two transcription factors, *Hr38* and *atonal*, in this group. GO-enrichment analysis revealed an enrichment for "alpha-amylase" activity, due to up-regulation of two amylase genes *Amy-p* and *Amy-d* (Figure 2.7A). In humans, alpha-amylase was recently found to be expressed in neuronal dendritic spines, astrocytes, and pericytes, and patients with Alzheimer's disease showed a reduction in alpha-amylase gene expression, but an up-regulation in protein and enzyme activity (Byman et al. 2018). In addition, an increase in salivary alpha-amylase indicates adrenergic activation and correlates with emotional memory recall in humans (Segal and Cahill 2009), suggesting the importance of amylase regulation for cognitive function. The second cluster, UP2, contains 104 genes whose expression rose sharply at 10 minutes and returned to baseline levels within 20 minutes of the start of exposure (Figure 2.5B). Two transcription factors were included in this quickly-induced group: the JAK-STAT-responsive *slbo* which is required for proper cell migration (Segal and Cahill 2009; Rørth, Szabo, and Texido 2000), and the zinc finger transcription factor CG30431. The UP2 group was enriched for the "serine-type carboxypeptidase activity", as well as several actin cytoskeleton-associated molecular function terms (Figure 2.7B). This suggests that many of the genes in the UP2 group are likely to play a role in protein modification and regulation of the cytoskeleton in the adult brain. Finally, cluster 3 (UP3) contains 186 genes that showed peaks at 10 and 30 minutes and did not return to baseline levels within the timeframe of these experiments (Figure 2.5C). This suite of genes was enriched for several metabolic processes as well as for genes involved in translation (Figure 2.7C). Taken together, the up-regulated

genes in our study carry out a broad range of molecular functions. Moreover, groups of genes with similar expression profiles appear to control specific sets of functions.

To begin to understand how these gene groups might be differentially-regulated, we compared upstream sequences (2 kb) of genes within each cluster. Interestingly, we found that unique sets of 7-mer oligos were enriched within upstream regions of genes within each cluster, suggesting that these motifs may be involved in the precise regulation of the distinct gene groups that increase in abundance following sensory stimulation (Figure 2.6). Further work will be required to assess the functionality of these sequence motifs (van Helden 2003).

Our results with the 352 up-regulated genes following both olfactory and visual stimulation provide a framework for understanding their roles in the central nervous system of *Drosophila*. We next sought to examine whether extant *Drosophila* mutants of these genes showed any defects in olfactory-based learning. We utilized a convenient larval behavioral assay to assess both habituation and appetitive associative learning (Khurana and Siddiqi 2013), and another assay to evaluate appetitive or aversive associative learning separately (Figure 2.8C-E). Following the initial screens, we performed additional trials for mutants that showed promising preliminary results, or were mutants for genes that showed large fold-changes in our RNA-seq studies. Of the 14 mutants of up-regulated genes tested for habituation/appetitive associative learning (Figure 2.8A, B), and the 13 mutants tested for appetitive associative learning (Figure 2.8C, D), none showed learning and memory defects in these assays (Figure 2.8D). Only the *Hsp70Ab* mutant showed a deficit in habituation/appetitive associative learning, but not in appetitive associative learning alone (Figure 2.8B, C). This could indicate that this gene is required for proper habituation to occur.

The small group of 37 genes whose expression levels were reduced following sensory stimulation belong to the fourth and final cluster (Figure 2.5D). Most of these were significantly reduced by 20 minutes and many did not rise to baseline levels within the 45-minute testing period. The promoter regions of these genes were also enriched for sequences distinct from Clusters 1-3, consistent with the idea that their expression levels are controlled by independent regulatory networks (Figure 2.6). To date, nothing is known of the role of down-regulation of genes immediately following sensory stimulation. While there are no enriched molecular functions associated with this DOWN group, we did find that this group is enriched for genes that are involved in defense responses to both biotic and abiotic stimuli (data not shown). Interestingly, a mutant for one down-regulated gene that belongs to the heat shock family of proteins, Hsp70Ba, showed deficits in all three learning paradigms (habituation/appetitive associative learning, appetitive associative learning, and aversive associative learning) (Figure 2.8B, D, E). The level of Hsp70Ba was significantly reduced within 10 minutes of stimulation. While the mechanism of rapid down-regulation is unclear, there is a known role for Hsp70 in learning: over-expression of this gene in the hippocampus reduces learning in mice (Ammon-Treiber et al. 2008). The preliminary data suggests that some genes that we identified in response to sensory stimulation are involved in proper learning and memory formation.

Aging flies have declining memory and changes in ARGs in the brain

Normal aging is known to result in deficits in learning and memory, as well as changes in regulation of certain transcription factors (de Magalhães, Curado, and Church 2009). We compared the activity-induced transcriptome changes in juvenile (4-5 day), middle-aged (10 day), and old (25 day) adult *Drosophila melanogaster* brains. We

focused on the 30-minute time point since most of the differentially expressed genes in 5-day-old flies were significantly different within this time. We compared the juvenile gene profiles at 30 minutes with middle-aged and old flies exposed to the same light and odor blend for 30 minutes. The transcriptomes of each group were compared with their age-matched unstimulated controls (Figure 2.9). As seen with juvenile flies, many more genes were up-regulated in middle-aged flies (217, Fold-change>2, FDR<0.05) than were down-regulated (50, Fold-change <-2, FDR <0.05) (Figure 2.10A). As with 2 of the up-regulated groups in juvenile flies, genes up-regulated in middle-aged flies were also enriched for molecular function GO-terms “amylase activity” and “serine hydrolase activity,” suggesting that increases in these enzymes may continue to play important roles in response to neuronal activity (Figure 2.11). By contrast, the “chitin-binding” family of genes that was up-regulated in juvenile flies was enriched in the down-regulated genes of middle-aged flies (Figure 2.11).

We found a nearly 50% reduction in the number of genes that were up-regulated in old fly brains (119, Fold-change>2, FDR<0.05), while the number of down-regulated genes remained in a similar range as in middle-aged flies with 57 (Fold-change<-2, FDR <0.05) (Figure 2.10B). Once again, we found that the amylase genes (*Amy-p* and *Amy-d*) were upregulated. In older flies, we found that “serine hydrolase”-associated genes were enriched in both the up- and down-regulated gene sets (Figure 2.11). The down-regulated genes were also enriched for “light-activated ion channel” and “opsin binding” go terms (Figure 2.11).

A comparison of the up-regulated genes revealed that a small but significant number of genes were shared among the different ages. The highest degree of overlap was between the up genes for middle-aged and old flies (19, Figure 2.13). In total, there

were only 4 genes shared between all 3 ages at 30 minutes: Amylase-proximal, Amylase-distal, Syntaxin 1A, and Tetraspanin 29Fb (Table 2.2). For the down-regulated genes, there was only significant overlap between middle-aged and old flies (data not shown). With this age-specific effect of ARG gene expression in response to odor and light, we next tracked the expression levels of the up-regulated genes in juveniles across all ages tested (Figure 2.12). We found that up-regulated genes in juveniles were expressed at higher levels in middle-aged flies in baseline samples, as well as in those exposed to the sensory stimuli. For old fly brains, we found that most genes returned to the relatively low levels found in juveniles in control samples, but failed to be induced following sensory stimulation. These data demonstrate that gene expression changes following exposure to sensory stimuli vary widely between juvenile flies and older flies, hinting at possible mechanisms of age-dependent declines in learning and memory.

Histone deacetylase 6 mutants with memory decline show ARG decline

Mammalian IEG regulation is known to depend on chromatin structure, including increased acetylation along with open chromatin that is permissive to transcription (Fowler, Sen, and Roy 2011). Furthermore, the promoter regions of ARGs previously characterized in flies are in a permissive state before stimulation (Fowler, Sen, and Roy 2011; Chen et al. 2016a). We next sought to examine a potential role for histone deacetylase proteins (HDACs) in the regulation of ARGs in the fly brain in response to sensory stimulation. Previous work in our lab has demonstrated that while HDAC6 is predominantly cytoplasmic, it can be found in the nucleus of some neurons (Perry et al. 2017). Additionally, we uncovered a role for HDAC6 in both larval and adult neurons for proper learning and memory formation and synaptic plasticity (Perry et al. 2017). To test the involvement of HDAC6 in ARG regulation, we performed the same light and odor

exposure experiments using HDAC6 knockout (KO) mutant flies along with their white-eyed wild-type genetic controls (Figure 2.14). Each test group was exposed for 10, 20, or 30 minutes; the brains from each condition were pooled into the stimulated group and compared to the unstimulated controls. We found that in white-eyed wild-type flies, 150 genes were up-regulated (Fold-change>2, FDR<0.05) and 37 genes were down-regulated (Fold-change<-2, FDR<0.05) (Figure 2.15A). The up-regulated genes were enriched for many functions, including the previously seen “chitin binding” and “serine hydrolase activity” functions (Figure 2.17). By comparison, far fewer genes were induced in the HDAC6 (KO) mutants (29, Fold-change>2, FDR<0.05) and 40 genes were significantly down-regulated (Fold-change<-2, FDR<0.05) (Figure 2.15A). Of the up-regulated genes, only 3 overlapped between the two genotypes and only one single gene was common to the down-regulated genes, though this overlap was significant (Figure 2.15B). The genes down-regulated in HDAC6 (KO) mutants were enriched for “cation symporter activity,” as well as “transmembrane transport” (Figure 2.16).

When we examined expression of the up-regulated genes in the white-eyed wild-type fly brains across all four groups, we observed that nearly all of them require HDAC6 expression. Our experiments reveal a role for HDAC6 in regulating proper ARG expression following sensory stimulation. Comparison of HDAC6 (KO) mutants versus wild-type baseline levels revealed that only 35 genes are significantly up-regulated and 31 genes are down-regulated (data not shown). This suggests that while HDAC6 is required for ARG induction, it is dispensable for maintaining global patterns of gene expression in the adult fly brain. Whether this requirement of HDAC for ARG regulation is direct via histone modification within the nucleus, or indirect via alteration of protein complexes that regulate gene expression, remains to be studied.

Discussion

A prior study identifying ARGs in the fly was done by artificially activating all neurons using a pan-neuronal driver and a variety of effectors; it revealed that the stimulation paradigm has a dramatic effect on the suite of genes expressed. It follows then, that the network of genes activated in response to natural stimuli may be different and merits investigation. We selected the visual system because of its large representation in the brain, as well as the olfactory system, given the ease of access to the antenna, the broad requirement of *Orco* to generate peripheral activity, and the vital role of olfactory conditioning in the field of learning and memory (Sullivan et al. 2015; Aqrabawi and Kim 2018).

Our central nervous system findings confirm those of Rosbash and colleagues (Chen et al. 2016b), that immediate gene expression is highly variable in the *Drosophila* nervous system, and the source of activity can have a strong impact on the altered patterns of gene expression. Using a physiological stimulus in wild-type flies, we reliably picked up increases in the expression of two previously-identified robust fly ARGs *Hr38* and *sr* in the brain. In comparison to these previously reported genes, we found others that are more strongly increased following sensory stimulation and thus become intriguing targets for further study (Table 2.1).

Tracking the expression of *Drosophila* ARGs as a proxy for active neuronal circuits would have tremendous value in an organism that, while more tractable than mammalian nervous systems (approximately 100,000 neurons in *Drosophila* as compared to roughly 4 million neurons in mice, for example), is still capable of sophisticated behaviors that are easily quantifiable in the lab. Our catalog of visual and olfactory stimulated ARGs offers a set of candidate genes to track within these sensory

systems for future studies examining functional circuits that give rise to specific behaviors. We identified 4 genes that are induced in both the peripheral and central nervous systems that are excellent candidates for olfactory-specific examination of ARGs. The aim of our experiments was to examine the effects of neuronal activity on global nervous system expression. The current study, however, cannot detangle the contributions of neuronal populations from glia and other cell types in the peripheral and central tissues that were assayed.

Our screen to identify potential roles for these ARGs in larval learning and memory pointed to 2 members of the heat-shock protein family. Work on *Hsp70* in mice has revealed that increased levels of this gene in the hippocampus are associated with a defect in learning and memory (Ammon-Treiber et al. 2008). Consistent with this finding, Hsp70Ba was identified in our screen as a down-regulated gene in juvenile flies, and Hsp70Ab was aberrantly up-regulated in aged flies that are known to have learning and memory defects.

For the down-regulated genes in our study, there are several possible mechanisms by which transcript abundance could be reduced, including targeted mRNA degradation or increased translation leading to negative feedback and down-regulation of the gene's expression. For the up-regulated genes, we were unable to identify a role for learning and memory in the larval stage. This does not, however, rule out a role in adult learning and memory processes. Recent work has identified a need for increased expression of CREB and c-Fos in select cells of the mushroom body to regulate memory-associated behaviors that is seen after 5 or more training sessions (Miyashita et al. 2018). Consistent with these findings, we do not see any increase in abundance of

these transcripts in our study. Additionally, we note that our study is limited to the identification of activity markers and not tailored to associative learning markers.

Our findings that proper regulation of most 5-day ARGs is lost at 30 minutes in older flies is indicative of a pronounced effect of age on ARG expression following sensory stimulation. We found elevated levels of juvenile ARG expression in both control and stimulated groups of middle-aged fly brains. In older flies, relative expression of these ARGs was still slightly elevated, though not as high as that in middle-aged flies. Nevertheless, induction following sensory stimulation was not observed. The observed increase in baseline expression of ARGs in older flies is in contrast to the age-dependent decline in expression revealed in neurons of aging *Drosophila* via single cell RNA-seq (Davie et al. 2018). It remains to be studied whether the increase in juvenile ARGs without sensory stimulation is due to a general decline in mRNA levels in older flies, leading to relatively higher representation in RNA-seq analyses, or if there are age-specific mechanisms of increased transcription of these genes, or both. Nonetheless, our study provides a foundation to understand whether the loss of induction of particular 5-day ARGs in older flies is responsible for memory decline and to understand whether, and is so how, increase of new ARGs in older flies may be involved in age-dependent declines in learning and memory performance (Figure 2.18).

Finally, our study uncovers a novel role for the highly-conserved HDAC6 in the *Drosophila* adult nervous system (Figure 2.18). HDAC6 is involved in many diverse cellular functions, undoubtedly due to its ability to acetylate many non-histone targets (Hubbert et al. 2002; Kovacs et al. 2005; Miskiewicz et al. 2014; Zhang et al. 2007), and to bind ubiquitin and other protein complexes (Valenzuela-Fernández et al. 2008). The complexity of HDAC6 function in cells and its role in *Drosophila* learning and memory in

both larvae and adults make it an intriguing target in our ARG study. Expression of ARGs in juvenile flies depends on the presence of HDAC6. We found substantial differences in baseline gene expression in the brains of HDAC6 (KO) mutants as compared to wild-type counterparts. This is indicative of a broad role in nervous system gene regulation. Our findings invite further experiments to understand the precise mechanisms by which HDAC6 exerts its effect on both ARG expression and global nervous system gene expression.

Materials and Methods

Drosophila Stocks and Manipulations

Fly stocks were maintained on conventional cornmeal fly food under a 12 hr light:12 hr dark cycle at 25°C with 50% humidity. The OreR strain was used as wild-type control for sequencing experiments unless otherwise indicated. For the HDAC6 experiments, *w1118* backcrossed 5 times to *Canton-S* (*wCS*) was used as the white-eyed wild-type control and compared to *HDAC6(KO)* mutants (Bloomington 51182) that were backcrossed to *wCS* for 6 generations. For larval learning assays, control strains were *wCS*, *Canton-S* (CS), or *w1118*.

Sensory deprivation, stimulation, and dissection.

Small groups of 6 mated male flies were placed into vials containing a wet Kimwipe and housed overnight without food for 13-16 hours in dark temperature/humidity-controlled chambers. Flies were anesthetized and sorted using CO_2 at least 24 hours prior to placement into these sensory deprivation chambers. The following morning at 4-5 days-old, the flies were simultaneously exposed to ambient white light, 100 µl hexyl alcohol (1-hexanol, CAS 111-27-3), and 100 µl isobutyl acetate (CAS 110-19-0; odors diluted separately to 10^{-2} in paraffin oil) for 10, 20, 30, or 45 min.

All treatments and experiments were performed at room temperature. Odorants were chosen based on strong electrophysiological responses from a variety of antennal odorant receptors in *Drosophila* (Hallem et al., 2006), and light was used due to the large representation of the visual cortex in the fly brain. At the appropriate time points, flies were quickly anesthetized with CO_2 and stored on ice for no more than 10 min until dissection. The control condition consisted of flies that were immediately anesthetized and dissected following 13-16 hours of deprivation.

For experiments with 5, 10, and 25-day-old flies, 16 brains were pooled per condition tested. For brain experiments with wCS and HDAC(KO) flies, 15 brains were pooled per condition, with the stimulated group composed of 5 brains from each of the 10, 20, and 30 minute exposures. All samples were stored at -80°C until processing. N=2 (biological replicates) for all experiments except all 5-day old brain experiments, where N=3.

RNA isolation and preparation for transcriptome analysis

Tissues were mechanically crushed with disposable RNAse-free plastic pestles, and total RNA was isolated using a Trizol-based protocol. cDNA libraries were prepared from total RNA using the Illumina TruSeq RNA Sample Preparation Kit (v2) and 50 and 75 bps single-end sequencing was done using the HighSeq2000 and NextSeq500 platforms, respectively. There were an average of 53.7 million reads / replicate, with an average of 81% mapped.

Bioinformatic analysis of RNA-seq experiments

Reads were aligned to the latest release of the *Drosophila melanogaster* genome (dm6)) and quantified with kallisto (Version: kallisto 0.43.1) (Bray et al. 2016). Only libraries for which we obtained >75 % alignment were used for downstream analysis.

Transcript counts were summarized to gene-level using tximport package (version 1.4.0) (Soneson, Love, and Robinson 2015). For any instances of detected batch effects, we removed unwanted variation using RuvR in the RuvSeq package (version_1.10.0) (Risso et al. 2014). Differentially expressed gene (DEG) analysis was performed with the edgeR package (version 3.18.1) (Robinson, McCarthy, and Smyth 2010), using low count filtering (cpm >0.5) and TMM normalization. Clusters were generated using the MFuzz package (v.2.38.0) in R (Futschik and Carlisle 2005). GO-enrichment analysis was performed with GOrilla, using expressed genes as the background (Eden et al. 2009).

Larval learning assays

The "appetitive associative learning assay" was performed as in (Gerber, Biernacki, and Thum 2013) using pentyl acetate (CAS 628-63-7) diluted 1:50 in paraffin oil, and undiluted 1-octanol (CAS 111-87-5). For each training session, 2 caps from 200 ul microcentrifuge tubes were filled with 50 ul odorant each, and placed on opposite sides of the dish. The "habituation/appetitive associative learning assay" was a modification of the Gerber protocol using odorants identified in (Kreher et al. 2008), where trans-2-hexenal (E2-hexenal, CAS 6728-26-3) at 10^{-2} dilution in paraffin oil, but not 10^{-4} dilution, activated a variety of odorant receptors and elicited an attractive behavioral response. 25 ul of the appropriate odorant was applied to each of 2 Whatman filter paper squares (1" x 1") that were adhered to the inner lid of the training dish. The "aversive associative learning assay" was performed following the Gerber protocol, except that sucrose in the training dishes was replaced by an aversive concentration of NaCl (4M), and the testing agarose dish also contained 4M NaCl.

Training and tests were performed during the lights-on period under rearing conditions (above). All stocks were homozygous mutants unless otherwise noted. Third-instar feeding stage larvae (aged 5 days after eggs were laid) were extracted from their food using 15% sucrose and rinsed several times with water, then trained immediately for the associative learning assay, or starved in a humidified chamber for 2 hours prior to the habituation/associative learning training. 50-100 larvae were placed into a 10 cm Petri dish containing agarose and the first odorant, and the dish was placed under a dark box for a 3 minute exposure (associative learning assay) or a 5 minute exposure (habituation/associative learning assay). Larvae were then transferred using a damp paintbrush into another 10 cm Petri dish containing agarose with 2 M sucrose and the second odorant, and exposed under a dark box for 3 or 5 minutes. Training sessions were alternated such that larvae were exposed to a total of 3 agarose/1st odorant dishes and 3 sucrose/2nd odorant dishes, followed immediately by a final test in which each odorant was presented on opposite sides of an agarose dish, and larvae could move freely about the dish for 5 minutes. Larvae on each ½ of the dish were then counted, and the Learning Index or Preference Change was calculated.

For the associative learning assay, larvae were reciprocally trained such that one group was trained to pentyl acetate paired with sucrose, and another group was trained to 1-octanol paired with sucrose. The Preference Index (PI) was: (# larvae side 1) – (# larvae side 2) ÷ (total # larvae in the assay). The Learning Index was: Average of (PI trained to 1-octanol) and (PI trained to pentyl acetate).

For the habituation/associative learning assay, the Preference Index (PI) was calculated as above. The Preference Change was (Trained PI for E2-hexenal, 10^{-4}) – (Naive PI for E2-hexenal, 10^{-4}).

References

Abraham, W. C., S. E. Mason, J. Demmer, J. M. Williams, C. L. Richardson, W. P. Tate, P. A. Lawlor, and M. Dragunow. 1993. “Correlations between Immediate Early Gene Induction and the Persistence of Long-Term Potentiation.” *Neuroscience* 56 (3): 717–27.

Almendral, J. M., D. Sommer, H. Macdonald-Bravo, J. Burckhardt, J. Perera, and R. Bravo. 1988. “Complexity of the Early Genetic Response to Growth Factors in Mouse Fibroblasts.” *Molecular and Cellular Biology* 8 (5): 2140–48.

Ammon-Treiber, Susanne, Gisela Grecksch, Charalampos Angelidis, Patra Vezyraki, Volker Höllt, and Axel Becker. 2008. “Emotional and Learning Behaviour in Mice Overexpressing Heat Shock Protein 70.” *Neurobiology of Learning and Memory* 90 (2): 358–64.

Aqrabawi, Afif J., and Jun Chul Kim. 2018. “Hippocampal Projections to the Anterior Olfactory Nucleus Differentially Convey Spatiotemporal Information during Episodic Odour Memory.” *Nature Communications* 9 (1): 2735.

Bailey, C. H., P. Montarolo, M. Chen, E. R. Kandel, and S. Schacher. 1992. “Inhibitors of Protein and RNA Synthesis Block Structural Changes That Accompany Long-Term Heterosynaptic Plasticity in Aplysia.” *Neuron* 9 (4): 749–58.

Barth, A. L. 2004. “Alteration of Neuronal Firing Properties after In Vivo Experience in a FosGFP Transgenic Mouse.” *Journal of Neuroscience* 24 (29): 6466–75.

Brakeman, P. R., A. A. Lanahan, Richard O’Brien, K. Roche, C. A. Barnes, R. L. Huganir, and P. F. Worley. 1997. “Homer: A Protein That Selectively Binds Metabotropic Glutamate Receptors.” *Nature* 386 (6622): 284–88.

Bray, Nicolas L., Harold Pimentel, Páll Melsted, and Lior Pachter. 2016. “Erratum: Near-Optimal Probabilistic RNA-Seq Quantification.” *Nature Biotechnology* 34 (8): 888.

Byman, Elin, Nina Schultz, Netherlands Brain Bank, Malin Fex, and Malin Wennström. 2018. “Brain Alpha-Amylase: A Novel Energy Regulator Important in Alzheimer Disease?” *Brain Pathology* , February. https://doi.org/10.1111/bpa.12597.

Chen, Xiao, Reazur Rahman, Fang Guo, and Michael Rosbash. 2016a. “Genome-Wide Identification of Neuronal Activity-Regulated Genes in.” *eLife* 5 (December). https://doi.org/10.7554/eLife.19942.

Clayton, David F. 2000. “The Genomic Action Potential.” *Neurobiology of Learning and Memory* 74 (3): 185–216.

Cochran, Brent H., Angela C. Reffel, and Charles D. Stiles. 1983. “Molecular Cloning of Gene Sequences Regulated by Platelet-Derived Growth Factor.” *Cell* 33 (3): 939–47.

Cullinan, W. E., J. P. Herman, D. F. Battaglia, H. Akil, and S. J. Watson. 1995. “Pattern and Time Course of Immediate Early Gene Expression in Rat Brain Following Acute Stress.” *Neuroscience* 64 (2): 477–505.

Davie, Kristofer, Jasper Janssens, Duygu Koldere, Maxime De Waegeneer, Uli Pech, Łukasz Kreft, Sara Aibar, et al. 2018. “A Single-Cell Transcriptome Atlas of the Aging Drosophila Brain.” *Cell* 174 (4): 982–98.e20.

Eden, Eran, Roy Navon, Israel Steinfeld, Doron Lipson, and Zohar Yakhini. 2009. “GOrilla: A Tool for Discovery and Visualization of Enriched GO Terms in Ranked Gene Lists.” *BMC Bioinformatics* 10 (February): 48.

Fowler, Trent, Ranjan Sen, and Ananda L. Roy. 2011. “Regulation of Primary Response Genes.” *Molecular Cell* 44 (3): 348–60.

French, P. J., V. O’Connor, M. W. Jones, S. Davis, M. L. Errington, K. Voss, B. Truchet, et al. 2001. “Subfield-Specific Immediate Early Gene Expression Associated with Hippocampal Long-Term Potentiation in Vivo.” *The European Journal of Neuroscience* 13 (5): 968–76.

Futschik, Matthias E., and Bronwyn Carlisle. 2005. “Noise-Robust Soft Clustering of Gene Expression Time-Course Data.” *Journal of Bioinformatics and Computational Biology* 3 (4): 965–88.

Gerber, Bertram, Roland Biernacki, and Jeannette Thum. 2013. “Odor-Taste Learning Assays in Drosophila Larvae.” *Cold Spring Harbor Protocols* 2013 (3). https://doi.org/10.1101/pdb.prot071639.

Guan, Zhuo, Sudipta Saraswati, Bill Adolfsen, and J. Troy Littleton. 2005. “Genome-Wide Transcriptional Changes Associated with Enhanced Activity in the Drosophila Nervous System.” *Neuron* 48 (1): 91–107.

Guthrie, K. M., A. J. Anderson, M. Leon, and C. Gall. 1993. “Odor-Induced Increases in c-Fos mRNA Expression Reveal an Anatomical ‘Unit’ for Odor Processing in Olfactory Bulb.” *Proceedings of the National Academy of Sciences of the United States of America* 90 (8): 3329–33.

Hallem, Elissa A., and John R. Carlson. 2006. “Coding of Odors by a Receptor Repertoire.” *Cell* 125 (1): 143–60.

Helden, J. van. 2003. “Regulatory Sequence Analysis Tools.” *Nucleic Acids Research* 31 (13): 3593–96.

Hubbert, Charlotte, Amaris Guardiola, Rong Shao, Yoshiharu Kawaguchi, Akihiro Ito, Andrew Nixon, Minoru Yoshida, Xiao-Fan Wang, and Tso-Pang Yao. 2002. “HDAC6 Is a Microtubule-Associated Deacetylase.” *Nature* 417 (6887): 455–58.

Khurana, Sukant, and Obaid Siddiqi. 2013. “Olfactory Responses of Drosophila Larvae.”

Chemical Senses 38 (4): 315–23.

Kovacs, Jeffrey J., Patrick J. M. Murphy, Stéphanie Gaillard, Xuan Zhao, June-Tai Wu, Christopher V. Nicchitta, Minoru Yoshida, David O. Toft, William B. Pratt, and Tso-Pang Yao. 2005. "HDAC6 Regulates Hsp90 Acetylation and Chaperone-Dependent Activation of Glucocorticoid Receptor." *Molecular Cell* 18 (5): 601–7.

Kreher, Scott A., Dennis Mathew, Junhyong Kim, and John R. Carlson. 2008. "Translation of Sensory Input into Behavioral Output via an Olfactory System." *Neuron* 59 (1): 110–24.

Lau, L. F., and D. Nathans. 1985. "Identification of a Set of Genes Expressed during the G0/G1 Transition of Cultured Mouse Cells." *The EMBO Journal* 4 (12): 3145–51.

Lin, Dayu, Maureen P. Boyle, Piotr Dollar, Hyosang Lee, E. S. Lein, Pietro Perona, and David J. Anderson. 2011. "Functional Identification of an Aggression Locus in the Mouse Hypothalamus." *Nature* 470 (7333): 221–26.

Lyford, G. L., K. Yamagata, W. E. Kaufmann, C. A. Barnes, L. K. Sanders, N. G. Copeland, D. J. Gilbert, N. A. Jenkins, A. A. Lanahan, and P. F. Worley. 1995. "Arc, a Growth Factor and Activity-Regulated Gene, Encodes a Novel Cytoskeleton-Associated Protein That Is Enriched in Neuronal Dendrites." *Neuron* 14 (2): 433–45.

Magalhães, João Pedro de, João Curado, and George M. Church. 2009. "Meta-Analysis of Age-Related Gene Expression Profiles Identifies Common Signatures of Aging." *Bioinformatics* 25 (7): 875–81.

Miskiewicz, Katarzyna, Liya E. Jose, Wondwossen M. Yeshaw, Jorge S. Valadas, Jef Swerts, Sebastian Munck, Fabian Feiguin, Bart Dermaut, and Patrik Verstreken. 2014. "HDAC6 Is a Bruchpilot Deacetylase That Facilitates Neurotransmitter Release." *Cell Reports* 8 (1): 94–102.

Miyashita, Tomoyuki, Emi Kikuchi, Junjiro Horiuchi, and Minoru Saitoe. 2018. "Long-Term Memory Engram Cells Are Established by c-Fos/CREB Transcriptional Cycling." *Cell Reports* 25 (10): 2716–28.e3.

Morgan, J. I., D. R. Cohen, J. L. Hempstead, and T. Curran. 1987. "Mapping Patterns of c-Fos Expression in the Central Nervous System after Seizure." *Science* 237 (4811): 192–97.

Nedivi, E., D. Hevroni, D. Naot, D. Israeli, and Y. Citri. 1993. "Numerous Candidate Plasticity-Related Genes Revealed by Differential cDNA Cloning." *Nature* 363 (6431): 718–22.

Perry, Sarah, Beril Kiragasi, Dion Dickman, and Anandasankar Ray. 2017. "The Role of Histone Deacetylase 6 in Synaptic Plasticity and Memory." *Cell Reports* 18 (6): 1337–45.

Risso, Davide, John Ngai, Terence P. Speed, and Sandrine Dudoit. 2014.

"Normalization of RNA-Seq Data Using Factor Analysis of Control Genes or Samples." *Nature Biotechnology* 32 (9): 896–902.

Robinson, Mark D., Davis J. McCarthy, and Gordon K. Smyth. 2010. "edgeR: A Bioconductor Package for Differential Expression Analysis of Digital Gene Expression Data." *Bioinformatics* 26 (1): 139–40.

Rørth, P., K. Szabo, and G. Texido. 2000. "The Level of C/EBP Protein Is Critical for Cell Migration during Drosophila Oogenesis and Is Tightly Controlled by Regulated Degradation." *Molecular Cell* 6 (1): 23–30.

Saffen, D. W., A. J. Cole, P. F. Worley, B. A. Christy, K. Ryder, and J. M. Baraban. 1988. "Convulsant-Induced Increase in Transcription Factor Messenger RNAs in Rat Brain." *Proceedings of the National Academy of Sciences of the United States of America* 85 (20): 7795–99.

Segal, Sabrina K., and Larry Cahill. 2009. "Endogenous Noradrenergic Activation and Memory for Emotional Material in Men and Women." *Psychoneuroendocrinology* 34 (9): 1263–71.

Soneson, Charlotte, Michael I. Love, and Mark D. Robinson. 2015. "Differential Analyses for RNA-Seq: Transcript-Level Estimates Improve Gene-Level Inferences." *F1000Research* 4: 1521.

Sullivan, Regina M., Donald A. Wilson, Nadine Ravel, and Anne-Marie Mouly. 2015. "Olfactory Memory Networks: From Emotional Learning to Social Behaviors." *Frontiers in Behavioral Neuroscience* 9 (February): 36.

Valenzuela-Fernández, Agustín, J. Román Cabrero, Juan M. Serrador, and Francisco Sánchez-Madrid. 2008. "HDAC6: A Key Regulator of Cytoskeleton, Cell Migration and Cell-Cell Interactions." *Trends in Cell Biology* 18 (6): 291–97.

Worley, P. F., R. V. Bhat, J. M. Baraban, C. A. Erickson, B. L. McNaughton, and C. A. Barnes. 1993. "Thresholds for Synaptic Activation of Transcription Factors in Hippocampus: Correlation with Long-Term Enhancement." *The Journal of Neuroscience: The Official Journal of the Society for Neuroscience* 13 (11): 4776–86.

Zhang, Xiaohong, Zhigang Yuan, Yingtao Zhang, Sarah Yong, Alexis Salas-Burgos, John Koomen, Nancy Olashaw, et al. 2007. "HDAC6 Modulates Cell Motility by Altering the Acetylation Level of Cortactin." *Molecular Cell* 27 (2): 197–213.

Figure 2.1 Experiment design to capture ARG expression

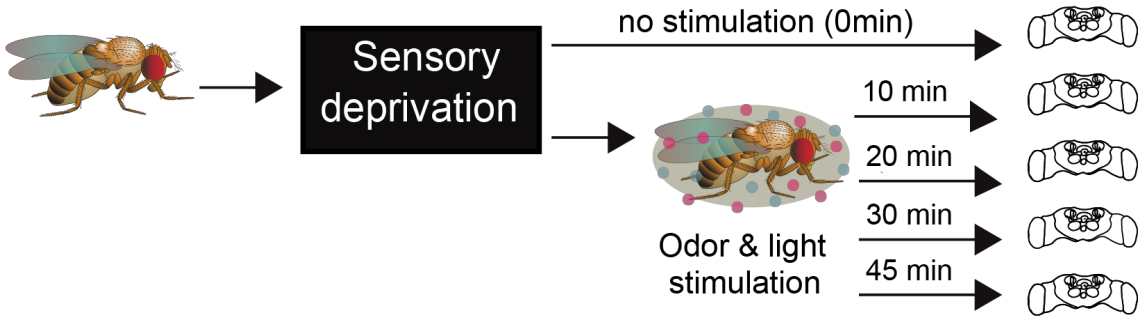

Figure 2.1 Experiment design to capture ARG expression
Stimulation paradigm for brain transcriptome analysis in 5-day-old wild-type flies

Figure 2.2 Differentially expressed genes in the 5-day-old brain following stimulation

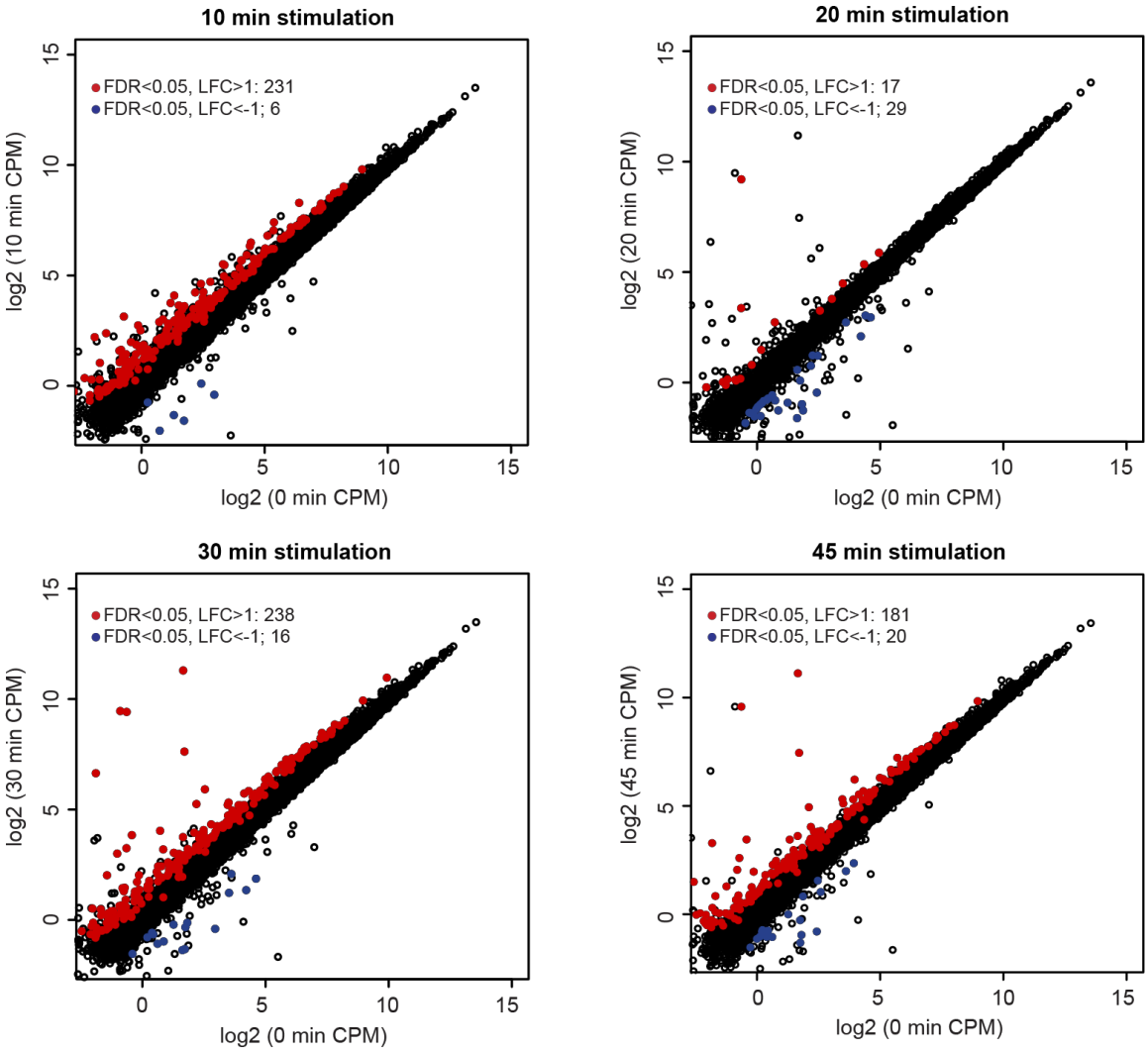

Figure 2.2 Differentially expressed genes in the 5-day-old brain following stimulation

Plots highlighting up- and down-regulated genes at the indicated time point. Red and blue dots represent up-regulated genes (Fold-change>2, FDR<0.05) and down-regulated genes (Fold-change<-2, FDR< 0.05), respectively.

Figure 2.3 A time series of ARG expression in the 5-day-old brain

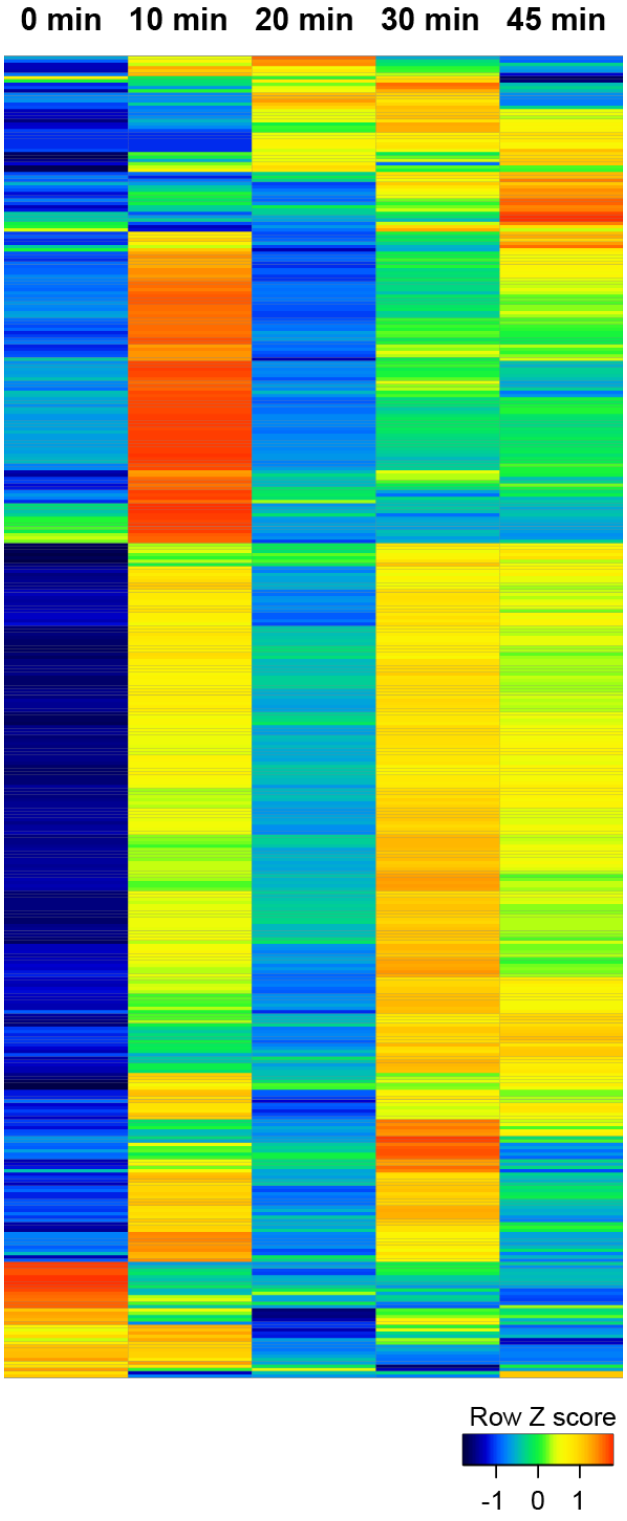

Figure 2.3 A time series of ARG expression in the 5-day-old brain

Heatmap following expression of all 399 differentially-expressed genes in the brain. Each column represents the expression of one gene, normalized across time points (red=high expression, blue=low expression).

Figure 2.4 Comparison of expression levels of previously identified ARGS

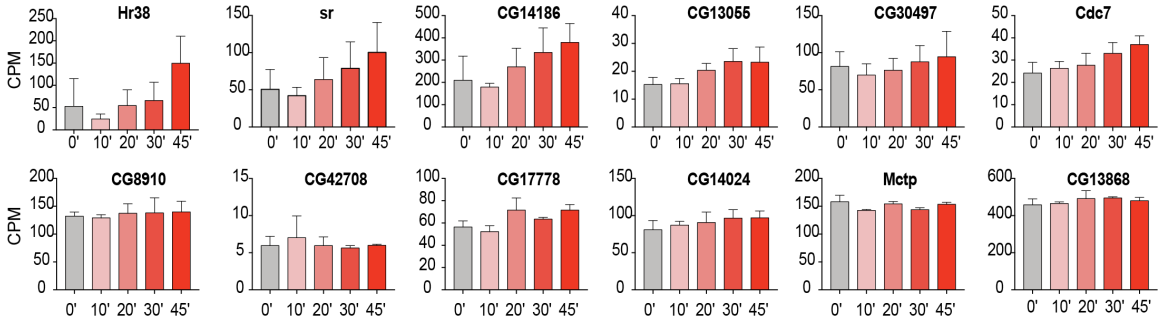

Figure 2.4 Comparison of expression levels of previously identified ARGS

Bar graphs showing normalized expression levels (in counts per million, CPM) for the common 12 ARGs identified in Chen et al., 2016.

Figure 2.5 ARGs can be divided into 4 different groups based on expression patterns

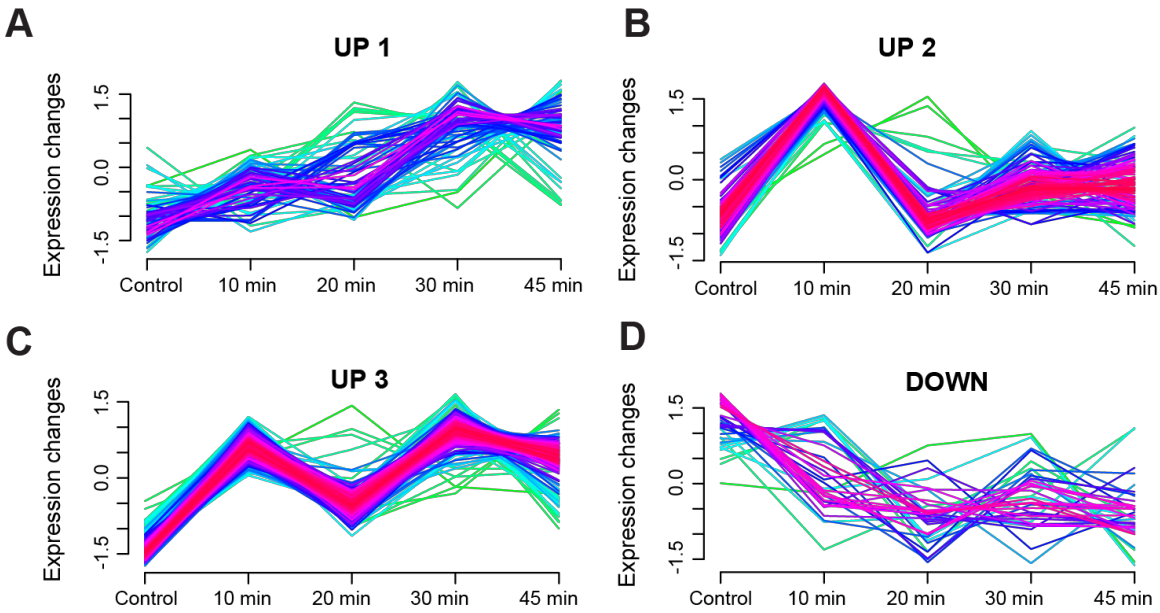

Figure 2.5 ARGs can be divided into 4 different groups based on expression patterns

(A) Cluster UP1 gene membership expression across each time point.

(B) Cluster UP2 gene membership expression across each time point.

(C) Cluster UP3 gene membership expression across each time point.

(D) Cluster DOWN1 gene membership expression across each time point.

For all cluster graphs: genes with low membership value are marked yellow/green and genes with high membership value are marked with red/ purple lines.

Figure 2.6 Each cluster has unique sequences enriched upstream of their transcription start site

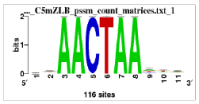

Sequence	Observed	Expected	P-value
atacgatg|catcgtat	9	1.4	1.7 x 10^{-5}
tcgccaa|ttggcga	25	10.13	5.6 x 10^{-5}
aactaa|ttagtt	111	72.83	1.9 x 10^{-5}

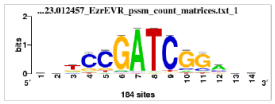

Sequence	Observed	Expected	P-value
ccgatcgc|gcgatcgg	15	3.31	6.5 x 10^{-8}
ccgatcg|cgatcgg	32	10.45	1.6 x 10^{-6}
ccgatc|gatcgg	97	45.18	1.5 x 10^{-11}

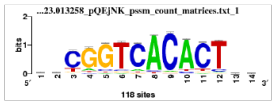

Sequence	Observed	Expected	P-value
agtgtgac|gtcacact	25	7.28	2.2x 10^{-7}
agcactg|cagtgct	48	20.67	2.0 x 10^{-7}
ggtcac|gtgacc	84	45.83	2.8 x 10^{-7}

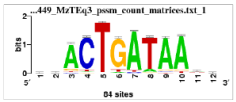

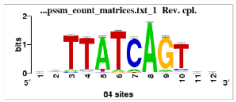

Sequence	Observed	Expected	P-value
ctgataa|ttatcag	34	12.55	4.2 x 10^{-7}
cttatca|tgataag	32	13.49	1.3 x 10^{-5}
ccataac|gttatgg	19	6.57	5.8 x 10^{-5}

Figure 2.6 Each cluster has unique sequences enriched upstream of their transcription start site

Table of over-represented 7-mer oligos found 2 kb upstream of the transcription start site (TSS) of genes indicated clusters.

Figure 2.7 Characterization of the ARGs in the 5-day-old brain

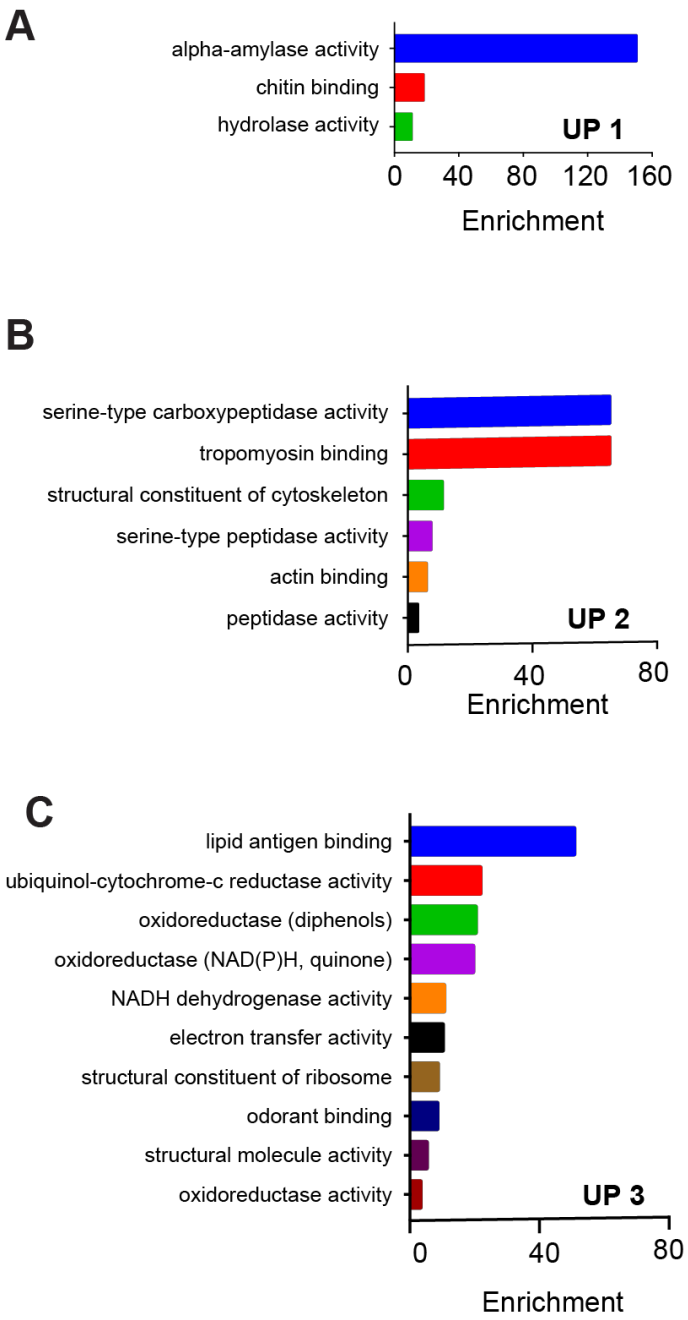

Figure 2.7 Characterization of the ARGs in the 5-day-old brain

(A) Bar graph showing fold-enrichment for molecular function GO terms in cluster UP1 compared to all genes expressed in the 5-day brain RNA-seq experiments ($p<0.05$).

(B) Bar graph showing fold-enrichment for molecular function GO terms in cluster UP2 compared to all genes expressed in the 5-day brain RNA-seq experiments ($p<0.05$).

(C) Bar graph showing fold-enrichment for molecular function GO terms in cluster UP3 compared to all genes expressed in the 5-day brain RNA-seq experiments ($p<0.05$).

Figure 2.8 Learning defects in mutants of ARGs

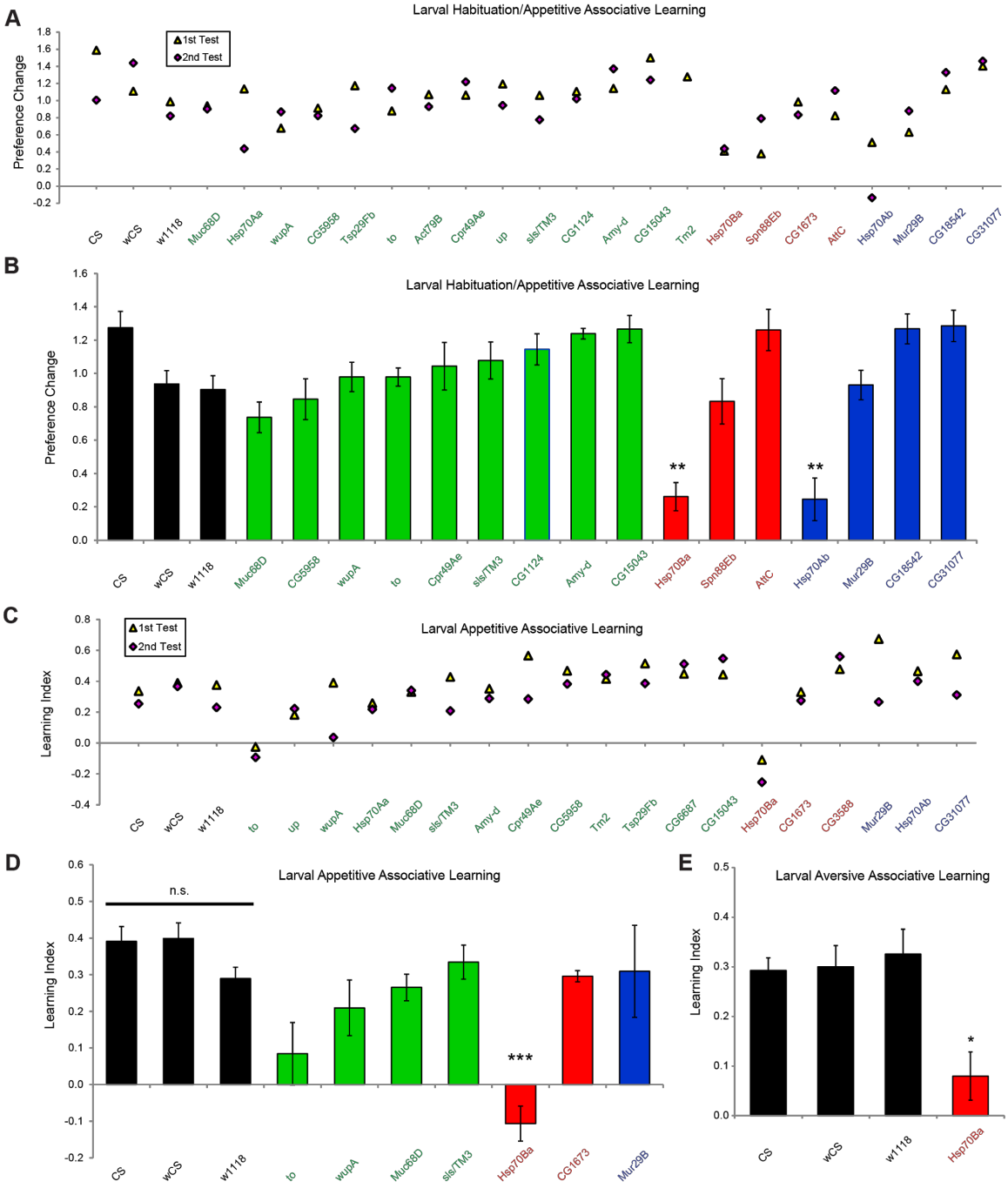

Figure 2.8 Learning defects in mutants of ARGs

(A) Preference change for each test performed (n=1-2) in the larval habituation/appetitive associative learning screen.

(B) Average preference change and SEM for several mutants that were chosen for further testing (n=4-10). **, $p<0.01$ using two-tailed Student's t-test (compared to the appropriate control, w1118). Black font or bars, control flies; green font or bars, up-regulated genes (5-day-old flies); red font or bars, down-regulated genes (5-day-old flies); blue font or bars, genes changing only in the aged (10 or 25-day-old) flies.

(C) Learning index for each test performed (n=2) in the larval appetitive associative learning screen.

(D) Average learning index and SEM for several mutants that were chosen for further testing (n=4-6). n.s, not significantly different; ***, $p<0.001$ using two-tailed Student's t-test (compared to w1118).

(E) Learning index for the Hsp70Ba mutant in the aversive associative learning test. *, $p<0.05$ using two-tailed Student's t-test (compared to w1118).

Figure 2.9 Identification of ARG expression following 30 minutes of sensory stimulation in the aging brain

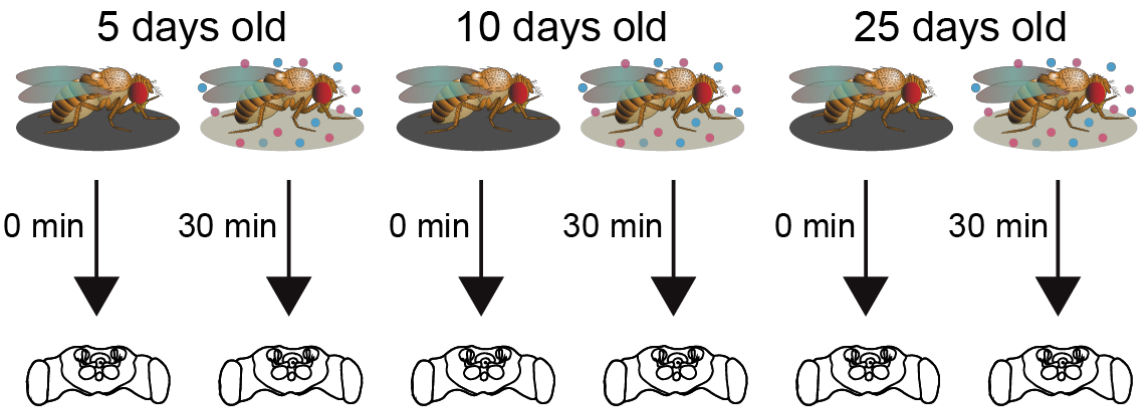

Figure 2.9 Identification of ARG expression following 30 minutes of sensory stimulation in the aging brain

Stimulation paradigm for brain transcriptome analysis in 5, 10, and 25-day-old wild-type flies.

Figure 2.10 ARGs are expressed within 30 minutes of sensory stimulation in aging brains

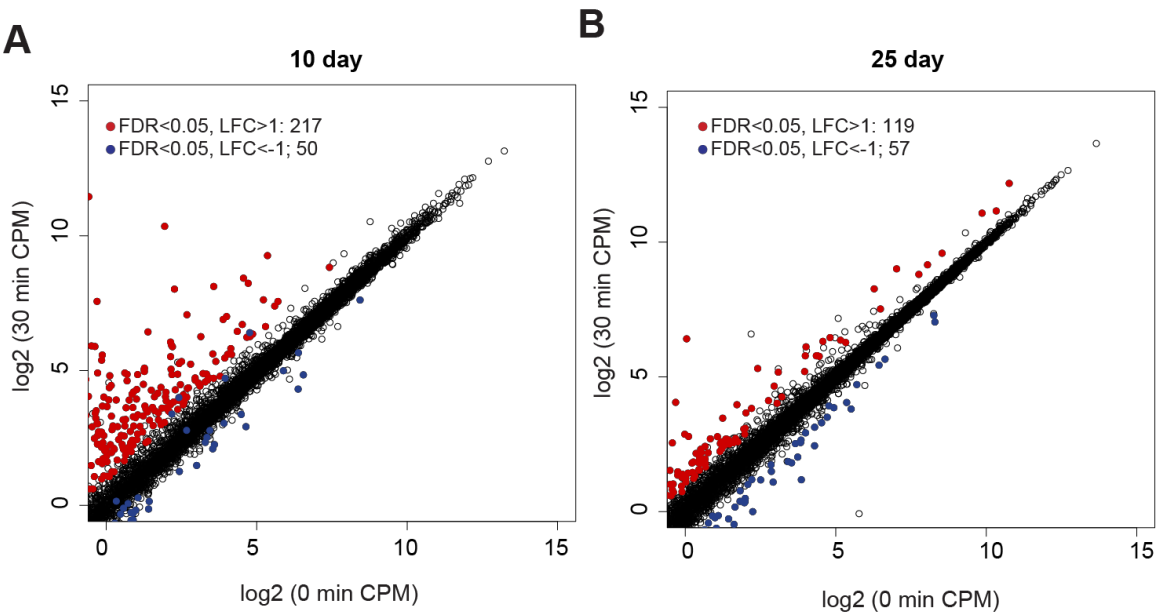

Figure 2.10 ARGs are expressed within 30 minutes of sensory stimulation in aging brains

(A) Plot highlighting up- and down-regulated genes at 30 minutes in 10-day old fly brains. Red and blue dots represent up-regulated genes (Fold-change>2, FDR<0.05) and down-regulated genes (Fold-change<-2, FDR< 0.05), respectively.

(B) Plot highlighting up- and down-regulated genes at 30 minutes in 25-day-old fly brains. Red and blue dots represent up-regulated genes (Fold-change>2, FDR<0.05) and down-regulated genes (Fold-change<-2, FDR< 0.05), respectively.

Figure 2.11 Characterization of ARGs in the aging brain

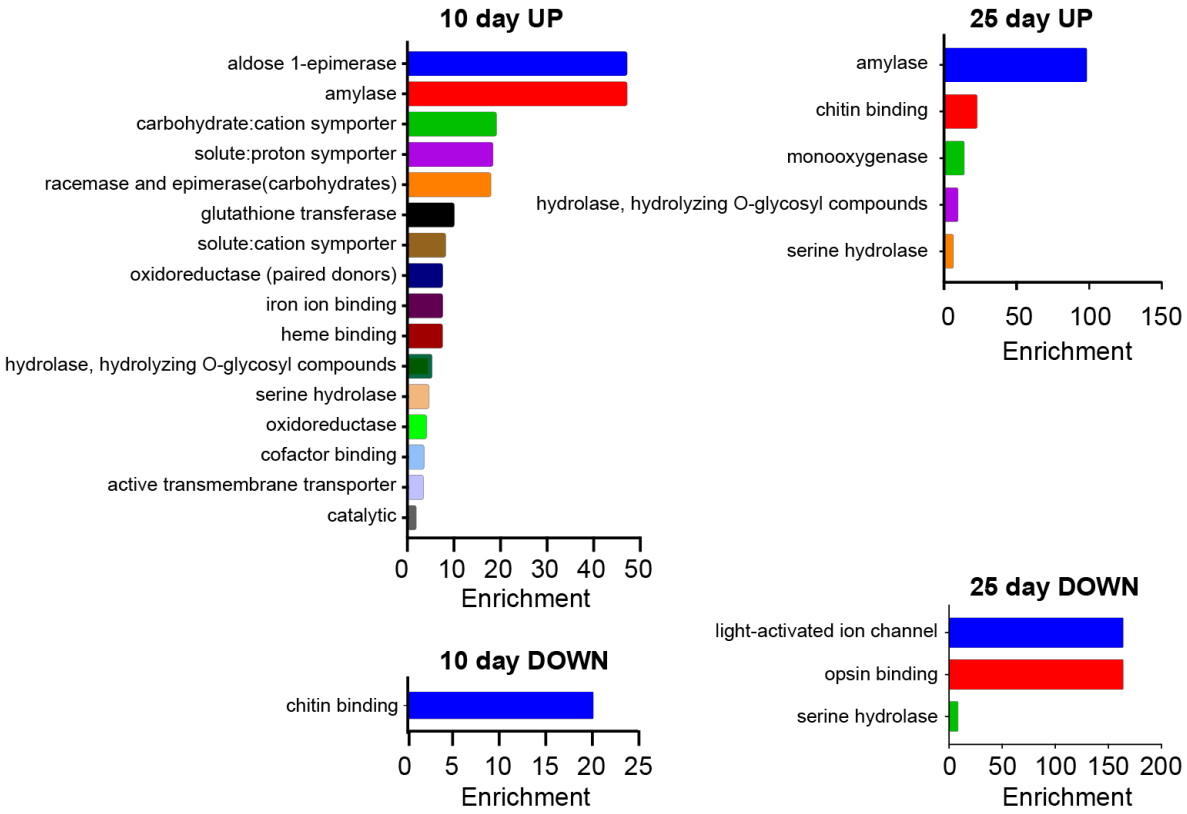

Figure 2.11 Characterization of ARGs in the aging brain

(D) Bar graph showing fold-enrichment for molecular function GO terms for ARGs in 10-day-old brains compared to all genes expressed in the 10-day-old brain RNA-seq experiments ($p<0.05$) (left) and ARGs in 25-day-old brain compared to all genes expressed in the 25-day-old brain RNA-seq experiments ($p<0.05$) (right).

Figure 2.12 Most ARGs in the 5-day-old brain are misexpressed in older flies

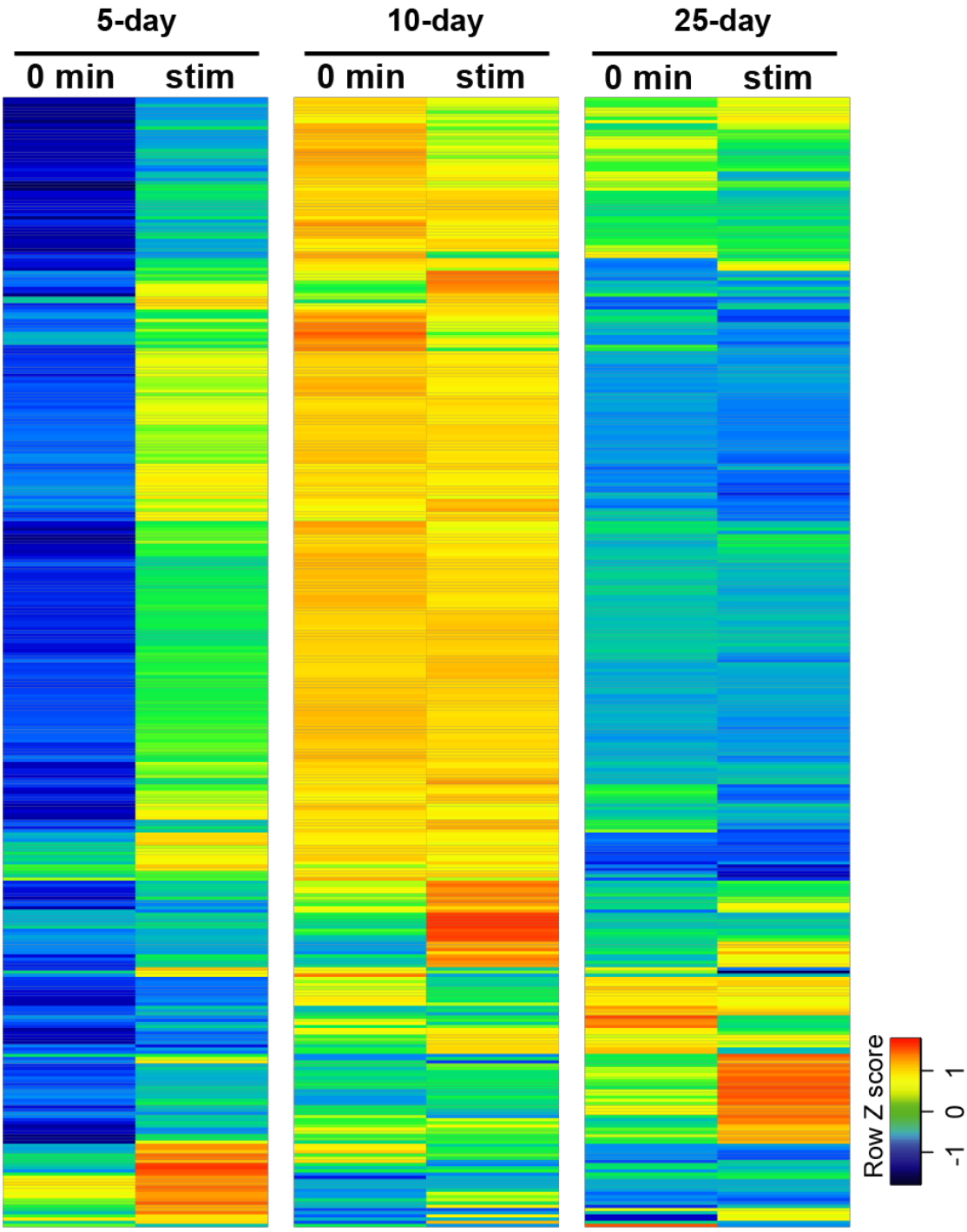

Figure 2.12 Most ARGs in the 5-day-old brain are misexpressed in older flies

Heatmap following expression of all 352 up-regulated ARGs in the 5-day-old brain across all ages and treatments. Each column represents the expression of one gene, normalized across all ages/ time points (red=high expression, blue=low expression).

Figure 2.13 Few genes are induced in all three ages tested

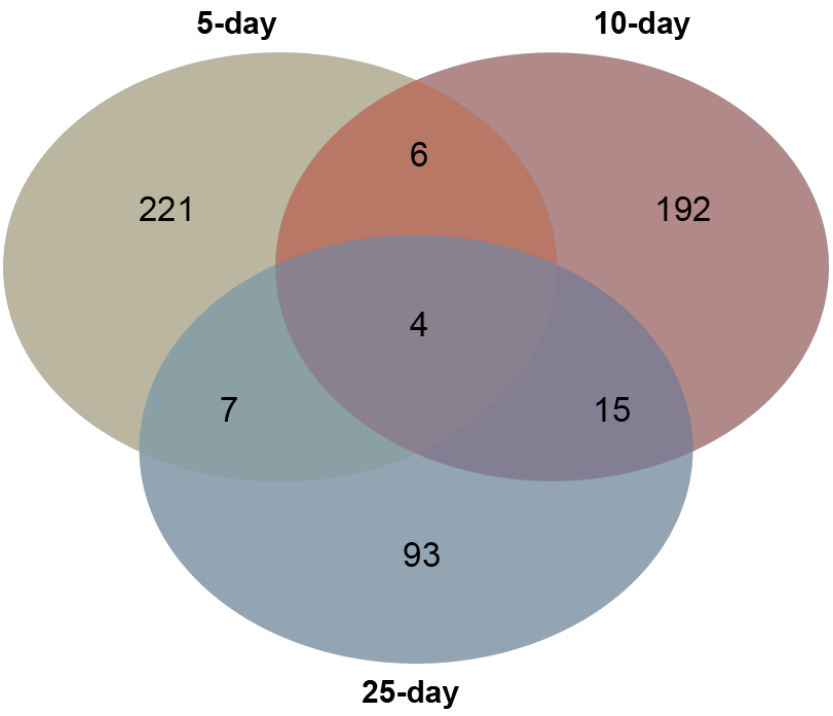

Figure 2.13 Few genes are induced in all three ages tested

Venn plot comparing the overlap of all up-regulated genes for each age tested.

\

Figure 2.14 Experiment design to examine the role of HDAC6 in ARG expression

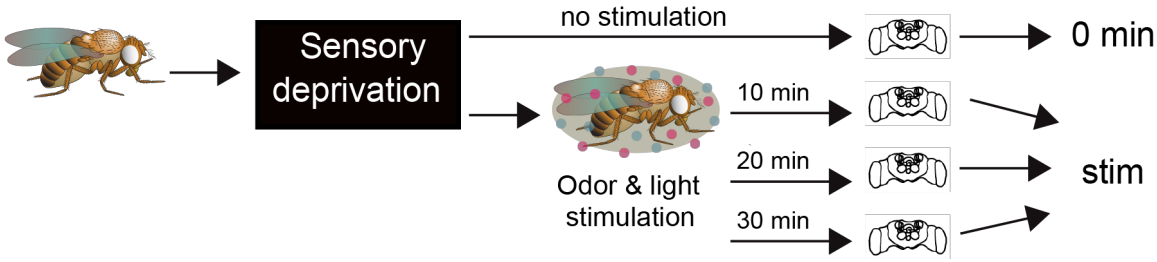

Figure 2.14 Experiment design to examine the role of HDAC6 in ARG expression

Stimulation paradigm for brain transcriptome analysis in 5-day-old white-eyed wild-type and HDAC6 (KO) mutant flies.

Figure 2.15 Differentially expressed genes in *Drosophila melanogaster* brain following neuronal activation depend on HDAC6

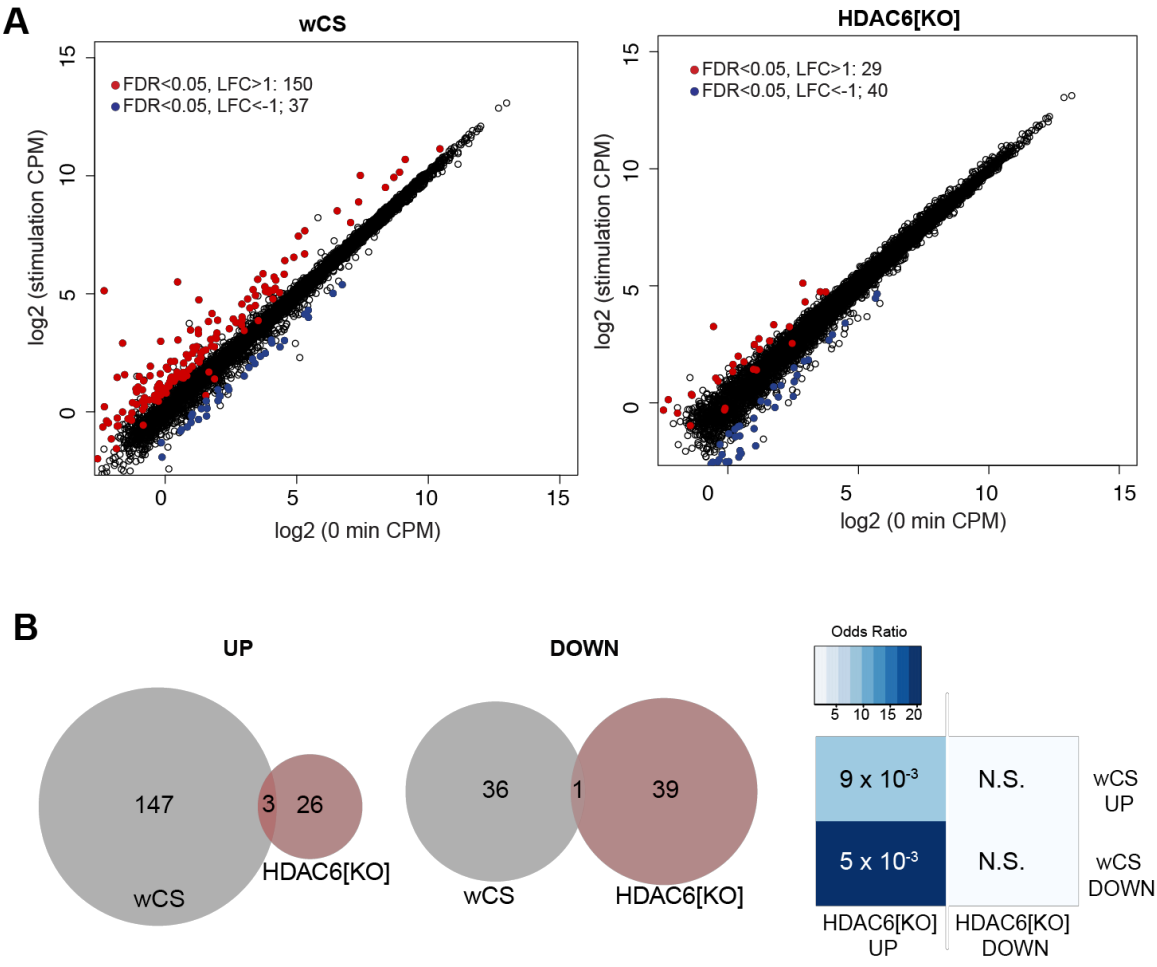

Figure 2.15 Differentially expressed genes in *Drosophila melanogaster* brain following neuronal activation depend on HDAC6

(A) Plot highlighting up- and down-regulated genes in the stimulated group of white-eyed wild-type flies (left) and white-eyed HDAC6 [KO] mutant flies (right). Red and blue dots represent up-regulated genes (Fold-change>2, FDR<0.05) and down-regulated genes (Fold-change<-2, FDR<0.05), respectively.

(B) Venn plot comparing the overlap of all up- and down-regulated genes in the brain of each genotype following sensory stimulation. The far right box shows significance of overlap of indicated gene sets (P-value indicated in box; color denotes odds ratio from Fisher's exact test).

Figure 2.16 Characterization of ARGs in wCS and HDAC6 mutant flies

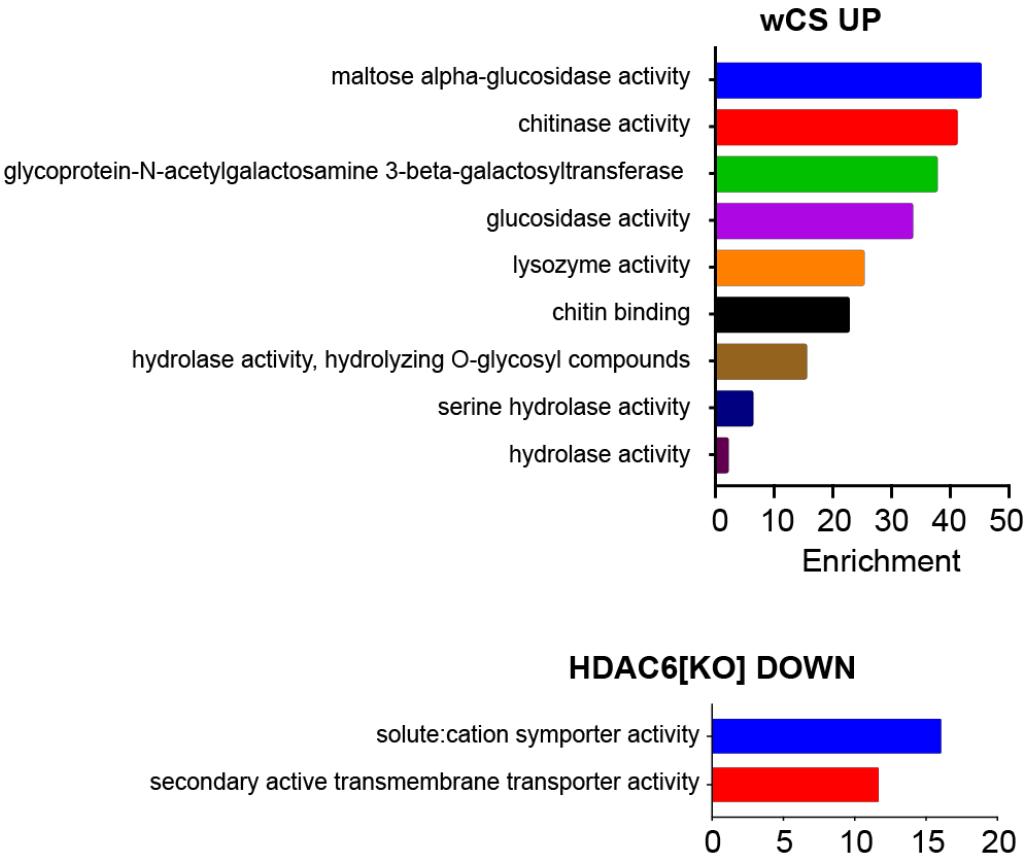

Figure 2.16 Characterization of ARGs in wCS and HDAC6 mutant flies

Bar graph showing fold-enrichment for molecular function GO terms for up-regulated genes in wCS brain compared to all genes expressed in the brain RNA-seq experiments ($p<0.05$) (left) and down-regulated genes in HDAC6[KO] mutant brains compared to all genes expressed in the brain RNA-seq experiments ($p<0.05$) (right).

Figure 2.17 Loss of ARG expression in HDAC6 mutants

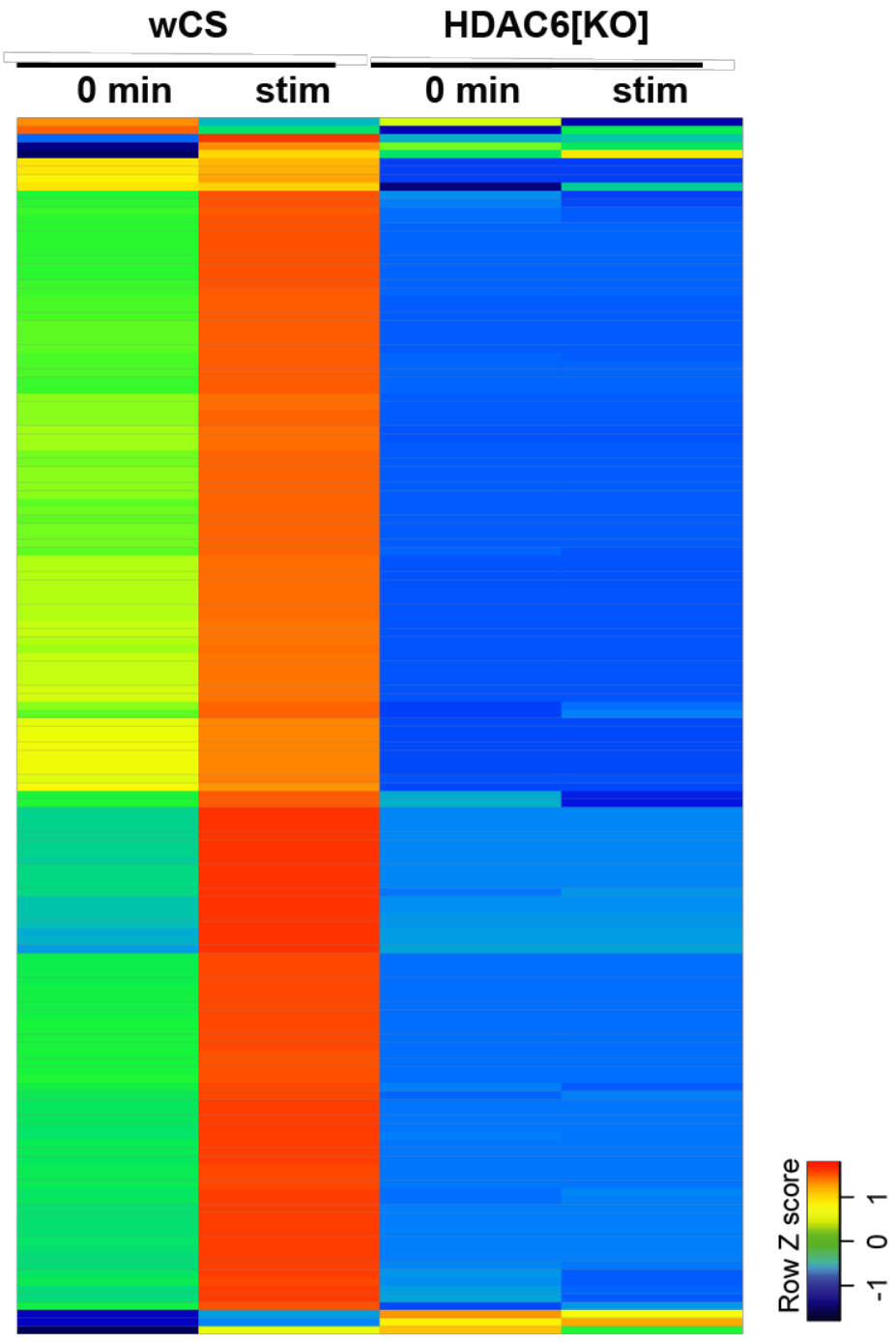

Figure 2.17 Loss of ARG expression in HDAC6 mutants

Heatmap following expression of 150 up-regulated genes in the white-eyed, wild-type brain across all experiments. Each column represents the expression of one gene, normalized across samples (red=high expression, blue=low expression).

Figure 2.18 Model

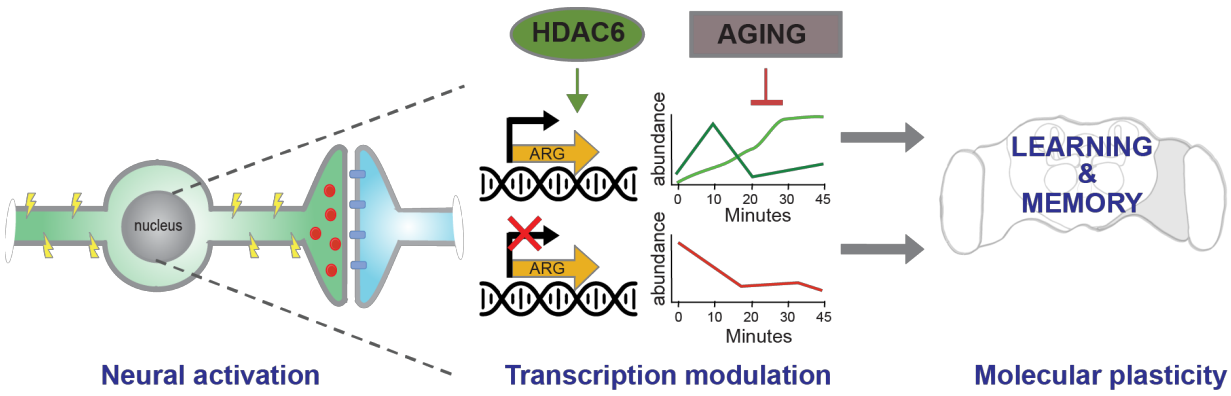

Figure 2.18 Model

A schematic representing the interaction between ARG modulation and key players in learning and memory: age and HDAC6.

Table 2.1 Top ARGs induced following sensory stimulation

Gene	Peak fold change	Peak Time	Description	Human Ortholog
CG34324	1,574	30 min	chitin binding	
CG13330	1,370	10 min		
Muc68D	1,075	30 min	chitin binding; extracellular matrix structural constituent	
CG34220	622	30 min	chitin binding	
CG3906	340	30 min		
CG34330	70	10 min		
Skp2	56	30 min	contributes to ubiquitin-protein transferase activity	SKP2
CG31821	49	45 min	serine-type carboxypeptidase activity	SCPEP1
Cht8	35	45 min	chitin binding; chitinase activity	CHIA, CHIT1
to	24	30 min	hemolymph juvenile hormone binding; takeout superfamily	
…	…	…	…	…
Hr38	4	45 min	DNA binding transcription factor activity; nuclear receptor activity; steroid hormone receptor activity	NR4A1

Table 2.2 ARGs induced in the young and aging adult brain.

Symbol	Gene	log_2 Fold Change after stimulation		
		5 days	10 days	25 days
Amy-p	Amylase-proximal	3.81	2.78	1.24
Amy-d	Amylase-distal	3.27	2.90	1.35
Syx1A	Syntaxin 1A	2.44	6.48	1.38
Tsp29Fb	Tetraspanin 29Fb	1.73	2.13	1.04

Table 2.3 ARGs at 10 minutes in the adult brain

Gene	logFC	PValue	FDR
FBgn0085359	6.133263101	2.56E-31	2.37E-27
FBgn0033679	1.806938224	9.54E-13	4.42E-09
FBgn0038774	2.937776801	1.25E-11	3.05E-08
FBgn0032285	2.640662788	1.32E-11	3.05E-08
FBgn0031313	1.593364866	3.67E-11	6.81E-08
FBgn0035544	3.621012253	1.55E-10	2.40E-07
FBgn0039038	3.505203249	1.05E-09	1.39E-06
FBgn0039800	1.989853077	1.36E-09	1.57E-06
FBgn0040398	1.268704333	1.51E-08	1.46E-05
FBgn0033848	10.41543919	1.73E-08	1.46E-05
FBgn0053502	1.416024061	1.88E-08	1.46E-05
FBgn0002789	2.106978558	1.89E-08	1.46E-05
FBgn0028543	1.482747474	3.31E-08	2.27E-05
FBgn0086695	3.872765864	3.43E-08	2.27E-05
FBgn0039347	1.931061286	3.97E-08	2.45E-05
FBgn0031089	2.660863538	5.10E-08	2.95E-05
FBgn0011296	1.423943075	6.90E-08	3.76E-05
FBgn0051550	1.640152416	7.58E-08	3.91E-05
FBgn0030160	1.421199281	2.43E-07	0.000118731
FBgn0259715	1.358943773	3.17E-07	0.000147141
FBgn0036825	1.919610907	3.37E-07	0.000148927
FBgn0004057	1.425825922	6.58E-07	0.000277367
FBgn0017566	1.439456073	8.45E-07	0.000327293
FBgn0261602	2.334296926	8.47E-07	0.000327293
FBgn0038948	1.522431653	8.83E-07	0.000327582
FBgn0035144	2.029901219	9.73E-07	0.000347159
FBgn0031261	1.490164078	1.25E-06	0.000430338
FBgn0027790	1.84240683	1.39E-06	0.00045985
FBgn0000047	3.48020746	2.34E-06	0.000749663
FBgn0039801	1.435442061	2.74E-06	0.000845849
FBgn0028396	2.39489378	2.87E-06	0.000858523
FBgn0034743	1.292680405	3.48E-06	0.001008564
FBgn0037146	1.128255413	4.43E-06	0.001246045
FBgn0051810	3.645396473	4.58E-06	0.001248967

FBgn0003149	2.236202232	5.78E-06	0.001530544
FBgn0036728	1.089259948	7.19E-06	0.001852657
FBgn0031093	1.610646978	7.54E-06	0.001883729
FBgn0032381	-2.546619323	8.11E-06	0.001883729
FBgn0052500	1.09917219	8.13E-06	0.001883729
FBgn0265356	2.25558453	8.33E-06	0.001883729
FBgn0036135	1.632574005	9.65E-06	0.002130533
FBgn0003887	1.07729567	1.02E-05	0.002149589
FBgn0034709	1.378244163	1.06E-05	0.002149589
FBgn0037342	1.098800411	1.10E-05	0.002149589
FBgn0031913	1.904758415	1.12E-05	0.002149589
FBgn0000079	1.236183145	1.14E-05	0.002149589
FBgn0004169	1.963027234	1.15E-05	0.002149589
FBgn0051950	2.132144601	1.16E-05	0.002149589
FBgn0039682	1.440127628	1.23E-05	0.002191273
FBgn0040813	1.176144709	1.23E-05	0.002191273
FBgn0030051	1.690886718	1.26E-05	0.002191273
FBgn0017579	1.524376765	1.29E-05	0.002191273
FBgn0026268	2.229795019	1.30E-05	0.002191273
FBgn0004654	1.019998678	1.32E-05	0.002191273
FBgn0024289	1.009615299	1.39E-05	0.002234094
FBgn0033879	1.349921518	1.40E-05	0.002234094
FBgn0039635	1.262942106	1.46E-05	0.002286604
FBgn0034793	1.202744035	1.53E-05	0.00233062
FBgn0052726	3.065845884	1.53E-05	0.00233062
FBgn0250814	1.927638291	1.64E-05	0.002411864
FBgn0266446	1.835224223	1.79E-05	0.002513743
FBgn0034137	1.585537145	2.08E-05	0.002839775
FBgn0051823	2.274669226	2.21E-05	0.002839775
FBgn0264695	2.008992417	2.22E-05	0.002839775
FBgn0039685	1.3547734	2.24E-05	0.002839775
FBgn0016920	-2.905016503	2.27E-05	0.002839775
FBgn0014857	1.46997654	2.33E-05	0.002843726
FBgn0031050	1.101795341	2.37E-05	0.002859246
FBgn0259209	1.809126407	2.41E-05	0.002867453
FBgn0259219	1.181839375	2.62E-05	0.003052897
FBgn0000150	1.485165303	2.63E-05	0.003052897

FBgn0033480	1.256565108	2.85E-05	0.003235881
FBgn0039110	1.26440319	2.86E-05	0.003235881
FBgn0052564	1.408211232	3.07E-05	0.003431519
FBgn0020618	1.101905084	3.22E-05	0.003552493
FBgn0040342	1.246975924	3.35E-05	0.003652541
FBgn0085353	2.528890621	3.51E-05	0.003755766
FBgn0027794	1.175255703	3.52E-05	0.003755766
FBgn0261606	1.042903599	3.61E-05	0.003799266
FBgn0030605	1.348670348	3.67E-05	0.003820459
FBgn0031021	1.365969141	3.78E-05	0.003836986
FBgn0029860	1.132319279	3.85E-05	0.003836986
FBgn0032171	1.100690967	4.12E-05	0.004067167
FBgn0033949	1.544119311	4.21E-05	0.004110094
FBgn0034497	3.155792817	4.26E-05	0.004116748
FBgn0037356	1.064471029	4.39E-05	0.004196486
FBgn0020235	1.020303123	4.50E-05	0.004257958
FBgn0040931	2.137273188	4.72E-05	0.004396687
FBgn0031106	1.907614868	4.74E-05	0.004396687
FBgn0033728	2.565724559	4.79E-05	0.004397098
FBgn0031908	1.643465985	4.99E-05	0.004496146
FBgn0027585	1.257645932	5.00E-05	0.004496146
FBgn0032803	1.027331436	5.09E-05	0.004496146
FBgn0031538	1.006345421	5.12E-05	0.004496146
FBgn0034879	1.294875657	5.18E-05	0.004496146
FBgn0021944	1.037101234	5.19E-05	0.004496146
FBgn0038878	1.147771495	5.26E-05	0.004511744
FBgn0030853	1.139856545	5.30E-05	0.004511744
FBgn0034645	1.661611515	5.70E-05	0.004803187
FBgn0030569	1.484274291	5.79E-05	0.004839052
FBgn0036203	2.760258237	5.88E-05	0.004846965
FBgn0034755	1.493965339	5.93E-05	0.004846965
FBgn0027586	1.097298816	6.02E-05	0.004846965
FBgn0024234	1.260943488	6.06E-05	0.004846965
FBgn0013343	3.691382442	6.06E-05	0.004846965
FBgn0003062	1.078577235	6.84E-05	0.005326966
FBgn0005638	1.72749511	7.15E-05	0.005524369
FBgn0039151	1.061963984	7.21E-05	0.005524369

FBgn0034517	1.288402065	7.38E-05	0.0055607
FBgn0085360	1.345696444	7.42E-05	0.0055607
FBgn0004047	1.24023769	7.45E-05	0.0055607
FBgn0023540	1.575117938	7.50E-05	0.0055607
FBgn0266448	2.090519206	7.88E-05	0.00579883
FBgn0011722	1.085646297	8.52E-05	0.006173964
FBgn0037351	1.907568828	8.81E-05	0.006319533
FBgn0037329	1.061504222	8.86E-05	0.006319533
FBgn0033162	1.005146044	0.000100072	0.006981012
FBgn0083961	1.160604577	0.00010129	0.006987537
FBgn0027563	1.403478732	0.000101738	0.006987537
FBgn0039406	1.097509604	0.000102618	0.006996151
FBgn0004117	1.573035796	0.000104889	0.007098787
FBgn0039298	2.467140276	0.000106582	0.007161046
FBgn0013764	1.141205607	0.000111206	0.007402612
FBgn0030365	1.14014306	0.000114995	0.007561945
FBgn0050431	1.410841612	0.000117951	0.007701684
FBgn0014028	1.242793295	0.000119375	0.00773734
FBgn0034920	1.497982895	0.000120637	0.00773734
FBgn0085195	1.43552603	0.000121	0.00773734
FBgn0033321	1.322239662	0.000128745	0.008158417
FBgn0037328	1.744012907	0.000129345	0.008158417
FBgn0044030	1.632320307	0.000131131	0.008215149
FBgn0029857	1.143790363	0.00013468	0.008262702
FBgn0039667	1.935529008	0.00013609	0.008262702
FBgn0039713	1.310544294	0.000142517	0.008525299
FBgn0031381	1.10269407	0.000147937	0.008656342
FBgn0000044	1.765673777	0.000148442	0.008656342
FBgn0042112	1.258256472	0.000150789	0.008738229
FBgn0031022	1.126238467	0.000160762	0.009258315
FBgn0031879	1.776018884	0.0001621	0.009271287
FBgn0010424	1.504029697	0.000163987	0.009271287
FBgn0034885	1.412732476	0.000165083	0.00927667
FBgn0001989	1.266059705	0.000168657	0.009308253
FBgn0037433	1.233799803	0.000174744	0.009587122
FBgn0027497	3.417772642	0.000182014	0.00990781
FBgn0000045	1.99302762	0.000183324	0.00990781

FBgn0053548	1.321680481	0.000183795	0.00990781
FBgn0003462	1.105573134	0.000189368	0.010057041
FBgn0038299	-2.285140876	0.000205808	0.010720508
FBgn0043783	1.148763375	0.000216418	0.011123512
FBgn0037686	1.887364845	0.000217345	0.011123512
FBgn0011272	1.173348345	0.00022269	0.011282947
FBgn0037164	1.391114969	0.0002265	0.01129316
FBgn0033603	1.291812946	0.000226545	0.01129316
FBgn0030945	1.583257795	0.00024051	0.011675416
FBgn0036415	1.898871295	0.000243187	0.011709859
FBgn0025382	1.225190323	0.00024906	0.011903507
FBgn0004862	1.351036597	0.000252304	0.011996748
FBgn0030640	1.223443214	0.000254371	0.012023694
FBgn0033365	1.213572957	0.000255465	0.012023694
FBgn0051809	2.526755512	0.000256971	0.012033514
FBgn0032833	1.093644164	0.000259397	0.012086098
FBgn0004404	1.351302198	0.000262292	0.012099372
FBgn0033961	1.680143018	0.000274158	0.012399952
FBgn0031251	2.277904861	0.000275782	0.012412863
FBgn0002174	1.317266972	0.000287025	0.012832731
FBgn0053349	1.880387909	0.000310112	0.013499351
FBgn0030103	1.054557541	0.000313377	0.013577702
FBgn0038806	1.1186002	0.000326884	0.014031812
FBgn0002773	1.972702108	0.000329938	0.01409763
FBgn0000046	2.079130489	0.000332861	0.014157288
FBgn0022355	1.128480512	0.000342079	0.014417077
FBgn0038043	1.28950098	0.000347939	0.014597709
FBgn0037937	1.276072261	0.00040174	0.016555256
FBgn0033351	1.431365954	0.000407404	0.016649507
FBgn0052783	2.042301131	0.00041598	0.016916518
FBgn0036481	1.685117132	0.000423134	0.016928081
FBgn0034162	1.196681676	0.000423567	0.016928081
FBgn0037131	1.290255994	0.000431821	0.01718389
FBgn0000084	1.309681373	0.000437765	0.017295105
FBgn0025286	1.186212106	0.000438347	0.017295105
FBgn0261363	1.105710868	0.000456631	0.017940196
FBgn0040074	1.081841684	0.000478279	0.018632794

FBgn0031737	1.457346253	0.000538988	0.020002905
FBgn0030156	1.39271916	0.000539307	0.020002905
FBgn0042201	1.198602718	0.000540163	0.020002905
FBgn0004028	1.539209495	0.000551112	0.020197264
FBgn0031092	1.078737977	0.000556524	0.020315316
FBgn0032167	1.500415807	0.000576406	0.020795486
FBgn0037024	1.032948006	0.000615931	0.021944501
FBgn0053519	1.58842454	0.000625137	0.022121526
FBgn0030584	1.000005094	0.000634577	0.022160213
FBgn0052573	1.200122941	0.000635702	0.022160213
FBgn0033566	1.055778305	0.000638481	0.022160213
FBgn0003515	1.341847319	0.000640524	0.022160213
FBgn0027334	1.620004118	0.000666741	0.022811902
FBgn0032293	1.213126272	0.000698661	0.023642284
FBgn0041581	-2.65280967	0.00073576	0.024539464
FBgn0003279	1.300315196	0.00075009	0.024927737
FBgn0034331	1.018119068	0.000760828	0.025104612
FBgn0266451	1.646661041	0.00078503	0.025811348
FBgn0052536	1.243244872	0.000792609	0.025968444
FBgn0039527	1.289195144	0.000823101	0.026872519
FBgn0014869	1.022566949	0.000828079	0.026940176
FBgn0039564	1.157574518	0.000841996	0.027173224
FBgn0013277	-1.971117182	0.000844035	0.027173224
FBgn0086906	1.908254774	0.000861253	0.027496005
FBgn0029858	1.126333361	0.000960256	0.029978101
FBgn0035344	1.482258049	0.001051755	0.032078535
FBgn0030645	1.609050955	0.001061094	0.03225725
FBgn0010078	1.098957482	0.001096521	0.032722477
FBgn0038820	1.581914344	0.001124913	0.033217184
FBgn0038516	1.15623564	0.00113889	0.03341704
FBgn0040606	1.64748	0.001147649	0.03356783
FBgn0013348	3.806590911	0.001153537	0.033633945
FBgn0035501	1.313808796	0.0011577	0.033649505
FBgn0039108	-1.074950488	0.001190943	0.034400076
FBgn0030925	1.064463723	0.001195886	0.034435565
FBgn0038294	1.562356278	0.001200935	0.034473908
FBgn0030292	1.675874326	0.001364854	0.037889004

FBgn0002772	1.519045889	0.001379571	0.03809302
FBgn0031464	1.039808386	0.001460813	0.039488803
FBgn0034142	1.251701799	0.001480983	0.039801961
FBgn0002565	1.237172196	0.001533211	0.04108652
FBgn0033942	1.151372974	0.001565019	0.041818026
FBgn0033140	1.163341473	0.00161654	0.042824466
FBgn0033850	1.028069349	0.001669347	0.043723681
FBgn0035241	1.261212968	0.001692281	0.044075366
FBgn0030005	1.63846644	0.001714817	0.044463796
FBgn0039486	1.147096826	0.001735446	0.044821886
FBgn0259678	1.472006434	0.001757131	0.045043405
FBgn0033341	1.243902031	0.0017969	0.045752017
FBgn0035181	1.09362554	0.001810935	0.045752017
FBgn0037312	1.048991838	0.001830638	0.045874792
FBgn0035240	1.087635368	0.00195013	0.047947643
FBgn0026372	1.202108626	0.002011238	0.048689811
FBgn0029093	3.41284372	0.002035378	0.049145889
FBgn0053105	1.004837415	0.002086911	0.049742526

Table 2.4 ARGs at 20 minutes in the adult brain

Gene	logFC	PValue	FDR
FBgn0033848	4.404305455	2.44E-20	2.24E-16
FBgn0015035	-2.236397994	5.27E-16	2.42E-12
FBgn0013343	1.956097225	8.02E-16	2.46E-12
FBgn0010241	-2.152398322	1.07E-14	2.45E-11
FBgn0025643	-2.116616227	7.94E-10	1.22E-06
FBgn0034647	-1.285924104	7.40E-09	9.72E-06
FBgn0039347	1.334277131	3.87E-08	3.95E-05
FBgn0052671	-1.678524679	6.90E-08	6.34E-05
FBgn0016920	-1.447954405	8.02E-08	6.70E-05
FBgn0086695	1.652436287	1.22E-07	8.59E-05
FBgn0051086	1.833023041	1.81E-07	0.000118507
FBgn0031106	1.010784343	3.44E-07	0.000210784
FBgn0030482	-1.270457942	1.06E-06	0.000513388
FBgn0041579	-2.90721892	2.69E-06	0.00095051
FBgn0259918	-1.109705894	6.64E-06	0.002032867
FBgn0028396	1.501854412	8.03E-06	0.002306378
FBgn0038299	-2.814728727	1.05E-05	0.002484141
FBgn0028519	-1.416918948	1.13E-05	0.002570533
FBgn0066292	-1.122973752	1.54E-05	0.003071251
FBgn0085353	7.245754922	1.66E-05	0.003106764
FBgn0030588	-1.188525943	2.62E-05	0.004383167
FBgn0034276	-1.120959193	4.25E-05	0.006512538
FBgn0032116	3.497252906	9.90E-05	0.011914423
FBgn0039040	-1.816433335	0.000100141	0.011914423
FBgn0010433	1.159160044	0.000101113	0.011914423
FBgn0005391	1.292504184	0.000103046	0.011988553
FBgn0052786	-1.417839607	0.000119644	0.013248789
FBgn0260004	-1.117811937	0.00012733	0.013824973
FBgn0013772	-1.365287341	0.000127856	0.013824973
FBgn0053470	-2.968549931	0.000137923	0.014398915
FBgn0038398	-2.243571502	0.000152875	0.014691141
FBgn0039486	1.438648813	0.000163635	0.015191569
FBgn0015568	-1.11435524	0.00020814	0.01839437
FBgn0032835	-1.237999138	0.000237437	0.020072915

FBgn0037131	1.044867283	0.00027541	0.02122664
FBgn0053329	-1.09858973	0.000278697	0.02122664
FBgn0051778	-1.136249375	0.000339456	0.024375636
FBgn0052564	1.039064023	0.000405939	0.027233489
FBgn0050489	-1.194589355	0.00058112	0.035371353
FBgn0004047	1.043553023	0.000730768	0.04021848
FBgn0051950	1.068749617	0.000737019	0.040321066
FBgn0037836	-1.051252881	0.000766545	0.041443038
FBgn0037755	2.294355672	0.000873988	0.043704792
FBgn0040211	-1.279836656	0.000879843	0.043711563
FBgn0259229	-1.126241316	0.000932728	0.044883286
FBgn0033387	-1.049273631	0.001014418	0.04708847

Table 2.5 ARGs at 30 minutes in the adult brain

Gene	logFC	PValue	FDR
FBgn0033848	7.821325646	4.04E-47	3.74E-43
FBgn0040931	2.343818325	1.11E-19	5.15E-16
FBgn0034645	2.091719265	5.28E-18	1.63E-14
FBgn0015035	-3.137905558	1.86E-15	4.31E-12
FBgn0016726	1.661583284	2.29E-14	4.25E-11
FBgn0010387	1.710204309	1.60E-13	2.48E-10
FBgn0030292	1.928770543	5.02E-13	6.65E-10
FBgn0039347	1.783156268	7.65E-13	8.87E-10
FBgn0040532	1.81913942	1.04E-12	1.07E-09
FBgn0250814	1.977466263	4.09E-12	3.79E-09
FBgn0039635	1.29110693	1.68E-11	1.42E-08
FBgn0044810	2.743279546	2.24E-11	1.73E-08
FBgn0085353	10.59897587	4.67E-11	3.33E-08
FBgn0036203	10.07412849	5.85E-11	3.73E-08
FBgn0000150	1.612321928	6.03E-11	3.73E-08
FBgn0085271	2.605923084	6.58E-11	3.81E-08
FBgn0033961	1.785878413	7.29E-11	3.98E-08
FBgn0040899	1.675594028	1.44E-10	7.44E-08
FBgn0037686	2.207517094	4.07E-10	1.99E-07
FBgn0051950	2.172444009	5.96E-10	2.76E-07
FBgn0261602	2.401707845	8.09E-10	3.57E-07
FBgn0266375	1.118077477	9.42E-10	3.91E-07
FBgn0025558	1.50667364	9.70E-10	3.91E-07
FBgn0034871	8.406709876	1.09E-09	4.20E-07
FBgn0026879	1.867380149	1.35E-09	5.01E-07
FBgn0261844	1.335060892	1.73E-09	5.72E-07
FBgn0031092	1.336688276	1.76E-09	5.72E-07
FBgn0017566	1.400146952	1.81E-09	5.72E-07
FBgn0014869	1.145098908	1.84E-09	5.72E-07
FBgn0037351	2.126051208	1.85E-09	5.72E-07
FBgn0083953	1.391116449	2.18E-09	6.41E-07
FBgn0085249	9.275425915	2.21E-09	6.41E-07
FBgn0030645	2.073088499	2.61E-09	7.33E-07
FBgn0031313	1.441467987	2.86E-09	7.79E-07

FBgn0044030	1.81266522	3.13E-09	8.28E-07
FBgn0029529	1.352096055	3.79E-09	9.76E-07
FBgn0031735	1.78343798	9.29E-09	2.33E-06
FBgn0037328	2.000680017	1.03E-08	2.50E-06
FBgn0052564	1.742945666	1.20E-08	2.85E-06
FBgn0036825	2.002201154	1.34E-08	3.10E-06
FBgn0002174	1.367476368	1.41E-08	3.19E-06
FBgn0030605	1.280862408	1.55E-08	3.43E-06
FBgn0032833	1.161027799	1.65E-08	3.55E-06
FBgn0031106	1.937177602	1.83E-08	3.85E-06
FBgn0029857	1.152348379	2.61E-08	5.38E-06
FBgn0004404	1.617937142	2.70E-08	5.44E-06
FBgn0032812	1.705091961	2.87E-08	5.66E-06
FBgn0033480	1.321233366	3.08E-08	5.95E-06
FBgn0031021	1.363442171	3.40E-08	6.43E-06
FBgn0036135	1.592428743	4.17E-08	7.74E-06
FBgn0032835	-1.600269762	4.48E-08	8.15E-06
FBgn0000084	1.420429548	5.35E-08	9.55E-06
FBgn0003887	1.015703404	6.23E-08	1.09E-05
FBgn0003279	1.504579445	6.40E-08	1.10E-05
FBgn0031561	2.659822299	7.34E-08	1.24E-05
FBgn0031093	1.574117605	8.54E-08	1.40E-05
FBgn0039800	1.841841535	8.59E-08	1.40E-05
FBgn0030945	1.671472444	9.02E-08	1.42E-05
FBgn0017579	1.604369306	9.04E-08	1.42E-05
FBgn0025352	1.03950726	1.03E-07	1.59E-05
FBgn0031381	1.249850405	1.17E-07	1.75E-05
FBgn0032293	1.285596964	1.17E-07	1.75E-05
FBgn0014857	1.470777502	1.27E-07	1.85E-05
FBgn0011272	1.400758606	1.28E-07	1.85E-05
FBgn0025382	1.341010193	1.31E-07	1.86E-05
FBgn0036728	1.067648326	1.53E-07	2.15E-05
FBgn0066292	-1.474984485	1.62E-07	2.25E-05
FBgn0038678	1.083429857	1.67E-07	2.27E-05
FBgn0034743	1.392957977	2.24E-07	2.96E-05
FBgn0033566	1.192859888	3.03E-07	3.96E-05
FBgn0001989	1.257662662	3.13E-07	4.04E-05

FBgn0035753	1.272896315	4.16E-07	5.29E-05
FBgn0030974	1.028857875	4.27E-07	5.31E-05
FBgn0010078	1.289843084	4.29E-07	5.31E-05
FBgn0038948	1.489705846	4.70E-07	5.74E-05
FBgn0030853	1.05933951	4.83E-07	5.81E-05
FBgn0031971	1.311242637	4.97E-07	5.91E-05
FBgn0000047	3.121045167	5.26E-07	6.06E-05
FBgn0014028	1.22753307	5.29E-07	6.06E-05
FBgn0031099	1.382099306	5.62E-07	6.36E-05
FBgn0032285	2.339374244	5.88E-07	6.49E-05
FBgn0000079	3.806408859	6.18E-07	6.74E-05
FBgn0030272	1.047766262	6.25E-07	6.74E-05
FBgn0030584	1.027686555	6.50E-07	6.85E-05
FBgn0040575	1.787398	6.83E-07	7.09E-05
FBgn0013764	1.170042283	6.88E-07	7.09E-05
FBgn0034517	1.293131334	7.13E-07	7.27E-05
FBgn0038043	1.308872315	7.43E-07	7.49E-05
FBgn0027794	1.094008785	7.57E-07	7.49E-05
FBgn0027334	1.89785232	7.59E-07	7.49E-05
FBgn0263911	1.599180719	7.94E-07	7.75E-05
FBgn0051550	1.468204005	8.64E-07	8.27E-05
FBgn0027497	3.341465767	8.67E-07	8.27E-05
FBgn0261597	1.536774735	8.73E-07	8.27E-05
FBgn0022224	2.005026731	9.41E-07	8.82E-05
FBgn0037342	1.157730538	1.06E-06	9.60E-05
FBgn0042112	1.27776756	1.08E-06	9.69E-05
FBgn0037329	1.037621671	1.11E-06	9.87E-05
FBgn0033879	1.375246815	1.21E-06	0.000106567
FBgn0031261	1.487440985	1.25E-06	0.00010913
FBgn0086695	3.511050051	1.37E-06	0.000118737
FBgn0034877	1.427753063	1.39E-06	0.000119465
FBgn0039713	1.406847226	1.63E-06	0.000139046
FBgn0004654	1.063060073	1.68E-06	0.000141539
FBgn0026562	1.157207614	1.74E-06	0.000145608
FBgn0015379	1.029111089	1.76E-06	0.000145886
FBgn0040751	1.96947077	2.12E-06	0.000172762
FBgn0033341	1.433715906	2.17E-06	0.000173687

FBgn0034879	1.319435789	2.27E-06	0.000179326
FBgn0037236	5.795356626	2.71E-06	0.000211023
FBgn0037312	1.218503138	2.81E-06	0.000217139
FBgn0038806	1.097646825	3.41E-06	0.000258995
FBgn0026372	1.417938271	3.59E-06	0.000268174
FBgn0033691	1.049079747	3.78E-06	0.00027841
FBgn0039110	1.161579085	4.08E-06	0.000295563
FBgn0033351	1.504629032	4.17E-06	0.000299909
FBgn0003462	1.126122656	4.28E-06	0.000305339
FBgn0030569	2.135950465	4.34E-06	0.000307108
FBgn0031050	1.051612998	4.51E-06	0.000316664
FBgn0004057	1.550989622	4.61E-06	0.000320285
FBgn0033122	1.291577793	4.65E-06	0.000320285
FBgn0027791	1.588936926	4.66E-06	0.000320285
FBgn0030103	1.314843198	4.92E-06	0.000332885
FBgn0031068	1.020269396	5.00E-06	0.000336176
FBgn0261606	1.216723773	5.29E-06	0.000348795
FBgn0028396	2.816395768	5.42E-06	0.000353847
FBgn0015521	1.260179119	5.68E-06	0.000368719
FBgn0032171	1.080583334	5.92E-06	0.00038134
FBgn0040623	1.269713413	6.47E-06	0.00041395
FBgn0039298	4.594496071	6.81E-06	0.000432331
FBgn0025286	1.318207641	6.97E-06	0.000439697
FBgn0086355	1.318065641	7.14E-06	0.000444698
FBgn0035592	1.032409111	7.14E-06	0.000444698
FBgn0030640	1.197278855	7.49E-06	0.000459814
FBgn0052069	1.984866101	8.46E-06	0.00051276
FBgn0003062	1.075075952	9.29E-06	0.000559245
FBgn0034793	1.264852333	9.57E-06	0.00057265
FBgn0030365	1.060310788	1.03E-05	0.000606614
FBgn0051086	2.017540335	1.04E-05	0.000609834
FBgn0037024	1.082189815	1.09E-05	0.000632212
FBgn0035181	1.092521073	1.10E-05	0.000632212
FBgn0040398	1.220302601	1.15E-05	0.000655843
FBgn0037131	1.375838446	1.21E-05	0.000678695
FBgn0265187	1.795600602	1.24E-05	0.000686939
FBgn0003275	1.021273884	1.27E-05	0.000700782

FBgn0023540	1.044651954	1.37E-05	0.000734834
FBgn0029860	1.078264838	1.51E-05	0.000793384
FBgn0052808	1.033628905	1.63E-05	0.000856458
FBgn0039682	1.374696768	1.77E-05	0.000924039
FBgn0034497	2.06888644	1.84E-05	0.000953427
FBgn0020618	1.118355	1.89E-05	0.000973047
FBgn0036919	1.036203792	1.90E-05	0.000974066
FBgn0069923	2.309291595	1.92E-05	0.000980608
FBgn0039406	1.067785479	2.02E-05	0.001000949
FBgn0003330	1.015483721	2.13E-05	0.001049736
FBgn0000078	3.266452726	2.14E-05	0.001049736
FBgn0035544	2.863942771	2.26E-05	0.001104265
FBgn0010381	1.954186012	2.38E-05	0.001153306
FBgn0029897	1.320012968	2.54E-05	0.001210257
FBgn0053502	1.876115332	2.56E-05	0.001210257
FBgn0052536	1.239051263	2.63E-05	0.001233986
FBgn0034902	1.042274164	2.89E-05	0.001320046
FBgn0033679	1.262544485	2.91E-05	0.001320046
FBgn0024234	1.232840585	2.92E-05	0.001320046
FBgn0028543	1.439301555	2.99E-05	0.001344204
FBgn0031022	1.159389938	3.49E-05	0.001550482
FBgn0023477	1.015043556	3.72E-05	0.001628079
FBgn0039697	1.075203129	3.80E-05	0.001652694
FBgn0033268	1.136963746	3.83E-05	0.001658699
FBgn0033949	1.42028478	3.84E-05	0.001658699
FBgn0083961	1.256734046	3.97E-05	0.001697552
FBgn0031538	1.067133855	4.12E-05	0.00174648
FBgn0050410	1.159921884	4.31E-05	0.001801611
FBgn0039151	1.183061225	4.33E-05	0.001801611
FBgn0036667	2.368881939	4.47E-05	0.001833968
FBgn0040606	1.866843982	4.57E-05	0.001866588
FBgn0041579	-2.640475376	5.12E-05	0.002013962
FBgn0021906	1.112516895	5.60E-05	0.002174503
FBgn0037396	1.661609556	6.02E-05	0.002307448
FBgn0034755	1.439306687	6.54E-05	0.002482264
FBgn0040890	1.059984337	6.65E-05	0.002498787
FBgn0039757	1.043454654	7.07E-05	0.002621447

FBgn0034053	1.249070353	7.38E-05	0.002695248
FBgn0015031	1.469878426	7.55E-05	0.002733806
FBgn0035587	1.42384332	8.40E-05	0.002963131
FBgn0037146	1.15427701	8.56E-05	0.003008406
FBgn0038032	1.485066677	9.30E-05	0.003217228
FBgn0010408	1.032578007	9.37E-05	0.003232124
FBgn0050157	1.090060913	9.54E-05	0.003253779
FBgn0039665	1.364249577	9.90E-05	0.003364615
FBgn0039558	1.019250454	0.000103257	0.003495299
FBgn0029858	1.123027058	0.000104468	0.003510639
FBgn0085195	1.402649043	0.000113617	0.003777045
FBgn0040534	1.496770147	0.000129307	0.004164301
FBgn0034885	1.541127812	0.000131804	0.004230034
FBgn0030160	1.455938276	0.000161347	0.005023527
FBgn0028740	1.519851879	0.000164697	0.005108897
FBgn0022355	1.25507646	0.000191937	0.00579875
FBgn0033603	1.05846419	0.000198361	0.005972576
FBgn0004403	1.00207939	0.000202395	0.00603607
FBgn0014368	1.106171757	0.000240367	0.006951559
FBgn0039801	1.326749869	0.000249715	0.007051241
FBgn0052573	1.261255868	0.000250119	0.007051241
FBgn0030051	1.67263826	0.000251643	0.007072691
FBgn0013343	2.441139941	0.000320754	0.008613768
FBgn0039500	1.375384219	0.000330048	0.008715786
FBgn0259715	1.09351852	0.000331072	0.008715786
FBgn0030653	2.013346348	0.000331799	0.008715786
FBgn0032751	1.097725522	0.000332656	0.008715786
FBgn0033850	1.127179814	0.000348135	0.008994288
FBgn0051810	2.069809479	0.000367203	0.009382387
FBgn0031108	1.403044336	0.000381959	0.009705953
FBgn0038774	1.227487425	0.000410403	0.010371892
FBgn0038353	3.664134126	0.000426236	0.010742775
FBgn0003517	1.094151749	0.000432537	0.010755439
FBgn0004862	1.11235795	0.000433701	0.010755544
FBgn0053470	-2.448729285	0.000467272	0.011405128
FBgn0038236	-1.897252769	0.00051324	0.012138988
FBgn0039040	-1.55497831	0.000520795	0.012197906

FBgn0043536	1.363904368	0.000529869	0.012348083
FBgn0034187	-1.202569305	0.000553856	0.012760574
FBgn0026570	-1.056659397	0.00057127	0.013082782
FBgn0259209	1.229872715	0.000573983	0.013112538
FBgn0037290	2.730665156	0.000586102	0.013323754
FBgn0039620	1.386812361	0.00064121	0.014227816
FBgn0030588	-1.047687418	0.000658975	0.014449151
FBgn0033365	1.398131012	0.00066657	0.014512766
FBgn0085360	1.140595199	0.000676067	0.014650743
FBgn0013277	-2.010148647	0.000760429	0.015920949
FBgn0038398	-1.478009335	0.00079523	0.016500578
FBgn0052783	1.858261895	0.000845956	0.017094205
FBgn0031089	1.741617844	0.000848586	0.017101902
FBgn0039685	1.863820672	0.000889863	0.017711336
FBgn0032381	-2.231538201	0.000905116	0.017976343
FBgn0039084	-1.390662787	0.000923139	0.018256114
FBgn0038070	1.176768809	0.00095895	0.01879898
FBgn0013275	3.854420393	0.001075566	0.020696836
FBgn0002789	1.293279165	0.001097208	0.020896518
FBgn0015561	1.304278646	0.001201778	0.022160023
FBgn0031913	1.027346521	0.001274305	0.023107549
FBgn0040923	1.186520889	0.001287523	0.023278318
FBgn0027793	1.191199062	0.001334049	0.02407257
FBgn0030484	1.109503972	0.001416528	0.025217454
FBgn0011722	1.347030081	0.001422343	0.025248183
FBgn0039486	1.623926222	0.001597794	0.027596902
FBgn0036659	1.152933269	0.001641169	0.028136498
FBgn0030846	-1.868914607	0.001699802	0.028717059
FBgn0037602	1.004351903	0.001938999	0.031418609
FBgn0032116	3.482659622	0.001941009	0.031418609
FBgn0015568	-1.051989685	0.002073598	0.033154623
FBgn0032075	1.727077785	0.002220827	0.034853074
FBgn0037937	1.058769042	0.002837893	0.041846514
FBgn0033942	1.029026146	0.003089645	0.04484735
FBgn0029835	1.058922365	0.003204647	0.046058153

Table 2.6 ARGs at 45 minutes in the adult brain

Gene	logFC	PValue	FDR
FBgn0033848	6.397782279	1.72E-41	1.60E-37
FBgn0053502	2.84671601	1.12E-39	5.18E-36
FBgn0016726	1.759379201	1.98E-19	6.13E-16
FBgn0040931	2.184034924	5.14E-16	1.03E-12
FBgn0036622	3.860959884	5.57E-16	1.03E-12
FBgn0034645	1.881563644	5.42E-12	8.38E-09
FBgn0030569	2.426369821	1.35E-11	1.79E-08
FBgn0039620	1.365430791	2.02E-11	2.34E-08
FBgn0004057	1.375693677	4.23E-11	4.36E-08
FBgn0010381	2.630111577	5.92E-11	5.50E-08
FBgn0033679	1.419839597	1.27E-10	1.07E-07
FBgn0261844	1.439281707	2.28E-10	1.76E-07
FBgn0266375	1.055512717	2.83E-10	1.95E-07
FBgn0040751	2.438896269	2.94E-10	1.95E-07
FBgn0083953	1.406238545	3.15E-10	1.95E-07
FBgn0040899	1.69562127	1.03E-09	6.00E-07
FBgn0040532	1.800814605	1.68E-09	9.19E-07
FBgn0010387	1.278005828	2.66E-09	1.37E-06
FBgn0014859	1.92958564	3.08E-09	1.51E-06
FBgn0066292	-1.624016084	3.76E-09	1.74E-06
FBgn0038017	2.061727478	4.09E-09	1.81E-06
FBgn0261602	2.025433475	6.70E-09	2.82E-06
FBgn0037686	1.743960683	1.07E-08	4.30E-06
FBgn0000150	1.493835866	1.63E-08	6.31E-06
FBgn0036825	1.783505635	2.45E-08	8.88E-06
FBgn0037328	1.660190534	2.49E-08	8.88E-06
FBgn0017579	1.410918366	4.89E-08	1.68E-05
FBgn0034743	1.261034222	5.10E-08	1.69E-05
FBgn0030292	1.505926325	5.30E-08	1.69E-05
FBgn0033961	1.510231023	6.30E-08	1.95E-05
FBgn0250814	1.641696071	8.10E-08	2.42E-05
FBgn0004554	1.919525858	8.60E-08	2.49E-05
FBgn0026879	1.864851018	1.16E-07	3.24E-05
FBgn0037351	1.540678321	1.19E-07	3.24E-05

FBgn0039347	1.626051597	1.36E-07	3.61E-05
FBgn0051821	5.614054943	2.13E-07	5.48E-05
FBgn0085271	2.039100196	2.57E-07	6.39E-05
FBgn0002789	1.456357205	2.62E-07	6.39E-05
FBgn0031106	1.623921031	2.70E-07	6.41E-05
FBgn0010078	1.15278684	3.51E-07	8.13E-05
FBgn0004404	1.52147672	4.36E-07	9.87E-05
FBgn0027334	1.303889414	4.99E-07	0.000106313
FBgn0032293	1.153032853	5.12E-07	0.000106313
FBgn0030484	1.075965105	5.16E-07	0.000106313
FBgn0022355	1.081835942	6.01E-07	0.000119965
FBgn0000473	1.158453917	6.08E-07	0.000119965
FBgn0029857	1.042965117	7.29E-07	0.000140897
FBgn0044030	1.651806822	9.16E-07	0.000173488
FBgn0040582	-1.129372564	1.11E-06	0.000202343
FBgn0039527	1.408927601	1.11E-06	0.000202343
FBgn0030605	1.189422756	1.75E-06	0.00030712
FBgn0031313	1.186697748	1.81E-06	0.000311045
FBgn0035592	1.087289	1.94E-06	0.000316476
FBgn0031093	1.313257463	1.97E-06	0.000316476
FBgn0038299	-3.125011158	2.25E-06	0.00035333
FBgn0014857	1.331736519	2.37E-06	0.000365969
FBgn0262858	1.010162841	2.64E-06	0.000401585
FBgn0017566	1.249282887	3.04E-06	0.00044581
FBgn0029529	1.194002848	3.10E-06	0.00044581
FBgn0035544	3.02105031	3.17E-06	0.00044581
FBgn0003279	1.153857665	3.25E-06	0.000450685
FBgn0261606	1.111797386	3.32E-06	0.000452807
FBgn0261597	1.22444697	3.79E-06	0.000510074
FBgn0013275	4.484244558	3.95E-06	0.000523113
FBgn0040623	1.232042787	4.87E-06	0.000636189
FBgn0030945	1.171104548	5.06E-06	0.000651333
FBgn0039713	1.179626251	5.69E-06	0.000697272
FBgn0032812	1.210734995	5.71E-06	0.000697272
FBgn0025286	1.098284917	5.99E-06	0.000721245
FBgn0033351	1.317136468	6.13E-06	0.000727107
FBgn0266172	2.502407003	6.19E-06	0.000727107

FBgn0030653	1.33957201	6.30E-06	0.000730489
FBgn0033340	2.005113344	6.56E-06	0.000751336
FBgn0052564	1.75227029	7.00E-06	0.000792302
FBgn0038043	1.081163476	7.49E-06	0.000826783
FBgn0039635	1.029415128	8.17E-06	0.000892052
FBgn0052857	-2.05238705	9.68E-06	0.001032096
FBgn0038948	1.323865426	1.02E-05	0.001053772
FBgn0051950	1.775378275	1.02E-05	0.001053772
FBgn0000084	1.112591263	1.04E-05	0.001053772
FBgn0003062	1.044303095	1.04E-05	0.001053772
FBgn0011272	1.17080501	1.05E-05	0.001053772
FBgn0025382	1.141999193	1.17E-05	0.001169776
FBgn0031381	1.051061593	1.20E-05	0.00117857
FBgn0037312	1.018967282	1.21E-05	0.00117857
FBgn0034879	1.232858769	1.24E-05	0.001201135
FBgn0263911	1.39048343	1.33E-05	0.001261015
FBgn0030645	1.429502896	1.33E-05	0.001261015
FBgn0030051	1.405609822	1.39E-05	0.001305146
FBgn0025558	1.187953198	1.49E-05	0.001364087
FBgn0002174	1.102139674	1.67E-05	0.001475896
FBgn0042112	1.215689172	1.70E-05	0.001484592
FBgn0031092	1.110230392	1.98E-05	0.001704332
FBgn0036135	1.452698601	1.98E-05	0.001704332
FBgn0032472	-1.380950457	2.18E-05	0.001822359
FBgn0037131	1.369389194	2.53E-05	0.002079224
FBgn0014028	1.03681636	2.76E-05	0.002206453
FBgn0031099	1.094781966	2.81E-05	0.002212597
FBgn0031050	1.023806691	2.94E-05	0.002271725
FBgn0031021	1.160970266	3.02E-05	0.00230623
FBgn0015521	1.022063148	3.06E-05	0.00230623
FBgn0013764	1.076747968	3.06E-05	0.00230623
FBgn0011722	1.046620531	3.17E-05	0.002367925
FBgn0027794	1.023684854	3.26E-05	0.002419511
FBgn0027791	1.317487607	3.37E-05	0.002461626
FBgn0265356	1.383998403	3.42E-05	0.002481941
FBgn0033520	1.062563467	3.55E-05	0.002508429
FBgn0267649	1.304587951	3.57E-05	0.002508429

FBgn0035587	1.468031161	3.62E-05	0.002522209
FBgn0051550	1.485869649	4.48E-05	0.00299061
FBgn0030103	1.096304686	4.63E-05	0.003055128
FBgn0033341	1.248590558	4.65E-05	0.003055128
FBgn0040890	1.108774491	4.68E-05	0.003055128
FBgn0024234	1.043511353	4.76E-05	0.003068324
FBgn0040534	2.032445509	5.08E-05	0.003226094
FBgn0032638	-2.728172499	5.22E-05	0.003256616
FBgn0034877	1.177206035	6.35E-05	0.003824563
FBgn0039665	1.290995883	6.39E-05	0.003824563
FBgn0036667	2.263365554	7.24E-05	0.004224938
FBgn0266448	1.428270627	7.48E-05	0.004308529
FBgn0051809	1.656287646	7.66E-05	0.004327347
FBgn0033879	1.160163057	7.68E-05	0.004327347
FBgn0026372	1.060534156	8.16E-05	0.004530397
FBgn0051810	3.28254491	8.18E-05	0.004530397
FBgn0033603	1.088634315	8.74E-05	0.004795874
FBgn0027497	3.029115744	9.18E-05	0.004935624
FBgn0029747	1.011380492	9.52E-05	0.005003759
FBgn0037356	1.013042216	9.56E-05	0.005003759
FBgn0039406	1.052799972	9.60E-05	0.005003759
FBgn0033480	1.079880691	9.97E-05	0.005166783
FBgn0039038	2.466172343	0.00010491	0.005289428
FBgn0001989	1.105775386	0.000105747	0.005302774
FBgn0034647	-1.05856794	0.000112915	0.005565317
FBgn0259140	1.395921465	0.000115103	0.005565317
FBgn0004047	1.027600961	0.000132589	0.006252513
FBgn0266451	1.117104362	0.00014056	0.006487436
FBgn0031148	1.013013728	0.000144521	0.006637218
FBgn0031913	1.024616041	0.000147579	0.006744298
FBgn0086695	3.632131252	0.000150249	0.006799308
FBgn0040342	1.09054399	0.00015303	0.006825298
FBgn0040211	-1.257296358	0.00015977	0.007074166
FBgn0040575	1.40420747	0.000171782	0.007441034
FBgn0267650	3.031348992	0.00017245	0.007441034
FBgn0010433	1.241290327	0.000190856	0.007963989
FBgn0032075	1.537117173	0.000200068	0.008212508

FBgn0083961	1.125449503	0.000206222	0.008390899
FBgn0020618	1.016711561	0.000209296	0.008478781
FBgn0042206	-1.405680574	0.000212192	0.008558736
FBgn0069923	2.326448054	0.000214937	0.008606849
FBgn0034793	1.133714645	0.000234366	0.009135345
FBgn0036415	1.546005558	0.000240698	0.009296737
FBgn0035144	1.340189375	0.000248591	0.00945155
FBgn0030588	-1.308179813	0.000267976	0.01002424
FBgn0052536	1.133987988	0.00026974	0.010049715
FBgn0029897	1.067306003	0.000286825	0.010601115
FBgn0015031	1.301639409	0.000297071	0.010936239
FBgn0028740	1.519886042	0.000349201	0.01250785
FBgn0034580	5.106368285	0.000354605	0.012556001
FBgn0261363	1.040720596	0.000356829	0.012586692
FBgn0260004	-1.077403844	0.000364277	0.012800741
FBgn0034517	1.080992692	0.00036672	0.012810675
FBgn0040923	1.239550827	0.000372867	0.012859076
FBgn0032171	1.081321312	0.000414464	0.01403278
FBgn0031261	1.079783617	0.000421577	0.014119014
FBgn0051823	1.467582251	0.00043105	0.01438437
FBgn0003149	1.079027164	0.000461778	0.015031275
FBgn0000046	1.006353898	0.000503549	0.016109299
FBgn0087041	1.187825505	0.000513976	0.016329292
FBgn0086355	1.039536752	0.000560254	0.017550625
FBgn0050052	-1.628911639	0.000596042	0.018309534
FBgn0040682	-1.046762482	0.000605848	0.018549356
FBgn0033728	1.981108554	0.000633242	0.019197983
FBgn0035199	1.001894934	0.000782522	0.022268285
FBgn0032835	-1.538155923	0.000811574	0.022815075
FBgn0015568	-1.161291917	0.000819562	0.022840848
FBgn0038774	1.496083666	0.000896556	0.024680558
FBgn0033850	1.021142725	0.0009113	0.025012228
FBgn0031735	1.239485648	0.000916067	0.025068897
FBgn0053307	-1.144386807	0.000965077	0.026255194
FBgn0039084	-1.185364342	0.00110248	0.028973678
FBgn0083956	1.02095889	0.001280123	0.031753203
FBgn0034755	1.178480007	0.001338107	0.032593963

FBgn0052783	1.977827797	0.001409973	0.033650366
FBgn0036778	1.105891111	0.001411016	0.033650366
FBgn0040736	-1.662934106	0.001444922	0.034195256
FBgn0029835	1.033240048	0.001452465	0.034286308
FBgn0030005	1.556311186	0.001506902	0.035212914
FBgn0031879	1.045337013	0.001535638	0.035349583
FBgn0262954	1.893470131	0.001544303	0.035374073
FBgn0052069	1.619656495	0.001626634	0.036626913
FBgn0010435	1.085248876	0.001694394	0.03742594
FBgn0030846	-1.847323218	0.001756127	0.038303711
FBgn0085353	8.159035248	0.001758907	0.038303711
FBgn0259229	2.158084099	0.001907613	0.040220285
FBgn0031080	1.130766653	0.002095678	0.042728798
FBgn0039298	3.019518198	0.002210113	0.044669325
FBgn0029858	1.009044872	0.002380194	0.047181748
FBgn0036752	-1.089843062	0.002414555	0.047558011
FBgn0085249	8.53777027	0.002429164	0.047643448
FBgn0037236	5.373080745	0.002552435	0.049024728
FBgn0031737	1.051375759	0.002611371	0.04994988

Table 2.7 ARGs in the 10 day old adult brain

Gene	logFC	PValue	FDR
FBgn0051077	-67.96325343	2.42E-101	2.32E-97
FBgn0040687	-64.3403938	1.51E-66	7.23E-63
FBgn0036766	-60.42555255	1.97E-61	6.29E-58
FBgn0034582	-51.23475793	6.18E-48	1.34E-44
FBgn0030773	4.353589946	6.98E-48	1.34E-44
FBgn0030929	4.399435759	9.61E-45	1.53E-41
FBgn0013343	6.477529387	4.14E-42	5.66E-39
FBgn0040502	4.738084731	5.72E-40	6.84E-37
FBgn0051104	3.950157182	1.30E-39	1.38E-36
FBgn0034247	3.714831522	3.06E-38	2.93E-35
FBgn0037563	-47.78745511	4.94E-37	4.29E-34
FBgn0038756	-46.32755415	6.21E-36	4.96E-33
FBgn0000078	2.904950959	1.80E-34	1.33E-31
FBgn0259918	-6.46116109	4.02E-34	2.75E-31
FBgn0010246	3.590335317	7.98E-33	5.09E-30
FBgn0034031	3.501923574	1.51E-29	9.01E-27
FBgn0261930	3.452637264	2.38E-29	1.34E-26
FBgn0043575	3.937257099	4.57E-29	2.43E-26
FBgn0262608	-38.94008486	1.34E-28	6.77E-26
FBgn0259101	3.165142866	2.22E-28	1.06E-25
FBgn0039310	3.446638411	3.33E-28	1.52E-25
FBgn0000079	2.777103814	5.52E-28	2.40E-25
FBgn0051288	2.926181755	8.93E-28	3.72E-25
FBgn0037386	2.741876897	1.20E-27	4.77E-25
FBgn0267408	2.55756371	2.71E-27	1.04E-24
FBgn0051004	2.876700289	7.87E-27	2.89E-24
FBgn0036022	4.11938418	2.95E-26	1.05E-23
FBgn0038257	3.099993795	1.66E-25	5.67E-23
FBgn0038652	2.532999011	2.43E-25	8.00E-23
FBgn0038135	3.23647172	2.61E-25	8.32E-23
FBgn0039154	3.370125802	3.03E-25	9.34E-23
FBgn0046302	2.696894666	3.44E-25	1.03E-22
FBgn0040349	3.155902781	7.32E-25	2.12E-22
FBgn0036607	-36.57952069	2.85E-24	8.01E-22

FBgn0037973	2.476724908	9.87E-24	2.70E-21
FBgn0039315	2.804280959	3.19E-23	8.47E-21
FBgn0051148	3.130258517	5.75E-23	1.49E-20
FBgn0002570	5.99574402	6.01E-23	1.51E-20
FBgn0025454	2.291254004	6.21E-23	1.52E-20
FBgn0264750	2.66561068	7.15E-23	1.71E-20
FBgn0030777	2.895139094	7.32E-23	1.71E-20
FBgn0026755	2.663497229	1.13E-22	2.57E-20
FBgn0040252	2.840124531	2.81E-22	6.25E-20
FBgn0030396	2.63250745	4.69E-22	1.02E-19
FBgn0035094	2.618877131	4.84E-22	1.03E-19
FBgn0030775	2.783719237	2.83E-21	5.89E-19
FBgn0036752	2.839050911	5.23E-21	1.07E-18
FBgn0261575	5.246593916	1.12E-20	2.23E-18
FBgn0035476	2.682206892	1.36E-19	2.66E-17
FBgn0031741	2.391488468	2.76E-19	5.28E-17
FBgn0027843	2.142853427	5.86E-19	1.10E-16
FBgn0040299	2.437198401	6.62E-19	1.22E-16
FBgn0030594	2.338799659	1.45E-18	2.61E-16
FBgn0050052	3.103276752	4.90E-18	8.67E-16
FBgn0003053	2.467489478	5.57E-18	9.69E-16
FBgn0031801	2.10994154	6.35E-18	1.09E-15
FBgn0030040	2.406349437	7.30E-18	1.22E-15
FBgn0010241	2.142488029	8.85E-18	1.46E-15
FBgn0030776	2.420114268	4.81E-17	7.79E-15
FBgn0051300	2.139242647	6.60E-17	1.05E-14
FBgn0034085	2.909228639	8.26E-17	1.29E-14
FBgn0053514	2.473838655	1.33E-16	2.05E-14
FBgn0039092	2.913565541	4.27E-16	6.48E-14
FBgn0033981	2.364410882	4.81E-16	7.19E-14
FBgn0030774	2.484519938	7.68E-16	1.13E-13
FBgn0001258	1.915253618	9.15E-16	1.33E-13
FBgn0010223	2.081775696	2.25E-15	3.21E-13
FBgn0040827	3.130040755	2.57E-15	3.61E-13
FBgn0038466	2.101802106	4.09E-15	5.68E-13
FBgn0024361	2.119687054	9.13E-15	1.25E-12
FBgn0037146	1.99042562	1.24E-14	1.67E-12

FBgn0050489	2.08220882	1.43E-14	1.90E-12
FBgn0003863	6.143709857	1.65E-14	2.16E-12
FBgn0033079	1.973383603	5.46E-14	7.06E-12
FBgn0032235	1.990560908	6.99E-14	8.90E-12
FBgn0029932	1.701037066	7.07E-14	8.90E-12
FBgn0033782	2.14138356	7.68E-14	9.54E-12
FBgn0035360	1.826744435	1.40E-13	1.71E-11
FBgn0027562	1.912720629	3.56E-13	4.31E-11
FBgn0004552	-2.030543281	3.70E-13	4.43E-11
FBgn0034717	1.870177769	4.54E-13	5.36E-11
FBgn0029766	1.712458452	7.77E-13	9.06E-11
FBgn0051091	2.093267912	1.07E-12	1.23E-10
FBgn0050456	1.799520229	1.24E-12	1.41E-10
FBgn0033234	1.743929361	1.96E-12	2.21E-10
FBgn0037678	1.783144868	2.46E-12	2.74E-10
FBgn0038292	1.775266009	2.77E-12	3.05E-10
FBgn0037288	1.815390807	2.88E-12	3.13E-10
FBgn0032187	1.937949247	3.34E-12	3.59E-10
FBgn0041156	1.7578858	8.11E-12	8.62E-10
FBgn0027106	2.027729057	1.17E-11	1.22E-09
FBgn0038194	1.696336374	1.18E-11	1.22E-09
FBgn0039326	1.633680256	1.74E-11	1.79E-09
FBgn0032116	2.460031187	2.42E-11	2.46E-09
FBgn0025709	2.201041842	2.86E-11	2.89E-09
FBgn0039316	1.589552271	4.36E-11	4.34E-09
FBgn0038353	2.758132272	5.65E-11	5.57E-09
FBgn0032726	1.60824314	6.15E-11	6.01E-09
FBgn0011280	1.527376437	6.67E-11	6.45E-09
FBgn0032283	2.463689113	6.91E-11	6.61E-09
FBgn0036493	1.867695388	8.11E-11	7.69E-09
FBgn0063492	1.684573908	1.22E-10	1.15E-08
FBgn0033395	1.822000225	1.36E-10	1.26E-08
FBgn0037714	1.826625416	2.02E-10	1.85E-08
FBgn0037387	1.421919043	2.46E-10	2.24E-08
FBgn0085428	1.986486646	2.60E-10	2.35E-08
FBgn0028491	1.492258926	2.73E-10	2.44E-08
FBgn0001089	1.405455466	3.43E-10	3.04E-08

FBgn0029835	1.862519026	3.55E-10	3.12E-08
FBgn0025643	1.93798094	4.37E-10	3.80E-08
FBgn0034394	1.565391098	5.15E-10	4.44E-08
FBgn0040503	-2.188499589	5.32E-10	4.54E-08
FBgn0034509	2.207075717	5.62E-10	4.76E-08
FBgn0038398	1.946987518	7.31E-10	6.14E-08
FBgn0030993	1.580346445	1.02E-09	8.48E-08
FBgn0040291	-6.517828278	1.09E-09	8.95E-08
FBgn0030484	1.918087272	1.09E-09	8.95E-08
FBgn0032770	2.083855796	1.16E-09	9.44E-08
FBgn0040923	1.655173099	1.20E-09	9.67E-08
FBgn0267651	-1.624031305	2.22E-09	1.76E-07
FBgn0042119	2.164738761	2.24E-09	1.76E-07
FBgn0034612	1.694947389	2.24E-09	1.76E-07
FBgn0035313	-21.39030181	2.40E-09	1.87E-07
FBgn0038236	2.028942416	2.65E-09	2.04E-07
FBgn0038299	-1.495798965	3.04E-09	2.33E-07
FBgn0028394	1.547581004	4.27E-09	3.24E-07
FBgn0040250	1.914664891	5.05E-09	3.80E-07
FBgn0011770	1.39506643	6.00E-09	4.47E-07
FBgn0025620	1.578462393	6.03E-09	4.47E-07
FBgn0036835	-1.654623522	6.17E-09	4.54E-07
FBgn0036756	1.457560899	7.46E-09	5.45E-07
FBgn0030747	1.357732541	7.82E-09	5.67E-07
FBgn0036205	1.54717132	8.54E-09	6.14E-07
FBgn0063497	1.344902217	8.73E-09	6.24E-07
FBgn0033978	1.693950557	1.07E-08	7.55E-07
FBgn0085256	-1.946975807	1.54E-08	1.08E-06
FBgn0012037	1.281229297	1.67E-08	1.17E-06
FBgn0035189	1.558091001	1.80E-08	1.25E-06
FBgn0034628	1.296618211	1.81E-08	1.25E-06
FBgn0063493	1.344857438	1.86E-08	1.27E-06
FBgn0037731	-3.734465239	2.22E-08	1.51E-06
FBgn0037354	1.277877099	2.41E-08	1.62E-06
FBgn0035040	1.657154042	2.88E-08	1.93E-06
FBgn0034629	1.512657845	2.94E-08	1.96E-06
FBgn0063491	1.378700972	2.98E-08	1.97E-06

FBgn0050339	1.401204065	3.14E-08	2.06E-06
FBgn0032715	1.303151706	3.32E-08	2.15E-06
FBgn0039685	-1.386052934	3.32E-08	2.15E-06
FBgn0035355	1.353919446	3.75E-08	2.41E-06
FBgn0001248	1.205123139	5.27E-08	3.36E-06
FBgn0050479	1.538993431	6.24E-08	3.96E-06
FBgn0015039	1.265712805	6.84E-08	4.31E-06
FBgn0031418	1.300611618	7.01E-08	4.38E-06
FBgn0259236	1.441635233	7.13E-08	4.43E-06
FBgn0036727	2.418930402	7.35E-08	4.54E-06
FBgn0015714	2.034024535	7.46E-08	4.57E-06
FBgn0051089	1.422409322	7.86E-08	4.79E-06
FBgn0003892	1.358670672	8.25E-08	5.00E-06
FBgn0035264	1.394677902	1.07E-07	6.45E-06
FBgn0010504	1.258900468	1.08E-07	6.47E-06
FBgn0050411	1.97381978	1.19E-07	7.09E-06
FBgn0052633	-19.41738484	1.21E-07	7.10E-06
FBgn0033582	1.622285801	1.22E-07	7.10E-06
FBgn0026061	1.343486598	1.22E-07	7.10E-06
FBgn0032075	2.130232474	1.47E-07	8.52E-06
FBgn0039084	1.48554877	2.55E-07	1.47E-05
FBgn0037174	1.438570971	3.01E-07	1.72E-05
FBgn0032505	-8.406388207	3.06E-07	1.75E-05
FBgn0259678	1.34244557	3.33E-07	1.88E-05
FBgn0039040	1.780253384	3.46E-07	1.95E-05
FBgn0003187	-1.869345204	4.44E-07	2.48E-05
FBgn0040992	1.311140642	5.65E-07	3.13E-05
FBgn0260228	1.311140642	5.65E-07	3.13E-05
FBgn0031559	-1.920356088	7.39E-07	4.06E-05
FBgn0043783	1.230556925	7.67E-07	4.19E-05
FBgn0037974	1.275837013	8.95E-07	4.87E-05
FBgn0036996	1.979246913	1.10E-06	5.93E-05
FBgn0002985	1.64125781	1.12E-06	6.03E-05
FBgn0259834	1.109198013	1.13E-06	6.05E-05
FBgn0050098	-1.565826216	1.20E-06	6.38E-05
FBgn0031432	1.258057282	1.33E-06	7.04E-05
FBgn0033075	1.128853576	1.41E-06	7.43E-05

FBgn0015038	1.409172346	1.55E-06	8.10E-05
FBgn0261393	1.236138727	1.99E-06	0.000103695
FBgn0032167	1.229897492	2.57E-06	0.000133155
FBgn0031548	1.350305827	2.65E-06	0.00013637
FBgn0036289	1.22470885	3.13E-06	0.000160017
FBgn0038804	1.138695751	3.40E-06	0.00017317
FBgn0029657	-1.751418401	3.46E-06	0.000174988
FBgn0038680	1.077505794	3.51E-06	0.000176912
FBgn0038914	-1.93169947	3.62E-06	0.000181557
FBgn0034647	-1.316849417	4.45E-06	0.000221161
FBgn0032685	1.536445161	4.46E-06	0.000221161
FBgn0024997	1.067272443	4.78E-06	0.000235803
FBgn0039008	-2.984863863	4.82E-06	0.000236501
FBgn0029091	2.184094543	5.27E-06	0.000257272
FBgn0037144	1.205242968	5.46E-06	0.000264446
FBgn0051720	1.195167713	5.47E-06	0.000264446
FBgn0039207	1.02591825	5.69E-06	0.000273674
FBgn0031012	1.117745296	5.90E-06	0.000282175
FBgn0002562	-1.155214348	7.82E-06	0.000372221
FBgn0085424	1.057048523	8.41E-06	0.000398308
FBgn0039038	-1.818189333	8.54E-06	0.000402316
FBgn0004167	1.175751678	8.86E-06	0.000415653
FBgn0085195	-1.180691687	9.10E-06	0.000424663
FBgn0035679	1.008081166	9.14E-06	0.000424663
FBgn0033820	-1.063619847	9.30E-06	0.000429715
FBgn0038327	-4.689999694	1.01E-05	0.000464364
FBgn0052476	1.147127083	1.11E-05	0.00050877
FBgn0030737	1.250091798	1.81E-05	0.000815583
FBgn0020416	-1.015861307	1.88E-05	0.000843784
FBgn0038419	1.153462358	1.90E-05	0.000845505
FBgn0046876	-1.766102045	2.06E-05	0.000910311
FBgn0032124	1.190139453	2.42E-05	0.001063386
FBgn0036806	1.006731489	2.64E-05	0.001154326
FBgn0260479	1.031663495	3.26E-05	0.001419411
FBgn0010497	1.754582588	4.04E-05	0.001750817
FBgn0034736	1.075158681	4.41E-05	0.001902058
FBgn0262794	1.413613894	4.53E-05	0.001941934

FBgn0040942	1.172428583	4.95E-05	0.002113941
FBgn0014903	1.056440539	5.13E-05	0.002179779
FBgn0038897	1.123209291	5.27E-05	0.002229833
FBgn0053460	-1.828567252	5.29E-05	0.002230754
FBgn0038391	-11.98153352	5.44E-05	0.00228449
FBgn0039754	1.621577191	6.56E-05	0.00274144
FBgn0033296	4.353485837	8.88E-05	0.003677438
FBgn0029990	-1.046001965	9.34E-05	0.003851709
FBgn0035904	1.060132746	0.000105523	0.004315247
FBgn0027521	1.011098715	0.000120236	0.0048337
FBgn0038516	1.350629577	0.000125552	0.005025119
FBgn0038706	1.243568602	0.000126104	0.005025119
FBgn0004427	-10.54029882	0.000126573	0.005025119
FBgn0038404	2.014498147	0.000128373	0.005054613
FBgn0032835	1.047211439	0.000186355	0.007277718
FBgn0034229	1.177788803	0.000189548	0.007342485
FBgn0032085	1.06873136	0.000199201	0.007623839
FBgn0032945	1.440447596	0.000227476	0.008671264
FBgn0065035	1.50284408	0.000233301	0.008858025
FBgn0021776	1.036188204	0.000244266	0.009201319
FBgn0034047	1.304471339	0.000245824	0.009223707
FBgn0052686	1.152281411	0.000255943	0.009565883
FBgn0067052	-1.218337551	0.000273797	0.010153834
FBgn0038179	1.147655153	0.00027776	0.01026104
FBgn0034490	1.099534264	0.000290332	0.010684224
FBgn0038820	1.233751033	0.000333696	0.012232959
FBgn0003250	-1.505933329	0.000343687	0.012551132
FBgn0038380	1.000941895	0.000355408	0.012880844
FBgn0037936	1.044160953	0.00041888	0.014971093
FBgn0043069	-1.13206064	0.000419341	0.014971093
FBgn0024920	-1.296363519	0.000486674	0.016994509
FBgn0051205	1.223300337	0.000528917	0.018335774
FBgn0051321	1.001465941	0.000576969	0.019786536
FBgn0033970	1.175841048	0.000585783	0.020017052
FBgn0069973	-1.106437258	0.000657326	0.02214542
FBgn0050269	1.010677517	0.000721163	0.023958639
FBgn0013772	1.154299338	0.000729519	0.024152374

FBgn0028841	-1.742171121	0.000789685	0.025875695
FBgn0032161	1.042138827	0.000897312	0.029005007
FBgn0039821	1.29620553	0.000998876	0.032071291
FBgn0032896	-1.101461712	0.001120552	0.035857657
FBgn0261628	-1.399464405	0.001138188	0.036300612
FBgn0053099	1.416752895	0.001271683	0.040024539
FBgn0030310	-1.025741897	0.001335959	0.041511862
FBgn0036622	1.113265998	0.001344477	0.041630914
FBgn0003132	1.075366574	0.001350601	0.041685657
FBgn0031700	-1.296516092	0.001437879	0.043675005
FBgn0263321	-1.236146119	0.001511223	0.045044812

Table 2.8 ARGs in the 25-day-old adult brain

Gene	logFC	PValue	FDR
FBgn0003863	6.38280846	1.97E-140	1.90E-136
FBgn0028841	2.084964952	1.20E-48	5.21E-45
FBgn0050360	4.204187353	1.62E-48	5.21E-45
FBgn0037755	3.034703332	1.35E-35	3.27E-32
FBgn0030688	3.041586015	2.90E-32	5.60E-29
FBgn0263235	2.372705506	1.57E-29	2.52E-26
FBgn0263234	2.34963981	5.02E-27	6.94E-24
FBgn0033696	1.944735582	7.22E-27	8.72E-24
FBgn0051956	1.847190528	1.81E-22	1.94E-19
FBgn0263748	1.836525887	2.23E-22	2.15E-19
FBgn0037563	1.811737573	3.86E-22	3.40E-19
FBgn0003357	3.315616153	8.54E-22	6.88E-19
FBgn0034582	1.829560234	6.17E-21	4.59E-18
FBgn0010241	-1.512369446	1.31E-20	9.06E-18
FBgn0034647	-1.685041469	4.31E-19	2.78E-16
FBgn0031701	-2.062201073	1.22E-17	7.36E-15
FBgn0039298	1.298693643	1.68E-17	9.57E-15
FBgn0038756	1.569585756	3.80E-17	2.04E-14
FBgn0042129	2.566787481	1.39E-16	7.07E-14
FBgn0036362	1.974846789	6.27E-16	3.03E-13
FBgn0261845	2.219714212	1.26E-15	5.81E-13
FBgn0039670	1.455493745	6.61E-15	2.90E-12
FBgn0085481	1.830433887	8.02E-15	3.34E-12
FBgn0261714	-1.620096477	8.29E-15	3.34E-12
FBgn0038299	-1.13147535	2.10E-14	8.12E-12
FBgn0053349	-1.611974386	5.64E-14	2.10E-11
FBgn0033835	-1.596782226	8.46E-14	3.03E-11
FBgn0042173	-7.421049094	1.67E-13	5.78E-11
FBgn0052786	2.221849959	2.01E-13	6.70E-11
FBgn0260234	-1.318292598	2.08E-13	6.71E-11
FBgn0035880	-1.055564324	2.22E-13	6.93E-11
FBgn0004623	-1.278196573	8.47E-13	2.56E-10
FBgn0261631	2.263602431	1.71E-12	4.78E-10
FBgn0053808	-7.281216452	1.73E-12	4.78E-10

FBgn0053099	1.638541523	2.74E-12	7.36E-10
FBgn0037534	1.126474214	3.04E-12	7.95E-10
FBgn0033079	1.277125799	4.19E-12	1.07E-09
FBgn0032783	1.033110254	4.40E-12	1.09E-09
FBgn0262608	1.5184828	4.61E-12	1.11E-09
FBgn0038404	1.633678852	6.03E-12	1.42E-09
FBgn0034871	1.238634373	7.81E-12	1.80E-09
FBgn0035636	1.813599992	1.11E-11	2.49E-09
FBgn0040687	1.214210976	1.99E-11	4.37E-09
FBgn0051077	1.215372976	2.17E-11	4.65E-09
FBgn0024943	-1.217473702	2.33E-11	4.89E-09
FBgn0032639	-1.498795553	2.50E-11	5.14E-09
FBgn0000120	-1.167021761	2.55E-11	5.14E-09
FBgn0038749	-1.524671472	2.71E-11	5.35E-09
FBgn0033785	1.553558139	2.89E-11	5.59E-09
FBgn0002938	-1.122832387	3.61E-11	6.71E-09
FBgn0036831	1.365589531	3.90E-11	7.09E-09
FBgn0041156	1.324318863	3.96E-11	7.09E-09
FBgn0000497	1.519751758	1.25E-10	2.20E-08
FBgn0038079	1.219622005	1.38E-10	2.38E-08
FBgn0053470	-1.392972686	2.16E-10	3.67E-08
FBgn0028396	-1.088884011	4.39E-10	7.31E-08
FBgn0036220	1.664262255	4.72E-10	7.74E-08
FBgn0000071	-1.480137907	6.47E-10	1.04E-07
FBgn0038391	1.478161048	6.58E-10	1.04E-07
FBgn0000121	-1.163222177	6.86E-10	1.07E-07
FBgn0058198	1.568012063	7.66E-10	1.18E-07
FBgn0032025	1.172189972	8.32E-10	1.26E-07
FBgn0003248	-1.64432682	1.05E-09	1.54E-07
FBgn0013343	1.378684371	1.21E-09	1.75E-07
FBgn0036203	1.153329937	1.31E-09	1.86E-07
FBgn0030569	1.499245532	1.35E-09	1.89E-07
FBgn0032665	2.051545634	1.66E-09	2.29E-07
FBgn0036622	1.616488905	1.79E-09	2.43E-07
FBgn0052633	1.332820669	1.88E-09	2.52E-07
FBgn0037724	1.249730493	1.96E-09	2.60E-07
FBgn0051106	1.506176806	2.44E-09	3.19E-07

FBgn0004784	-1.350038478	2.98E-09	3.84E-07
FBgn0028518	1.435808013	4.29E-09	5.45E-07
FBgn0036766	1.073168617	4.35E-09	5.46E-07
FBgn0003861	-1.185500187	5.81E-09	7.20E-07
FBgn0033541	1.114529445	5.93E-09	7.26E-07
FBgn0267435	-1.329952711	6.34E-09	7.67E-07
FBgn0035571	1.517671907	6.74E-09	8.05E-07
FBgn0039486	1.509565413	6.92E-09	8.16E-07
FBgn0085353	1.042106241	8.08E-09	9.42E-07
FBgn0036066	1.719442781	9.24E-09	1.05E-06
FBgn0050365	2.709148016	9.36E-09	1.05E-06
FBgn0085256	-1.723992064	1.07E-08	1.18E-06
FBgn0039107	2.047244707	1.14E-08	1.26E-06
FBgn0035313	1.218742703	1.18E-08	1.28E-06
FBgn0259918	-1.944805994	1.59E-08	1.69E-06
FBgn0036287	-1.070938302	1.66E-08	1.75E-06
FBgn0036607	1.335351774	3.38E-08	3.51E-06
FBgn0040503	-1.106901767	3.54E-08	3.65E-06
FBgn0040069	1.241696353	4.42E-08	4.45E-06
FBgn0036232	1.100345473	5.62E-08	5.54E-06
FBgn0030984	1.179003347	6.18E-08	6.03E-06
FBgn0025709	1.220720163	6.72E-08	6.49E-06
FBgn0044812	-1.011947454	7.55E-08	7.23E-06
FBgn0032082	1.36114919	1.24E-07	1.15E-05
FBgn0029827	1.129226964	1.61E-07	1.47E-05
FBgn0000206	-1.038827741	2.16E-07	1.95E-05
FBgn0032638	-1.672227722	2.20E-07	1.97E-05
FBgn0035043	1.475861457	3.04E-07	2.67E-05
FBgn0040363	1.281609763	3.26E-07	2.84E-05
FBgn0034321	1.310917227	3.46E-07	2.96E-05
FBgn0003187	-1.439332945	3.93E-07	3.30E-05
FBgn0042102	1.263373471	3.97E-07	3.31E-05
FBgn0033124	1.782738119	4.31E-07	3.53E-05
FBgn0265185	1.556256782	5.02E-07	4.08E-05
FBgn0050098	-1.204508203	5.22E-07	4.21E-05
FBgn0032055	-1.252083379	6.12E-07	4.81E-05
FBgn0036727	2.102132201	7.81E-07	5.99E-05

FBgn0032075	1.04234506	7.81E-07	5.99E-05
FBgn0042086	1.669226365	9.98E-07	7.60E-05
FBgn0005614	-1.103891081	1.02E-06	7.67E-05
FBgn0065035	-1.033462438	1.16E-06	8.63E-05
FBgn0037520	1.404086455	1.39E-06	0.000100774
FBgn0000594	-1.441551831	1.54E-06	0.000110338
FBgn0033787	1.002223543	1.86E-06	0.000131416
FBgn0039821	1.262933736	1.99E-06	0.000138727
FBgn0051718	-1.238094799	2.10E-06	0.00014529
FBgn0033633	1.262882596	2.22E-06	0.000152405
FBgn0054054	-1.493685457	2.39E-06	0.000163044
FBgn0030756	1.414147647	2.53E-06	0.000169976
FBgn0015336	1.004370779	2.62E-06	0.000174658
FBgn0035398	1.550796141	2.97E-06	0.000196921
FBgn0038412	1.238554393	3.60E-06	0.000233606
FBgn0010388	-1.996532688	3.89E-06	0.000249096
FBgn0034509	1.209254704	3.96E-06	0.000250015
FBgn0035308	1.311747441	4.25E-06	0.000265189
FBgn0034758	1.108641942	4.49E-06	0.00027823
FBgn0002936	-1.378484887	5.07E-06	0.00031025
FBgn0035611	1.141597637	5.10E-06	0.000310355
FBgn0035574	1.189790095	6.23E-06	0.00037427
FBgn0028381	1.156593635	7.82E-06	0.000455582
FBgn0030331	-1.345451733	1.01E-05	0.000571293
FBgn0010381	-1.810389523	1.03E-05	0.000580046
FBgn0000047	-1.76704644	1.15E-05	0.000637254
FBgn0013772	1.218892941	1.21E-05	0.000662069
FBgn0067052	-1.182970754	1.47E-05	0.000789923
FBgn0051901	1.322536387	1.56E-05	0.000832505
FBgn0050343	1.259948567	1.71E-05	0.000902796
FBgn0034470	2.576156714	1.72E-05	0.000906156
FBgn0038631	1.333369435	1.86E-05	0.000966106
FBgn0016013	-1.94439335	1.88E-05	0.000969733
FBgn0036264	1.685895837	1.96E-05	0.001000978
FBgn0011279	1.097236325	3.48E-05	0.001674541
FBgn0004009	1.472830011	3.55E-05	0.001690049
FBgn0040291	-1.721155151	4.44E-05	0.002062428

FBgn0041581	-1.02219076	4.65E-05	0.002129677
FBgn0037427	1.496794166	5.15E-05	0.002340294
FBgn0050008	-1.425689254	5.39E-05	0.002433442
FBgn0034293	-1.2026646	6.35E-05	0.0028312
FBgn0002570	2.958752561	7.73E-05	0.003351751
FBgn0001321	1.177688878	8.06E-05	0.003465757
FBgn0040074	-1.331275735	8.20E-05	0.003509307
FBgn0038846	1.291637745	8.75E-05	0.003710284
FBgn0028887	1.36616601	9.86E-05	0.004076279
FBgn0036778	1.051672872	9.94E-05	0.004090306
FBgn0030928	1.283842954	0.000114634	0.004580638
FBgn0035379	-1.145793526	0.000158747	0.006214919
FBgn0039523	1.141197816	0.000164549	0.006390317
FBgn0031554	1.403476147	0.000170148	0.006581309
FBgn0035583	1.034856468	0.000257571	0.009579662
FBgn0013275	-3.749828786	0.000346489	0.01269148
FBgn0051104	1.486621351	0.000367919	0.013324989
FBgn0042119	1.295626277	0.000415865	0.014837437
FBgn0028920	1.510165657	0.000488716	0.016932075
FBgn0013276	2.873589264	0.000503702	0.017333812
FBgn0000078	1.353644419	0.000529652	0.018034263
FBgn0085249	1.005123898	0.00054699	0.018429951
FBgn0032286	-1.036217892	0.000813634	0.025881045
FBgn0083974	1.077967096	0.000846836	0.02682094
FBgn0053105	1.23706062	0.000868425	0.027353976
FBgn0031471	-1.141274955	0.001008419	0.030568685
FBgn0261341	1.225183288	0.001028875	0.031035294
FBgn0032770	1.146089133	0.001212897	0.03554155
FBgn0000079	1.240388977	0.00124189	0.036171918
FBgn0000357	-1.118735957	0.001729109	0.048325101
FBgn0028377	1.386918886	0.001785992	0.04977103

Table 2.9 ARGs in adult brain of wCS flies

Gene	logFC	PValue	FDR
FBgn0031176	5.716240376	5.20E-53	5.07E-49
FBgn0034289	4.358698738	4.82E-52	2.35E-48
FBgn0031277	5.924461407	5.22E-44	1.70E-40
FBgn0032505	5.142934016	8.57E-44	2.09E-40
FBgn0085241	5.323170468	6.22E-38	1.21E-34
FBgn0263762	4.378811099	6.86E-33	1.12E-29
FBgn0052726	-4.671454386	4.27E-29	5.95E-26
FBgn0260390	5.496429148	4.13E-27	5.03E-24
FBgn0036024	3.581653303	3.69E-26	4.00E-23
FBgn0031910	7.196965397	9.23E-26	9.01E-23
FBgn0053109	3.679053525	2.48E-25	2.20E-22
FBgn0004429	4.048326446	6.16E-21	5.01E-18
FBgn0023197	3.284691609	7.09E-21	5.32E-18
FBgn0264991	4.790750477	2.27E-20	1.58E-17
FBgn0053265	2.920353841	4.21E-18	2.74E-15
FBgn0004427	3.1762408	5.85E-17	3.57E-14
FBgn0038180	2.206380138	1.76E-14	1.01E-11
FBgn0004425	2.616642741	2.28E-14	1.24E-11
FBgn0004428	3.099094387	4.11E-14	2.11E-11
FBgn0037724	2.495633909	4.60E-14	2.24E-11
FBgn0010357	2.29177788	2.20E-13	1.02E-10
FBgn0263235	2.300509474	1.94E-12	8.22E-10
FBgn0039670	2.07319444	1.94E-12	8.22E-10
FBgn0053532	2.765031014	8.18E-11	3.33E-08
FBgn0012042	-1.552596478	9.51E-11	3.71E-08
FBgn0010359	2.898920299	1.67E-10	6.27E-08
FBgn0003067	-1.31982273	2.42E-10	8.45E-08
FBgn0266488	-1.31982273	2.42E-10	8.45E-08
FBgn0034276	-1.438887819	2.91E-10	9.79E-08
FBgn0038795	-1.614592184	3.64E-09	1.18E-06
FBgn0029091	1.9606443	4.52E-09	1.41E-06
FBgn0002563	-1.356989971	4.61E-09	1.41E-06
FBgn0040606	-1.141803894	8.34E-09	2.47E-06
FBgn0039685	-1.234899693	1.24E-08	3.55E-06

FBgn0040653	-1.396862958	1.43E-08	3.96E-06
FBgn0043578	-1.342230024	1.46E-08	3.96E-06
FBgn0013307	-1.476582201	2.08E-08	5.49E-06
FBgn0039800	-1.182974967	2.29E-08	5.89E-06
FBgn0042102	1.970835855	2.99E-08	7.48E-06
FBgn0066084	1.849497314	3.29E-08	8.03E-06
FBgn0051956	1.943658645	3.77E-08	8.97E-06
FBgn0051778	-1.34977406	4.25E-08	9.78E-06
FBgn0032082	2.024406661	4.33E-08	9.78E-06
FBgn0035781	1.236538303	4.41E-08	9.78E-06
FBgn0050360	1.872654134	5.03E-08	1.09E-05
FBgn0030929	3.229009966	8.29E-08	1.76E-05
FBgn0029831	-1.276954615	8.51E-08	1.77E-05
FBgn0015336	2.365935298	9.46E-08	1.92E-05
FBgn0265187	2.006293309	1.05E-07	2.06E-05
FBgn0052557	1.475192101	1.06E-07	2.06E-05
FBgn0053346	4.087041001	1.16E-07	2.23E-05
FBgn0034197	1.174096332	1.50E-07	2.83E-05
FBgn0032285	-1.247736085	1.90E-07	3.50E-05
FBgn0033789	3.384357058	2.31E-07	4.18E-05
FBgn0039486	1.363590781	4.68E-07	8.31E-05
FBgn0034887	-1.396461104	5.45E-07	9.50E-05
FBgn0061356	-1.294314722	6.22E-07	0.000106454
FBgn0030425	-1.009950619	8.22E-07	0.000138358
FBgn0053099	1.738392851	8.79E-07	0.000145456
FBgn0036362	3.36498773	1.02E-06	0.000166501
FBgn0022700	4.087787487	1.41E-06	0.000220618
FBgn0030311	2.170213236	1.42E-06	0.000220618
FBgn0033633	1.40118898	1.42E-06	0.000220618
FBgn0036220	1.471909057	1.87E-06	0.00027938
FBgn0032435	2.167659904	1.89E-06	0.00027938
FBgn0035398	1.626609401	1.89E-06	0.00027938
FBgn0262608	4.931104165	1.92E-06	0.00027938
FBgn0031514	1.599236849	2.02E-06	0.000289977
FBgn0003863	4.169960554	2.17E-06	0.000305611
FBgn0052633	2.379940499	2.19E-06	0.000305611
FBgn0085453	-1.035605668	2.27E-06	0.000311933

FBgn0027556	1.429227455	2.31E-06	0.000312587
FBgn0038391	1.768672794	3.27E-06	0.00043777
FBgn0038353	4.159979395	3.57E-06	0.000470815
FBgn0035198	2.324289377	3.68E-06	0.000476852
FBgn0034140	-1.05705098	3.71E-06	0.000476852
FBgn0034582	3.581252509	5.35E-06	0.000669388
FBgn0030984	1.651452715	6.15E-06	0.000759762
FBgn0051901	3.879570667	6.64E-06	0.000810737
FBgn0032235	1.95086333	6.82E-06	0.000822187
FBgn0036575	1.771452032	6.98E-06	0.000830501
FBgn0002531	1.575301529	7.61E-06	0.000884531
FBgn0039801	-1.181895806	8.23E-06	0.00094273
FBgn0085481	1.448465181	8.30E-06	0.00094273
FBgn0039299	2.422234653	9.01E-06	0.001010874
FBgn0038431	1.27173891	9.12E-06	0.001011695
FBgn0035571	1.705725336	9.60E-06	0.001052648
FBgn0001208	-1.082256352	1.05E-05	0.001139595
FBgn0037236	4.529830665	1.09E-05	0.001173552
FBgn0032075	1.332648296	1.11E-05	0.001176752
FBgn0039073	-1.016733381	1.24E-05	0.001287583
FBgn0024912	2.511019334	1.36E-05	0.001397737
FBgn0037627	-1.260319842	1.42E-05	0.001447726
FBgn0262531	2.002917585	1.47E-05	0.001480625
FBgn0002570	2.475791697	1.50E-05	0.001496537
FBgn0085428	1.309773714	1.66E-05	0.001630616
FBgn0040060	3.530396195	1.67E-05	0.001630616
FBgn0011227	1.587024752	1.95E-05	0.001879575
FBgn0037570	1.809497717	1.96E-05	0.001879575
FBgn0037684	-1.188311538	1.99E-05	0.001883283
FBgn0032025	1.069824173	2.03E-05	0.001901494
FBgn0000079	3.282390148	2.25E-05	0.002088856
FBgn0030396	1.0991901	2.27E-05	0.002088925
FBgn0032116	3.381793346	2.32E-05	0.002117926
FBgn0033788	4.522999719	2.45E-05	0.002187357
FBgn0051106	1.305842415	2.46E-05	0.002187357
FBgn0037065	1.331365258	2.67E-05	0.002351601
FBgn0034580	3.61403321	2.82E-05	0.002438509

FBgn0035325	1.873503819	2.98E-05	0.002554348
FBgn0024289	-1.0610146	3.09E-05	0.002626847
FBgn0053533	2.046618137	3.22E-05	0.002712177
FBgn0037563	5.565844948	3.32E-05	0.002767789
FBgn0034511	-1.156261581	3.85E-05	0.003156686
FBgn0032287	-1.022144504	4.37E-05	0.003552395
FBgn0023001	1.005745982	4.54E-05	0.003636138
FBgn0032194	-1.397903069	5.19E-05	0.004050744
FBgn0038466	1.559799049	5.86E-05	0.004526344
FBgn0004892	1.892075083	5.89E-05	0.004526344
FBgn0036203	7.323857113	6.68E-05	0.005096701
FBgn0050026	1.119857216	6.83E-05	0.005151984
FBgn0037290	3.247687008	6.86E-05	0.005151984
FBgn0033170	-1.049460441	6.99E-05	0.005212172
FBgn0250815	4.112039546	7.39E-05	0.005462206
FBgn0015010	1.447835916	7.60E-05	0.005537235
FBgn0035313	1.909694595	7.99E-05	0.005775153
FBgn0002565	-1.0122064	8.32E-05	0.005943534
FBgn0052695	-1.271913508	8.40E-05	0.005943534
FBgn0004009	1.529158001	8.48E-05	0.005956736
FBgn0038589	1.751357882	8.70E-05	0.006065086
FBgn0034871	6.716371538	8.94E-05	0.006186764
FBgn0035665	3.839855615	9.16E-05	0.006215962
FBgn0029762	1.20005837	9.16E-05	0.006215962
FBgn0036659	1.772768329	9.17E-05	0.006215962
FBgn0036607	4.041579363	9.80E-05	0.006550886
FBgn0039107	1.479589065	9.90E-05	0.006576125
FBgn0028518	1.976266625	0.000100724	0.006599804
FBgn0050411	1.044027935	0.000102721	0.006641487
FBgn0085265	2.56414352	0.00011466	0.007178361
FBgn0031860	-1.023168091	0.000115087	0.007178361
FBgn0004197	1.796323539	0.000115436	0.007178361
FBgn0051077	6.71443425	0.000125354	0.007745789
FBgn0010246	1.117595649	0.000136667	0.008339253
FBgn0039620	1.394990638	0.000142748	0.008656182
FBgn0261840	5.185574802	0.000149026	0.008926023
FBgn0036831	5.551507932	0.000150328	0.008949114

FBgn0036766	6.173576806	0.000155326	0.009135254
FBgn0031585	2.256214839	0.000157227	0.009155487
FBgn0085353	6.715183806	0.00015784	0.009155487
FBgn0034053	2.803479872	0.000158484	0.009155487
FBgn0042101	1.370959496	0.000160465	0.009215416
FBgn0037520	1.23329054	0.000170631	0.009685301
FBgn0033787	1.988399	0.000178171	0.010054828
FBgn0039298	3.960823982	0.000182351	0.010231555
FBgn0028381	1.439486127	0.000186001	0.010376709
FBgn0040687	7.073864458	0.000205421	0.011141797
FBgn0038756	4.770880958	0.000206852	0.011157429
FBgn0024244	1.270764644	0.000211715	0.01129495
FBgn0036727	1.438350398	0.000227568	0.011880999
FBgn0013343	5.803642077	0.000252597	0.013048186
FBgn0039821	1.09836421	0.00026626	0.013555148
FBgn0038404	1.472949771	0.000297881	0.014913889
FBgn0040069	3.068262027	0.000314095	0.015645439
FBgn0031735	2.385250953	0.000316999	0.015709941
FBgn0036493	1.049394515	0.000334597	0.01639834
FBgn0036232	6.455372466	0.000335928	0.01639834
FBgn0085249	6.121649121	0.000349079	0.016871581
FBgn0034085	1.017756076	0.000365475	0.017526592
FBgn0053808	1.484159673	0.000366522	0.017526592
FBgn0051806	1.456143293	0.000416314	0.019436465
FBgn0034195	1.341723886	0.000427472	0.019779173
FBgn0004003	1.473841179	0.000461395	0.020663312
FBgn0034563	2.704139836	0.00047675	0.021156887
FBgn0063495	1.18507588	0.000484141	0.021387656
FBgn0036066	1.25430895	0.000504863	0.022028865
FBgn0032896	-1.088000157	0.000505425	0.022028865
FBgn0002578	3.441000676	0.000537262	0.023209253
FBgn0033138	1.087859418	0.000578221	0.02475953
FBgn0039749	-2.258797716	0.000589908	0.025149643
FBgn0051088	1.307781636	0.000608893	0.025846181
FBgn0034363	-1.11203087	0.000626853	0.026379142
FBgn0037409	1.425807955	0.000649281	0.027205715
FBgn0034142	1.060076151	0.000750248	0.031168812

FBgn0263748	6.110232333	0.000885375	0.036318959
FBgn0035043	1.459020675	0.001011903	0.040823176
FBgn0052351	1.280572329	0.001105772	0.043752369
FBgn0033271	1.910850386	0.001157882	0.045582265
FBgn0032381	3.967595702	0.001188214	0.046402142

Table 2.10 ARGs in adult brain of HDAC6 mutant flies

Gene	logFC	PValue	FDR
FBgn0026388	5.365289679	6.08E-21	5.77E-17
FBgn0013275	3.085651247	6.75E-14	3.21E-10
FBgn0037731	2.692807515	3.08E-12	9.75E-09
FBgn0011227	4.056115954	1.30E-10	3.08E-07
FBgn0263830	2.357146401	1.02E-09	1.95E-06
FBgn0034580	-3.074250606	1.50E-09	2.10E-06
FBgn0010424	-2.173765441	1.59E-09	2.10E-06
FBgn0035969	-2.014267923	1.77E-09	2.10E-06
FBgn0033819	-3.173578131	2.75E-09	2.90E-06
FBgn0058198	-2.798917981	5.40E-09	5.13E-06
FBgn0032414	-2.447562371	7.95E-09	6.87E-06
FBgn0025700	2.978832315	1.11E-08	8.81E-06
FBgn0037755	3.188185062	2.96E-08	2.17E-05
FBgn0030311	2.880615977	5.89E-08	4.00E-05
FBgn0038525	-1.569495405	6.59E-08	4.17E-05
FBgn0010015	-2.61316582	7.87E-08	4.67E-05
FBgn0263118	-2.521105352	1.08E-07	6.06E-05
FBgn0063496	1.862965131	2.13E-07	0.000107097
FBgn0032181	2.132575158	2.14E-07	0.000107097
FBgn0035239	1.617636448	2.57E-07	0.000122002
FBgn0266172	3.475150266	7.29E-07	0.000319474
FBgn0033521	1.476694029	7.40E-07	0.000319474
FBgn0034275	-2.500703742	1.07E-06	0.000442182
FBgn0260997	-2.562708021	1.94E-06	0.000758344
FBgn0031692	-1.596031685	2.00E-06	0.000758344
FBgn0030159	-1.186424472	4.45E-06	0.001626867
FBgn0002565	1.209464147	5.95E-06	0.002092251
FBgn0033821	-1.200955977	6.81E-06	0.00231194
FBgn0031857	-1.38280935	8.73E-06	0.0028066
FBgn0000079	1.433811079	9.26E-06	0.0028066
FBgn0037565	-1.578683234	9.35E-06	0.0028066
FBgn0086695	1.612325999	9.45E-06	0.0028066
FBgn0003089	-2.166620194	1.29E-05	0.003711547
FBgn0035550	-1.20686756	1.38E-05	0.003858316

FBgn0034647	-2.915962319	1.83E-05	0.004977364
FBgn0035402	1.112829772	1.92E-05	0.005074234
FBgn0263986	-2.029578346	2.11E-05	0.005430603
FBgn0030880	-1.785942348	2.51E-05	0.006100429
FBgn0263076	1.569852816	2.53E-05	0.006100429
FBgn0031558	2.864496275	2.57E-05	0.006100429
FBgn0035022	1.836075839	2.94E-05	0.006814308
FBgn0029762	-2.204513321	3.72E-05	0.008359036
FBgn0008646	1.725460173	3.78E-05	0.008359036
FBgn0032299	1.822045596	4.03E-05	0.00870453
FBgn0032194	3.323807705	4.68E-05	0.009870695
FBgn0085229	2.772890466	5.10E-05	0.010543401
FBgn0038071	-1.105904522	5.31E-05	0.010736961
FBgn0037730	-1.497300401	5.47E-05	0.010827626
FBgn0029831	-1.081985649	5.85E-05	0.011347464
FBgn0037683	-2.117151164	6.53E-05	0.01240195
FBgn0034293	-1.21790232	7.61E-05	0.014167916
FBgn0053196	-1.034683734	7.88E-05	0.014398823
FBgn0031289	2.322424746	9.11E-05	0.016322237
FBgn0042201	-1.268166932	9.55E-05	0.016807011
FBgn0037263	-1.387768764	0.00013206	0.02281278
FBgn0032803	1.1960139	0.000136232	0.023113168
FBgn0031261	1.061998973	0.000161868	0.026924983
FBgn0038277	1.602202995	0.000164367	0.026924983
FBgn0259794	-1.496369425	0.000176046	0.02750394
FBgn0039595	-1.043329885	0.000178725	0.02750394
FBgn0267649	-2.700461005	0.000179067	0.02750394
FBgn0001323	-1.502445004	0.000179481	0.02750394
FBgn0031854	1.086173797	0.000191582	0.028892341
FBgn0034439	-1.122903796	0.000198648	0.029489873
FBgn0063667	-1.804420233	0.000219263	0.03204957
FBgn0010038	-1.072420229	0.000262342	0.037765328
FBgn0040514	-2.100026977	0.000277508	0.039352321
FBgn0035574	-1.224849574	0.000350788	0.048785916
FBgn0034928	-1.41114711	0.000354303	0.048785916

Table 2.11 Library details

Name	Tissue	Length	Reads Mapped	Percent
OreR_ant_0min_A	Antenna	single-75	18,529,552	79.41807814
OreR_ant_0min_B	Antenna	single-75	23,894,763	71.7579823
OreR_ant_stim_A	Antenna	single-75	20,092,639	75.54944663
OreR_ant_stim_B	Antenna	single-75	33,455,045	73.72828737
Orco2_ant_0min_B	Antenna	single-75	54,864,913	81.14724325
Orco2_ant_0min_C	Antenna	single-75	29,859,334	77.10841936
Orco2_ant_stim_B	Antenna	single-75	54,881,246	82.48969966
Orco2_ant_stim_C	Antenna	single-75	39,255,666	76.8848725
5d_0min_A	Brain	single-50	29,882,030	83.15720907
5d_0min_B	Brain	single-50	24,131,069	80.6821327
5d_0min_C	Brain	single-75	67,036,144	79.88741709
5d_10min_A	Brain	single-50	29,515,532	82.86845757
5d_10min_B	Brain	single-50	27,881,672	82.50462145
5d_10min_C	Brain	single-75	52,054,831	84.33122939
5d_20min_A	Brain	single-50	24,427,803	82.95678388
5d_20min_B	Brain	single-50	31,510,110	82.67848493
5d_20min_C	Brain	single-75	45,340,869	81.73585788
5d_30min_A	Brain	single-50	20,381,088	82.54369398
5d_30min_B	Brain	single-50	28,878,084	83.10398077
5d_30min_C	Brain	single-75	56,926,188	84.40540491
5d_45min_A	Brain	single-50	24,463,926	82.50356587
5d_45min_B	Brain	single-50	20,922,541	82.30506523
5d_45min_C	Brain	single-75	52,614,413	84.12594938
10d_0min_A	Brain	single-50	42,717,478	81.88120525
10d_0min_B	Brain	single-75	82,319,821	87.2728012
10d_30min_A	Brain	single-50	52,276,262	83.63683372
10d_30min_B	Brain	single-75	79,253,246	85.67977953
25d_0min_A	Brain	single-50	33,230,912	83.60310591
25d_0min_B	Brain	single-75	48,639,247	81.99957405
25d_30min_A	Brain	single-50	27,777,935	83.9534021
25d_30min_B	Brain	single-75	50,359,125	80.44143532
wCS_0min_A	Brain	single-75	32,425,356	76.37508624
wCS_0min_B	Brain	single-75	70,959,597	78.54719996

wCS_stim_A	Brain	single-75	28,171,007	79.27491513
wCS_stim_B	Brain	single-75	95,911,941	78.07041975
HDAC6_0min_A	Brain	single-75	104,095,958	78.9861107
HDAC6_0min_B	Brain	single-75	53,881,104	77.18462279
HDAC6_stim_A	Brain	single-75	53,214,437	81.03952724
HDAC6_stim_B	Brain	single-75	39,815,076	77.56878633

Chapter 3

Activity-regulated gene expression in the *Drosophila* antenna depends upon the presence *Orco* and stimulus-type

Overview

Activity regulated genes (ARGs) are induced quickly in the brain in response to activation of neuronal circuits. As we and others have characterized previously, the protein products of these ARGs belong to a multitude of classes and vary widely with age and stimulus type. In our study, the entire brain is used to examine gene expression, although the activated neurons are limited to those with responsiveness to light and our selected odorants. Identifying the contributions of individual circuits in this context would be challenging. To isolate the contribution of olfactory signaling to ARG expression, we utilize the relatively simple *Drosophila* antenna to characterize ARG expression in the peripheral nervous system. We find 85 and 51 genes that increase and decrease, respectively following exposure to a fruit-odor blend. The reliable expression of most of these antennal ARGs is lost in the *Orco* coreceptor mutant that has severe defects in detection of the odorants tested. Additionally, we uncover a previously unknown role for *Orco* in the regulation of baseline gene expression in the *Drosophila* antenna including other olfactory receptors (*Or*s) and ARGs. Finally, we find that the pattern of ARG expression at the periphery depends on the odor type. Brief exposure to the common repellent DEET (N,N-Diethyl-3-methylbenzamide) leads to a reduced number of induced ARGs, many of which are distinct from ARGs induced by the attractive fruit odor blend.

Introduction

Compared to the 100,000 neurons of the fruit fly brain, the antenna represents a more simplified nervous system at the periphery. Approximately 1000 olfactory sensory neurons (OSNs) coat the surface of the antennal 3rd segment (Stocker 1994). These neurons exist in a stereotypic manner and are characterized into functional classes based on their capacity to respond to various odorants (de Bruyne, Foster, and Carlson 2001). Neuronal activity is generated when odorants bind transmembrane receptors belonging to one of three families of chemoreceptor genes: odor receptor (*Or)* (Peter J. Clyne et al. 1999; Leslie B. Vosshall et al. 1999; Gao, Yuan, and Chess 2000)*,* *ionotropic receptor* (*Ir*) (Benton et al. 2009; Ai et al. 2010; Silbering et al. 2011), or *gustatory receptor* (*Gr*) genes (P. J. Clyne, Warr, and Carlson 2000; Scott et al. 2001; Yao and Carlson 2010)*.* A majority of neurons in the antenna express just a single *Or;* all of the neurons within this group require the obligate coreceptor *Orco* to allow the *Or* to reach the dendrite, to form a heteromeric complex, and ultimately to generate an olfactory response (Leslie B. Vosshall et al. 1999; L. B. Vosshall, Wong, and Axel 2000; Larsson et al. 2004; Neuhaus et al. 2005). The binding of an odorant to a select Or/Orco receptor leads to an electrical response of a characteristic type (excitatory or inhibitory), strength, and temporal decay. Many fruit volatiles, for example activate a distinct set of *Ors,* and their corresponding OSNs, and lead to attraction behaviors.

Some odorants can activate different channels that lead to aversion. The common insect repellent DEET (N, N-diethyl-*m*-toluamide) , for example, is detected by olfactory and gustatory neurons, and leads to aversive behaviors in both cases. Volatile DEET evokes repellency, observed in flies where contact with DEET is prohibited. The mechanisms of volatile DEET repellency are controversial and several different models

have been put forth for its action on OSNs: one in which DEET activates repellent OSNs in an Orco-dependent fashion (Syed and Leal 2008; Ditzen, Pellegrino, and Vosshall 2008), and a second in which DEET modifies responses of some OSNs to their cognate ligands thereby acting to confuse normal olfactory coding (Pellegrino et al. 2011). DEET also acts as a contact repellent, relying on bitter taste neuron-mediated rejection of DEET-laced substrates, which occurs even with severely reduced olfactory input (Lee, Kim, and Montell 2010).

This well studied chemosensory organ provides a suitable environment to further study the principles of activity regulated gene (ARG) expression. We are interested in understanding the differences in gene expression at the periphery, compared to the central nervous system. The antenna also affords the ability to examine how olfactory activity directly contributes to the observed change in gene expression through use of the *Orco* co-receptor mutant, which has severe defects in detection of the odorants tested. Finally, given the the differences in the way flies respond to odorants (i.e. attractive vs aversive), we can examine what differences, if any these odorant types have on the gene expression programs immediately following exposure in the antenna.

Results

Sensory activation differentially modulates the antennal transcriptome

In order to identify changes in mRNA abundance in response to neural activation, we housed flies overnight in vials with no food, odor, or light, and exposed the sensory-deprived flies simultaneously to room lighting and a fruit odor blend known to activate several antennal Ors for 10, 20, or 30 minutes (Hallem and Carlson 2006). Antennae from each group were pooled and the transcriptome changes were compared to antennae from the “0 minute” unstimulated control group (Figure 3.1). We found that a

small fraction of genes (0.6%) in the genome, 85 genes, were significantly up-regulated in response to olfactory stimulation (Fold-change >2, FDR <0.05) (Figure 3.2A, left panel). Interestingly, we also found 51 genes that were significantly lower in levels following sensory stimulation (Fold-change < -2, FDR <0.05) (Figure 3.2A, left panel). The up-regulated ARG set was enriched for genes that are involved in "microtubule plus-end binding" by > 30-fold, suggesting a role in regulating the cytoskeleton (Figure 3.3). Only one transcription factor, the repressor *hairy*, was significantly up-regulated. GO-enrichment analysis of the down-regulated ARGs showed significant enrichment for genes involved in "neuropeptide hormone" and "transmembrane transporter" activities (Figure 3.3). Thus, even a brief period of olfactory stimulation in the *Drosophila* antenna is sufficient to alter the expression of 136 genes.

In order to check whether regulation of these ARGs depends on olfactory stimulation of neurons, we used *Orco*-mutant flies ($\Delta Orco^2$) that lack the obligate co-receptor of the olfactory receptor (*Or*) gene family, thus rendering all Ors non-functional (Larsson et al. 2004). Since the odorants in our stimulus mainly act on members of the Or family, and far fewer receptors from the ionotropic receptor (Ir) or gustatory receptors (Gr) families, we anticipate considerably lower activation of ORNs in the $\Delta Orco^2$ mutant. We performed the same stimulation experiment in $\Delta Orco^2$ mutant antenna and found a substantial drop to only 15 genes that were up-regulated (Fold change >2, FDR<0.05) (Figure 3.2A, right panel). About 83 out of the 85 up-regulated genes were not modulated in the mutant, suggesting that their regulation is dependent upon a functional olfactory receptor in ORNs (Figure 3.2B). However, more than half of the antennal ARGs were found at high baseline levels in $\Delta Orco^2$ mutants, and within this group, most genes continued to be activity-modulated but were down-regulated instead of up-regulated after

odor exposure (Figure 3.2C). The simplest interpretation is that the majority of ARGs observed in the antenna are induced in response to olfactory activity.

Interestingly, a sizeable number of genes (255) showed a reduction in abundance after the stimulus (Fold-change<-2, FDR<0.05) (Figure 3.2A, right panel). In all, 250 out of the 255 genes with sensory-reduced levels in Δ*Orco*^{2} mutants were not significantly modulated in wild-type antennae (Figure 3.2B). These were enriched for the GO terms "retinol dehydrogenase activity" and various "transmembrane transporter activity" terms (Figure 3.3). However, examining the overlap between the up- and down-regulated genes in each genotype, we found the strongest overlap in genes up-regulated in wild-type and down-regulated in Δ*Orco*^{2} mutants ($p<9 \times 10^{-15}$) (Figure 3.2B). This is consistent with the idea that Orco has a strong influence on odor-induced ARG expression in the *Drosophila* antenna.

Changes in antennal transcriptome in partially anosmic Orco mutants extend beyond activity-regulated genes

Given these initial findings, changes in baseline expression levels in the Δ*Orco*^{2} mutant merited additional investigation. Not only do Δ*Orco*^{2} flies not have functional OrX-Orco receptors, they also lack baseline action potential responses in all Or-expressing olfactory neurons (majority of the olfactory neurons), and it has been shown that lack of activity can lead to neuronal degeneration (Chiang et al. 2009). More than 900 genes were significantly different in abundance when comparing the expression in wild-type and Δ*Orco*^{2} mutant antennae (Figure 3.4A). Many of the antennal ARGs identified were significantly different between wild-type and Δ*Orco*^{2} mutants (Figure 3.4B). Several antennal chemoreceptor genes were down-regulated in Δ*Orco*^{2} mutant antenna as well including 27 Ors in the antenna, but only 3 Irs (Figure 3.6). In fact, "detection of chemical

stimulus involved in sensory perception of smell" was the GO term most strongly enriched (>18-fold) among transcripts that were lower in Δ*Orco*^{2} mutants (Figure 3.5). This highlights a previously unknown requirement of Orco for proper expression levels of many chemosensory genes in the *Drosophila* antenna. Whether this is an indirect effect of lack of spontaneous neuronal firing, or of neuronal death, or some other regulatory method remains to be studied. Among the genes whose levels were significantly higher in Δ*Orco*^{2} mutant antennae, there was an enrichment for rhodopsin mediated signaling and GPCR signaling (Figure 3.5). One possibility is that these genes are expressed in non-*Orco* neurons, such as IR+ ORNs, support cells, or even cells of the 2nd antennal segment responsible for hearing, which is attached to the tissue that was sequenced. Alternatively, the mRNAs of these genes could be destabilized due to lack of RNA binding proteins in the *Orco* mutant, or if the mRNA stability was negatively regulated downstream of spontaneous activity. Overall, these results suggest a prominent role for Orco in antennal gene expression, not only in terms of ARG regulation, but also in sensory gene expression.

DEET exposure leads to a different pattern of immediate gene expression in the antenna

To examine ARG expression following exposure to an aversive odorant, we also exposed flies to the common repellent DEET in the same manner as was done with the fruit odor blend, with the exception of placement (Figure 3.7). Due to the low volatility of DEET, we placed the odor in closer proximity to the adult flies. As with the fruit odors, we find that exposure to DEET is sufficient to alter the expression of genes in the antenna in a matter of minutes. We find only 50 genes whose expression increased following DEET exposure (Fold-change>2, FDR<0.05) (Figure 3.8A). In addition to no found Go terms enriched in this reduced gene set, there is surprisingly little overlap between the genes

induced by DEET than those induced following exposure to fruit odors (Figure 3.8B). We find only 4 genes that are induced in response to both fruit odors and DEET: *CG3999*, *Unc115b*, *Acp1*, and the transcriptional repressor *hairy.* This small, yet significant overlap indicates that only few odorant-independent genes are induced after antennal activity (Figure 3.8B).

There are 102 genes that showed reduced expression in the antenna following exposure to this repellent (Fold-change<-2, FDR<0.05) (Figure 3.8A). The overlap with genes that also decrease in abundance following treatment with fruit odors is much stronger ($p<6x10^{-30}$) (Figure 3.8B). We performed GO enrichment analysis with these decreasing genes and observed similarities with those down-regulated in response to fruit odors. Once again, we find "neurotransmitter transporter activity" and "neuropeptide hormone activity" significantly enriched among genes that decrease following olfactory stimulation (Figure 3.9). Additionally, we find a reduction in genes that are associated with visual system function, including "retinol dehydrogenase activity" which is enriched by more than 100-fold and "G protein-coupled photoreceptor activity" (Figure 3.9). Collectively, we find that while there is statistically significant overlap among the gene expression changes in response to fruit odors and DEET, there are also many unique gene targets following immediate exposure (Figure 3.10).

Discussion

In this study, we have identified a collection of ARGs that change in the antenna of *Drosophila melanogaster* in response to light and odor cues across a range of time points as we did for the brain. We characterize striking differences in genes induced in this tissue from those induced in the brains of juvenile flies. We find only 4 genes

commonly induced in both tissues. These 4 genes have yet to be characterized and warrant further investigation.

We find only a single transcription factor, the repressor *hairy,* that is induced in the antenna, in contrast to the several found to increase in the brain. We fail to detect the canonical *Drosophila* ARG transcription factors *Hr38* and *sr* in the antenna. However, our experiment only extended to 30 minutes, and given the large gene size of these transcription factors (Hr38:~31 kb and sr: :~11 kb), there may not have been enough time to expose this difference. This suggests that this peripheral group of neurons, immediately in response to stimulation, express more effector genes, including many cytoskeletal genes, rather than regulatory genes that further alter the genetic landscape of the antenna.

Induction of the antennal ARGs is dependent upon the presence of the obligate olfactory co-receptor, Orco. Comparison of baseline levels of gene expression in unstimulated control groups of wild-type and $\Delta Orco^2$ mutants uncovers a previously unknown role for Orco in the expression of many chemosensory genes, including Ors, Grs, Irs and Trp channels, as well as many others. It remains to be seen exactly how the presence of the Orco subunit has such a profound effect on antennal gene expression.

Interestingly, we find several visual system genes significantly altered in antenna from flies lacking *Orco*. Further work is required to understand if there is any light-responsiveness in either the 2^{nd} or 3^{rd} segment of the antenna, and if this sensitivity is increased in $\Delta Orco^2$ mutants.

Our comparative transcriptome analysis with DEET, reveals that the pattern of ARG expression in the antenna is highly sensitive to the odorant delivered. We find a lack of strong overlap between genes induced by fruit odors and those induced by the

repellent DEET. This suggests that the suite of genes altered in the antenna following brief stimulation are specifically tailored to the type of odorant, and thus the population of OSNs that are active during this period. Future studies where these experiments are replicated with other odorants would provide useful information as to whether these changes are due to the odorant behavior valence (attractive or aversive) or to the exact populations of activated neurons.

We do, however, observe strong overlap between genes that are reduced in response to fruit odors and those reduced in response to DEET. This group of down-regulated genes have not been studied in any context, and the consistency of their down-regulation despite the odorant type makes them interesting subject for future studies. We previously have shown that one down-regulated gene we identified in the brain is involved in learning and memory; it is possible that these genes down-regulated at the periphery play similar roles in olfactory-based learning.

Materials and Methods

Drosophila Stocks and Manipulations

Fly stocks were maintained on conventional cornmeal fly food under a 12 hr light:12 hr dark cycle at 25°C with 50% humidity. The OreR strain was used as wild-type control for sequencing experiments. Δ*Orco*^{2} mutants were obtained from the Bloomington Stock Center (23130).

Sensory deprivation, stimulation, and dissection.

Small groups of 10 mated male flies were placed into vials containing a wet Kimwipe and housed overnight without food for 13-16 hours in dark temperature/humidity-controlled chambers. Flies were anesthetized and sorted using CO_2 at least 24 hours prior to placement into these sensory deprivation chambers. The

following morning at 4-5 days-old, the flies were simultaneously exposed to ambient white light, 100 µl hexyl alcohol (1-hexanol, CAS 111-27-3), and 100 µl isobutyl acetate (CAS 110-19-0; odors diluted separately to 10^{-2} in paraffin oil) for 10, 20, 30, or 45 min. Experiments with DEET used the same protocol, except the odor was placed in closer proximity due to its low volatility. All treatments and experiments were performed at room temperature.. At the appropriate time points, flies were quickly anesthetized with CO_2 and stored on ice for no more than 10 min until dissection. The control condition consisted of flies that were immediately anesthetized and dissected following 13-16 hours of deprivation.

20 pairs of antenna were hand dissected to include the 2nd and 3rd segments and immediately frozen in liquid nitrogen for each time point. These were pooled with the additional timepoints to serve as the "stimulated" group in all experiments.

RNA isolation and preparation for transcriptome analysis

Tissues were mechanically crushed with disposable RNAse-free plastic pestles, and total RNA was isolated using a Trizol-based protocol. cDNA libraries were prepared from total RNA using the Illumina TruSeq RNA Sample Preparation Kit (v2) and 50 and 75 bps single-end sequencing was done using the HighSeq2000 and NextSeq500 platforms, respectively. There were an average of 53.7 million reads / replicate, with an average of 81% mapped.

Bioinformatic analysis of RNA-seq experiments

Reads were aligned to the latest release of the *Drosophila melanogaster* genome (dm6)) and quantified with kallisto (Version: kallisto 0.43.1) (Bray et al. 2016). Only libraries for which we obtained >75 % alignment were used for downstream analysis. Transcript counts were summarized to gene-level using tximport package (version 1.4.0)

(Soneson, Love, and Robinson 2015). For any instances of detected batch effects, we removed unwanted variation using RuvR in the RuvSeq package (version_1.10.0) (Risso et al. 2014). Differentially expressed gene (DEG) analysis was performed with the edgeR package (version 3.18.1) (Robinson, McCarthy, and Smyth 2010), using low count filtering (cpm >0.5) and TMM normalization. Clusters were generated using the MFuzz package (v.2.38.0) in R (Futschik and Carlisle 2005). GO-enrichment analysis was performed with GOrilla, using expressed genes as the background (Eden et al. 2009).

References

Ai, Minrong, Soohong Min, Yael Grosjean, Charlotte Leblanc, Rati Bell, Richard Benton, and Greg S. B. Suh. 2010. “Acid Sensing by the Drosophila Olfactory System.” *Nature* 468 (7324): 691–95.

Benton, Richard, Kirsten S. Vannice, Carolina Gomez-Diaz, and Leslie B. Vosshall. 2009. “Variant Ionotropic Glutamate Receptors as Chemosensory Receptors in Drosophila.” *Cell* 136 (1): 149–62.

Bruyne, M. de, K. Foster, and J. R. Carlson. 2001. “Odor Coding in the Drosophila Antenna.” *Neuron* 30 (2): 537–52.

Chiang, Albert, Rashi Priya, Mani Ramaswami, K. Vijayraghavan, and Veronica Rodrigues. 2009. “Neuronal Activity and Wnt Signaling Act through Gsk3-Beta to Regulate Axonal Integrity in Mature Drosophila Olfactory Sensory Neurons.” *Development* 136 (8): 1273–82.

Clyne, Peter J., Coral G. Warr, Marc R. Freeman, Derek Lessing, Junhyong Kim, and John R. Carlson. 1999. “A Novel Family of Divergent Seven-Transmembrane Proteins: Candidate Odorant Receptors in Drosophila.” *Neuron* 22 (2): 327–38.

Clyne, P. J., C. G. Warr, and J. R. Carlson. 2000. “Candidate Taste Receptors in Drosophila.” *Science* 287 (5459): 1830–34.

Ditzen, Mathias, Maurizio Pellegrino, and Leslie B. Vosshall. 2008. “Insect Odorant Receptors Are Molecular Targets of the Insect Repellent DEET.” *Science* 319 (5871): 1838–42.

Gao, Q., B. Yuan, and A. Chess. 2000. “Convergent Projections of Drosophila Olfactory Neurons to Specific Glomeruli in the Antennal Lobe.” *Nature Neuroscience* 3 (8): 780–85.

Hallem, Elissa A., and John R. Carlson. 2006. “Coding of Odors by a Receptor Repertoire.” *Cell* 125 (1): 143–60.

Larsson, Mattias C., Ana I. Domingos, Walton D. Jones, M. Eugenia Chiappe, Hubert Amrein, and Leslie B. Vosshall. 2004. “Or83b Encodes a Broadly Expressed Odorant Receptor Essential for Drosophila Olfaction.” *Neuron* 43 (5): 703–14.

Lee, Youngseok, Sang Hoon Kim, and Craig Montell. 2010. “Avoiding DEET through Insect Gustatory Receptors.” *Neuron* 67 (4): 555–61.

Neuhaus, Eva M., Günter Gisselmann, Weiyi Zhang, Ruth Dooley, Klemens Störtkuhl, and Hanns Hatt. 2005. “Odorant Receptor Heterodimerization in the Olfactory System of Drosophila Melanogaster.” *Nature Neuroscience* 8 (1): 15–17.

Pellegrino, Maurizio, Nicole Steinbach, Marcus C. Stensmyr, Bill S. Hansson, and Leslie B. Vosshall. 2011. “A Natural Polymorphism Alters Odour and DEET Sensitivity in an Insect Odorant Receptor.” *Nature* 478 (7370): 511–14.

Scott, K., R. Brady Jr, A. Cravchik, P. Morozov, A. Rzhetsky, C. Zuker, and R. Axel. 2001. “A Chemosensory Gene Family Encoding Candidate Gustatory and Olfactory Receptors in Drosophila.” *Cell* 104 (5): 661–73.

Silbering, Ana F., Raphael Rytz, Yael Grosjean, Liliane Abuin, Pavan Ramdya, Gregory S. X. E. Jefferis, and Richard Benton. 2011. “Complementary Function and Integrated Wiring of the Evolutionarily Distinct Drosophila Olfactory Subsystems.” *The Journal of Neuroscience: The Official Journal of the Society for Neuroscience* 31 (38): 13357–75.

Stocker, Reinhard F. 1994. “The Organization of the Chemosensory System in Drosophila Melanogaster: A Rewiew.” *Cell and Tissue Research* 275 (1): 3–26.

Syed, Zainulabeuddin, and Walter S. Leal. 2008. “Mosquitoes Smell and Avoid the Insect Repellent DEET.” *Proceedings of the National Academy of Sciences of the United States of America* 105 (36): 13598–603.

Vosshall, L. B., A. M. Wong, and R. Axel. 2000. “An Olfactory Sensory Map in the Fly Brain.” *Cell* 102 (2): 147–59.

Vosshall, Leslie B., Hubert Amrein, Pavel S. Morozov, Andrey Rzhetsky, and Richard Axel. 1999. “A Spatial Map of Olfactory Receptor Expression in the Drosophila Antenna.” *Cell* 96 (5): 725–36.

Yao, C. Andrea, and John R. Carlson. 2010. “Role of G-Proteins in Odor-Sensing and CO2-Sensing Neurons in Drosophila.” *The Journal of Neuroscience: The Official Journal of the Society for Neuroscience* 30 (13): 4562–72.

Figure 3.1 Antennal experiment design with fruit odor blend

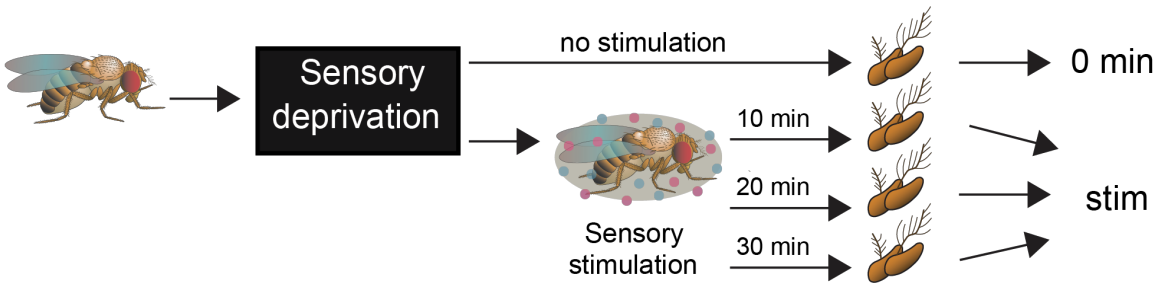

Figure 3.1 Antennal experiment design with fruit odor blend
Stimulation paradigm for antennal transcriptome analysis in 5 day-old wild-type and $\Delta Orco^2$ mutant flies

Figure 3.2 Differentially expressed genes in antenna following neuronal activation depend on the Orco co-receptor

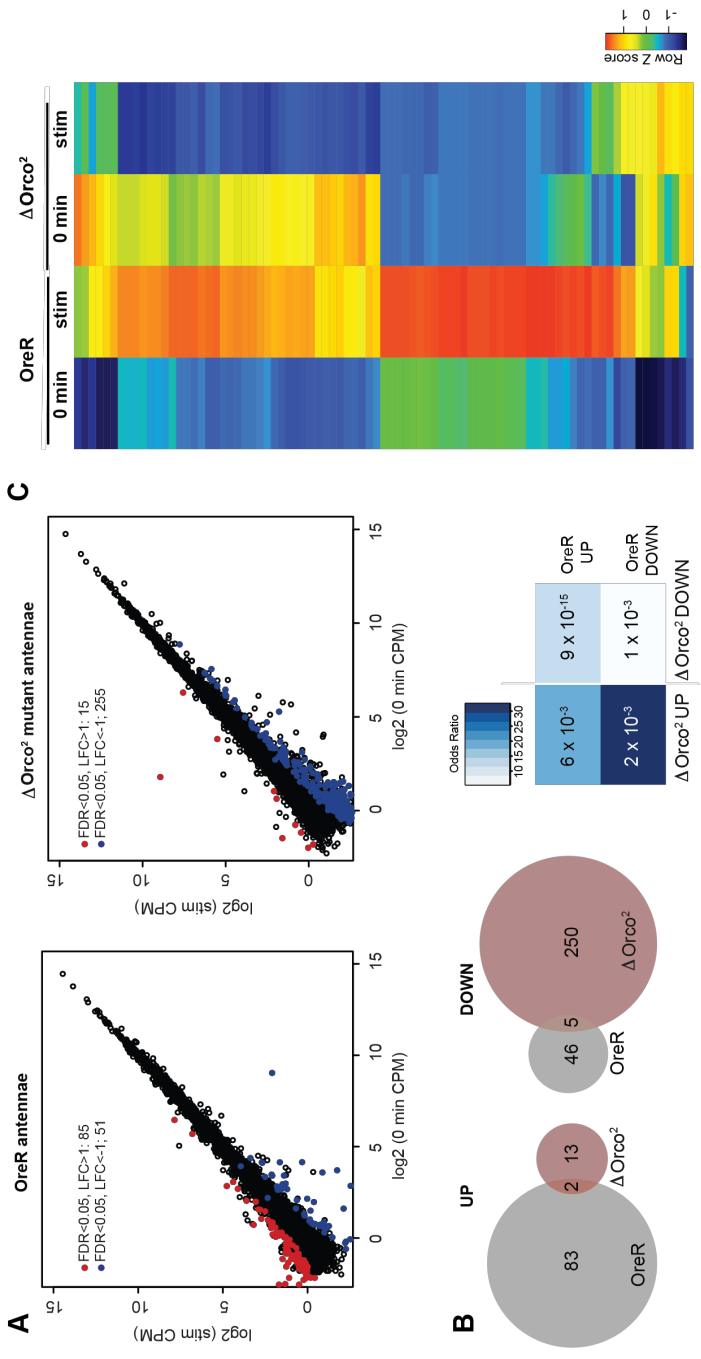

Figure 3.2 Differentially expressed genes in antenna following neuronal activation depend on the Orco co-receptor

(A) Plot highlighting up- and down-regulated genes in the stimulated group. Red and blue dots represent up-regulated genes (Fold-change > 2, FDR< 0.05) and down-regulated genes (Fold-change < -2, FDR< 0.05), respectively.

(B) Venn plot comparing the overlap of up- and down-regulated antennal genes for wild-type and $\Delta Orco^2$ mutants. The far right box shows significance of overlap of indicated gene sets (P-value indicated in box; color denotes odds ratio from Fisher's exact test).

(C) Heatmap following expression of 85 up-regulated genes in the wild-type antenna across all experiments. Each column represents the expression of one gene, normalized across samples (red= high expression, blue= low expression).

Figure 3.3 Antennal ARGs are enriched for cytoskeleton genes

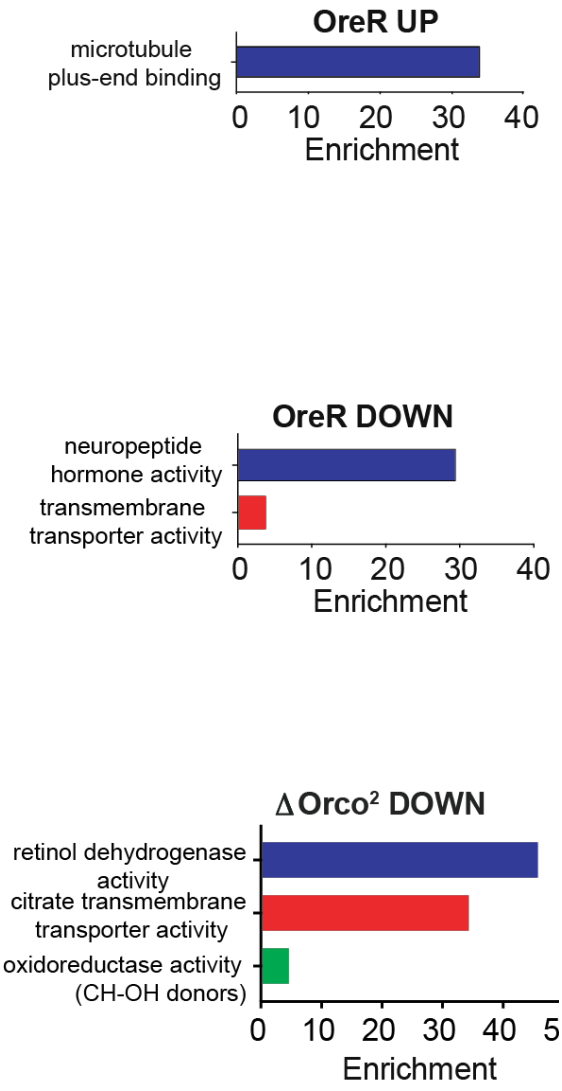

Figure 3.3 Antennal ARGs are enriched for cytoskeleton genes.

Bar graphs showing fold-enrichment for biological process GO terms in indicated gene lists compared to all genes expressed in antennal RNA-seq experiments ($p<0.05$).

Figure 3.4. Orco mutant antenna have altered gene expression relative to wild-type.

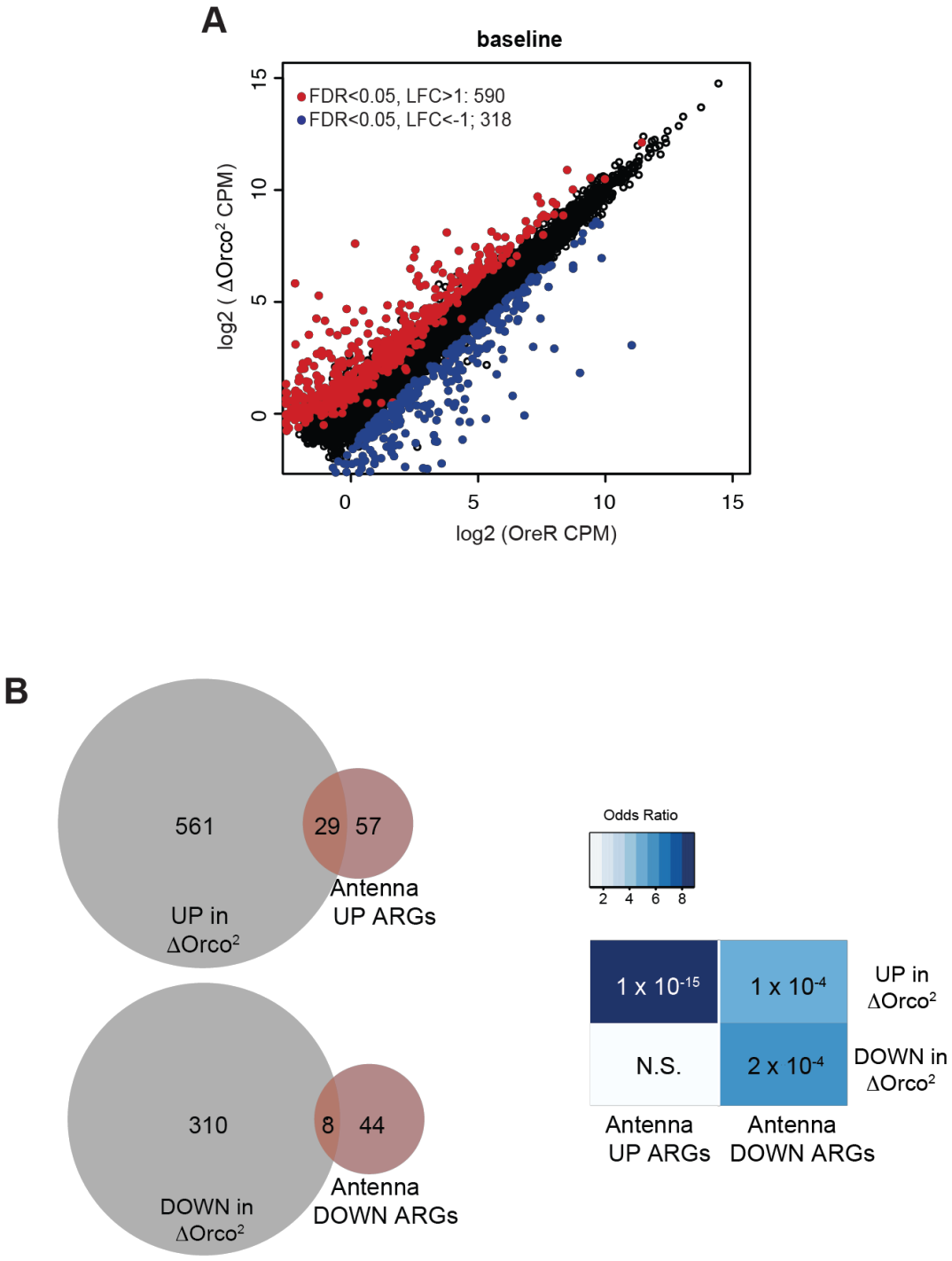

Figure 3.4. Orco mutant antenna have altered gene expression relative to wild-type.

(A) Plot highlighting up- and down-regulated genes in ΔOrco^2 mutants. Red and blue dots represent up-regulated genes (Fold-change > 2, FDR< 0.05) and down-regulated genes (Fold-change < -2, FDR< 0.05), respectively.

(B) Venn plot comparing the overlap of up- and down-regulated genes in the baseline of ΔOrco^2 mutants compared to ARGs identified in wild-type antennae. The far right box shows significance of overlap of indicated gene sets (P-value indicated in box; color denotes odds ratio from Fisher's exact test).

Figure 3.5 Characterization of baseline genes altered in *Orco* mutants

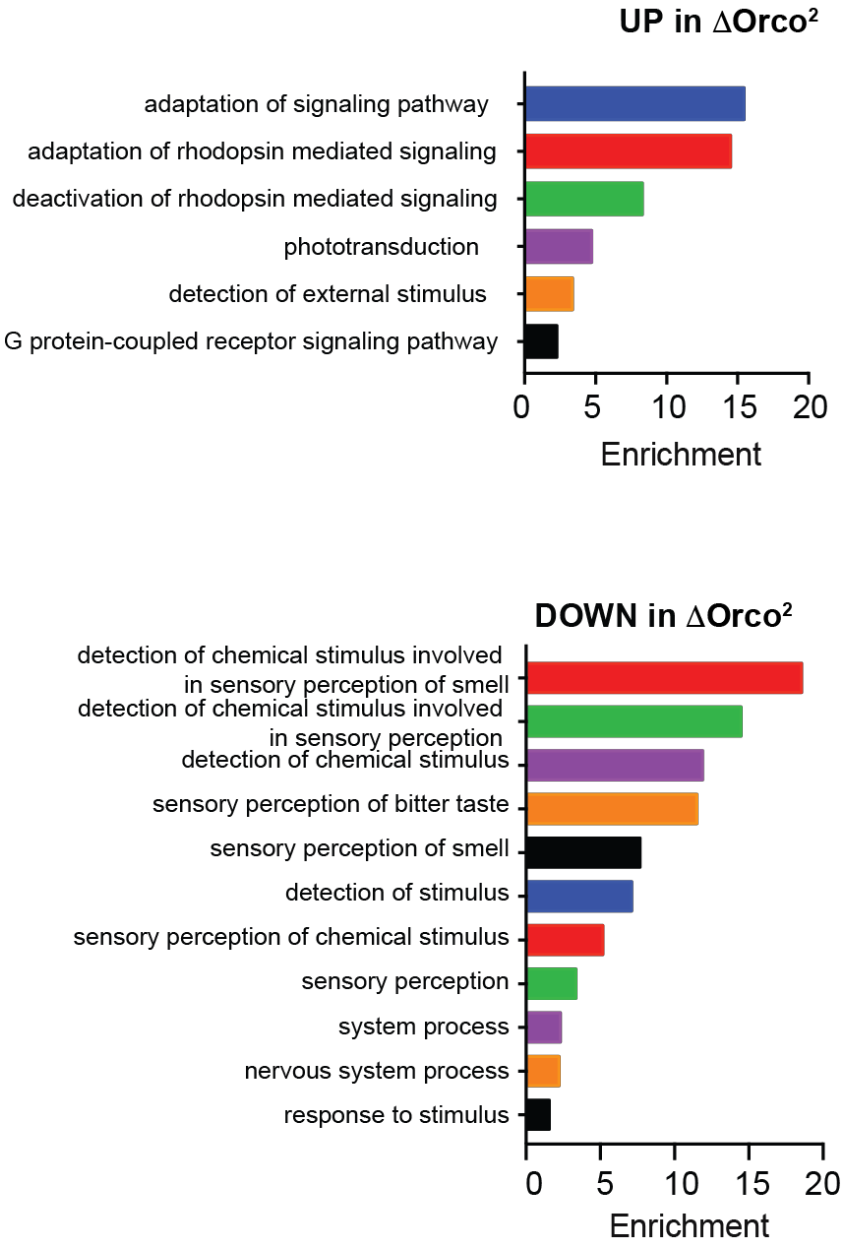

Figure 3.5 Characterization of baseline genes altered in *Orco* mutants

Bar graphs showing fold-enrichment for biological process GO terms in indicated gene lists compared to all genes expressed in antennal RNA-seq experiments ($p<0.05$).

FIgure 3.6 Loss of *Orco* leads to misregulation of many *Or* genes

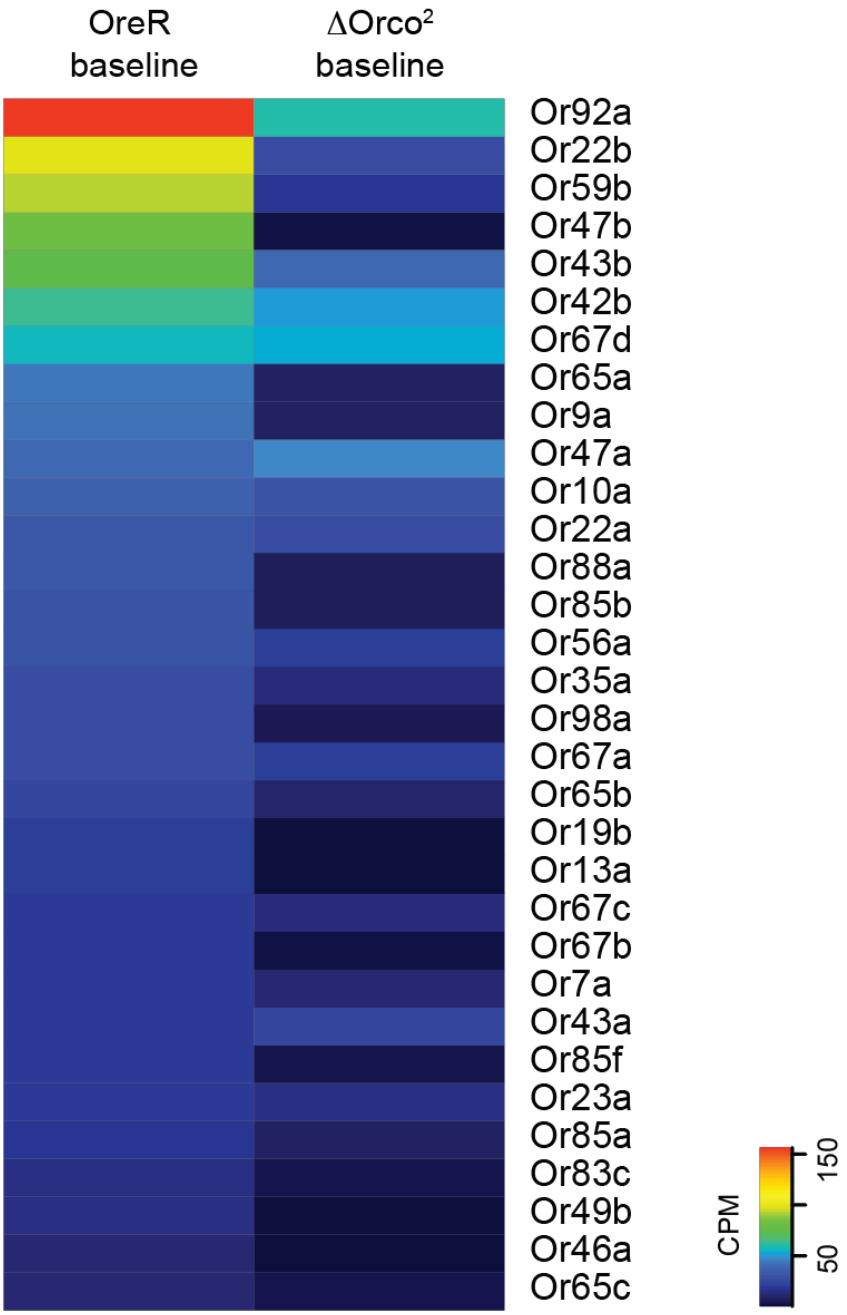

FIgure 3.6 Loss of *Orco* leads to misregulation of many *Or* genes

Heatmap following expression of 32 down-regulated Or genes at baseline in wild-type and $\Delta Orco^2$ mutant antennae. Each column represents the expression of one gene, normalized across samples (red= high expression, blue= low expression).

Figure 3.7 Antennal experiment design with DEET

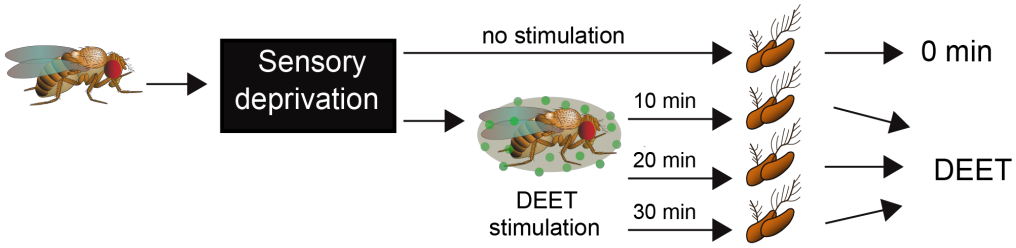

Figure 3.7 Antennal experiment design with DEET
Stimulation paradigm for antennal transcriptome analysis in 5 day-old wild-type flies

Figure 3.8 Differentially-expressed genes in antenna differ with exposure to DEET repellent

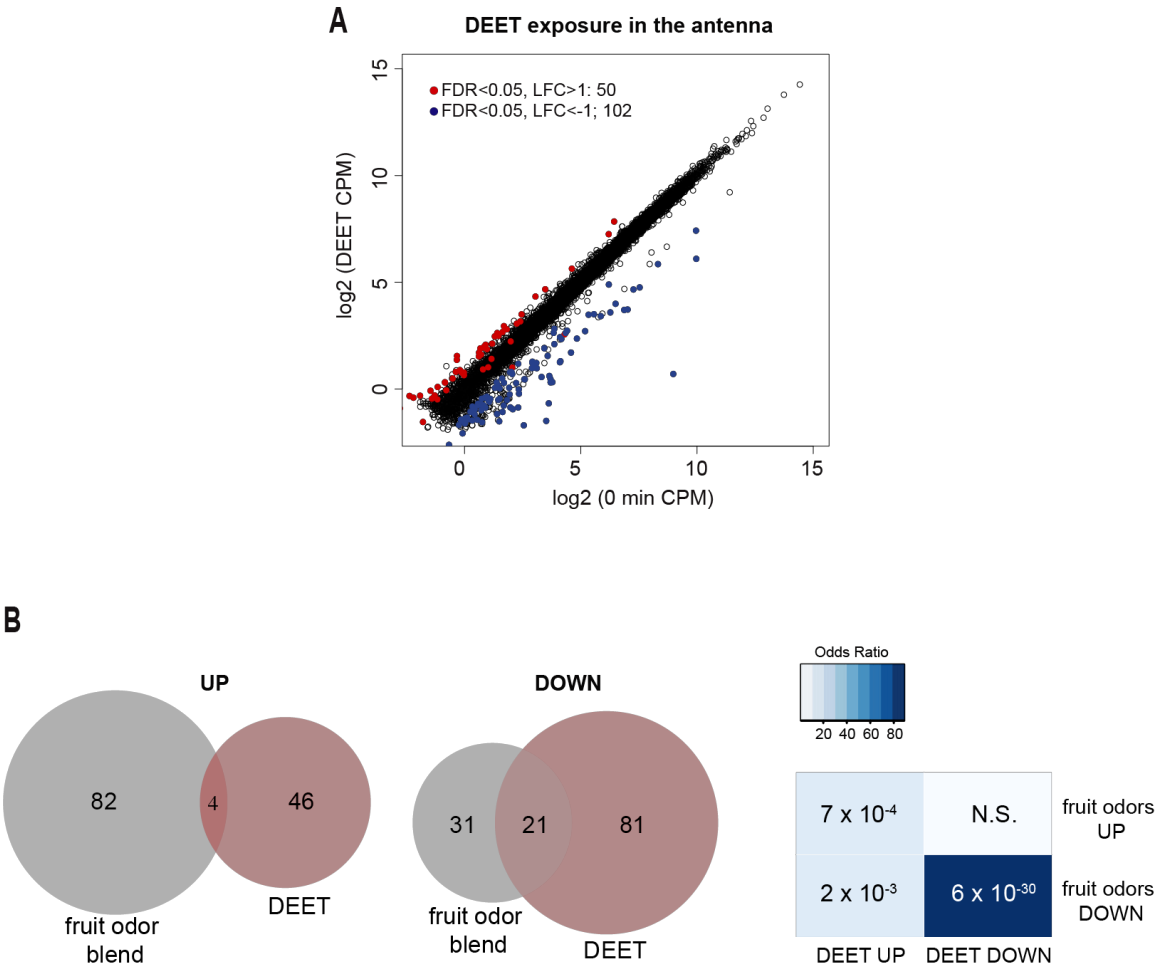

Figure 3.8 Differentially-expressed genes in antenna differ with exposure to DEET repellent

(A) Plot highlighting up- and down-regulated genes in the stimulated group. Red and blue dots represent up-regulated genes (Fold-change > 2, FDR< 0.05) and down-regulated genes (Fold-change < -2, FDR< 0.05), respectively.

(B) Venn plot comparing the overlap of up- and down-regulated antennal genes for fruit odor- and DEET- exposed flies[]. The far right box shows significance of overlap of indicated gene sets (P-value indicated in box; color denotes odds ratio from Fisher's exact test).

Figure 3.9 Characterization of down-regulated genes following DEET exposure reveals similarities with fruit odor-reduced genes.

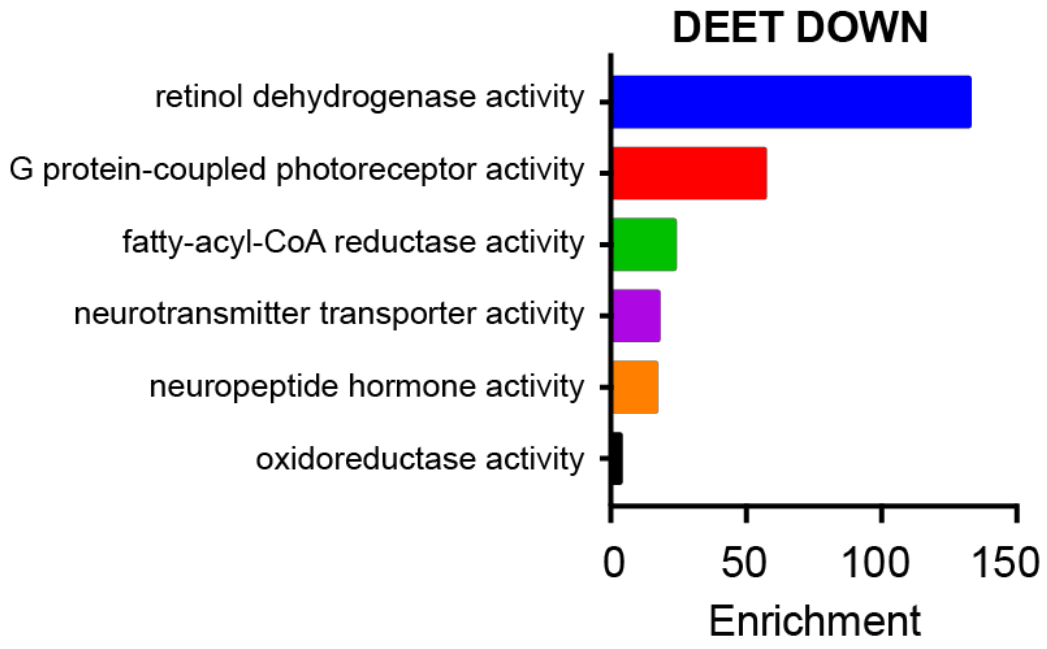

Figure 3.9 Characterization of down-regulated genes following DEET exposure reveals similarities with fruit odor-reduced genes.

Bar graphs showing fold-enrichment for biological process GO terms in genes down-regulated following DEET exposure compared to all genes expressed in antennal RNA-seq experiments ($p<0.05$).

Figure 3.10 Expression patterns of all ARGs that change in response to either fruit odors or DEET

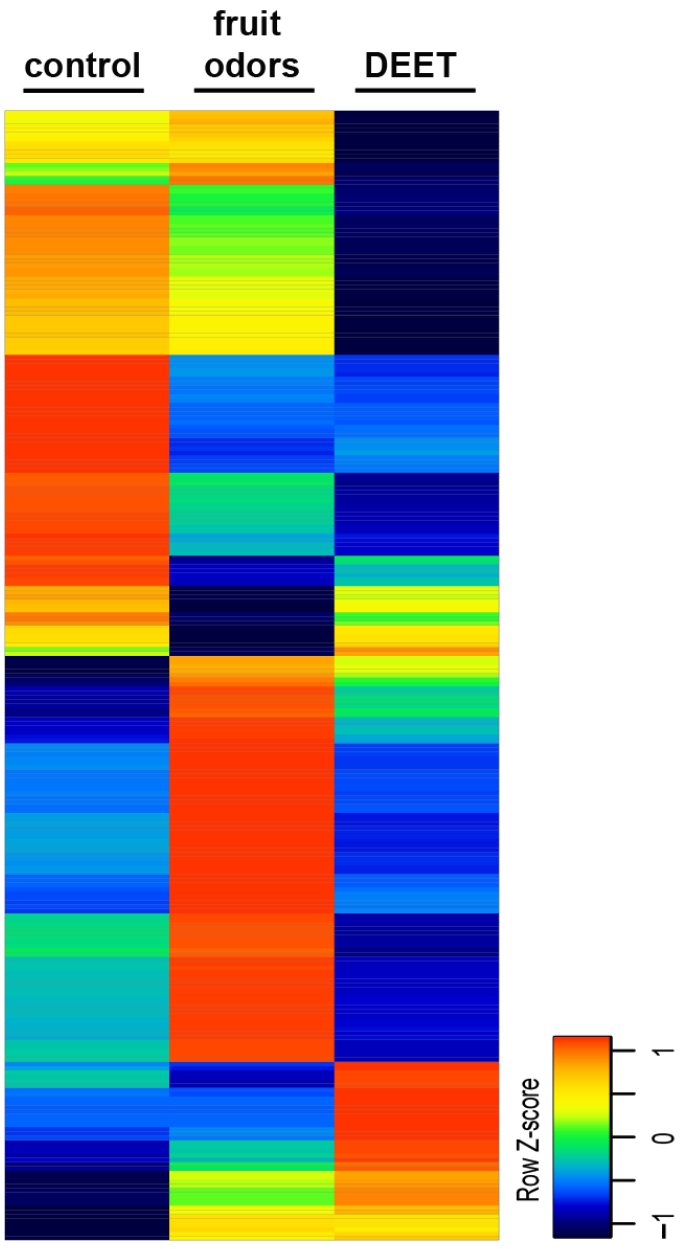

Figure 3.10 Expression patterns of all ARGs that change in response to either fruit odors or DEET

Heatmap following expression of all activity-regulated genes in the wild-type antenna across both odor stimulation paradigms. Each column represents the expression of one gene, normalized across samples (red= high expression, blue= low expression).

Table 3.1 Results for top ARGs, fruit odors in wild type antennae

Gene	logFC	PValue	FDR
FBgn0051274	-9.070918085	7.07E-35	7.35E-31
FBgn0043069	8.786479242	2.86E-27	1.49E-23
FBgn0037895	-3.995281736	6.98E-24	2.42E-20
FBgn0259974	1.835140267	1.54E-21	4.00E-18
FBgn0037232	-3.511771592	3.98E-20	8.28E-17
FBgn0034133	4.041382337	1.12E-19	1.95E-16
FBgn0013343	-2.864923263	1.36E-19	2.02E-16
FBgn0001168	1.37849442	1.75E-18	2.27E-15
FBgn0010381	2.49633099	3.78E-17	4.37E-14
FBgn0051665	-2.45217935	2.13E-15	2.21E-12
FBgn0033834	3.178330148	1.74E-13	1.65E-10
FBgn0259977	1.410798792	1.96E-13	1.70E-10
FBgn0032636	3.586062656	2.30E-13	1.84E-10
FBgn0052786	-1.670892666	1.64E-12	1.14E-09
FBgn0033848	-2.442641644	1.56E-12	1.14E-09
FBgn0001257	1.088482153	1.06E-11	6.90E-09
FBgn0020399	3.655588627	1.73E-11	1.06E-08
FBgn0030191	2.461914768	5.66E-11	3.27E-08
FBgn0266177	-1.479417651	1.25E-10	6.85E-08
FBgn0032055	-3.787958397	2.06E-10	1.07E-07
FBgn0011596	2.403185297	3.51E-10	1.74E-07
FBgn0000047	-1.44004834	1.65E-09	7.78E-07
FBgn0031546	2.932431219	1.92E-09	8.70E-07
FBgn0029950	-1.873076993	6.92E-09	3.00E-06
FBgn0038630	2.036110345	1.65E-08	6.69E-06
FBgn0052282	-1.820772438	1.67E-08	6.69E-06
FBgn0036311	1.980666904	2.18E-08	8.41E-06
FBgn0031542	-1.583683171	2.63E-08	9.78E-06
FBgn0038225	2.413099734	2.76E-08	9.89E-06
FBgn0036807	3.852299549	3.04E-08	1.05E-05
FBgn0034128	-2.002644892	4.21E-08	1.41E-05
FBgn0000405	1.788798897	4.81E-08	1.56E-05
FBgn0052819	1.34232647	1.27E-07	4.01E-05
FBgn0085344	2.443904617	3.45E-07	0.000102501

FBgn0030260	-2.454946559	6.98E-07	0.000201691
FBgn0033403	-1.822156685	7.67E-07	0.000215659
FBgn0061197	1.223317338	9.23E-07	0.000239934
FBgn0037676	-1.075917896	9.22E-07	0.000239934
FBgn0039332	-4.53418582	9.10E-07	0.000239934
FBgn0267326	1.874669114	9.81E-07	0.000248905
FBgn0039536	-1.296855104	1.27E-06	0.000315229
FBgn0003124	1.543860491	1.47E-06	0.000356228
FBgn0051099	2.251013602	2.32E-06	0.000536346
FBgn0033705	1.222272654	2.29E-06	0.000536346
FBgn0062517	1.195159795	2.38E-06	0.000539115
FBgn0004619	-1.773988677	3.43E-06	0.000743513
FBgn0263983	-1.122196836	4.83E-06	0.0009535
FBgn0028531	2.006185516	5.34E-06	0.001018343
FBgn0042627	-3.310262038	5.38E-06	0.001018343
FBgn0040519	1.350480402	5.54E-06	0.001028669
FBgn0033520	1.214774787	6.69E-06	0.00122137
FBgn0029730	1.994574815	8.28E-06	0.001436137
FBgn0038052	1.337800912	8.18E-06	0.001436137
FBgn0086915	1.114033481	8.88E-06	0.001514466
FBgn0037512	2.060197389	9.29E-06	0.001558679
FBgn0031424	-1.693021639	1.08E-05	0.001779726
FBgn0030477	-1.523401433	1.20E-05	0.001951313
FBgn0015831	1.67502014	1.37E-05	0.002184573
FBgn0031735	-1.545876717	1.80E-05	0.002790758
FBgn0037396	1.209339776	1.88E-05	0.002868956
FBgn0042201	-1.334445202	1.99E-05	0.002958969
FBgn0032269	1.24134486	2.21E-05	0.003243579
FBgn0037915	1.675772872	2.31E-05	0.003333768
FBgn0261839	-1.277949633	2.39E-05	0.003408858
FBgn0033645	-1.347217967	2.51E-05	0.003521228
FBgn0052783	1.105090687	3.09E-05	0.004279495
FBgn0051907	1.355536977	3.68E-05	0.004795208
FBgn0033963	1.285656752	3.57E-05	0.004795208
FBgn0032471	1.261318314	3.66E-05	0.004795208
FBgn0001981	1.825236253	3.85E-05	0.004949022
FBgn0000500	-2.029820086	4.14E-05	0.005249508

FBgn0037730	-1.801233594	4.84E-05	0.005998154
FBgn0000039	-1.968248149	5.44E-05	0.0065825
FBgn0085384	-1.200855707	5.51E-05	0.006592064
FBgn0039052	-1.556632234	5.65E-05	0.006680767
FBgn0032639	1.667881692	5.87E-05	0.006864434
FBgn0034173	1.490394994	5.97E-05	0.006902428
FBgn0038299	1.044971487	6.92E-05	0.007661211
FBgn0262002	1.689514322	7.87E-05	0.008352365
FBgn0053503	1.20072369	7.86E-05	0.008352365
FBgn0262881	1.938772323	8.14E-05	0.008555387
FBgn0054054	1.548359971	8.63E-05	0.008973658
FBgn0261842	-1.606533538	9.29E-05	0.009571699
FBgn0067903	1.455637967	9.72E-05	0.009818388
FBgn0260455	1.455637967	9.72E-05	0.009818388
FBgn0038450	-4.781718304	0.000103317	0.010333663
FBgn0261998	1.345537375	0.000107119	0.010511807
FBgn0036713	-2.200861712	0.000107057	0.010511807
FBgn0036474	1.795271297	0.000108192	0.010517884
FBgn0039511	1.228649444	0.000111558	0.010744649
FBgn0031805	1.148544337	0.000116037	0.010962544
FBgn0036731	1.734097176	0.000125712	0.011675547
FBgn0003312	1.427201675	0.000129907	0.011958387
FBgn0034205	1.611317802	0.000132496	0.012089681
FBgn0032797	-1.455217123	0.000138489	0.012312531
FBgn0040074	-1.941783453	0.000154939	0.01331963
FBgn0051391	1.628857604	0.000173248	0.014533243
FBgn0039071	1.489570861	0.000215192	0.017625416
FBgn0039083	1.690043792	0.000220737	0.017938351
FBgn0260463	1.710104043	0.000242413	0.019102918
FBgn0010019	-7.635477743	0.000241101	0.019102918
FBgn0035143	1.445374922	0.000253668	0.019691478
FBgn0030815	-1.55975772	0.000252944	0.019691478
FBgn0031585	1.332129668	0.000276439	0.021221089
FBgn0004197	-1.249661122	0.000277453	0.021221089
FBgn0003023	1.482884314	0.000279964	0.021256848
FBgn0035240	1.036490398	0.000289125	0.021793338
FBgn0035800	1.346820394	0.000300044	0.022362164

FBgn0261362	-1.379805296	0.000318624	0.023340327
FBgn0035781	1.124283679	0.000350671	0.025111496
FBgn0039398	1.08479301	0.000348498	0.025111496
FBgn0036565	-1.037376201	0.000352459	0.025111496
FBgn0003515	-1.337770916	0.000395769	0.028005396
FBgn0036778	1.462236585	0.000400123	0.028122127
FBgn0011227	-1.112713442	0.00040369	0.028182435
FBgn0030033	1.670878477	0.000429516	0.029393614
FBgn0050361	-1.333092836	0.000436718	0.029691096
FBgn0032507	-1.186661613	0.000464697	0.031185686
FBgn0037059	1.428247393	0.00047172	0.031454016
FBgn0003248	-1.148221701	0.000502357	0.032659471
FBgn0033911	-1.16018767	0.000520828	0.033442323
FBgn0034144	1.042703343	0.000537852	0.033907517
FBgn0014454	1.305919032	0.000548397	0.034364018
FBgn0035196	1.123380975	0.000577026	0.035516101
FBgn0033137	-1.095912743	0.00064421	0.038414479
FBgn0035857	1.386956247	0.000725683	0.040982899
FBgn0028569	1.433418249	0.00076144	0.042583354
FBgn0028848	1.168344488	0.000776507	0.043193724
FBgn0051028	-1.742237758	0.000832434	0.045814682
FBgn0030377	1.482479239	0.000845273	0.046276454
FBgn0037994	1.554775646	0.000873248	0.047064898
FBgn0038135	1.689235289	0.000899163	0.048211817
FBgn0040508	1.446563557	0.000903854	0.048214821
FBgn0037801	1.011116666	0.000920404	0.048599214
FBgn0032448	1.146434092	0.000926482	0.048673057
FBgn0038979	1.508090548	0.000947201	0.049511505

Table 3.2 Results for top ARGs, fruit odors in ΔOrco^2 mutant antennae

Gene	logFC	PValue	FDR
FBgn0261843	10.76419945	1.49E-42	1.53E-38
FBgn0052823	-6.578865604	1.34E-29	6.86E-26
FBgn0266175	9.85910449	3.89E-29	1.33E-25
FBgn0050160	8.735207239	1.16E-19	2.96E-16
FBgn0034152	8.10627588	9.55E-16	1.96E-12
FBgn0250904	-3.772252981	8.63E-15	1.47E-11
FBgn0046873	-4.133851213	1.46E-14	2.08E-11
FBgn0047334	5.812560251	1.62E-14	2.08E-11
FBgn0085353	-2.579076157	2.57E-13	2.93E-10
FBgn0265627	-3.766584	4.73E-13	4.85E-10
FBgn0033834	-3.32969462	5.60E-13	5.21E-10
FBgn0034659	-4.390580712	4.38E-12	3.74E-09
FBgn0053017	-2.880765807	1.13E-11	8.93E-09
FBgn0033848	3.099027552	1.28E-11	9.34E-09
FBgn0259151	-3.880739239	1.52E-11	1.03E-08
FBgn0265625	-4.096710157	2.16E-11	1.38E-08
FBgn0051682	-4.083625108	2.75E-11	1.66E-08
FBgn0040074	-3.172845855	6.60E-11	3.76E-08
FBgn0032636	-2.799861868	3.77E-10	2.03E-07
FBgn0015831	-3.871349899	1.19E-09	6.10E-07
FBgn0040687	-2.750828494	2.73E-09	1.31E-06
FBgn0052106	-3.62059896	2.82E-09	1.31E-06
FBgn0032269	-2.745904589	3.10E-09	1.38E-06
FBgn0051601	-3.624568896	4.05E-09	1.73E-06
FBgn0038665	-3.125486801	5.13E-09	2.10E-06
FBgn0014019	-1.874815684	5.93E-09	2.33E-06
FBgn0052220	-2.140722947	9.04E-09	3.43E-06
FBgn0038092	-2.675505984	9.66E-09	3.54E-06
FBgn0032638	-1.703113214	1.80E-08	6.35E-06
FBgn0036310	-3.581260068	2.63E-08	8.97E-06
FBgn0034871	-2.572741708	3.00E-08	9.77E-06
FBgn0032338	-3.020105328	3.05E-08	9.77E-06
FBgn0265626	-3.257829978	3.80E-08	1.18E-05
FBgn0052655	-3.365933041	7.93E-08	2.39E-05

FBgn0036945	-2.081896109	9.91E-08	2.90E-05
FBgn0030015	-2.926725676	1.06E-07	3.02E-05
FBgn0260758	-2.621779256	1.16E-07	3.21E-05
FBgn0031775	-2.332892885	2.29E-07	6.16E-05
FBgn0029703	-3.552102981	3.84E-07	0.000100765
FBgn0037502	-2.448370093	7.44E-07	0.00019051
FBgn0031620	-3.957894169	7.73E-07	0.000193127
FBgn0039071	-3.444872099	8.41E-07	0.000205084
FBgn0038708	-2.671210865	1.06E-06	0.0002526
FBgn0039070	-2.286802873	1.10E-06	0.0002526
FBgn0030317	-1.380801346	1.11E-06	0.0002526
FBgn0050430	-2.438607808	1.25E-06	0.000278531
FBgn0030014	-1.769838412	1.56E-06	0.000333161
FBgn0030033	-2.114285876	1.57E-06	0.000333161
FBgn0010019	4.717700627	1.59E-06	0.000333161
FBgn0050278	-3.065876599	1.76E-06	0.000360348
FBgn0036311	-2.227573479	2.04E-06	0.000408796
FBgn0051525	-2.628734651	2.10E-06	0.000412802
FBgn0050411	2.06590283	2.34E-06	0.000444899
FBgn0001281	-2.394021451	2.35E-06	0.000444899
FBgn0034835	-3.056096792	2.54E-06	0.000472719
FBgn0011693	-1.555378119	2.64E-06	0.00048377
FBgn0001168	1.307193524	2.75E-06	0.000493709
FBgn0033279	-2.867379849	2.80E-06	0.000494163
FBgn0003249	-1.256411473	4.11E-06	0.000714302
FBgn0085454	-2.879321871	4.34E-06	0.000740998
FBgn0050366	-2.081826979	4.99E-06	0.000838334
FBgn0042201	-1.906944193	5.47E-06	0.000891048
FBgn0036014	-2.428864171	5.54E-06	0.000891048
FBgn0033794	-2.411404386	5.57E-06	0.000891048
FBgn0031560	-2.238284708	6.75E-06	0.001064327
FBgn0259713	-2.257578894	6.98E-06	0.001084144
FBgn0000047	-1.656486869	7.24E-06	0.001107214
FBgn0042173	-2.02822331	7.59E-06	0.001143351
FBgn0032291	-2.125452626	8.13E-06	0.001207689
FBgn0002862	-3.040941013	9.18E-06	0.001343743
FBgn0039593	-1.604513016	1.03E-05	0.001486327

FBgn0031526	-2.405589975	1.16E-05	0.001642208
FBgn0033366	-1.212167212	1.17E-05	0.001642208
FBgn0028938	1.613502409	1.20E-05	0.001659007
FBgn0011270	-3.164570613	1.31E-05	0.00178381
FBgn0032276	-4.081256263	1.36E-05	0.001835494
FBgn0038897	-1.565156832	1.41E-05	0.001875432
FBgn0033817	-1.457577642	1.44E-05	0.001889953
FBgn0026755	-1.473188112	1.58E-05	0.002045449
FBgn0260453	-2.076715371	1.60E-05	0.002045449
FBgn0032287	-1.296901815	1.86E-05	0.002347171
FBgn0038697	-2.533734303	1.96E-05	0.002451224
FBgn0036785	-1.970516533	2.04E-05	0.002521637
FBgn0261842	-1.229913692	2.07E-05	0.002524284
FBgn0003124	-2.389206559	2.15E-05	0.002593412
FBgn0015591	-2.039101247	2.21E-05	0.002629651
FBgn0031305	-1.185788267	2.60E-05	0.003038434
FBgn0032314	-3.288711087	2.61E-05	0.003038434
FBgn0051820	-2.108007175	2.67E-05	0.003070649
FBgn0032109	-1.915862265	2.92E-05	0.00327596
FBgn0034957	-2.98924855	2.95E-05	0.00327596
FBgn0031546	-3.85913196	2.96E-05	0.00327596
FBgn0036924	-1.498970798	2.97E-05	0.00327596
FBgn0014465	-1.599903195	3.18E-05	0.003461146
FBgn0263402	-1.93931296	3.32E-05	0.003580418
FBgn0035921	-1.525406406	3.57E-05	0.003807139
FBgn0069354	-2.746497289	3.62E-05	0.003825698
FBgn0039251	-1.802067833	3.70E-05	0.003864508
FBgn0085249	-1.382277597	3.78E-05	0.003907156
FBgn0038295	-1.764115456	3.82E-05	0.003917275
FBgn0067861	-3.265813553	4.10E-05	0.004156213
FBgn0036415	-2.095234531	4.14E-05	0.004159422
FBgn0038946	-1.3906445	4.82E-05	0.004796422
FBgn0028526	-1.116868266	5.03E-05	0.004959249
FBgn0037811	-1.346016645	5.31E-05	0.005177932
FBgn0031723	-1.687604642	5.36E-05	0.005177932
FBgn0053493	-1.267889297	5.43E-05	0.005195352
FBgn0033439	-1.739394446	5.73E-05	0.00540525

FBgn0037410	-2.025948665	5.75E-05	0.00540525
FBgn0031561	-1.226787918	6.15E-05	0.005697215
FBgn0033730	-1.611527644	6.17E-05	0.005697215
FBgn0030895	-1.514626634	6.48E-05	0.005925785
FBgn0034435	-2.365977994	6.66E-05	0.006034579
FBgn0036620	-1.369007535	6.89E-05	0.006189288
FBgn0002936	-1.235718008	7.11E-05	0.006335405
FBgn0029831	-1.106898932	7.66E-05	0.006766135
FBgn0033512	-2.195687499	7.79E-05	0.006816842
FBgn0053337	1.692695947	8.22E-05	0.007140387
FBgn0036619	-1.081884106	8.35E-05	0.007186992
FBgn0039629	-1.172425016	8.42E-05	0.007188894
FBgn0041194	-1.425479225	8.92E-05	0.007551906
FBgn0030157	-1.236394811	9.30E-05	0.007807395
FBgn0032464	-2.241157052	9.52E-05	0.007927
FBgn0052548	-3.153508459	9.67E-05	0.007985698
FBgn0035800	-2.771358142	0.000102249	0.008379513
FBgn0028567	-2.382711089	0.000105402	0.008512965
FBgn0028379	-2.353690138	0.000105539	0.008512965
FBgn0262100	-2.293180301	0.0001091	0.008731373
FBgn0035709	-2.795095242	0.000111301	0.008838478
FBgn0032773	-1.106823471	0.000112694	0.008880312
FBgn0051161	-1.461274919	0.000114584	0.008960292
FBgn0036778	-2.000864291	0.000116016	0.009003546
FBgn0038172	-1.1489842	0.000129108	0.009944197
FBgn0000406	-1.0405076	0.000137466	0.010397055
FBgn0053120	-1.182035668	0.00013771	0.010397055
FBgn0039083	-2.255868508	0.000138032	0.010397055
FBgn0086348	-1.790726733	0.000149136	0.011088163
FBgn0034133	-3.044404139	0.000149372	0.011088163
FBgn0259918	-1.062607722	0.000155034	0.011425648
FBgn0262150	-1.183261199	0.000156448	0.011447535
FBgn0030697	-4.149964852	0.000161357	0.011723013
FBgn0050098	-1.340992015	0.000165342	0.011927938
FBgn0032820	-1.180433695	0.000167187	0.011976665
FBgn0029501	-2.595503074	0.000176627	0.012565073
FBgn0029154	-1.770341869	0.000180268	0.012735609

FBgn0019650	-1.13910113	0.000188972	0.013259125
FBgn0261714	-1.077265026	0.0001929	0.013442607
FBgn0037915	-2.584189417	0.000198276	0.013723896
FBgn0050365	-2.018399352	0.000199714	0.013730643
FBgn0053696	-1.298111693	0.000206111	0.01407599
FBgn0038934	-3.949288329	0.000207958	0.014108065
FBgn0031751	-2.142431599	0.000213046	0.014264343
FBgn0037939	-2.544248842	0.000215574	0.014339863
FBgn0001263	-1.076583961	0.000226837	0.014991728
FBgn0033170	-1.071244636	0.000228575	0.015009775
FBgn0036652	-2.187567673	0.00023182	0.015125902
FBgn0050362	-1.62378457	0.000240746	0.015608904
FBgn0003067	-1.02143706	0.000248436	0.015906126
FBgn0266488	-1.02143706	0.000248436	0.015906126
FBgn0031128	-3.236578864	0.000254519	0.01599923
FBgn0036731	-2.186116119	0.000255973	0.01599923
FBgn0250849	-2.806762901	0.000256138	0.01599923
FBgn0263387	-2.806762901	0.000256138	0.01599923
FBgn0034416	-1.661126962	0.00026705	0.016579781
FBgn0051231	-1.949423431	0.000270194	0.016673875
FBgn0032894	-2.273884213	0.000271965	0.016682686
FBgn0267366	-3.708183652	0.000280485	0.017102934
FBgn0013949	-1.024408099	0.000284417	0.01724002
FBgn0037612	-1.288622153	0.00028649	0.017263532
FBgn0031343	-2.594271358	0.000291962	0.017490428
FBgn0036323	-1.384789625	0.000297341	0.017617908
FBgn0038706	-2.519493548	0.00029753	0.017617908
FBgn0050393	-2.810837491	0.000302417	0.017804393
FBgn0033287	-3.254197946	0.000305783	0.017899644
FBgn0031127	-1.864573516	0.000311331	0.018120895
FBgn0038000	-2.345141161	0.000313907	0.018167606
FBgn0040735	-1.449035949	0.000317059	0.018246902
FBgn0085229	-1.720617161	0.000334586	0.019142184
FBgn0037040	-3.19641198	0.000336352	0.019142184
FBgn0261362	-1.069179477	0.000343979	0.019468075
FBgn0053284	-3.412093711	0.000357406	0.020023929
FBgn0044810	-2.173622687	0.000357813	0.020023929

FBgn0052695	-1.128587717	0.000359664	0.020023929
FBgn0010381	-1.510516161	0.000365993	0.020266104
FBgn0260463	1.738816491	0.000370259	0.020358606
FBgn0051029	-1.59807888	0.000371638	0.020358606
FBgn0004623	-1.029560708	0.000387881	0.021067686
FBgn0259714	-1.047900209	0.000389018	0.021067686
FBgn0052181	-1.722958915	0.000390752	0.021067686
FBgn0038589	-1.760506595	0.000407415	0.021851086
FBgn0005558	-1.103241651	0.000411144	0.021936236
FBgn0267253	-1.499778042	0.000436268	0.023156106
FBgn0033863	-2.881170924	0.000448941	0.023584356
FBgn0260428	-2.019924895	0.000453497	0.023702178
FBgn0260466	-2.261667248	0.000470654	0.024473991
FBgn0036218	-3.023559783	0.000486352	0.025162564
FBgn0038655	-2.922802126	0.00048928	0.025186869
FBgn0033074	-1.416452475	0.000501929	0.025628663
FBgn0051226	-2.517623791	0.00050659	0.025690627
FBgn0003861	-1.008626487	0.000510305	0.025714808
FBgn0035263	-1.552666883	0.000512132	0.025714808
FBgn0250845	-2.47801447	0.000514597	0.025714808
FBgn0036925	-2.914312413	0.000521007	0.025908724
FBgn0267726	-2.524951789	0.000540735	0.026759867
FBgn0028848	-2.131598156	0.000557813	0.027472302
FBgn0052119	-3.318633895	0.000563326	0.027480814
FBgn0039817	-1.21782375	0.000563351	0.027480814
FBgn0035124	-2.269287224	0.000586743	0.028486213
FBgn0031129	-2.583998589	0.000600043	0.028865883
FBgn0085330	-1.506623776	0.000600446	0.028865883
FBgn0038334	-2.326551806	0.000603016	0.028865883
FBgn0032588	-2.478524351	0.000612241	0.029171152
FBgn0265263	-2.786878203	0.000621872	0.029205564
FBgn0039088	-2.579156291	0.000624754	0.029205564
FBgn0035240	-1.582910446	0.000626124	0.029205564
FBgn0035218	-2.572399169	0.000627218	0.029205564
FBgn0031785	-3.748438309	0.000637402	0.029478689
FBgn0039611	-1.202282215	0.000638839	0.029478689
FBgn0030859	1.541207129	0.000656164	0.030007804

FBgn0033020	-1.458542139	0.000675282	0.030744852
FBgn0039801	-1.008323269	0.000700842	0.031767361
FBgn0050364	-1.43920479	0.000725037	0.032575773
FBgn0037402	-1.939113472	0.000739753	0.033091834
FBgn0027929	-1.107115277	0.000746567	0.033202293
FBgn0031853	-1.326272064	0.000748705	0.033202293
FBgn0030592	-1.34332814	0.000758669	0.033499172
FBgn0262983	-1.605972062	0.000774215	0.034038898
FBgn0034472	-3.370880537	0.000797119	0.0347476
FBgn0003515	-1.198358199	0.000820389	0.035437832
FBgn0038163	-2.553947422	0.000823331	0.035437832
FBgn0053125	-1.130045093	0.000844974	0.036217226
FBgn0052437	-2.967190755	0.000851998	0.036234955
FBgn0042086	-2.840030096	0.000871572	0.036874277
FBgn0052719	-1.508547149	0.000874702	0.036874277
FBgn0033862	-1.542369852	0.000888882	0.037318479
FBgn0034140	-1.166373505	0.000898895	0.037584798
FBgn0035007	-1.823269783	0.000903573	0.037608678
FBgn0037896	-1.053627237	0.000906808	0.037608678
FBgn0000045	-1.078152069	0.000941484	0.038889355
FBgn0051516	1.079514091	0.000963658	0.039645452
FBgn0032219	-2.704276254	0.000996846	0.040737029
FBgn0039797	-2.23861707	0.001008017	0.040737029
FBgn0037323	-1.152223812	0.001008139	0.040737029
FBgn0035186	-1.216683533	0.001024632	0.041162095
FBgn0035776	-2.872296347	0.001035775	0.041447199
FBgn0267347	-1.159997222	0.001045535	0.04163546
FBgn0267727	-2.183421567	0.001048609	0.04163546
FBgn0051865	-1.063013144	0.001059725	0.04191437
FBgn0039564	-1.229811172	0.001073345	0.042289795
FBgn0033821	-1.073209214	0.001112249	0.043654707
FBgn0003889	-3.659164498	0.001142499	0.04450097
FBgn0036162	-2.897158589	0.001149079	0.044571648
FBgn0034144	-2.020975599	0.001153015	0.044571648
FBgn0051777	-1.403867035	0.001185449	0.045653148
FBgn0034800	-1.793553655	0.001200567	0.046030477
FBgn0003965	-1.094822324	0.001205391	0.046030477

FBgn0265362	-1.310562697	0.001208727	0.046030477
FBgn0002565	-1.361873701	0.001213241	0.046031113
FBgn0042189	-1.942801315	0.001217731	0.046031113
FBgn0051740	-3.184758392	0.001227807	0.046241392
FBgn0039752	-1.965332346	0.001232973	0.046265856
FBgn0000405	-2.379998075	0.001247853	0.046653301
FBgn0052573	-1.024337791	0.00125445	0.046729407
FBgn0264364	-2.074842839	0.001264035	0.046915845
FBgn0039617	-2.280920282	0.001313125	0.048041623
FBgn0033285	-3.079212243	0.001342784	0.048826629
FBgn0040001	1.390842328	0.001344115	0.048826629
FBgn0035090	-1.091154738	0.001350662	0.048891089
FBgn0064119	-2.99659713	0.001386417	0.049840839
FBgn0050091	-1.150435979	0.00138663	0.049840839

Table 3.3 Results for top ARGs, DEET in wild type antennae

Gene	logFC	PValue	FDR
FBgn0010019	-6.669769142	4.41E-124	4.41E-120
FBgn0035434	-2.428166885	3.38E-66	1.69E-62
FBgn0013343	138.084424	3.42E-61	1.14E-57
FBgn0000047	-2.799612916	1.10E-47	2.76E-44
FBgn0032055	-4.012251141	9.28E-39	1.86E-35
FBgn0266170	-4.602147106	2.48E-37	4.14E-34
FBgn0261841	-3.731330162	2.43E-30	3.47E-27
FBgn0036619	-2.37229785	1.82E-28	2.27E-25
FBgn0038327	41.51815124	2.41E-28	2.68E-25
FBgn0030311	4.783096634	2.03E-26	2.03E-23
FBgn0037547	-2.496053795	1.18E-25	1.08E-22
FBgn0038450	-4.603851218	2.69E-23	2.24E-20
FBgn0001168	1.40994593	5.07E-23	3.91E-20
FBgn0025583	-2.190989875	1.52E-20	1.09E-17
FBgn0029093	1.543478761	4.58E-20	3.05E-17
FBgn0011693	-1.89759555	7.07E-20	4.42E-17
FBgn0030258	-3.008776696	7.24E-18	4.26E-15
FBgn0031424	-2.893032329	1.54E-16	8.55E-14
FBgn0052786	-1.808300924	2.00E-16	1.05E-13
FBgn0042627	-2.108947611	2.99E-15	1.50E-12
FBgn0038946	-1.461514829	1.53E-13	7.29E-11
FBgn0035402	1.221322315	5.29E-13	2.41E-10
FBgn0053105	4.046794364	9.33E-13	4.06E-10
FBgn0016726	-1.010106734	1.58E-12	6.57E-10
FBgn0261840	3.523625411	1.99E-12	7.99E-10
FBgn0051665	-2.468543063	5.28E-12	1.96E-09
FBgn0029950	-1.241190643	7.48E-12	2.68E-09
FBgn0000492	1.884277941	1.09E-11	3.77E-09
FBgn0261839	1.494625963	1.18E-11	3.92E-09
FBgn0259738	1.452119474	2.55E-11	8.23E-09
FBgn0034588	-1.245577531	2.64E-11	8.28E-09
FBgn0037895	-2.236825538	3.12E-11	9.47E-09
FBgn0260463	1.816073851	3.36E-11	9.88E-09
FBgn0032652	-1.442249291	1.11E-10	3.00E-08

FBgn0086348	-1.69641173	1.87E-10	4.93E-08
FBgn0260444	1.193698296	8.10E-10	1.93E-07
FBgn0031542	-1.351226934	8.47E-10	1.97E-07
FBgn0036681	3.792474421	1.77E-09	3.95E-07
FBgn0014019	-1.764268347	1.94E-09	4.21E-07
FBgn0033340	-1.75500144	3.07E-09	6.41E-07
FBgn0032797	-1.594873221	3.50E-09	7.14E-07
FBgn0003248	-2.128710786	5.98E-09	1.20E-06
FBgn0000038	-1.003026758	6.94E-09	1.36E-06
FBgn0002562	1.215057927	7.21E-09	1.39E-06
FBgn0039755	-2.067410944	9.15E-09	1.73E-06
FBgn0000594	1.252072974	2.57E-08	4.59E-06
FBgn0039052	-1.953756145	4.88E-08	8.42E-06
FBgn0039685	1.281350456	5.90E-08	9.68E-06
FBgn0037801	1.109668714	7.55E-08	1.20E-05
FBgn0036713	-3.310801425	8.99E-08	1.38E-05
FBgn0052580	1.016608011	1.19E-07	1.72E-05
FBgn0267727	-1.288679075	1.82E-07	2.61E-05
FBgn0069923	-1.560869853	2.91E-07	3.94E-05
FBgn0023489	-1.693017311	5.33E-07	6.68E-05
FBgn0040575	-1.879747266	5.57E-07	6.88E-05
FBgn0024943	-1.699008565	6.64E-07	8.01E-05
FBgn0022224	-1.480223074	7.43E-07	8.75E-05
FBgn0032879	-1.28055546	7.64E-07	8.90E-05
FBgn0042086	11.63843428	1.12E-06	0.000129182
FBgn0038565	-1.534316684	1.41E-06	0.000153697
FBgn0035921	-1.543079512	1.76E-06	0.000182012
FBgn0029859	-1.247851964	3.21E-06	0.000300725
FBgn0086782	1.105840814	3.37E-06	0.000311625
FBgn0037826	-1.100692311	3.39E-06	0.000311625
FBgn0030260	-1.962842592	3.85E-06	0.000343863
FBgn0085236	1.100676111	4.31E-06	0.000378573
FBgn0037939	-1.263010278	4.64E-06	0.000403852
FBgn0259716	1.004730842	6.25E-06	0.000530335
FBgn0031976	-1.421511014	6.55E-06	0.000550705
FBgn0019650	-1.043366188	7.20E-06	0.000596021
FBgn0033911	-1.378355421	8.13E-06	0.000652797

FBgn0050411	1.170918552	1.06E-05	0.000832605
FBgn0004102	-1.115538098	1.13E-05	0.000875298
FBgn0036620	-1.609595693	2.12E-05	0.001474086
FBgn0038148	1.106396468	2.24E-05	0.001549371
FBgn0085485	-1.065350832	2.27E-05	0.001559221
FBgn0013277	8.821568574	2.29E-05	0.001560172
FBgn0039722	-1.12103473	2.47E-05	0.001659055
FBgn0037612	1.203460119	2.53E-05	0.001687625
FBgn0041579	2.043705984	2.85E-05	0.001879721
FBgn0010241	1.05662566	2.91E-05	0.001901413
FBgn0033782	1.150999121	2.98E-05	0.001915022
FBgn0030764	2.346046779	3.21E-05	0.001998147
FBgn0003249	-2.275628736	3.26E-05	0.002016931
FBgn0035575	-1.22942971	3.34E-05	0.00202882
FBgn0038706	1.925206432	4.04E-05	0.002409894
FBgn0032609	-1.618538317	4.15E-05	0.002445509
FBgn0040534	-1.717798536	4.24E-05	0.002483352
FBgn0033623	-1.272902944	4.27E-05	0.002483821
FBgn0039651	-1.37298884	4.43E-05	0.002555275
FBgn0037232	3.185963179	4.44E-05	0.002555275
FBgn0050446	3.845966747	5.14E-05	0.002827928
FBgn0030317	-1.449525479	5.47E-05	0.002974876
FBgn0001228	1.684401791	5.62E-05	0.003039194
FBgn0259210	-1.339189367	5.97E-05	0.003178514
FBgn0004516	-2.540986424	6.64E-05	0.003481183
FBgn0261845	3.515973619	6.89E-05	0.003595242
FBgn0035880	-1.440354776	7.39E-05	0.00377651
FBgn0032654	-1.494764379	8.59E-05	0.004157362
FBgn0037896	-1.444298091	8.60E-05	0.004157362
FBgn0044328	3.361109293	8.84E-05	0.004235337
FBgn0267429	-1.451720221	9.65E-05	0.004542558
FBgn0038914	1.978766494	9.66E-05	0.004542558
FBgn0034486	-1.04299854	0.000122827	0.005589731
FBgn0051683	-1.090239733	0.000150793	0.006650817
FBgn0004784	-1.795356405	0.000168023	0.007251082
FBgn0053296	-1.311430057	0.000188633	0.007873983
FBgn0050090	1.636839555	0.000191108	0.007873983

FBgn0034684	-1.894208679	0.000192696	0.007906853
FBgn0267435	-1.869340581	0.000212856	0.008524471
FBgn0051865	-1.499805189	0.000215137	0.008547436
FBgn0037454	-1.508174899	0.000222202	0.008758604
FBgn0035663	1.090228803	0.000235746	0.009109076
FBgn0036583	1.333925065	0.000236552	0.009109076
FBgn0034128	-1.12951062	0.000258321	0.009650402
FBgn0005619	-1.259789605	0.000281894	0.01030046
FBgn0039770	-1.403987093	0.000311199	0.011288874
FBgn0004623	-1.787672397	0.000345248	0.012265596
FBgn0035855	-1.373904929	0.000350237	0.01239072
FBgn0260234	-1.250799568	0.00046637	0.015359528
FBgn0004795	-1.207910169	0.000479109	0.015593145
FBgn0042201	-1.256137687	0.00051318	0.016310987
FBgn0014454	1.249794208	0.000573383	0.017718235
FBgn0032525	-1.324483345	0.000602389	0.018331661
FBgn0039398	-1.131451819	0.000656366	0.019442413
FBgn0052814	1.057026944	0.000709389	0.020586665
FBgn0040609	-1.151033783	0.000733136	0.020976319
FBgn0050340	1.043124195	0.000740422	0.021119945
FBgn0266445	1.276330481	0.000745519	0.021204919
FBgn0004618	-1.469090214	0.00080353	0.022347073
FBgn0039415	1.157846482	0.000818685	0.022705465
FBgn0053502	-1.088359783	0.000890435	0.024029736
FBgn0003861	-1.603225594	0.000908788	0.024303772
FBgn0032061	-1.272867475	0.00093834	0.024788029
FBgn0037976	-1.380562831	0.001011033	0.026021759
FBgn0038749	-1.223640533	0.001119378	0.028444706
FBgn0029810	-2.014648846	0.00115557	0.029216081
FBgn0035271	-1.026136648	0.001182479	0.029671635
FBgn0039332	-2.178859996	0.001225717	0.030451307
FBgn0029821	-1.205939944	0.001264839	0.031191061
FBgn0004619	-1.111251081	0.001277736	0.031431673
FBgn0261714	-1.535776721	0.001324897	0.032274632
FBgn0265041	6.266751005	0.001376259	0.033010086
FBgn0031957	-1.259418874	0.001378168	0.033010086
FBgn0034127	1.52428876	0.001536795	0.035209144

FBgn0035171	-1.237389738	0.001752596	0.03858759
FBgn0040732	1.054757874	0.001776011	0.038739476
FBgn0029752	-1.268620537	0.001925417	0.041278971
FBgn0002936	-1.804935187	0.001953351	0.041699258
FBgn0037827	1.029611156	0.002118362	0.044185508
FBgn0259918	-1.878542956	0.002143773	0.044622558
FBgn0000121	-1.77410825	0.002176716	0.045214272

Chapter 4

Conserved odor detection pathway via HDAC and chromatin slows neurodegeneration in a Huntington's model

Overview

Odorant detection is mainly known to occur via specialized transmembrane receptors that are evolutionarily unrelated across eukaryotes. We show that one odorant, diacetyl which can cross the cell membrane, inhibits members of the ancient histone deacetylase enzyme (HDACs) family, serving as an atypical detection pathway by modulating gene expression via changes in chromatin. Up-regulated genes overlap with those for known HDAC inhibitors and inhibition is seen with purified human HDACs *in vitro*. Exposure increased histone H3K9 acetylation in a human cell line. Organisms spanning multiple taxa responded to diacetyl volatiles by altering gene expression, presumably via inhibition of HDACs. Inhibitors of HDACs 1 and 3 are known drugs for polyglutamine degeneration and remarkably exposure to diacetyl vapor slows progression of neurodegeneration in the *Drosophila* model for Huntington's disease. Our findings reveal a highly-conserved and slow-acting pathway for responding to odorants and raises questions about this pathway on physiology and health.

Introduction

Eukaryotes primarily detect volatile odorants in the environment using olfactory neurons that express a variety of transmembrane receptors, a family of genes that have independently evolved multiple times in different phyla. Examples of these unrelated genes include: the ionotropic 7-transmembrane (TM) odorant receptor *(*Or*)* family, which is insect-specific; 3-TM ionotropic receptors (IRs), which are present across most arthropods; the nematode-divergent 7-TM GPCRs belonging to the *str, sra, srg, srw, srz,*

srbc, srsx and *srr* families; the mammalian 7-TM GPCR olfactory receptor (OR) family; and the trace amine-associated receptor (TAAR) family (Buck and Axel 1991; Clyne et al. 1999; Troemel et al. 1995; Benton et al. 2009; Vosshall et al. 1999; Robertson 1998; Frank Zufall and Munger 2016). The activation of these receptors induces neuronal action potentials, and this information is conveyed to higher brain centers where olfactory perception is generated (Knaden and Hansson 2014). Odorant exposures typically lead to instantaneous organismal responses over a matter of seconds and, in animals that can move, generate rapid olfactory behaviors that have been the focus of intense study. However, for a critical sensory modality like chemosensation, we would expect additional, more ancient detection mechanisms that are highly-conserved across eukaryotes. Interestingly, while it is known that plants can respond to volatile compounds, the mechanisms of detection remain unclear. In this regard, it is particularly important to detect and respond to odorants that can disrupt the cell membrane or enter cells. The diversity in the species that are known to detect volatile odorants suggests that there are mechanisms of detection that evolutionarily predate divergent, tuned receptor complexes.

Furthermore, responses to long-term odor exposure are also relevant since most olfactory systems dampen their sensitivity soon after the onset of initial detection through a process called adaptation, which allows the animal to tolerate chronic exposure to odorants in the environment (F. Zufall and Leinders-Zufall 1998; Colbert and Bargmann 1995; Kurahashi and Menini 1997; Störtkuhl, Hovemann, and Carlson 1999). Direct absorption into cells can occur via exposed tissues such as the nasal epithelium, lungs and skin. However, the consequences of such persistent odor exposure are not fully known.

In order to study the physiological effects of long-term odor exposure, we started with the simple and genetically tractable *Drosophila melanogaster* model and analyzed gene expression changes in the antenna. We found expression of hundreds of genes to be modulated by prolonged exposure to volatile diacetyl, a highly volatile compound with a buttery smell found in many commonly-consumed foods such as butter, yoghurt, wine, fruits, beer, popcorn, etc (Martineau, Henick-Kling, and Acree 1995; Maarse 2017; Hughes and Denise Baxter 2007; Shibamoto 2014; de Bruyne, Foster, and Carlson 2001; Hallem, Ho, and Carlson 2004). Subsequent analyses revealed that this food-derived odor is able to inhibit histone deacetylases (HDACs) directly. HDACs are histone-modifying enzymes involved in the removal of acetyl groups from lysine residues and the remodeling of chromatin structure, which has a key role in the epigenetic regulation of gene expression (Shahbazian and Grunstein 2007; Gräff and Tsai 2013). Because of their dramatic impact on gene regulation, HDACs are promising targets in drug development for many diseases such as cancers and neurodegenerative disorders (Minucci and Pelicci 2006; Bolden, Peart, and Johnstone 2006; Kazantsev and Thompson 2008; Chuang et al. 2009). Indeed, several classes of HDAC inhibitors administered orally have been found to attenuate the progression of a repertoire of cancers and neurodegenerative diseases including Alzheimer's disease and Huntington's disease (Chuang et al. 2009). We find that simple exposure to diacetyl volatiles can substantially slow degeneration of photoreceptor cells in a Huntington's disease model in *Drosophila*. We also find that in mice, the volatile diacetyl affects gene expression changes in the brain, presumably via absorption through the nasal epithelium. Our discovery of a volatile HDAC inhibitor opens the possibility for new types of therapeutics and prophylactics that are natural, safe, affordable, and already used in human consumption, while simultaneously highlighting a need to understand how

small molecules present in our environment interact with and alter mammalian nervous systems.

Results

Diacetyl aroma regulates global gene expression

In order to test consequences of long-term odor exposure, we performed experiments using an odorant, diacetyl, which met several criteria for being important to detect by organisms. It is present widely in nature as a pH-neutral fermentation product of microorganisms such as yeasts and lactic acid bacteria and is found in many foods and beverages (Shibamoto 2014). It can react with arginine side chains in proteins which can have detrimental effects (Starek-Swiechowicz and Starek 2014). Importantly, it is known to traverse the cell membrane (Krogerus and Gibson 2013). Diacetyl is also produced by microbes in the oral cavity, and is found in the breath of healthy people but increased in both acute and chronic conditions that affect the lungs, such as cystic fibrosis (Whiteson et al. 2014; Mochalski et al. 2013). To test the effects of long-term exposure to this compound, we used the model system *Drosophila melanogaster,* and placed adult males in vials in a closed container exposed to headspace from a 1% diacetyl solution (in paraffin oil) for 5 days as in a previous long-term odor-exposure study (Sachse et al. 2007). The transcriptome of the primary olfactory organ, the antenna, was compared with that of the control group of age-matched flies that were exposed to the solvent (PO, Figure 4.1A).

Surprisingly, the antennal transcriptional profile of diacetyl-exposed flies showed substantial changes in gene expression when compared to the solvent control (Figure 4.1B). We identified 1234 differentially-expressed genes (DEGs) (false discovery rate, FDR < 0.05) in the antennal transcriptome of diacetyl-exposed flies compared to control animals. Of these, 645 genes were significantly up-regulated ($\log_2$ fold-change > 1; red

dots in Figure 4.1B) and 589 genes were significantly down-regulated (log_2 fold-change < -1; blue dots in Figure 4.1B). A broad range of genes was significantly altered, with several biological process GO terms significantly enriched in the up-regulated gene list including "response to biotic stimulus" ($p < 3x10^{-7}$),"response to bacterium" ($p < 3x10^{-7}$) and "defense response" ($p < 3x10^{-7}$) (Figure 4.2, 4.3). In the down-regulated gene set the GO term most enriched was "sensory perception of chemical stimulus" ($p< 6x10^{-72}$).

The large number (645) of up-regulated genes and their distribution across different chromosome arms suggested either a global mechanism of diacetyl-dependent gene modulation or of multiple mechanisms affected by the odor. One such mechanism could be through odor-dependent olfactory neural activation-dependent increases in calcium or cAMP, altering expression via the transcription factor CREB. However, we found that only 14 genes between both the up and down sets of 1234 genes had the known CRE site within 500 bp of their transcription start site. Each gene set also contained >30 genes with at least one CRE half site, the same frequency that is found within the upstream sequences genome-wide in *Drosophila.*

Diacetyl acts as a histone deacetylase inhibitor in vitro

Since diacetyl is known to penetrate eukaryotic cells, we considered the possibility that it could interact directly with intracellular proteins by reacting with arginine side-chains through covalent modification or through non-covalent binding in a protein pocket. One potential outcome therefore could be interactions with proteins that influence gene expression. A structural comparison of diacetyl to bioactive compounds revealed that it is structurally similar to beta-hydroxybutyrate, which is a known inhibitor of histone deacetylase enzymes (HDACs) that is produced by the liver (Figure 4.4A) (Shimazu et al. 2013). HDAC inhibitors are known to modulate gene expression broadly by promoting the

acetylation of lysine residues on histone tails, thereby promoting accessible chromatin structure. This suggested a potential mechanism for diacetyl odor exposure to alter gene expression. While the gene-regulatory effect of covalent modification of arginine across a wide array of protein types is difficult to conduct, the HDAC inhibition hypothesis can be tested. To that end, we tested two known HDAC inhibitors (HDACis) that can be administered orally, sodium butyrate and valproic acid, for overlap amongst diacetyl-modulated genes. Using the *Drosophila* antennae, we performed RNA-seq after raising the flies on food containing sodium butyrate (SB) or valproic acid (VA) (Steffan et al. 2001) and compared gene expression with flies raised on untreated food for 5 days. We next compared the up-regulated gene profiles following each treatment to the one induced by exposure to diacetyl. As expected, feeding SB and VA induced significant changes in expression levels of several genes (Figure 4.4B, C). Interestingly we found that 133 of diacetyl up-regulated genes were also up-regulated in either SB, VA or both treatment conditions (Figure 4.5). Pairwise statistical analysis of each gene set revealed a significant overlap of diacetyl-induced genes with SB-induced genes ($p=6x10^{-11}$) and with VA-induced genes ($p=2x10^{-65}$) (Figure 4.5). There was, as expected, also a significant overlap between SB- and VA- induced genes ($p=1x10^{-52}$) (Figure 4.5). This highly significant overlap among up-regulated genes supports the model that diacetyl vapors also act as an HDAC inhibitor *in vivo*. Interestingly, each of the 3 treatments also modulated a substantial number of unique genes. Of particular interest, the suite of diacetyl-suppressed genes did not overlap with the known HDAC inhibitor treatments. This suggests that diacetyl has additional mechanisms of altering gene expression, outside of up-regulation due to inhibition of histone deacetylase proteins.

These observations raise the question whether HDACs represent a conserved detection mechanism for odorants like diacetyl that link odor-detection to a specific gene expression response. Eukaryotes in particular have evolved very diverse trans-membrane odor receptor families, and for many species, odorant receptors are not yet known. Several, like plants, even lack neurons (Figure 4.6). HDAC proteins, however, are an ancient family of genes that predate even histones themselves (Gregoretti, Lee, and Goodson 2004; Postberg et al. 2010; Leipe and Landsman 1997). It is conceivable that odor detection mechanisms that emerged in ancient forms may not have involved specialized transmembrane receptors, or neurons, or resulted in rapid behavioral movements. Alterations in gene expression, however, could be a signaling mechanism indicating the presence of select environmental chemicals. In order to be considered an ancient odor-sensing pathway, it should match 6 expected criteria: (1) a highly-specific alteration of gene expression as response to volatile compounds, (2) partially reversible, (3) differential modulation of different members of a family of proteins (HDACs), (4) dose-dependent response *in vitro*, (5) dose-dependent response *in vivo*, and (6) conserved across eukaryotes such as invertebrates, vertebrates and plants. With gene expression profiles induced by diacetyl characterized as our response, we proceeded to test the 5 other criteria experimentally.

Diacetyl-upregulation of genes is partially reversible

To test for reversibility, we performed a recovery experiment following diacetyl exposure. We maintained 5-day diacetyl-exposed flies in clean air for 5 additional days (Figure 4.7A). In parallel, we performed age-matched mock experiments with paraffin oil solvent exposure alone. A large number of genes were down-regulated following the recovery in comparison to the untreated mock 10-day-old flies (Figure 4.7B). Interestingly,

there was a significant overlap of these down-regulated genes with the set that was up-regulated in the diacetyl treatment (Figure 4.7C). These results suggest that the effects of HDAC inhibitory odorant exposure are not permanent but dynamic, and removal of the odorant leads to subsequent changes in gene expression of the up-regulated set.

To examine if diacetyl can directly modulate HDACs, we performed *in vitro* acetylation assays with purified human HDACs. It has been shown that the structurally-related -hydroxybutyrate targets zinc-dependent HDACs (Shimazu et al. 2013), so we tested diacetyl for inhibition of these enzymes. We found that indeed, diacetyl inhibited all 4 purified human Class I HDACs (HDAC1, 2, 3 and 8). The inhibition occurred in a dose-dependent manner in the *in vitro* assay, albeit to different extents. The IC_{50} values for HDAC1, 2, 3, 8 and 6 were 7.3 mM, 23.1 mM, 7.5 mM, 14.3 mM and 24.5 mM respectively (Figure 4.8). The levels of inhibition for the more sensitive HDAC1 and HDAC3 are comparable to those of -hydroxybutyrate (Shimazu et al. 2013).

Diacetyl acts as a histone deacetylase inhibitor ex vivo

In order to test if diacetyl can act as an HDAC inhibitor in the nucleus of living cells, we evaluated acetylation of Histone 3 in the fly head after 5 days of exposure to diacetyl vapors and found it was increased 11.88% (data not shown). We also tested *Orco* co-receptor mutant (Larsson et al. 2004) antennae and it also showed an increase in acetylation of 11.53%, which is identical to the increase in wild type antenna(data not shown). While the difference was not statistically significant the trend is consistent with the interpretation that HDAC inhibitory activity of diacetyl is responsible for changes in acetylation and gene expression in a manner that is distinct from its detection by the olfactory system.

In order to directly test histone acetylation in a more tractable system we used human HEK293 cells which offer a tractable system to prepare nuclear extracts. We exposed the cells to different doses of diacetyl for 2 or 6 hours and monitored histone acetylation levels by Western blot analysis of nuclear extract. Compared to the mock treatment, 10 mM diacetyl significantly increased H3K9 acetylation levels within 2 hours of treatment, whereas the acetylation levels of H3K14 and H4K5 were not affected (Figure 4.9A). This specificity for an increase of the H3K9 mark is consistent with previous observations for -hydroxybutyrate (Shimazu et al. 2013). After 6 hours of treatment, the H3K9 acetylation induced by 10 mM diacetyl was further increased (Figure 4.9B). The increase in H3K9 acetylation with diacetyl treatment is dependent both on the duration of exposure and concentration of the odorant.

Organisms are constantly exposed to odorants commonly found in their food and environment for prolonged periods of time. In order to test the effect of a lower concentration of the odorant, we selected a 5-day exposure time at a 100-fold lower concentration, comparable to amounts found in certain foods (Shibamoto 2014). When we treated HEK293 cells with this lower dose of diacetyl (100 M), H3K9 acetylation level increased after 96 hrs of exposure and reached significantly higher levels than control after 120 hrs (Fig 4.9C,D). These results demonstrate that prolonged exposure to even low levels of diacetyl can greatly impact the epigenetic environment inside the cell. More importantly, a 5-day exposure was sufficient to alter the epigenetic state of cells at concentrations that are present in some food sources (~ 10 ppm). Taken together, these results demonstrate that diacetyl can act as an HDAC inhibitor, causing broad modulations of gene expression, histone acetylation in cells, and inhibition of purified HDAC enzymes in a dose-dependent manner.

Transcriptional response to odor exposure is conserved in vertebrates and plants

We next performed *in vivo* experiments to determine whether mammalian cells also alter gene expression in response to diacetyl as we would expect from an HDAC inhibitor. We performed transcriptome analyses on lung tissue of mice exposed to diacetyl headspace at different doses for a period of 5 days, as was done in *Drosophila* (Figure 4.10A). Indeed, expression of a substantial number of genes was modulated in the diacetyl-exposed lungs compared to the control. The changes were dose-dependent and more pronounced in mice exposed to 1% compared to those exposed to 0.1% diacetyl (Figure 4.10B, C). Among these diverse sets of regulated genes, a significant overlap was found between 1% and 0.1% exposed lungs for both up-regulated genes ($p=3x10^{-3}$) and down-regulated genes ($p=6x10^{-3}$, Figure 4.10D, Figure 4.11A,B, Figure 4.17), further supporting a dose-dependent effect of diacetyl on gene expression in the mouse lung.

The HDAC family members are highly-conserved across eukaryotes, spanning both animal and plant kingdoms. Volatile microbial metabolites have been present throughout the evolution of animals, insects, and plants, and have potential as signals for multi-domain communication because they can travel wide ranges; plants detect root infections and time their immune response using volatiles (Effantin et al. 2011), and microbial volatiles elicit olfactory behaviors in insects and nematodes. We predicted therefore that plant cells could also respond to odorants such as diacetyl using this pathway (Figure 4.12A). As predicted, we found that 321 genes are differentially-regulated in the leaflet of *Arabidopsis thaliana* following exposure to volatile diacetyl for 5 days (FDR<0.05) (Figure 4.12B, Figure 4.18). As with the invertebrate (*Drosophila*) and vertebrate (mouse) transcriptomes, these regulated plant genes are distributed across multiple chromosome locations and represent genes of diverse molecular functions (Figure 4.13). Taken

together, our results indicate that HDACs serve as highly-conserved pathways to transduce detection of odorants like diacetyl, resulting in specific alteration of gene expression in multiple tissues.

Volatile Diacetyl protects from neurodegeneration in Huntington's model Drosophila

HDAC inhibitors are an important class of drugs being tested for a number of different conditions including neurodegenerative diseases (A. Fischer 2010; André Fischer et al. 2010). A major design challenge for such drugs is the ability to cross the blood-brain barrier. An interesting possibility that arises due to the volatility and small size of odorants is that they could diffuse through the intranasal route to the brain directly (Chauhan and Chauhan 2015). In order to test whether cells in the brain respond to diacetyl vapors by altering gene expression we performed RNA-seq experiments on mice exposed only to aroma of diacetyl for 5 days. Littermate controls were exposed in a similar manner to the solvent (PO) headspace. Several genes were differentially expressed upon exposure to 0.1% diacetyl (49 up-regulated, 32 down regulated, $|\log_2$ fold-change$| > 1$, FDR<0.05) or to 1% diacetyl (748 up-regulated, 1031 down regulated, $|\log_2$ fold-change$| > 1$, FDR <0.01) (Figure 4.14 A,B,C). GO analysis of the regulated genes in the exposed mouse brain transcriptome revealed several interesting sets of genes were significantly altered in each set (Figure 4.15). Although the overall DEG sets are different across the lungs and brain, there is a statistically significant overlap as well as would be expected from using the same mechanism of action (data not shown).

In order to test the viability of the natural HDAC-inhibitory odorant delivered in volatile form as a treatment of neurodegenerative disorders, we tested a previously established *Drosophila* model of human Huntington's disease. This model was selected since polyglutamine disorders are well suited for targeting by inhibitors of HDAC1 and

HDAC3 such as diacetyl (Thomas 2014). In this model, the human Huntingtin protein with expanded poly-Q repeats is expressed in the neurons of the compound eye, causing progressive degeneration of the photoreceptor rhabdomere cells in each ommatidium (Jackson et al. 1998). Previous studies have shown that orally administered HDAC inhibitors such as sodium butyrate and SAHA can significantly reduce photoreceptor degeneration in this model (Steffan et al. 2001). When the transgenic flies expressing two copies of the human Huntingtin with poly-Q repeats (HTTQ120) under control of the eye-specific GMR promoter were raised at 18^{o}C, the number of rhabdomeres in each ommatidium was similar to that of control flies (7) immediately post-eclosion (day 1, Figure 4.15A-C). When these flies were moved to 25^{o} C following eclosion (Figure 4.15A), they showed dramatic degeneration of rhabdomeres over a period of 10 days (Figures 4.15B, D-G). The mean number of rhabdomeres was reduced from 7 to ~1 by day 10.

Remarkably, when the Huntingtin (HTTQ120)-expressing flies were exposed immediately after eclosion to volatile headspace of 1% diacetyl (in PO) (Figure 4.15A), they showed a substantial (~50%) inhibition of rhabdomere loss (Figures 4.15B, D-G). The majority of ommatidia retained 6-7 rhabdomeres at day 5 (Figures 4.15D and F). Even after 10 days, the majority of the ommatidia still had 2-3 rhabdomeres left in the odor-exposed flies, while the solvent controls had only ~1-2 rhabdomeres (Figures 4.15E and G). These results demonstrate that diacetyl odorant exposure slows down the photoreceptor degeneration caused in the Huntington's disease model flies. This odorant may have potential as a prophylactic against neurodegenerative disorders.

Discussion

In this study, we discovered that eukaryotic cells have the ability to alter gene expression in response to an odorant, in a manner independent of traditional neuronal

activity-induced pathways (Figure 4.7). Members of a conserved family of HDACs detect the concentration of diacetyl differentially. Diacetyl exposure increased levels of H3K9 acetylation in the nucleus in a dose-dependent manner, as well as changes in gene expression. The odorant diacetyl occurs naturally and is generated from the metabolism of a variety of food components, including triglycerides, sugars and amino acids (Shibamoto 2014). Moreover, the chemical is produced by the activity of microorganisms such as yeasts and lactic bacteria during fermentation in many foods and beverages (Shibamoto 2014). Although beyond the scope of this study, the discovery that cells can alter gene expression upon prolonged exposure to a common naturally occurring odorant raises important questions about the potential physiological consequences of the expression changes. Given our repeated exposure to particular flavors and fragrances, the findings outlined here highlight a new consideration for evaluating the safety of certain volatile chemicals that can cross the cell membrane.

In mammals, up-regulation of circulating -hydroxybutyrate during fasting or calorie restriction induces changes in the expression of a set of genes (Shimazu et al. 2013). The acetylation mark specificity and IC50 of -hydroxybutyrate is similar to that of diacetyl. Nevertheless determining whether the inhibitory effect is due to non-covalent interactions with HDACs, as proposed for -hydroxybutyrate and sodium butyrate, or via covalent modifications of arginine is beyond the scope of this study. We are also aware that diacetyl can also directly react to the lysine side chain under certain experimental conditions (Saraiva, Borges, and Florêncio 2006).

Any beneficial physiological effects of odor-detection at lower odor concentrations would also be countered by studies of potential risks at higher concentrations. In fact, the deleterious effect of exposure to high levels to diacetyl causing bronchiolitis obliterans, or

“popcorn lung”, and its toxicity in cultured cells is already known (More, Raza, and Vince 2012). Even so it is present in several foods we eat, and is on the GRAS (Generally Regarded as Safe) list of Flavor and Extract Manufacturers Association (FEMA) for use as a flavoring ingredient at low concentrations. Although outside the scope of this study, a careful evaluation of both the positive and negative effects of diacetyl in additional animal studies will be critical prior to understanding the extent of this HDAC-mediated detection pathway. While the specific mechanism of “popcorn lung” is unknown, it has previously been proposed that carbonyl groups of diacetyl can react to modify amino acid side chains on proteins or generate reactive dicarbonyl and reactive oxygen species, leading to excessive cytokine production and inflammation (Starek-Swiechowicz and Starek 2014). Our results raise the possibility that the molecular mechanisms underlying this disorder could be partially attributed to the unusually high HDAC-mediated genetic response to diacetyl by cells in the lungs. Several studies using rodent animal models have shown toxicity of high levels of diacetyl in the respiratory tracts including the nose and lungs (A. F. Hubbs et al. 2002; Ann F. Hubbs et al. 2008; Morgan et al. 2008; Palmer et al. 2011). Indeed, we observed that high levels of diacetyl treatment caused cell and animal death: 10 mM diacetyl treatment for 24 hours in HEK293 cells. The toxic effect of higher dosages has been observed for many types of HDAC inhibitors. For example, in one *Drosophila* study, feeding of a high dosage of 4-phenylbutyrate reduces survival rate, while a lower dosage extends longevity (Kang, Benzer, and Min 2002).

This dual detection of the olfactory cue diacetyl by a fast, transmembrane mechanism and a slower, enzymatic mechanism draws parallels with the multiple pathways in place to detect light. In the specialized cells of the eye, detection of light occurs via rhodopsins (7-transmembrane GPCRs) and leads to neuronal activity and

behavioral responses. However, other cells, including in plants, are also able to respond to changes in light intensity of certain wavelengths using the ancient, conserved cryptochrome proteins that are related to photolyases (Fogle et al. 2011, 2015). This suggests that vital sensory modalities can be detected via multiple pathways.

Taken together, our discovery that cells can alter gene expression in response to an odor that acts as an HDAC inhibitor and reprograms gene expression promises the pursuit of new types of odor-based therapeutics that are natural, safe, affordable, already approved for human consumption, and present in natural sources as prophylactics for a myriad of diseases. Simultaneously, they raise the concern of a new type of environmental agent which can reprogram gene expression and have widespread effects that are yet unknown.

Materials and Methods

Drosophila Stocks and Manipulations

Fly stocks were maintained on conventional fly food under a 12 hr light:12 hr dark cycle at 18°C or 25°C. The fly strain of *w1118* backcrossed 5 times to *Canton-S* (*wCS*) was used in all the *Drosophila* transcriptome experiments. P{GMR-HTT.Q120}2.4 (Bloomington # 8533) were used for neurodegeneration experiments.

Odor Exposure Protocol for Transcriptome Analysis

Flies were exposed to diacetyl (B85307, Sigma-Aldrich, St. Louis, MO) by placing them in vials in a cylindrical closed container (112 mm diameter x 151 mm height) along with an odor-containing glass vial. The odorant was dissolved in 10 mL paraffin oil at 1% dilution. For a given exposure protocol, two groups of flies were prepared: those exposed to 1% diacetyl headspace and those exposed to paraffin oil headspace alone (control flies). Adult male flies aged 1 d were transferred to fly vials containing fresh medium, and

put into the container with the odor vial. At the end of the fifth day of exposure, flies were collected, and their antennae were dissected for RNA extraction. All treatments and experiments were performed at room temperature. For the recovery experiment, flies were transferred to a container with a glass vial of paraffin oil after 5 days of diacetyl exposure. At the end of the fifth day of recovery, flies were collected, and their antennae were dissected for total RNA extraction. The second and third antennal segments from 40-60 male flies after treatment were carefully hand-dissected from the head and collected in 1.5 ml microfuge tubes kept cold in liquid nitrogen. Antennae were mechanically crushed with disposable RNAse-free plastic pestles, and total RNA was isolated using a Trizol-based protocol. cDNA libraries were prepared from total RNA using the Illumina TruSeq RNA Sample Preparation Kit (v2) and 50 bps single- and paired-end sequencing was done using the HighSeq2000. Two biological replicates were sequenced for each condition, with an average of 27 million reads / replicate, and with an average of 84% mapped.

Two-month old C57BL/6 male mice (2-3 for each condition in a single cage) were continually exposed to air flowing over headspace of paraffin oil (solvent control) or 1% diacetyl over a period of 5 days, then euthanized for recovery of the lung tissue and processing for mRNA isolation. All protocols for animal use and euthanasia were approved by the University of California, Riverside Institutional Animal Care and Use Committee (https://or.ucr.edu/ori/committees/iacuc.aspx; protocol A-20150028E) and were in accordance with the National Institutes of Health Guidelines. Animal studies are in accordance with the provisions established by the Animal Welfare Act and the Public Health Services (PHS) Policy on the Humane Care and Use of Laboratory Animals. In the transcriptome analysis, two replicates were performed for each condition, with an average of 123,687,411 reads / replicate, with an average of 88% mapped. Multiplexed libraries

were made from total RNA input using the Illumina TruSeq RNA sample preparation kit (v2) and 50 bps single-end sequencing was done using the NextSeq500.

Day 23 *A. thaliana* plants (Col-0) that had been transplanted at day 7 to soil were placed in the experimental room for 2 days to acclimate (23°C with a 12 hour light/dark cycle). A single potted plant was placed in a 4-liter clear glass jar, with openings attached to a vacuum to allow for air exchange. A small beaker containing 1ml of 1% diacetyl in PO or PO alone were placed inside the jar. Plants were watered at 2.5 days. After 5 days, individual leaflets were dissected and flash frozen in liquid nitrogen. Trizol-based RNA isolation was carried out as above. Two biological replicates were performed for each condition, with an average of 68,355,820 reads / replicate, with an average of 95% mapped. Multiplexed libraries were made from total RNA input using the Illumina TruSeq RNA sample preparation kit (v2) and 50 bps single-end sequencing was done using the NextSeq500.

HDAC inhibitor Treatment Protocol for Transcriptome Analysis

Sodium butyrate (B5887, Sigma-Aldrich) or valproic acid (P4543, Sigma-Aldrich) were dissolved in normal fly food medium at the final concentration of 10 mM. Three groups of flies were prepared: those treated with one of the HDAC inhibitors and those without HDAC inhibitor treatment (control flies). Adult flies aged 1 d were transferred to fly vials containing medium with or without a HDAC inhibitor. At the end of the fifth day of treatment, flies were collected, and their antennae were dissected for RNA extraction. All treatments and experiments were performed at room temperature. Two biological replicates with 60 flies/replicate were performed for each condition, with an average of 23 million reads / replicate, and with an average of 92% mapped. Multiplexed libraries were

made from total RNA input using the Illumina TruSeq RNA sample preparation kit (v2) and 50 bps paired-end sequencing was done using the HighSeq2000.

Bioinformatic analysis of RNA-seq experiments

Reads aligned to the latest release of each of the genomes used (dm6 for the *Drosophila* genome, GRCm38 for the *Mus Musculus* genome, and Araport11 for the *Arabidopsis* genome) and quantified with kallisto (version 0.43.1) (Bray et al. 2016). Only libraries for which we obtained >75 % alignment were used for downstream analysis. Transcript counts were summarized to gene-level using tximport package (version 1.4.0) (Soneson, Love, and Robinson 2015). For any instances of detected batch effects, we removed unwanted variation using RuvR in the RuvSeq package (version 1.10.0) . Differentially expressed gene (DEG) analysis was performed with the edgeR package (version 3.18.1) (Robinson, McCarthy, and Smyth 2010) using low count filtering (cpm >0.5) and TMM normalization. Protein classification analysis was performed with PANTHER (version 13.1) (Mi et al. 2017). All significance analyses of gene overlap were done using the GeneOverlap package in R package (version 1.14.0). GO enrichment analysis was performed using clusterProfiler (version 3.6.0) (Yu et al. 2012).

HDAC Activity Assays

HDAC activity of class I HDACs (HDAC1, 2, 3 and 8) was measured with the fluorometric HDAC Activity Assay kit: HDAC1 (10011563, Cayman Chemical, Ann Arbor, MI), HDAC2, HDAC 3, and HDAC 8 (50062, 50073 and 50068, BPS Bioscience, San Diego, CA), according to the manufacturer's instructions. Due to interference, concentrations of >30 mM were not used in the IC50 calculation. To account for any interference at lower concentrations, all baseline measurements of blank wells (no HDAC enzyme) were performed and subtracted with the various concentrations of diacetyl.

Cell Culture and Treatment

Human embryonic kidney 293 (HEK293) cells were grown in 100 mm cell culture dishes with Dulbecco's modified Eagle's medium (DMEM) (10-013, Corning, Manassas, VA), supplemented with 10% fetal bovine serum (FBS) (26140-079, Gibco, Carlsbad, CA) at 37 °C with 5% CO_2. Cells that were ~80% confluent were treated with freshly-prepared medium supplemented with diacetyl at concentrations indicated. The cells for mock controls were handled in the same manner without adding diacetyl to the medium. In order to prevent diffusion of diacetyl odor from the treatment dishes to the ones of mock control, the cell culture dishes in different conditions were cultured in separate CO_2 incubators.

Odor Exposure Protocol for Huntington's Disease Model Flies

Flies were exposed to diacetyl in a cylindrical container (112 mm diameter x 151 mm height). Each container was tightly closed but had 2 holes, one of which connected to an air suction port, and the other to a vial containing either of 5 mL paraffin oil or 5 mL 1% diacetyl in paraffin oil. A gentle suction was applied to pull the headspace from the odor or paraffin oil vials into the cylindrical structure. pGMR-HTTQ120 flies were maintained at 18 °C. Adult flies aged 1 d were transferred to fly vials containing fresh medium, and put into the odor-filled container at room temperature. Paraffin oil and 1% diacetyl solution were prepared and replaced every day. At the end of the fifth day of exposure, half of the flies were collected and subjected to pseudopupil analysis. The remaining flies were transferred to fresh medium and exposed to the odors for an additional 5 days. All treatments and experiments were performed at room temperature.

Preparation of Nuclear Extracts from HEK293 Cells

Nuclear extracts of HEK293 cells were prepared according to a protocol described previously (Andrews and Faller 1991), with minor modifications. In brief, HEK293 cells

were washed twice with cold phosphate-buffered saline (PBS) and lysed with hypotonic buffer (10 mM HEPES-KOH [pH 7.9], 1.5 mM $MgCl_2$, 10 mM KCl, protease inhibitor cocktail [Roche], 1 mM DTT, 1 mM TSA). Following a brief centrifugation, the pellet was resuspended in hypertonic buffer (20 mM HEPES-KOH [pH 7.9], 25% glycerol, 420 mM NaCl 1.5 mM $MgCl_2$, 0.2 mM EDTA, protease inhibitor cocktail (04693159001, Roche, Indianapolis, IN), 1 mM DTT, 1 mM TSA). The supernatant was recovered as nuclear extract.

Western Blot Analysis

Proteins in the nuclear extracts (60 µg protein) were separated by SDS–PAGE gels (456-1043, Bio-Rad, Hercules, CA), transferred onto PVDF membranes (162-0174, Bio-Rad), and incubated with anti-histone antibodies: acetylated H3K9 (1/2000: ab4441, abcam, Cambridge, MA), acetylated H3K14 (1/5000: 06-911, EMD Millipore, Billerica, MA), acetylated H4K5 (1/2000: 07-327, EMD Millipore). Bound antibody was detected by horseradish peroxidase-conjugated anti-rabbit secondary antibody (1/20000: 1705046, Bio-Rad) and developed using Clarity™ Western ECL Substrate (1705060, Bio-Rad). Signals were detected and captured by ImageQuant™ LAS 4000 mini (GE healthcare, Pittsburgh, PA), and band intensities were quantified with ImageJ software. H3K9 acetylation intensity in individual lanes was reported relative to the normalized Mock treatment (Mock H3K9ace / Mock PCNA), and calculated using this formula: Relative H3K9ace intensity for each timepoint = (Diacetyl H3K9ace / diacetyl PCNA) / (Mock H3K9ace / Mock PCNA).

Data availability

All transcriptome data sets in this chapter are available and have been deposited in the GEO repository with accession number GSE116502.

References

Andrews, Nancy C., and Douglas V. Faller. 1991. “A Rapid Micropreparation Technique for Extraction of DNA-Binding Proteins from Limiting Numbers of Mammalian Cells.” *Nucleic Acids Research* 19 (9): 2499–2499.

Benton, Richard, Kirsten S. Vannice, Carolina Gomez-Diaz, and Leslie B. Vosshall. 2009. “Variant Ionotropic Glutamate Receptors as Chemosensory Receptors in Drosophila.” *Cell* 136 (1): 149–62.

Bolden, Jessica E., Melissa J. Peart, and Ricky W. Johnstone. 2006. “Anticancer Activities of Histone Deacetylase Inhibitors.” *Nature Reviews. Drug Discovery* 5 (9): 769–84.

Bray, Nicolas L., Harold Pimentel, Páll Melsted, and Lior Pachter. 2016. “Near-Optimal Probabilistic RNA-Seq Quantification.” *Nature Biotechnology* 34 (5): 525–27.

Bruyne, M. de, K. Foster, and J. R. Carlson. 2001. “Odor Coding in the Drosophila Antenna.” *Neuron* 30 (2): 537–52.

Buck, Linda, and Richard Axel. 1991. “A Novel Multigene Family May Encode Odorant Receptors: A Molecular Basis for Odor Recognition.” *Cell* 65 (1): 175–87.

Chauhan, Mihir B., and Neelima B. Chauhan. 2015. “Brain Uptake of Neurotherapeutics after Intranasal versus Intraperitoneal Delivery in Mice.” *Journal of Neurology, Neurosurgery, and Psychiatry* 2 (1). https://www.ncbi.nlm.nih.gov/pubmed/26366437.

Chuang, De-Maw, Yan Leng, Zoya Marinova, Hyeon-Ju Kim, and Chi-Tso Chiu. 2009. “Multiple Roles of HDAC Inhibition in Neurodegenerative Conditions.” *Trends in Neurosciences* 32 (11): 591–601.

Clyne, Peter J., Coral G. Warr, Marc R. Freeman, Derek Lessing, Junhyong Kim, and John R. Carlson. 1999. “A Novel Family of Divergent Seven-Transmembrane Proteins: Candidate Odorant Receptors in Drosophila.” *Neuron* 22 (2): 327–38.

Colbert, Heather A., and Cornelia I. Bargmann. 1995. “Odorant-Specific Adaptation Pathways Generate Olfactory Plasticity in C. Elegans.” *Neuron* 14 (4): 803–12.

Effantin, Géraldine, Corinne Rivasseau, Marina Gromova, Richard Bligny, and Nicole Hugouvieux-Cotte-Pattat. 2011. “Massive Production of Butanediol during Plant Infection by Phytopathogenic Bacteria of the Genera Dickeya and Pectobacterium.” *Molecular Microbiology* 82 (4): 988–97.

Fischer, A. 2010. “HDAC Inhibitors as Therapy for Neural Disorders. Discovery of a New Therapy.” *Pharmazie in Unserer Zeit* 39 (3): 204–9.

Fischer, André, Farahnaz Sananbenesi, Alison Mungenast, and Li-Huei Tsai. 2010.

"Targeting the Correct HDAC(s) to Treat Cognitive Disorders." *Trends in Pharmacological Sciences* 31 (12): 605–17.

Fogle, Keri J., Lisa S. Baik, Jerry H. Houl, Tri T. Tran, Logan Roberts, Nicole A. Dahm, Yu Cao, Ming Zhou, and Todd C. Holmes. 2015. "CRYPTOCHROME-Mediated Phototransduction by Modulation of the Potassium Ion Channel β-Subunit Redox Sensor." *Proceedings of the National Academy of Sciences of the United States of America* 112 (7): 2245–50.

Fogle, Keri J., Kelly G. Parson, Nicole A. Dahm, and Todd C. Holmes. 2011. "CRYPTOCHROME Is a Blue-Light Sensor That Regulates Neuronal Firing Rate." *Science* 331 (6023): 1409–13.

Gräff, Johannes, and Li-Huei Tsai. 2013. "Histone Acetylation: Molecular Mnemonics on the Chromatin." *Nature Reviews. Neuroscience* 14 (2): 97–111.

Gregoretti, Ivan V., Yun-Mi Lee, and Holly V. Goodson. 2004. "Molecular Evolution of the Histone Deacetylase Family: Functional Implications of Phylogenetic Analysis." *Journal of Molecular Biology* 338 (1): 17–31.

Hallem, Elissa A., Michael G. Ho, and John R. Carlson. 2004. "The Molecular Basis of Odor Coding in the Drosophila Antenna." *Cell* 117 (7): 965–79.

Hubbs, A. F., L. A. Battelli, W. T. Goldsmith, D. W. Porter, D. Frazer, S. Friend, D. Schwegler-Berry, et al. 2002. "Necrosis of Nasal and Airway Epithelium in Rats Inhaling Vapors of Artificial Butter Flavoring." *Toxicology and Applied Pharmacology* 185 (2): 128–35.

Hubbs, Ann F., William T. Goldsmith, Michael L. Kashon, David Frazer, Robert R. Mercer, Lori A. Battelli, Gregory J. Kullman, Diane Schwegler-Berry, Sherri Friend, and Vincent Castranova. 2008. "Respiratory Toxicologic Pathology of Inhaled Diacetyl in Sprague-Dawley Rats." *Toxicologic Pathology* 36 (2): 330–44.

Hughes, Paul S., and E. Denise Baxter. 2007. *Beer: Quality, Safety and Nutritional Aspects*. Royal Society of Chemistry.

Jackson, George R., Iris Salecker, Xinzhong Dong, Xiang Yao, Norman Arnheim, Peter W. Faber, Marcy E. MacDonald, and S. Lawrence Zipursky. 1998. "Polyglutamine-Expanded Human Huntingtin Transgenes Induce Degeneration of Drosophila Photoreceptor Neurons." *Neuron* 21 (3): 633–42.

Kang, Hyung-Lyun, Seymour Benzer, and Kyung-Tai Min. 2002. "Life Extension in Drosophila by Feeding a Drug." *Proceedings of the National Academy of Sciences of the United States of America* 99 (2): 838–43.

Kazantsev, Aleksey G., and Leslie M. Thompson. 2008. "Therapeutic Application of Histone Deacetylase Inhibitors for Central Nervous System Disorders." *Nature Reviews. Drug Discovery* 7 (10): 854–68.

Knaden, Markus, and Bill S. Hansson. 2014. “Mapping Odor Valence in the Brain of Flies and Mice.” *Current Opinion in Neurobiology* 24 (1): 34–38.

Krogerus, Kristoffer, and Brian R. Gibson. 2013. “Influence of Valine and Other Amino Acids on Total Diacetyl and 2,3-Pentanedione Levels during Fermentation of Brewer’s Wort.” *Applied Microbiology and Biotechnology* 97 (15): 6919–30.

Kurahashi, T., and A. Menini. 1997. “Mechanism of Odorant Adaptation in the Olfactory Receptor Cell.” *Nature* 385 (6618): 725–29.

Larsson, Mattias C., Ana I. Domingos, Walton D. Jones, M. Eugenia Chiappe, Hubert Amrein, and Leslie B. Vosshall. 2004. “Or83b Encodes a Broadly Expressed Odorant Receptor Essential for Drosophila Olfaction.” *Neuron* 43 (5): 703–14.

Leipe, Detlef D., and David Landsman. 1997. “Histone Deacetylases, Acetoin Utilization Proteins and Acetylpolyamine Amidohydrolases Are Members of an Ancient Protein Superfamily.” *Nucleic Acids Research* 25 (18): 3693–97.

Maarse, Henk. 2017. *Volatile Compounds in Foods and Beverages*. Routledge.

Martineau, Brigitte, Thomas Henick-Kling, and Terry Acree. 1995. “Reassessment of the Influence of Malolactic Fermentation on the Concentration of Diacetyl in Wines.” *American Journal of Enology and Viticulture* 46 (3): 385–88.

Mi, Huaiyu, Xiaosong Huang, Anushya Muruganujan, Haiming Tang, Caitlin Mills, Diane Kang, and Paul D. Thomas. 2017. “PANTHER Version 11: Expanded Annotation Data from Gene Ontology and Reactome Pathways, and Data Analysis Tool Enhancements.” *Nucleic Acids Research* 45 (D1): D183–89.

Minucci, Saverio, and Pier Giuseppe Pelicci. 2006. “Histone Deacetylase Inhibitors and the Promise of Epigenetic (and More) Treatments for Cancer.” *Nature Reviews. Cancer* 6 (1): 38–51.

Mochalski, Paweł, Julian King, Martin Klieber, Karl Unterkofler, Hartmann Hinterhuber, Matthias Baumann, and Anton Amann. 2013. “Blood and Breath Levels of Selected Volatile Organic Compounds in Healthy Volunteers.” *The Analyst* 138 (7): 2134–45.

More, Swati S., Abbas Raza, and Robert Vince. 2012. “The Butter Flavorant, Diacetyl, Forms a Covalent Adduct with 2-Deoxyguanosine, Uncoils DNA, and Leads to Cell Death.” *Journal of Agricultural and Food Chemistry* 60 (12): 3311–17.

Morgan, Daniel L., Gordon P. Flake, Patrick J. Kirby, and Scott M. Palmer. 2008. “Respiratory Toxicity of Diacetyl in C57BL/6 Mice.” *Toxicological Sciences: An Official Journal of the Society of Toxicology* 103 (1): 169–80.

Palmer, Scott M., Gordon P. Flake, Fran L. Kelly, Helen L. Zhang, Julia L. Nugent, Patrick J. Kirby, Julie F. Foley, William M. Gwinn, and Dan L. Morgan. 2011. “Severe Airway

Epithelial Injury, Aberrant Repair and Bronchiolitis Obliterans Develops after Diacetyl Instillation in Rats." *PloS One* 6 (3): e17644.

Postberg, Jan, Sakeh Forcob, Wei-Jen Chang, and Hans J. Lipps. 2010. "The Evolutionary History of Histone H3 Suggests a Deep Eukaryotic Root of Chromatin Modifying Mechanisms." *BMC Evolutionary Biology* 10 (August): 259.

Robertson, Hugh M. 1998. "Two Large Families of Chemoreceptor Genes in the NematodesCaenorhabditis Elegans and Caenorhabditis Briggsae Reveal Extensive Gene Duplication, Diversification, Movement, and Intron Loss." *Genome Research* 8 (5): 449–63.

Robinson, Mark D., Davis J. McCarthy, and Gordon K. Smyth. 2010. "edgeR: A Bioconductor Package for Differential Expression Analysis of Digital Gene Expression Data." *Bioinformatics* 26 (1): 139–40.

Sachse, Silke, Erroll Rueckert, Andreas Keller, Ryuichi Okada, Nobuaki K. Tanaka, Kei Ito, and Leslie B. Vosshall. 2007. "Activity-Dependent Plasticity in an Olfactory Circuit." *Neuron* 56 (5): 838–50.

Saraiva, Marco A., Carlos M. Borges, and M. Helena Florêncio. 2006. "Reactions of a Modified Lysine with Aldehydic and Diketonic Dicarbonyl Compounds: An Electrospray Mass Spectrometry Structure/activity Study." *Journal of Mass Spectrometry: JMS* 41 (2): 216–28.

Shahbazian, Mona D., and Michael Grunstein. 2007. "Functions of Site-Specific Histone Acetylation and Deacetylation." *Annual Review of Biochemistry* 76: 75–100.

Shibamoto, Takayuki. 2014. "Diacetyl: Occurrence, Analysis, and Toxicity." *Journal of Agricultural and Food Chemistry* 62 (18): 4048–53.

Shimazu, Tadahiro, Matthew D. Hirschey, John Newman, Wenjuan He, Kotaro Shirakawa, Natacha Le Moan, Carrie A. Grueter, et al. 2013. "Suppression of Oxidative Stress by β-Hydroxybutyrate, an Endogenous Histone Deacetylase Inhibitor." *Science* 339 (6116): 211–14.

Soneson, Charlotte, Michael I. Love, and Mark D. Robinson. 2015. "Differential Analyses for RNA-Seq: Transcript-Level Estimates Improve Gene-Level Inferences." *F1000Research* 4 (December): 1521.

Starek-Swiechowicz, Beata, and Andrzej Starek. 2014. "Diacetyl Exposure as a Pneumotoxic Factor: A Review." *Roczniki Panstwowego Zakladu Higieny* 65 (2): 87–92.

Steffan, J. S., L. Bodai, J. Pallos, M. Poelman, A. McCampbell, B. L. Apostol, A. Kazantsev, et al. 2001. "Histone Deacetylase Inhibitors Arrest Polyglutamine-Dependent Neurodegeneration in Drosophila." *Nature* 413 (6857): 739–43.

Störtkuhl, Klemens F., Bernhard T. Hovemann, and John R. Carlson. 1999. “Olfactory Adaptation Depends on the Trp Ca 2+ Channel in Drosophila.” *The Journal of Neuroscience: The Official Journal of the Society for Neuroscience* 19 (12): 4839–46.

Thomas, Elizabeth A. 2014. “Involvement of HDAC1 and HDAC3 in the Pathology of Polyglutamine Disorders: Therapeutic Implications for Selective HDAC1/HDAC3 Inhibitors.” *Pharmaceuticals* 7 (6): 634–61.

Troemel, Emily R., Joseph H. Chou, Noelle D. Dwyer, Heather A. Colbert, and Cornelia I. Bargmann. 1995. “Divergent Seven Transmembrane Receptors Are Candidate Chemosensory Receptors in C. Elegans.” *Cell* 83 (2): 207–18.

Vosshall, Leslie B., Hubert Amrein, Pavel S. Morozov, Andrey Rzhetsky, and Richard Axel. 1999. “A Spatial Map of Olfactory Receptor Expression in the Drosophila Antenna.” *Cell* 96 (5): 725–36.

Whiteson, Katrine L., Simone Meinardi, Yan Wei Lim, Robert Schmieder, Heather Maughan, Robert Quinn, Donald R. Blake, Douglas Conrad, and Forest Rohwer. 2014. “Breath Gas Metabolites and Bacterial Metagenomes from Cystic Fibrosis Airways Indicate Active pH Neutral 2,3-Butanedione Fermentation.” *The ISME Journal* 8 (6): 1247–58.

Yu, Guangchuang, Li-Gen Wang, Yanyan Han, and Qing-Yu He. 2012. “clusterProfiler: An R Package for Comparing Biological Themes among Gene Clusters.” *Omics: A Journal of Integrative Biology* 16 (5): 284–87.

Zufall, F., and T. Leinders-Zufall. 1998. “Role of Cyclic GMP in Olfactory Transduction and Adaptation.” *Annals of the New York Academy of Sciences* 855 (November): 199–204.

Zufall, Frank, and Steven D. Munger. 2016. *Chemosensory Transduction: The Detection of Odors, Tastes, and Other Chemostimuli*. Academic Press.

Figure 4.1. *Drosophila* antenna alters gene expression on long-term exposure to odorant

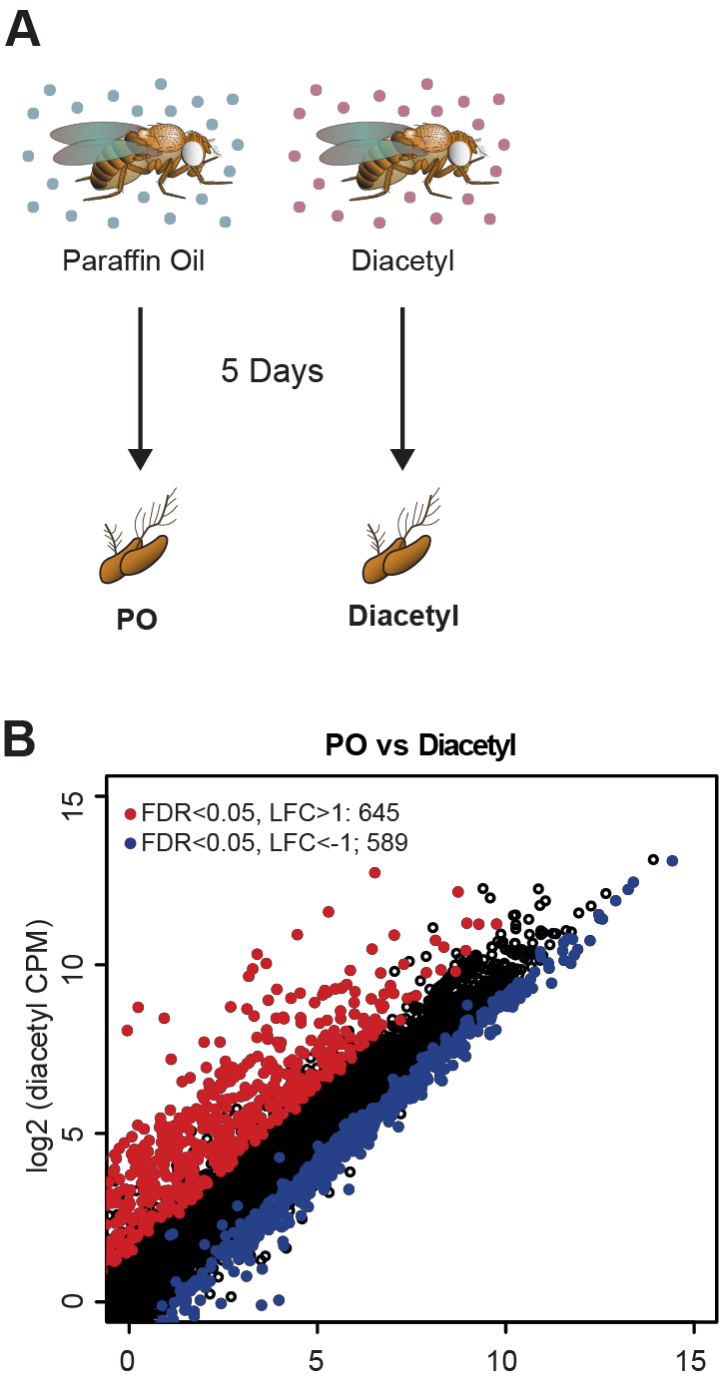

Figure 4.1. *Drosophila* antenna alters gene expression on long-term exposure to odorant

(A) Schematic of odor exposure protocol for transcriptome analysis from the antennae. (B) Plot highlighting up- and down-regulated genes in the diacetyl-exposed group. Red and blue dots represent up-regulated genes (false discovery rate (FDR) < 0.05, $\log_2$ fold change (LFC) > 1) and down-regulated genes (FDR < 0.05, LFC < 1), respectively.

Figure 4.2 GO enrichment for genes up-regulated in response to diacetyl

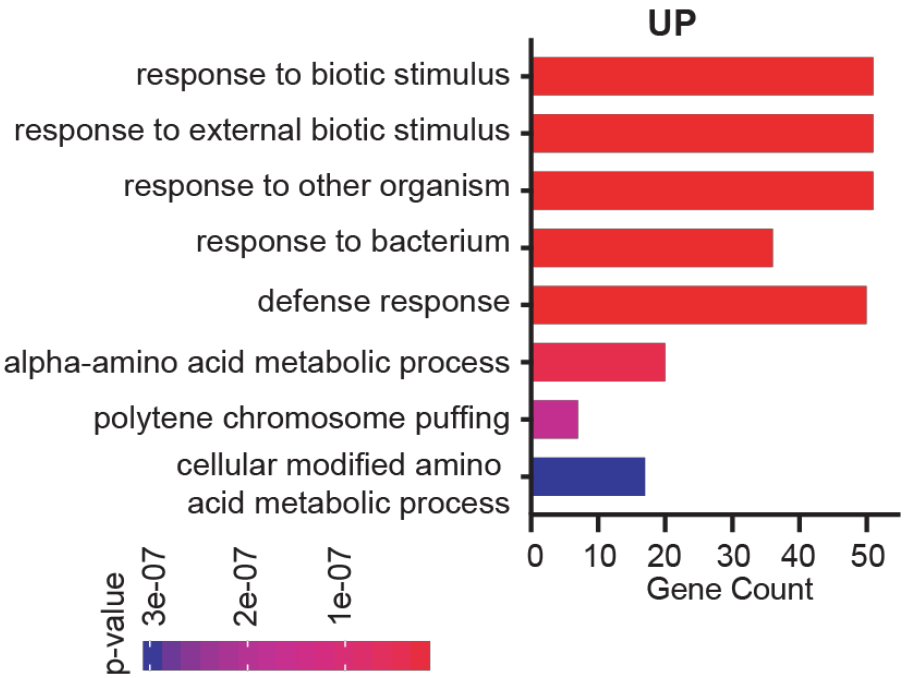

Figure 4.2 GO enrichment for genes up-regulated in response to diacetyl

Bar graphs showing enrichment for the top 8 biological process GO terms in the genes up-regulated after diacetyl treatment ($p < 0.05$). X-axis, Gene count for each GO-term. Y-axis, GO terms enriched in the diacetyl-exposed group. Bar color denotes p-value for enrichment.

Figure 4.3 Diacetyl exposure alters genes that encode a wide array of protein classes

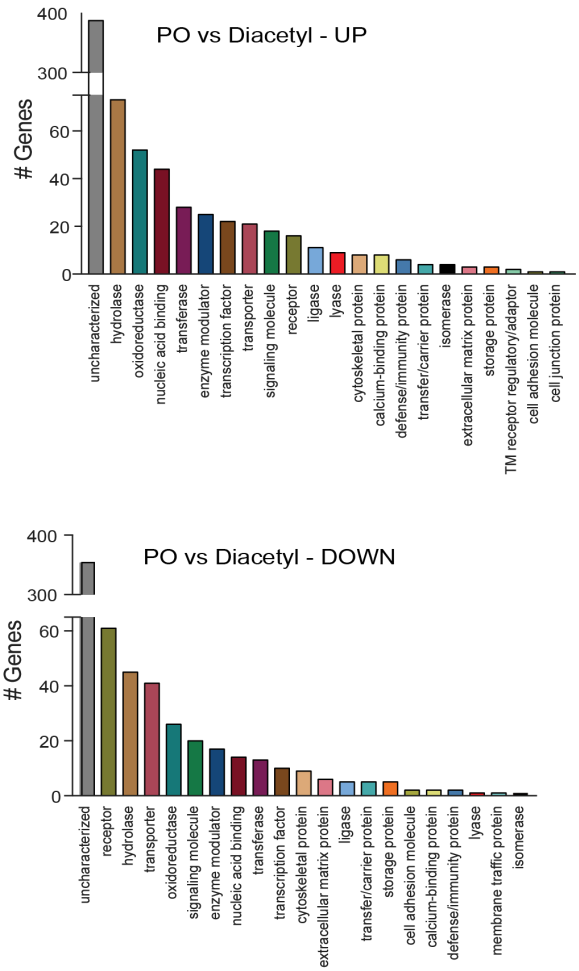

Figure 4.3 Diacetyl exposure alters genes that encode a wide array of protein classes

Bar graphs denoting the protein classification of the genes up- and down-regulated after odor exposure.

Figure 4.4 Differentially expressed in the antenna following treatment with two HDAC inhibitors

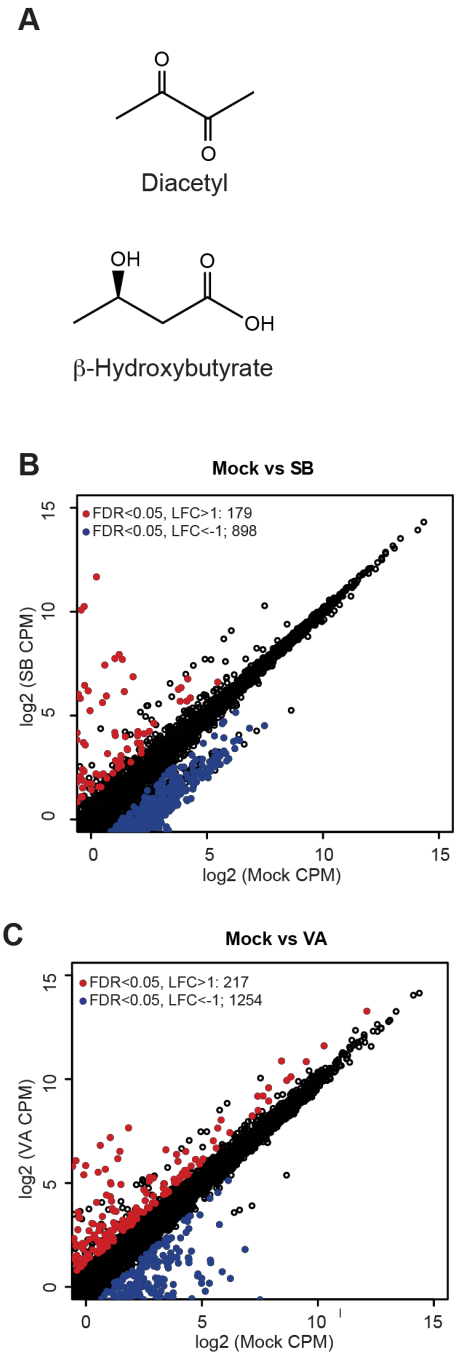

Figure 4.4 Differentially expressed in the antenna following treatment with two HDAC inhibitors

(A) Schematic chemical structures of diacetyl and -hydroxybutyrate.

(B and C) Plots showing enrichment of up- and down-regulated genes in sodium butyrate-(B) and valproic acid-treated (C) groups. Red and blue dots represent up-regulated genes (FDR < 0.05, LFC > 1) and down-regulated genes (FDR < 0.05, LFC < 1), respectively.

FIgure 4.5 Gene overlap between diacetyl and HDAC inhibitors

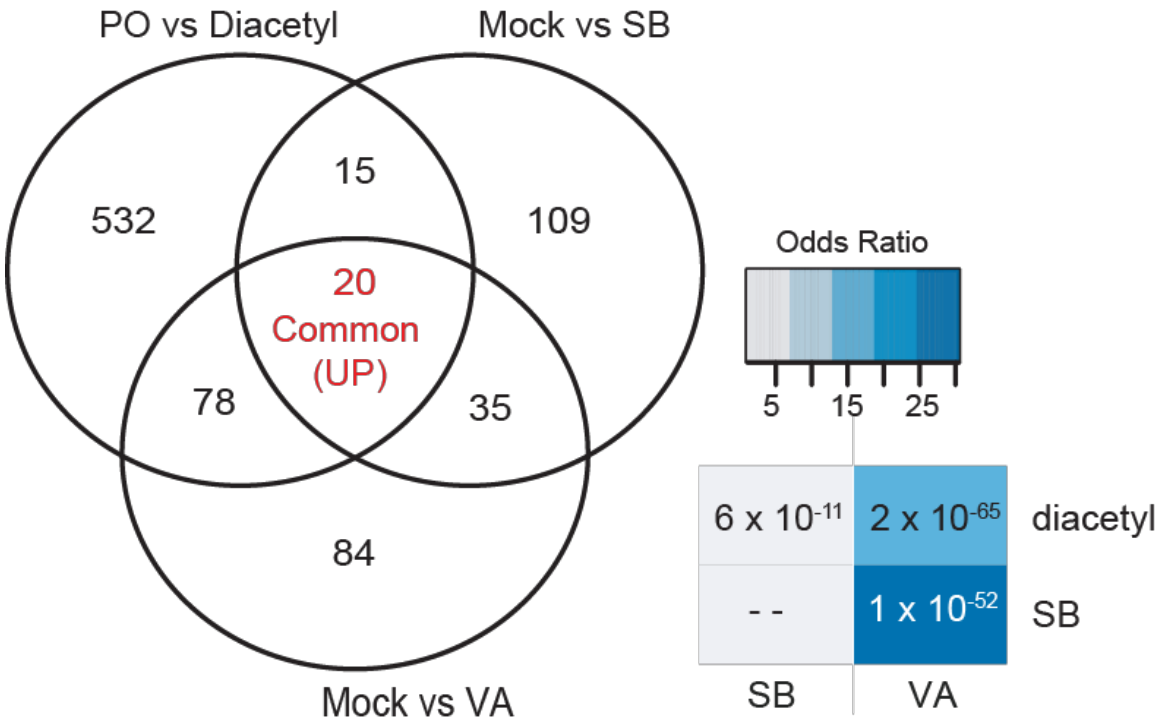

FIgure 4.5 Gene overlap between diacetyl and HDAC inhibitors

Left: Venn diagrams showing the overlaps of up-regulated genes among diacetyl-, sodium butyrate- and valproic acid-treated groups. *Right:* Table showing pairwise tests of significance of overlap between gene sets. P-values from Fisher's exact test.

Figure 4.6 HDACs are a more conserved family of proteins than olfactory receptors

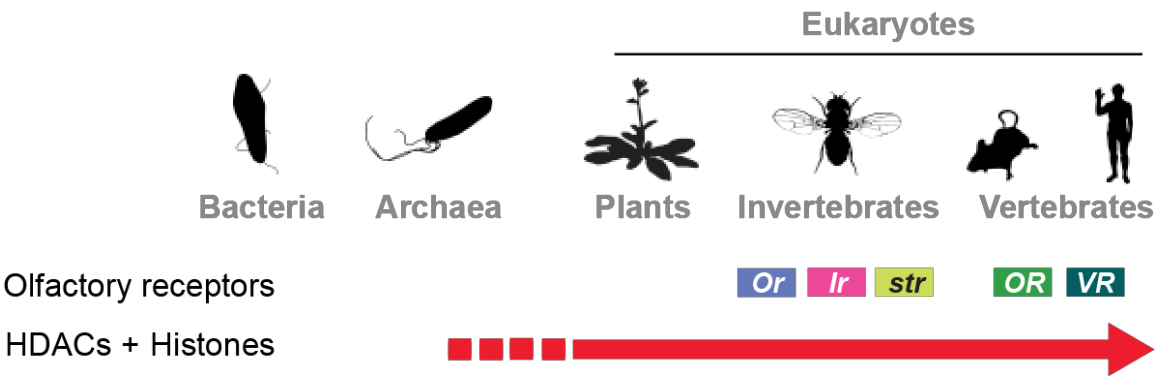

Figure 4.6 HDACs are a more conserved family of proteins than olfactory receptors

Schematic depicting the relatively low-conservation across different transmembrane olfactory receptor families, and the high-conservation of HDACs and histones.

Figure 4.7 Gene expression changes are partly reversible

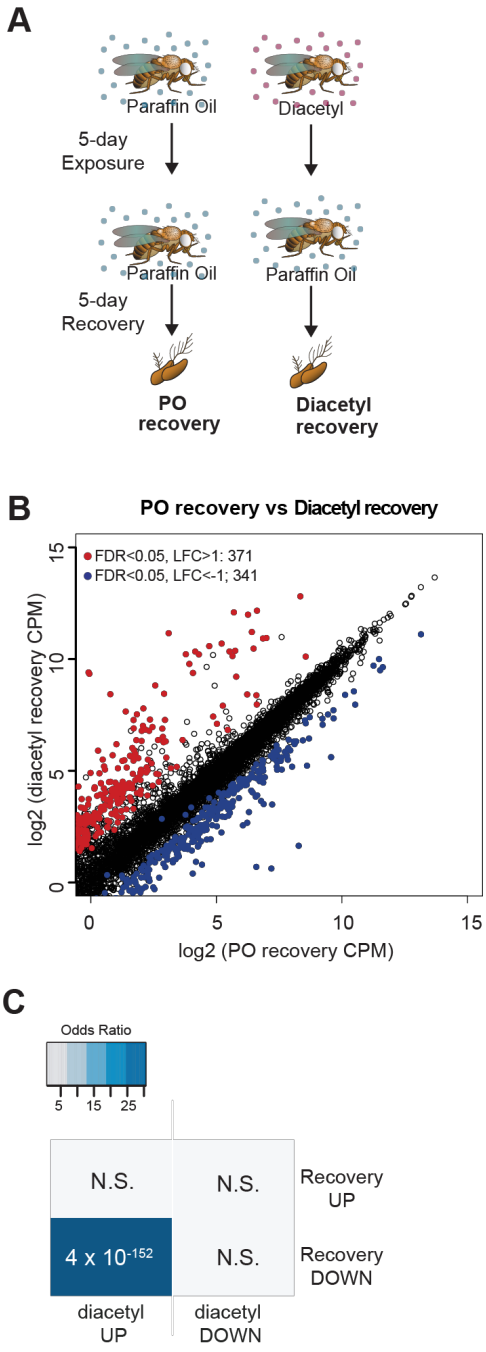

Figure 4.7 Gene expression changes are partly reversible

(A) Schematic of odor exposure and recovery protocol for transcriptome analysis from the antennae.

(B) Plot highlighting up- and down-regulated genes in the recovery from diacetyl exposure group. Red and blue dots represent up-regulated genes (FDR < 0.05, LFC > 1) and down-regulated genes (FDR < 0.05, LFC < 1), respectively.

(C) Table showing pairwise tests of significance of overlap between gene sets. P-values from Fisher's exact test, colored with associated odds ratio (strength of association).

Figure 4.8 Odor inhibits a family of HDACs *in vitro*

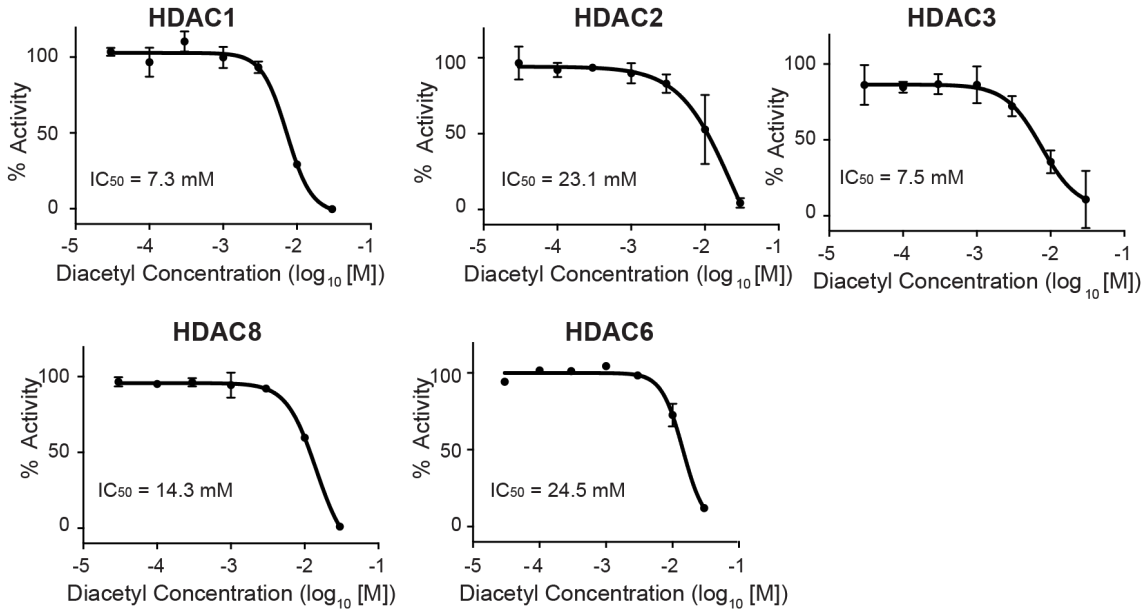

Figure 4.8 Odor inhibits a family of HDACs *in vitro*

Dose-activity curves of class I HDACs: HDAC1, HDAC2, HDAC3, HDAC8 and class II HDAC6 treated with various concentrations of diacetyl. IC50s are indicated in the chart areas. Error bars, S.E.M., n = 4-5.

Figure 4.9 Diacetyl increases H3K9 methylation in cell culture

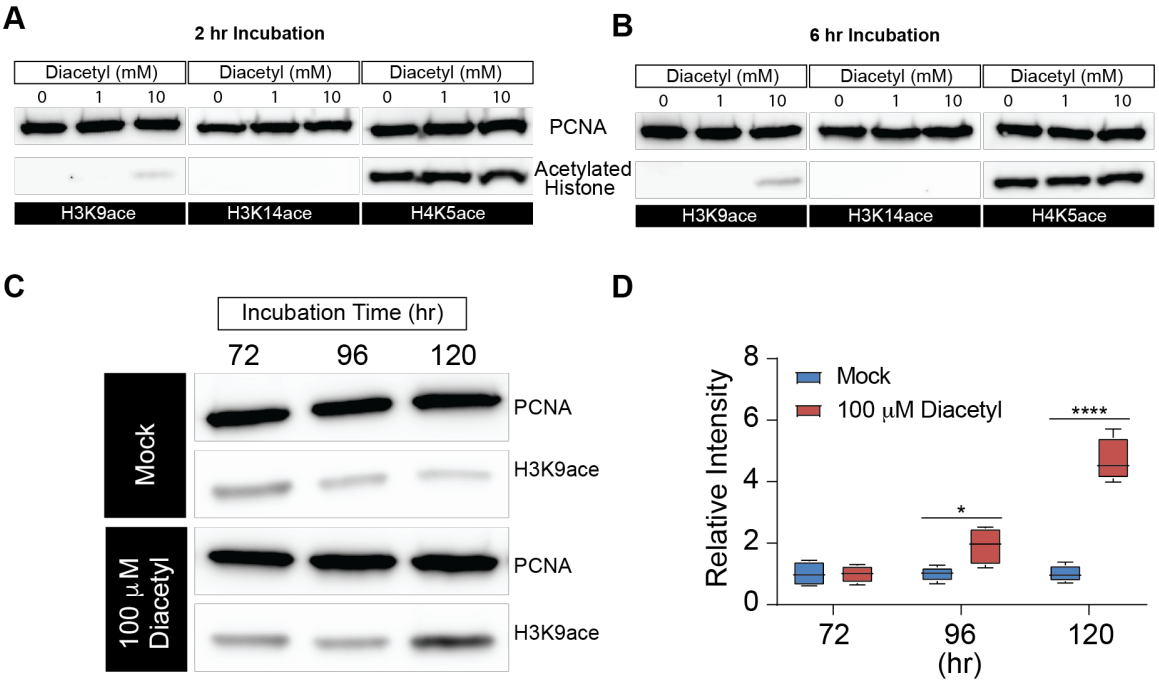

Figure 4.9 Diacetyl increases H3K9 methylation in cell culture

(A and B) Representative images from Western blots showing acetylation levels of H3K9 (left), H3K14 (middle) and H4K5 (right) in HEK293 cells after 2 hours (A) and 6 hours (B) of diacetyl exposure. PCNA (Proliferating cell nuclear antigen) is a 29 kDa nuclear protein used as a loading control for nuclear protein extracts.

(C) Western blots showing acetylation levels of H3K9 in HEK293 cells treated with 100 M diacetyl for 72 -120 hours. PCNA is used for a loading control.

(D) Box and whisker plot showing the relative intensities of acetylated H3K9 in HEK293 cells treated with 100 M diacetyl for 72 -120 hours. Box and whiskers represent minimum, 1st quartile, median, 3rd quartile, and maximum, n = 4 samples, *p*=0.9794, 0.0362 (*), <0.0001 (****) respectively determined by unpaired *t* test (two-tailed) against mock at each time point. (t= 0.02687, 2.688, 9.408 respectively, df= 6).

Figure 4.10 Exposure to diacetyl vapor alters gene expression in mouse lungs

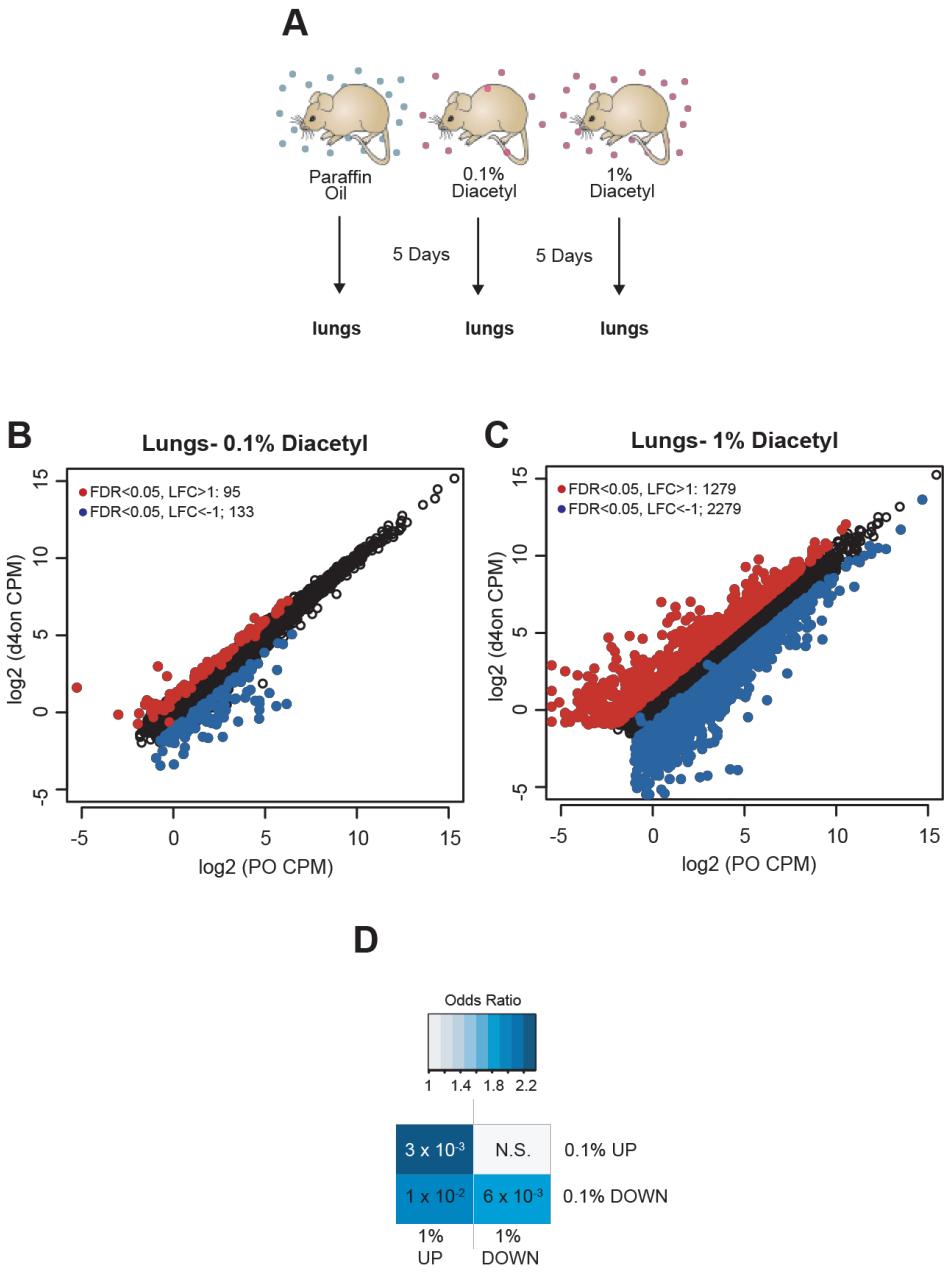

Figure 4.10 Exposure to diacetyl vapor alters gene expression in mouse lungs

(A) Schematic of diacetyl exposure protocol for transcriptome analysis of mouse lung tissue.

(B and C) Plot highlighting up- and down-regulated genes in the diacetyl-exposed groups. Red and blue dots represent up-regulated genes (FDR < 0.05, LFC > 1) and down-regulated genes (FDR < 0.05, LFC < 1), respectively in lungs.

(D) Table showing pairwise tests of significance of overlap between gene sets. P-values from Fisher's exact test, colored with associated odds ratio (strength of association).

Figure 4.11 Diacetyl exposure alters genes that encode a wide array of protein classes

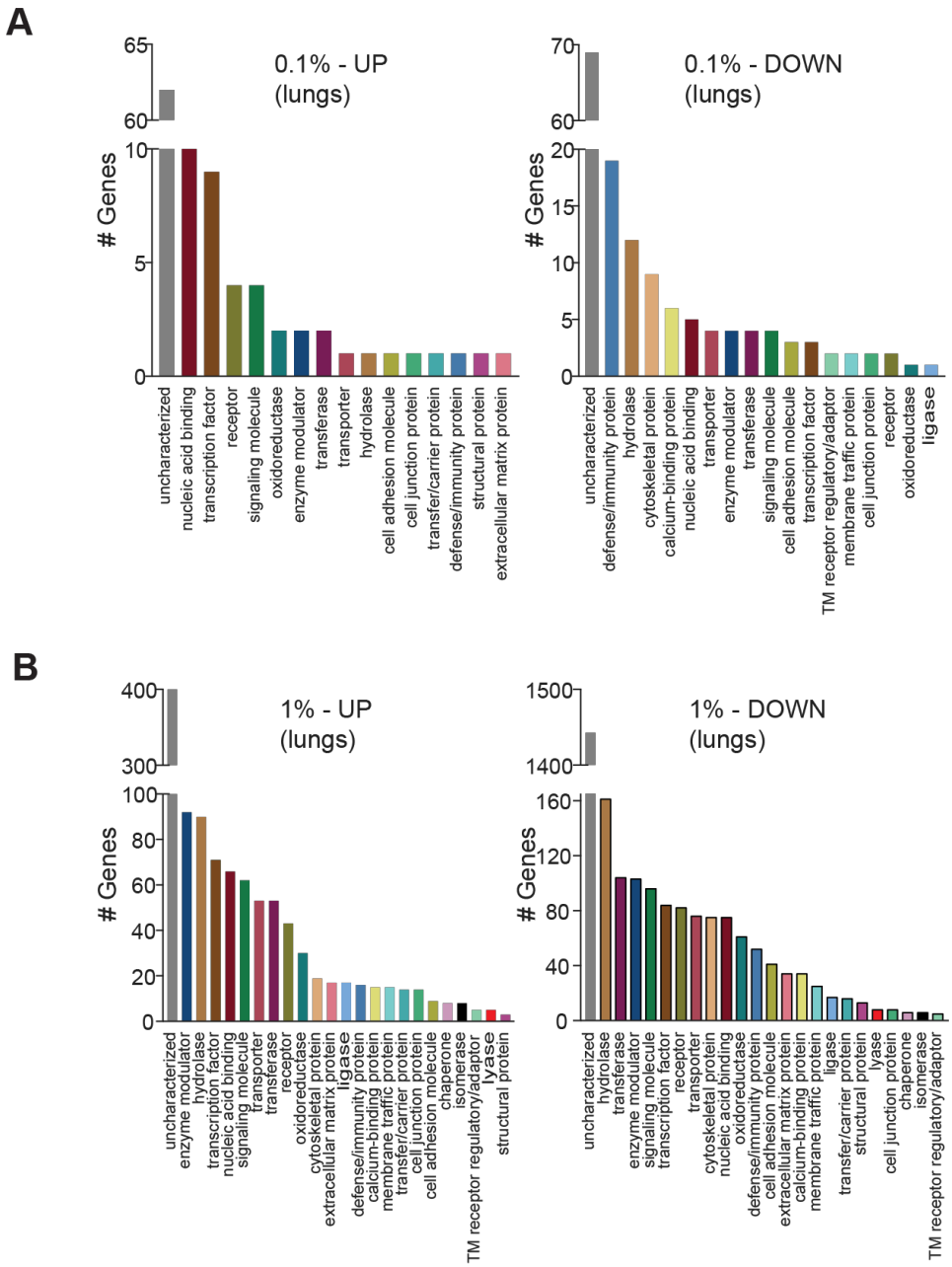

Figure 4.11 Diacetyl exposure alters genes that encode a wide array of protein classes

(A and B) Bar graphs denoting the protein classification of the genes up and down-regulated in the lung after odor exposure.

Figure 4.12 Exposure to diacetyl vapor alters gene expression in plant leaflets

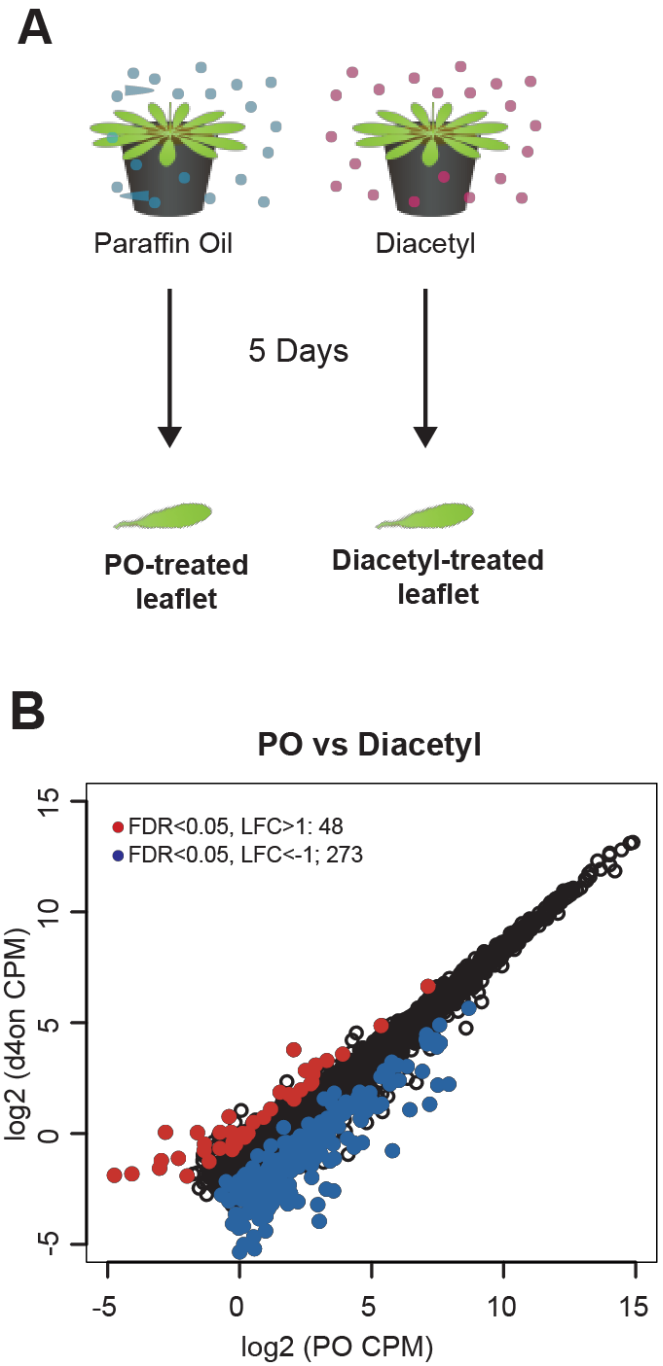

Figure 4.12 Exposure to diacetyl vapor alters gene expression in plant leaflets

(A) Schematic of diacetyl exposure protocol for transcriptome analysis of *Arabidopsis* leaflets.

(B) Plot highlighting up- and down-regulated genes in the diacetyl-exposed groups in leaves

Figure 4.13 Diacetyl exposure alters genes that encode a wide array of protein classes

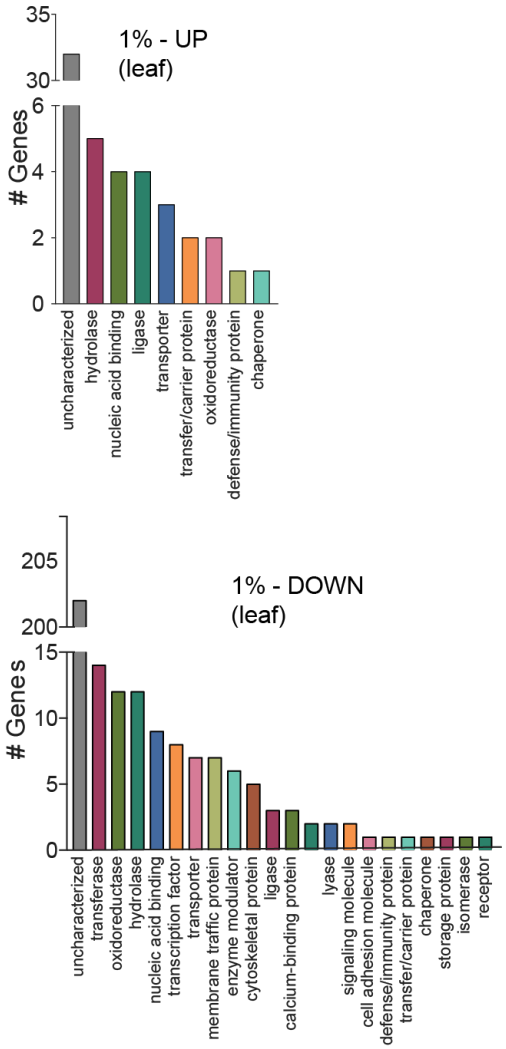

Figure 4.13 Diacetyl exposure alters genes that encode a wide array of protein classes

Bar graphs denoting the protein classification of the plant genes up- and down-regulated after odor exposure.

Figure 4.14 Exposure to diacetyl vapor alters gene expression in the mouse brain

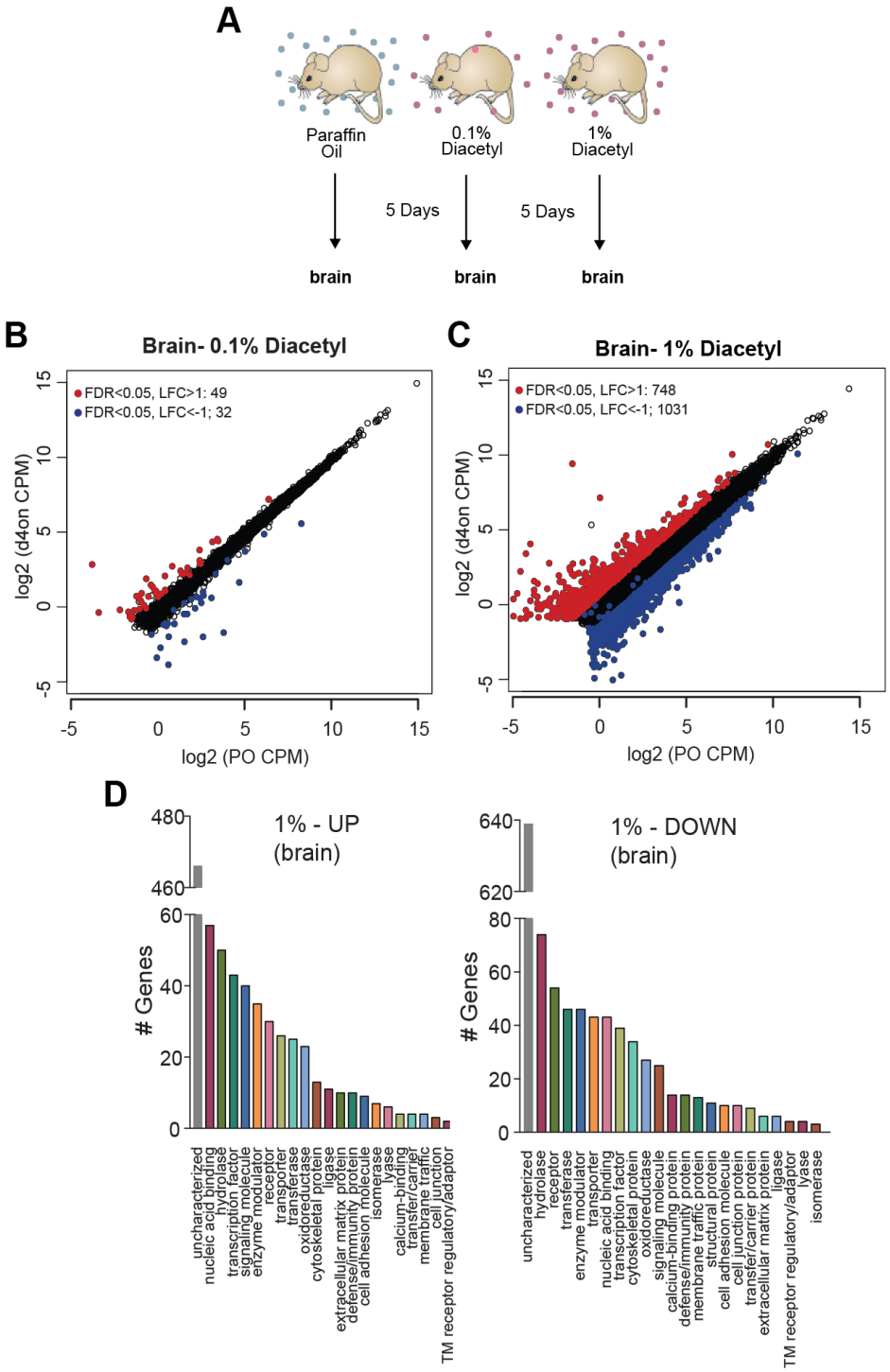

Figure 4.14 Exposure to diacetyl vapor alters gene expression in the mouse brain

(A) Schematic of diacetyl exposure protocol for transcriptome analysis of mouse brain tissues.

(B and C) Plot showing up- and down-regulated genes in the diacetyl-exposed groups. Red and blue dots represent up-regulated genes (FDR < 0.05, LFC > 1) and down-regulated genes (FDR < 0.05, LFC < 1), respectively in the brain.

(D) Bar graphs denoting the protein classification of the brain genes up- and down-regulated after odor exposure.

Figure 4.15 Odor exposure slows Huntington's neurodegeneration model in fly eye

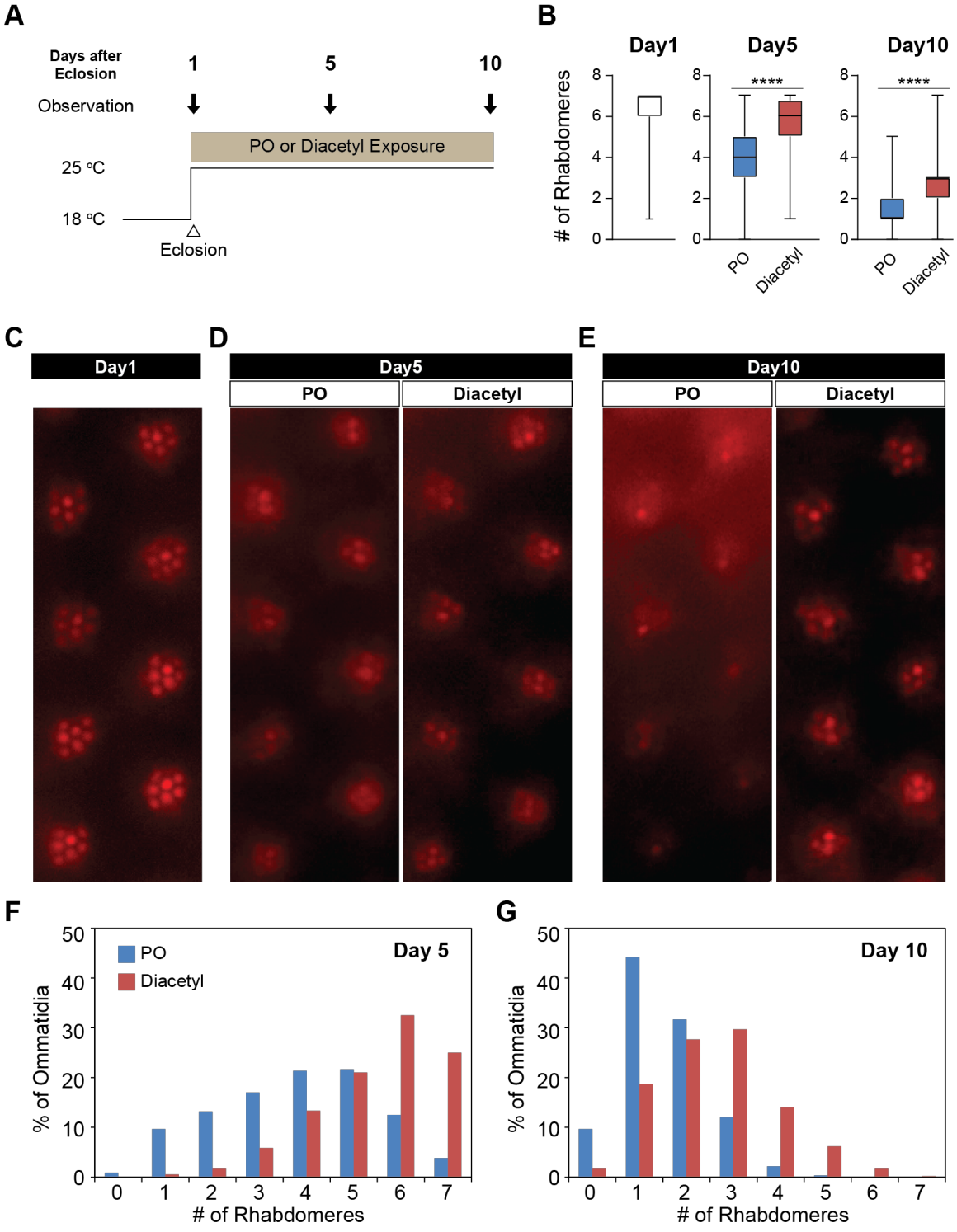

Figure 4.15 Odor exposure slows Huntington's neurodegeneration model in fly eye

(A) Schematic diagram showing temperature of experimental condition and timing of the eye examination in pGMR-HTTQ120 flies.

(B) Box and whisker plot showing mean number of rhabdomeres in each ommatidium in solvent PO (blue) and diacetyl-exposed (red) pGMR-HTTQ120 flies at 1, 5 and 10 day after eclosion (AE). Box and whiskers represent minimum, 1st quartile, median, 3rd quartile, and maximum, n = 600 ommatidia from 15 flies, p=<0.0001 (****) for both determined by unpaired *t* test (two-tailed) against PO at each time point. (t= 19.5, 16.83 respectively, df= 1198).

(C) A representative image of ommatidia of pGMR-HTTQ120 flies at AE 1 day.

(D and E) Representative images of ommatidia of pGMR-HTTQ120 flies exposed to paraffin oil (PO) or diaceyl after eclosion.

(F and G) Histogram showing the percent of the ommatidium with a given number of rhabdomeres indicated on the x axis.

Figure 4.16 Model

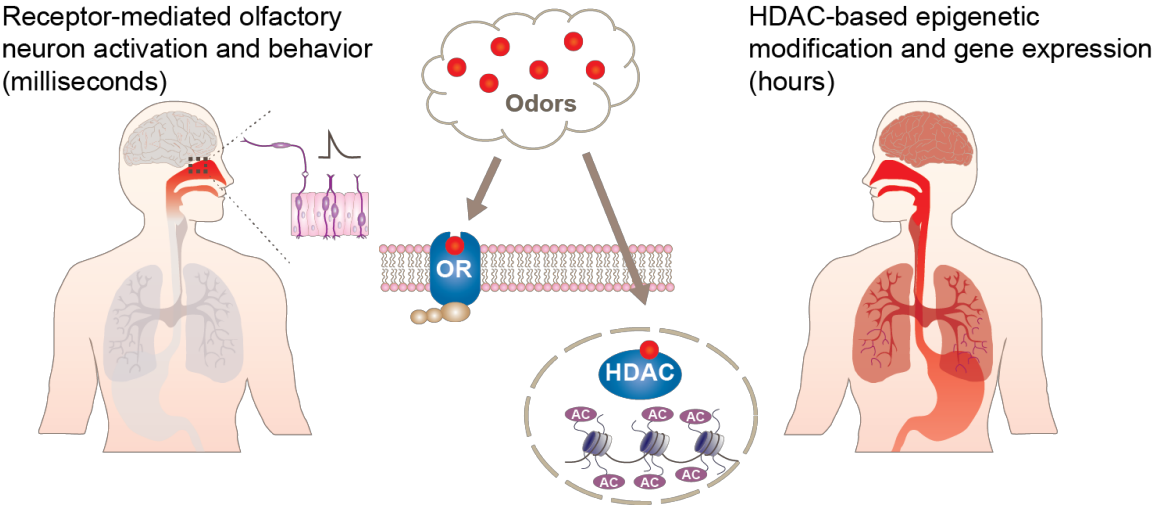

Figure 4.16 Model

A schematic depicting the 2 pathways through which odorants like diacetyl are likely to act. The red shading indicates tissues that we anticipate to be affected by diacetyl in each diagram.

Figure 4.17 Go enrichment for regulated genes common to mouse lungs exposed to 0.1% and 1% diacetyl

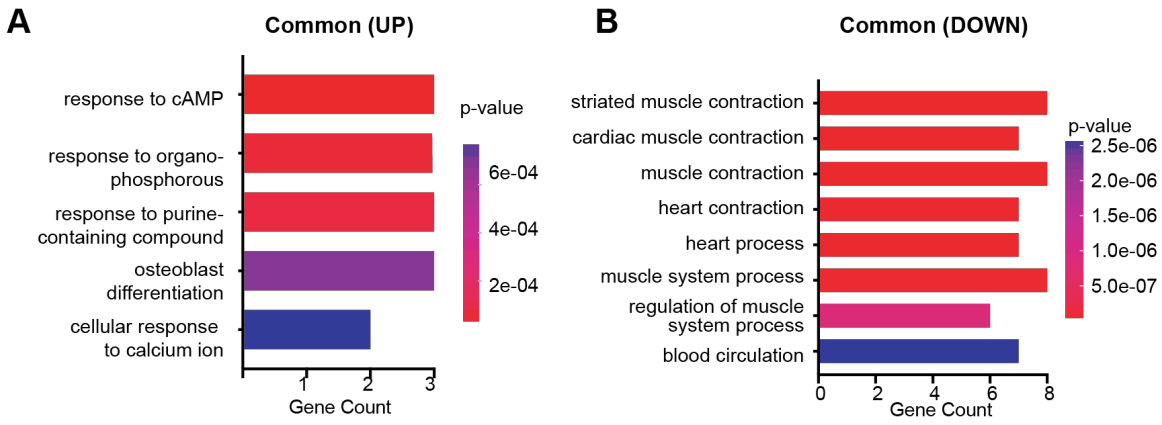

Figure 4.17 Go enrichment for regulated genes common to mouse lungs exposed to 0.1% and 1% diacetyl

(A) Bar graphs showing enrichment for biological process GO terms in the set of up-regulated genes in the mouse lung that were common between 0.1% and 1% treatments

(B) Bar graphs showing enrichment for the top 8 biological process GO terms in the set of down-regulated genes in the mouse lung that were common between 0.1% and 1% treatments ($p < 0.05$). X-axis, Gene count for each GO-term. Y-axis, GO terms enriched in the diacetyl-exposed group. Bar color denotes p-value for enrichment.

Figure 4.18 Exposure to diacetyl leads to gene expression changes in *Arabidopsis thaliana*

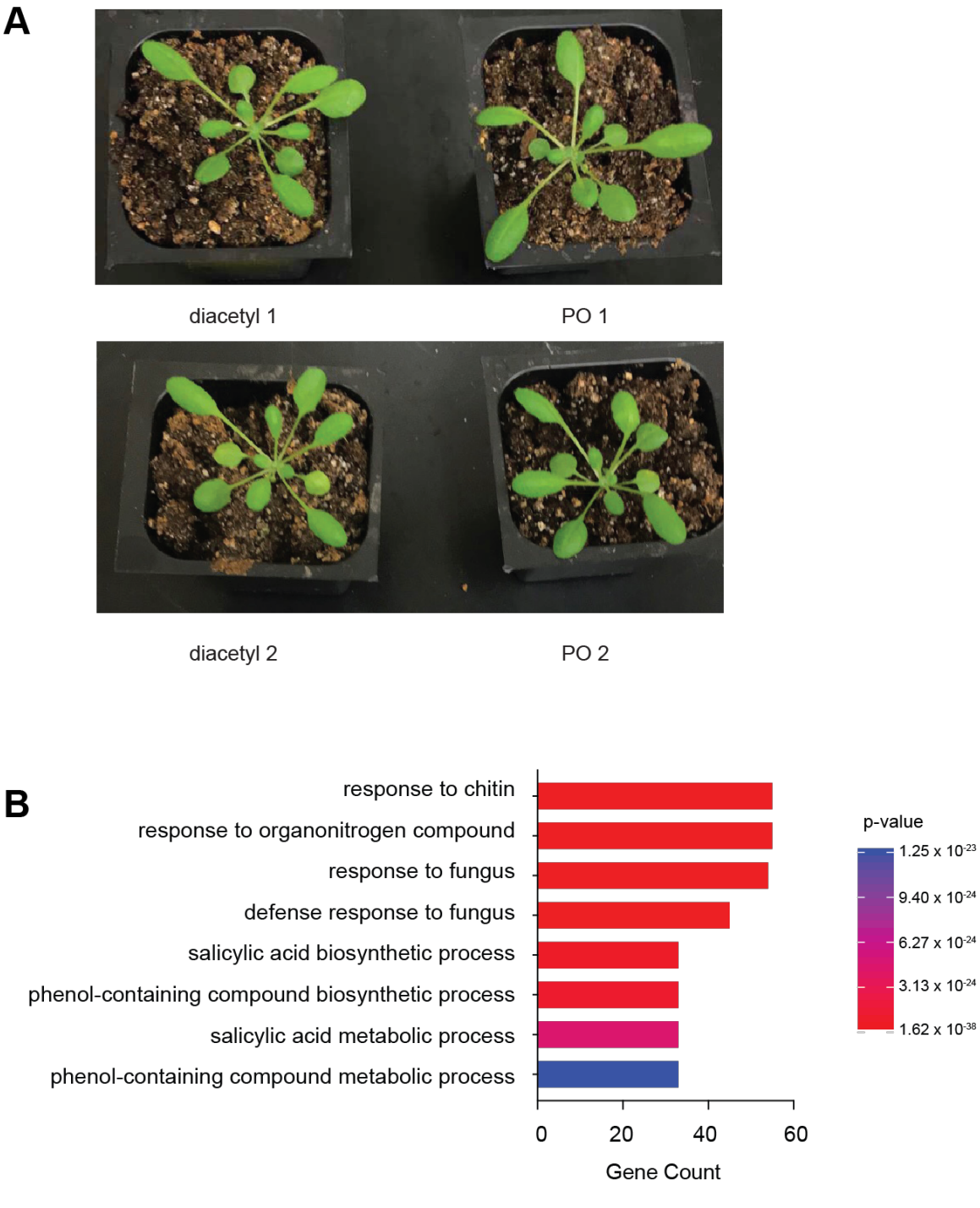

Figure 4.18 Exposure to diacetyl leads to gene expression changes in *Arabidopsis thaliana*

(A) *Arabidopsis* plants after exposure to either diacetyl or paraffin oil for 5 days.

(B) Bar graphs showing enrichment for the top 8 biological process GO terms in the set of down-regulated genes in *Arabidopsis* leaflets ($p < 0.05$). X-axis, Gene count for each GO-term. Y-axis, GO terms enriched in the diacetyl-exposed group. Bar color denotes p-value for enrichment. No enrichment found for up-regulated genes.

Table 4.1 Top 100 genes altered in response to 1% diacetyl in the fly antenna

Gene	logFC	PValue	FDR
FBgn0010041	7.760970184	5.09E-38	5.74E-34
FBgn0039670	8.698907337	2.60E-32	1.47E-28
FBgn0052557	7.093599468	6.02E-26	2.26E-22
FBgn0013277	5.366238773	5.38E-25	1.52E-21
FBgn0034756	6.00503928	4.97E-20	1.12E-16
FBgn0259140	5.539325146	3.30E-19	5.38E-16
FBgn0261845	-9.325517842	3.34E-19	5.38E-16
FBgn0002565	4.956830894	8.36E-19	1.18E-15
FBgn0010040	5.329046059	2.64E-18	3.32E-15
FBgn0033296	-14.87154321	3.29E-18	3.71E-15
FBgn0040837	5.914570636	4.39E-18	4.50E-15
FBgn0036996	9.266369948	1.13E-17	1.06E-14
FBgn0053757	-4.51217275	1.81E-17	1.57E-14
FBgn0033926	4.808233011	2.75E-16	2.22E-13
FBgn0013276	3.824799924	1.70E-15	1.28E-12
FBgn0013278	3.992119206	1.17E-14	8.26E-12
FBgn0002563	3.891419575	1.30E-14	8.60E-12
FBgn0033928	3.448999537	1.10E-13	6.87E-11
FBgn0085195	3.303687231	1.28E-13	7.59E-11
FBgn0039685	3.237172356	1.50E-12	8.11E-10
FBgn0032144	4.697364407	1.51E-12	8.11E-10
FBgn0031746	4.219255945	1.59E-12	8.17E-10
FBgn0262540	-3.249944721	1.70E-12	8.31E-10
FBgn0003067	3.15904828	2.93E-12	1.32E-09
FBgn0266488	3.15904828	2.93E-12	1.32E-09
FBgn0052602	4.000136952	3.09E-12	1.34E-09
FBgn0034741	3.605950638	6.54E-12	2.73E-09
FBgn0262856	-3.753193099	6.82E-12	2.75E-09
FBgn0085256	3.101637955	9.23E-12	3.59E-09
FBgn0038074	3.725718836	1.27E-11	4.77E-09
FBgn0001225	3.860862732	1.31E-11	4.78E-09
FBgn0031888	3.632617089	2.17E-11	7.64E-09
FBgn0030904	4.358516976	2.37E-11	8.12E-09

FBgn0001223	3.962946534	2.48E-11	8.24E-09
FBgn0260474	3.364864581	3.26E-11	1.05E-08
FBgn0032726	3.128746406	3.42E-11	1.07E-08
FBgn0034276	3.212123584	3.59E-11	1.10E-08
FBgn0001230	3.360869248	5.35E-11	1.53E-08
FBgn0003248	3.945707188	5.37E-11	1.53E-08
FBgn0053542	4.397756941	5.43E-11	1.53E-08
FBgn0261501	-4.185635151	6.19E-11	1.70E-08
FBgn0040732	3.340749283	8.04E-11	2.16E-08
FBgn0013279	3.247261573	9.47E-11	2.48E-08
FBgn0022772	3.425054177	1.60E-10	4.09E-08
FBgn0029766	2.973762569	1.87E-10	4.69E-08
FBgn0005655	3.456590862	2.49E-10	6.10E-08
FBgn0264541	-3.200753351	2.68E-10	6.42E-08
FBgn0266420	2.957150652	2.80E-10	6.59E-08
FBgn0085358	-11.39169828	3.35E-10	7.72E-08
FBgn0263076	-3.248258507	4.28E-10	9.65E-08
FBgn0066293	-3.148858407	4.37E-10	9.68E-08
FBgn0039801	2.907330979	5.49E-10	1.19E-07
FBgn0039827	3.069261483	8.24E-10	1.75E-07
FBgn0250842	4.280584327	8.62E-10	1.80E-07
FBgn0033153	3.979830438	9.99E-10	2.05E-07
FBgn0039031	2.93417695	1.05E-09	2.11E-07
FBgn0038795	2.995329108	1.16E-09	2.29E-07
FBgn0023415	3.984394755	1.28E-09	2.48E-07
FBgn0037151	3.052427376	1.38E-09	2.64E-07
FBgn0035186	3.226312429	2.08E-09	3.90E-07
FBgn0035781	2.919528247	2.22E-09	4.11E-07
FBgn0259716	2.997439484	2.73E-09	4.96E-07
FBgn0040096	4.091490081	3.22E-09	5.73E-07
FBgn0038732	-3.049955769	3.25E-09	5.73E-07
FBgn0001187	2.670348979	3.38E-09	5.83E-07
FBgn0039073	2.823024228	3.41E-09	5.83E-07
FBgn0026397	-3.814129449	3.92E-09	6.60E-07
FBgn0259683	-4.030629056	4.26E-09	7.06E-07
FBgn0033110	-3.291682114	4.34E-09	7.10E-07
FBgn0035439	2.840036166	5.06E-09	8.16E-07

FBgn0039682	2.786330441	5.17E-09	8.22E-07
FBgn0026314	-2.554350499	5.35E-09	8.38E-07
FBgn0035604	-3.955087798	6.21E-09	9.60E-07
FBgn0032538	3.246529116	6.79E-09	1.03E-06
FBgn0039800	2.738530917	7.14E-09	1.07E-06
FBgn0051354	3.52100875	8.67E-09	1.29E-06
FBgn0263830	-3.528105755	8.80E-09	1.29E-06
FBgn0038350	-3.893145617	9.64E-09	1.39E-06
FBgn0036232	6.416455344	1.10E-08	1.58E-06
FBgn0010043	2.945163097	1.15E-08	1.63E-06
FBgn0020638	-7.380030289	1.21E-08	1.67E-06
FBgn0037590	-4.101760835	1.22E-08	1.67E-06
FBgn0033835	2.643100619	1.23E-08	1.67E-06
FBgn0053057	2.728258087	1.26E-08	1.69E-06
FBgn0038798	-4.32212991	1.27E-08	1.69E-06
FBgn0034117	2.876262106	1.40E-08	1.84E-06
FBgn0033520	2.470145837	1.44E-08	1.87E-06
FBgn0034865	-4.493515355	1.47E-08	1.89E-06
FBgn0262539	-2.469299291	1.54E-08	1.95E-06
FBgn0031800	-2.920953659	1.58E-08	1.98E-06
FBgn0036078	-4.42193368	1.63E-08	2.01E-06
FBgn0050489	2.848045148	1.64E-08	2.01E-06
FBgn0033170	3.094002821	1.72E-08	2.09E-06
FBgn0011703	2.644401571	2.04E-08	2.44E-06
FBgn0041627	2.510227751	2.23E-08	2.65E-06
FBgn0039551	-5.627327423	2.47E-08	2.90E-06
FBgn0000078	2.758283581	2.69E-08	3.11E-06
FBgn0041337	2.639922684	2.71E-08	3.11E-06
FBgn0000492	2.876598924	2.73E-08	3.11E-06
FBgn0033043	-3.727553888	2.78E-08	3.14E-06

Table 4.2 Library details

Name	Tissue	Length	Reads Mapped	Percent
d4on_A	Antenna	single-50	31242412	85.78719449
d4on_B	Antenna	paired-50	13506165	75.4315606
PO_A	Antenna	paired-50	20793443	89.13641332
PO_B	Antenna	paired-50	17611515	87.56529169
d4onR_A	Antenna	single-50	43758561	83.74239823
d4onR_B	Antenna	paired-50	15423350	86.30606773
POR_A	Antenna	single-50	28313854	81.78774241
POR_B	Antenna	paired-50	14263894	84.57587085
sodium_butyrate_A	Antenna	paired-50	19608425	89.46434204
sodium_butyrate_B	Antenna	paired-50	22406913	90.43924656
valproic_acid_A	Antenna	paired-50	20590722	93.15393272
valproic_acid_B	Antenna	paired-50	21077614	92.22686316
untreated_A	Antenna	paired-50	21565274	93.14662492
untreated_B	Antenna	paired-50	18753848	90.98069092
LC1	Lung	single-75	76814780	88.94367805
LC2	Lung	single-75	61467930	87.82770091
LD1	Lung	single-75	65188581	85.84393257
LD2	Lung	single-75	73483737	85.88325672
MLC_A	Lung	single-75	145289543	88.6872915
MLC_B	Lung	single-75	173355517	87.88601589
MLD_A	Lung	single-75	143550725	90.56070108
MLD_B	Lung	single-75	132434053	87.09205325
AC_A	Leaflet	single-75	68986878	95.76666104
AC_B	Leaflet	single-75	62383893	95.18273732
AD_A	Leaflet	single-75	70238224	96.03548415
AD_B	Leaflet	single-75	57861048	92.27076357
BC1	Brain	single-75	63149574	88.8412849
BC2	Brain	single-75	75729660	87.20762097
BD1	Brain	single-75	62524044	85.96768069
BD2	Brain	single-75	67187011	84.74950412
MBC_A	Brain	single-75	53389853	84.37919492
MBC_B	Brain	single-75	57991303	81.90528369
MBD_A	Brain	single-75	71030375	83.3375258
MBD_B	Brain	single-75	89893087	80.9092616

Chapter 5

Coordinated regulation of olfactory receptors and axon guidance molecules by POU-domain transcription factors *acj6* and *pdm3*

Overview

The genetic programs that underlie nervous system development and eventually give rise to complex circuitry and behaviors are poorly understood. POU-domain transcription factors *acj6* and *pdm3* have previously been shown to be required for proper specification of olfactory sensory neuron (OSN) identity in *Drosophila melanogaster*. Both of these genes are also necessary, in a subset of OSN classes, for guidance of OSN axons to their proper glomerulus in the antennal lobe. Given this role in the development of the fly olfactory system, we employed a genome-wide microarray approach to isolate the genomic targets of *acj6* and *pdm3* in the adult. We examined the transcript profiles of the head tissue of mutants versus wild-type and identified 857 and 425 genes whose expression levels differ significantly in *acj6* and *pdm3* null mutants, respectively. A significant number of these targets are shared between the two factors, supporting a combinatorial role for POU-domain transcription factors in the adult nervous system. Amongst these target genes, we find olfactory receptors (*Ors)* that were known to be regulated by these factors are detected along with several novel chemosensory targets. Furthermore, we identify many known and putative axon guidance genes are likely direct targets of *acj6* and *pdm3.* This supports a dual function for POU-domain transcription factors in coordinating *Or* and axon guidance gene choice in a subset of neurons of the developing insect olfactory system.

Introduction

The main challenge for any olfactory system is to extract qualitative information about odorants present in the environment. In the *Drosophila* olfactory system, odors are detected by olfactory receptor sensory hairs, or sensilla, that cover the two main olfactory organs on the head: the third segment of the antenna and the maxillary palps (Shanbhag, Müller, and Steinbrecht 2000; Stocker 1994). OSN identity is determined by the specific *Or* expressed, as each OSN typically expresses only a single *Or* from a family of approximately 60 genes (Clyne, Warr, et al. 1999; L. B. Vosshall, Wong, and Axel 2000). This "one receptor to one neuron" principle of odor coding is also found in vertebrate olfactory systems (Mombaerts 2004).

The *Drosophila* olfactory system provides an ideal model to study development due to its numerical simplicity, which has led to detailed characterizations of the peripheral olfactory organs at the molecular and functional levels (Hallem, Ho, and Carlson 2004; Hallem and Carlson 2006; Dahanukar, Hallem, and Carlson 2005; Leslie B. Vosshall and Stocker 2007). In the antenna, the sensilla are divided into 4 morphologically distinct classes: large basiconics, small basiconics, coeloconics, and trichoids, each of which are found in distinct but partially overlapping zones of the antenna (Fuss and Ray 2009). Each sensillum contains 1-4 OSN classes arranged in stereotypic combinations (Marien de Bruyne, Clyne, and Carlson 1999; M. de Bruyne, Foster, and Carlson 2001). Although a course spatial organization of sensilla types exists at the antennal surface (L. B. Vosshall et al. 1999), the cell bodies of neurons that belong to different OSN classes are intermixed at the periphery. Despite this intermixing, the axons of all OSNs that express *Or* gene all converge onto a single, defined spherical region within the antennal lobe (AL); this region is known as a glomerulus and its shape and location are defined for each OSN class (L.

B. Vosshall, Wong, and Axel 2000; Gao, Yuan, and Chess 2000; Fishilevich and Vosshall 2005; Couto, Alenius, and Dickson 2005). These glomeruli in the AL are the site where the axons of a given OSN class form synapses with the dendrites of projection neurons (PNs), each of which also typically map to a single glomerulus, allowing the information of the odor stimulus detected at the periphery to be faithfully transmitted to higher brain centers (G. S. Jefferis et al. 2001).

Several axon guidance molecules have been implicated in the formation of the *Drosophila* olfactory circuit, including growth cone signaling molecules Dock and Pak (Ang et al. 2003), the alternatively spliced Dscam cell adhesion molecule (Hummel et al. 2003), and Robo receptors (Jhaveri et al. 2004).]. The developmental processes that govern the stereotypic connections from the periphery to the AL, however, are not fully understood. Recent studies have suggested a strong link between Or gene choice and glomerular targeting. Taken together, it is likely that the programmed pattern of gene expression throughout development of the olfactory system leads to the selection of a single Or as well as the expression of an OSN-unique combination of axon guidance molecules. These cell surface axon guidance molecules then govern the local and long range interaction during axon pathfinding, leading to precise connections of OSNs, with or without the expression of the endogenous OR.

Additionally, the Or itself does not play a role in guiding the OSN axons to the AL, as Or gene expression occurs after the OSN axons have formed their specific connections in their stereotypic glomeruli (G. S. X. E. Jefferis et al. 2004).

POU-domain transcription factors *acj6* and *pdm3* have been shown to have control over Or gene expression(Bai, Goldman, and Carlson 2009; Clyne, Certel, et al. 1999; Tichy, Ray, and Carlson 2008). With respect to these POU-domain transcription factors,

OSNs can be divided into three groups: those whose Or expression rely on Acj6 alone, those that rely on both Acj6 and Pdm3, and those that do not rely on either for Or gene expression (Bai, Goldman, and Carlson 2009; Tichy, Ray, and Carlson 2008) . The overlapping functions of these transcription factors give insight into a possible combinatorial code of transcription factors, where the unique combination of transcription factor expression specifies Or gene choice. Acj6 has been shown to both positively and negatively regulate Or gene expression, depending on which alternatively spliced form(s) of the transcription factor were present in the OSN (Bai, Goldman, and Carlson 2009; Tichy, Ray, and Carlson 2008; Bai and Carlson 2010). Mutants of these POU-domain transcription factors also displayed defects in axon guidance at the level of the AL (Tichy, Ray, and Carlson 2008; Komiyama, Carlson, and Luo 2004). These studies suggest that this combinatorial code of Or gene expression is identical to that used to specify the suite of axon guidance molecules expressed in a given OSN.

Results

Genome-wide identification of acj6 targets in the Drosophila head.

To explore the hypothesis that *acj6* coordinates *Or* gene choice with proper axon guidance molecule expression we used Agilent DNA microarrays to identify the genomic targets of *acj6.* We performed a comparative analysis between the transcriptome isolated for wild type and *acj6* null mutant adult heads and found 530 genes that are higher in expression levels and 327 genes that are lower in *acj6* mutants (Figure 5.1A). GO-term analysis performed on these 837 differentially expressed genes yielded several classes of genes were enriched amongst the up- and down-regulated groups. As expected, genes involved in the sensory perception of smell were enrichmed in the down-regulated gene set, which is consistent with the previously identified role for *acj6* in *Or* gene expression

(Figure 5.2A). Surprisingly, we found enrichment for genes involved in reproduction and mating behavior within the genes that are higher in *acj6* mutants (Figure 5.2A). This suggests a novel role for *acj6* in social behavior, perhaps acting as a repressor for reproductive gene expression. Finally, in both gene sets we find enrichment for genes with extracellular regions, supporting our hypothesis that axon guidance molecules are regulated by *acj6* (Figure 5.2A).

Genome-wide identification of pdm3 targets in the Drosophila head.

We performed identical microarray analysis comparing gene expression in the adult head between wild type and *pdm3* mutants. We found 309 genes and 116 genes whose expression is significantly increased and decreased, respectively in the heads of *pdm3* mutants (Figure 5.1B). The total number of differentially expressed genes is reduced by nearly half in *pdm3* mutants, suggesting it plays a significantly smaller role in regulation gene expression in the adult nervous system than does *acj6.* GO-term analysis reveals that *pdm3* also regulated genes with diverse functions, including a potential reporessor role for genes involved in flight, defense response to other organisms, and proteolysis (Figure 5.2B). Interestingly, the most enriched term among the genes lost in *pdm3* mutants is “photoreactive repair” which is also enriched in genes lost in *acj6* mutants. This strongly suggests that both *acj6* and *pdm3* POU-domain transcription factors are required for proper expression of DNA repair machinery (Figure 5.2A,B). Lastly, we see an increase in genes that are at least in-part located in the extracellular space as seen with *acj6* mutants (Figure 5.2B). This supports the notion that *pdm3* also regulates axon guidance molecules in the *Drosophila* adult.

Overlap analysis between acj6 and pdm3 targets reveals a subset of genes that require both transcription factors.

We next sought to examine a potential combinatorial role for *acj6* and *pdm3* for proper gene expression in the adult head. Comparison of the genes higher in each mutant than in wild type reveals 118 genes that are common between the two ($p< 9 \times 10^{-89}$, Figure 5.1 C,E). Similarly, 36 genes were shared among the genes reduced in these mutants ($p< 8 \times 10^{-31}$, Figure 5.1D,E). Taken together, a significant subset of genes require both *acj6* and *pdm3* for proper expression in the adult head. The overlap is only significant for genes that change in the same direction (up or down in both mutants) and not for genes that change in the opposite direction, suggesting that *acj6* and *pdm3* share positive and negative regulatory roles with respect to these genes (Figure 5.1E).

Identification of chemosensory gene targets.

Within these differentially regulated gene sets, we were curious to examine the chemosensory genes that are misregulated in the POU-domain transcription factor mutants. We searched within the list of genes altered in *acj6* mutants for known chemosensory receptors. We relaxed our fold-change cutoff from 2 to 1.4-fold to include genes that are known to be *acj6*-dependent and to account for the relatively low expression of these genes confined to small organs on the adult head tissue. We find 25 chemosensory genes (18 *Ors*, 4 *Grs*, and 3 *Irs*) whose expression is reduced in *acj6* mutants (Figure 5.2C). This includes previously identified targets along with several novel ones (Bai, Goldman, and Carlson 2009). Among these, we identify two broadly expressed receptors: *Orco* and *Ir76b* are reduced, which can have a large impact on receptor function in the olfactory system (Figure 5.2C). We also identify 6 chemosensory receptors whose expression increases in the absence of *acj6* , a finding that is inline with a previous report

that *acj6* also works to repress ectopic *Or* expression (Bai, Goldman, and Carlson 2009). It is worth noting, however, that we do not find increases in the larval *Or45b* in *acj6* mutants which is known to be ectopically expressed in mutant palps (Bai, Goldman, and Carlson 2009).

By contrast, far fewer chemosensory genes rely on *pdm3* for expression in the adult olfactory system. Our microarray analysis yielded only 5 down-regulated and 4 up-regulated chemosensory genes in *pdm3* mutants (Figure 5.2D). Interestingly, 8 out of these 9 genes are also dependent upon *acj6.* This suggests two things. First, *pdm3* has a considerable smaller role in olfactory receptor gene choice in the *Drosophila* adult than does *acj6.* Second, *pdm3* does not act independently of *acj6* in *Or* gene selection, but rather supports a combinatorial role along with *acj6* for positive and negative regulation of select chemosensory genes.

Identification of direct targets of acj6 using binding site analysis.

The *acj6* binding site identified by Bai and colleagues has been shown to play a vital role in *acj6*-dependent regulation of olfactory receptors (Bai, Goldman, and Carlson 2009). To determine the number of genes regulated by *acj6* that are likely direct targets, we extracted the sequence that lie 5kb upstream of each differentially regulated gene and scanned these sequences with the acj6-binding site matrix. Using a cutoff score >6, we identify 93.7% and 92.8 % of up- and down-regulated genes, respectively, contain at least one *acj6*-binding site within their upstream region (Table 5.1). This supports a role for *acj6* as a “terminal selector” transcription factor acting directly on gene targets, rather than regulating other transcription factor networks to indirectly modulate gene expression (Hobert 2008).

Regulation of known and putative axon guidance molecules.

Given the reliable identification of *Or* gene regulation and the overwhelming presence of *acj6*-binding sites upstream of its target genes, we next sought to ask whether *acj6* and *pdm3* have similar roles in regulating expression of axon guidance molecules. We compiled a list of 870 known and putative axon guidance genes (i.e. those with similar protein domains to known families of axon guidance molecules) and genes predicted to be expressed on the cell surface in *Drosophila (Kurusu et al. 2008)*. We find that 41 of these genes are increased, while 22 of the known and putative axon guidance molecules are reduced in *acj6* mutant heads. As with *Or* gene regulation, we identify a smaller role for *pdm3,* with 25 genes that are up-regulated and 12 genes down-regulated in *pdm3* mutants. Just as we observed with chemosensory genes, there is significant overlap between known and putative axon guidance molecules regulated by *acj6* and *pdm3* (Figure 5.3 A-C). Similarly, a closer look at these 17 overlapping genes once again suggests that a subset of regulated genes require both *acj6* and *pdm3* for proper expression (Figure 5.3D). These findings provide evidence in support of the long-held hypothesis that the regulatory machinery that manages the pattern of olfactory receptor gene expression also functions to regulate the suite of axon guidance molecules expressed, thereby coordinating these two fundamental aspects of *Drosophila* olfactory system development.

*acj6 regulates members of the semaphorin family of axon guidance proteins***.**

To examine the ensemble of known and putative axon guidance genes regulated by *acj6,* we performed phylogenetic analysis of these 63 genes. The peptide sequences of these genes were aligned with ClustalW (Thompson, Gibson, and Higgins 2002). We

find that members of the semaphorin family of axon guidance proteins, which are known to play a role in OSN axon targeting are among the different groups of genes regulated by *acj6.* We find 3 of the 5 known *Drosophila* semaphorins are significantly increased in *acj6* mutants, suggesting a repressive role for *acj6* in semaphorin regulation (Figure 5.4A). Each of the 3 regulated semaphorin genes have at least 1 acj6-binding site within 2kb of their transcription start site (TSS), suggesting that the repression occurs via direct binding of acj6 (Figure 5.4A). In addition to known roles in general nervous system axon guidance, many of the semaphorins have demonstrated roles specifically in proper wiring of the olfactory system. Sema-2a and Sema2-b are required for OSN axons to segregate into one of two main trajectories, the ventromedial bundle, en route to the antennal lobe (Joo et al. 2013; Sweeney et al. 2011; Komiyama et al. 2007). Interestingly, the signaling partner receptors to semaphorins, the plexin family are not among the *acj6* target genes. Sema-1b is also increased in *acj6* mutants. Sema-1b does not have a defined function within the wiring of the *Drosophila* olfactory system. We note that an additional semaphorin with a known role in olfactory system development, Sema-1a, is found to be significantly down-regulated in *acj6* mutants, although it did not meet our 2-fold expression change requirement (Fold-change -1.65, FDR < 0.05) (Lattemann et al. 2007). Identification of semaphorin-regulation by *acj6* provides compelling evidence for a role both in regulating chemosensory gene expression and specific axon guidance molecules within the *Drosophila* nervous system.

Regulation of an unknown group of putative axon guidance genes.

Finally, our phylogenetic analysis offers the potential to uncover other groups of *acj6*-regulated, related genes with potential roles in olfactory system axon guidance. As an example, we identify a group of genes that are currently uncharacterized in the adult

nervous system that cluster together based on similarities in peptide sequences (Figure 5.4B). Once again, most of the genes within this group contain at least 1 *acj6*-binding site within 2kb upstream of their TSS (Figure 5.4B). Each of these potential direct *acj6*-targets are found at higher levels in the *acj6*-mutant head; the one reduced gene in this group lacks a 2kb upstream binding site. Further investigation into the undescribed genes identified as *acj6*-targets will yield new insights into the dual role for *acj6* in the development of the *Drosophila* olfactory system.

Discussion

Beyond olfactory receptor gene choice.

The present study expands our understanding of *acj6* and *pdm3* function in the *Drosophila* nervous system to include other non-chemosensory functions, including a novel role for POU-domain transcription factors in regulating genes involved in social behavior and immune response. Both factors target genes involved in photoreactive repair. It remains to be studied if these POU-domain transcription factor mutants are more susceptible to UV-induced DNA damage.

In terms of gene targets, *pdm3* plays a considerably smaller role in regulation of gene expression in the *Drosophila* head. Much of these gene targets are shared with *acj6*, highlighting that *pdm3* often functions in conjunction with *acj6* for its regulatory functions. In fact, pairwise overlap analysis between all *acj6* and *pdm3* targets reveals that a significant subset of genes require both for positive and negative regulation, suggesting that the combinatorial action of acj6 and pdm3 extends beyond *Or* gene regulation .

Expanded roles in chemosensory gene regulation.

The detection of known olfactory receptor targets in our differentially regulated gene sets (Bai, Goldman, and Carlson 2009; Tichy, Ray, and Carlson 2008) bolsters the reliability of the genes identified in this study. We present novel chemosensory targets for both *acj6* and *pdm3.* For *acj6,* we find the broadly expressed receptors: *Orco* and *Ir76b* are significantly down-regulated. It remains to be studied whether the disruption of these genes is restricted to specific OSN classes or if there is a general reduction in these receptors. We also find a much smaller role for *pdm3* overall in olfactory receptor gene choice , and nearly all regulated chemoreceptor targets are shared with *acj6*. This suggests that *pdm3* acts only in conjunction with *acj6* in certain OSN classes, further supporting a combinatorial code of transcription factors in specifying the *Drosophila* olfactory map (Fuss and Ray 2009; Jafari et al. 2012).

Coordination of Or gene choice and axon guidance gene expression.

Our genome-scale approach also led to the identification of known and putative axon guidance molecules that are regulated by these transcription factors. Most notably, we identify 3 of the 5 *Drosophila* semaphorins are misexpressed at higher levels in *acj6* mutant heads. Many of these semaphorins have known roles in diverse olfactory system wiring processes including guidance to the proper axonal tract en route to the antennal lobe and intraclass repulsion at the boundaries of individual glomeruli (Barish and Volkan 2015). It is quite possible that disruption of these semaphorins is at least partially responsible for the wiring defects observed in *acj6* mutants, and to a lesser extent, *pdm3* muants. We note that our study is not restricted to wiring of axons coming from the peripheral nervous system. Our examination of head tissue would include changes in

higher order neuron classes within the olfactory system, a subset of which are known to require *acj6* for proper wiring (Komiyama et al. 2003).

The detection of these bona fide axon guidance molecules in conjunction with the well-established role in chemosensory gene regulation provides a missing connection between *Or* gene choice and specific axon guidance molecule gene expression by way of a single transcription factor, or combinatoria pair. As with chemosensory genes, most known and putative axon guidance targets identified for *acj6* have at least 1 binding site upstream of their TSS, linking this transcription factor to direct regulation of both olfactory receptors and axon guidance molecules. Again, *pdm3* is found to have a similar yet smaller role in regulating both of these gene categories.

It has been shown that OSNs require distinct combinations of the various *acj6* splice isoforms (Bai and Carlson 2010). The addition of differential splice isoform function expands the regulatory power of *acj6* in selecting the axon guidance determinants of OSN-class identity. Further studies are required to detangle the individual contributions of different isoforms to the regulation of expression of the axon guidance targets presented here.

It will be interesting to examine if other terminal selector transcription factors that are known players in *Or* gene choice: *E93*, *Fer1*, *onecut*, *Sim*, *xbp1*, and *zf30c* have similar dual functions in regulating axon guidance molecules in a similar regulatory matrix as described (Jafari et al. 2012).

Based on our understanding of terminal selector transcription factors in *Or* gene choice, it is reasonable to hypothesize that the regulation of axon guidance molecules is also specific to each OSN class and neuron type. These proteins could provide each class with a unique suite of axon guidance molecules, thereby establishing specific gradients of axon

guidance cues and altering the signaling capacity of each OSN class to respond to these cues for faithful guidance to their glomerular targets in the antennal lobe. Finally, our inclusion of putative axon guidance molecules/ cell-surface genes allows for the identification of candidate genes that are POU-domain targets which may have a role in the wiring of the *Drosophila* olfactory system in a class-specific manner.

Materials and Methods

Drosophila stocks and manipulations

Fly stocks were maintained on conventional cornmeal fly good under a 12 hr light: 12 hr dark cycle at 25℃ with 50% humidity. Wild-type flies were *w1118* backcrossed 5 times to *Canton-S* (*wCS)* for both sets of microarray experiments. For *acj6* mutants, we used *acj6*^{PGAL4} flies (Bloomington 30025) which have a GAL4 insertion that disrupts acj6 function (Bourbon et al. 2002; Bai and Carlson 2010). For *pdm3* mutant analysis, we used *PB{WH}pdm3*^{f00828} (Bloomington 18374) which contains a 10kb transposon insertion disrupting function (Thibault et al. 2004; Tichy, Ray, and Carlson 2008).

Tissue collection and RNA isolation

5-8 day old male flies were anesthetized with CO_2 and flash frozen in liquid nitrogen. 50 heads were collected for each experiment. Head tissues were mechanically crushed with disposable RNAse-free plastic pestles and total RNA was isolated using a trizol-based protocol. Total RNA samples were stored at -80℃ before being shipped for hybridization to *Agilent* DNA microarrays.

Bioinformatic analysis

Overlap analysis was done with the GeneOverlap package in R (Shen and Sinai 2013). Venn plots were generated in R with the VennDiagram package (v. 1.6.20). All analyses in R were run with R version 3.4.2. Go-enrichment analysis was performed with GOrilla

using expressed genes as the background (Eden et al. 2009). Phylogenetic trees were constructed with Clustal Omega (https://www.ebi.ac.uk/Tools/msa/clustalo/) using the neighbor-joining method. Upstream sequences were extracted from the BDGP6 genome. Binding sites were detected using the matrix scan function of the Regulatory Sequence Analysis Tools (Turatsinze et al. 2008). The position-weight matrix used for *acj6 (Bai, Goldman, and Carlson 2009)* was scanned using a weight score threshold >6.

References

Ang, Lay-Hong, Jenny Kim, Vitaly Stepensky, and Huey Hing. 2003. “Dock and Pak Regulate Olfactory Axon Pathfinding in Drosophila.” *Development* 130 (7): 1307–16.

Bai, Lei, and John R. Carlson. 2010. “Distinct Functions of acj6 Splice Forms in Odor Receptor Gene Choice.” *The Journal of Neuroscience: The Official Journal of the Society for Neuroscience* 30 (14): 5028–36.

Bai, Lei, Aaron L. Goldman, and John R. Carlson. 2009. “Positive and Negative Regulation of Odor Receptor Gene Choice in Drosophila by acj6.” *The Journal of Neuroscience: The Official Journal of the Society for Neuroscience* 29 (41): 12940–47.

Barish, Scott, and Pelin Cayirlioglu Volkan. 2015. “Mechanisms of Olfactory Receptor Neuron Specification in Drosophila.” *Wiley Interdisciplinary Reviews. Developmental Biology* 4 (6): 609–21.

Bourbon, Henri-Marc, Geneviève Gonzy-Treboul, Frédérique Peronnet, Marie-Francoise Alin, Claude Ardourel, Corinne Benassayag, David Cribbs, et al. 2002. “A P-Insertion Screen Identifying Novel X-Linked Essential Genes in Drosophila.” *Mechanisms of Development* 110 (1): 71–83.

Bruyne, Marien de, Peter J. Clyne, and John R. Carlson. 1999. “Odor Coding in a Model Olfactory Organ: TheDrosophilaMaxillary Palp.” *The Journal of Neuroscience: The Official Journal of the Society for Neuroscience* 19 (11): 4520–32.

Bruyne, M. de, K. Foster, and J. R. Carlson. 2001. “Odor Coding in the Drosophila Antenna.” *Neuron* 30 (2): 537–52.

Clyne, P. J., S. J. Certel, M. de Bruyne, L. Zaslavsky, W. A. Johnson, and J. R. Carlson. 1999. “The Odor Specificities of a Subset of Olfactory Receptor Neurons Are Governed by Acj6, a POU-Domain Transcription Factor.” *Neuron* 22 (2): 339–47.

Clyne, P. J., C. G. Warr, M. R. Freeman, D. Lessing, J. Kim, and J. R. Carlson. 1999. “A Novel Family of Divergent Seven-Transmembrane Proteins: Candidate Odorant Receptors in Drosophila.” *Neuron* 22 (2): 327–38.

Couto, Africa, Mattias Alenius, and Barry J. Dickson. 2005. “Molecular, Anatomical, and Functional Organization of the Drosophila Olfactory System.” *Current Biology: CB* 15 (17): 1535–47.

Dahanukar, Anupama, Elissa A. Hallem, and John R. Carlson. 2005. “Insect Chemoreception.” *Current Opinion in Neurobiology* 15 (4): 423–30.

Eden, Eran, Roy Navon, Israel Steinfeld, Doron Lipson, and Zohar Yakhini. 2009. “GOrilla: A Tool for Discovery and Visualization of Enriched GO Terms in Ranked Gene Lists.” *BMC Bioinformatics* 10 (February): 48.

Fishilevich, Elane, and Leslie B. Vosshall. 2005. “Genetic and Functional Subdivision of the Drosophila Antennal Lobe.” *Current Biology: CB* 15 (17): 1548–53.

Fuss, Stefan H., and Anandasankar Ray. 2009. “Mechanisms of Odorant Receptor Gene Choice in Drosophila and Vertebrates.” *Molecular and Cellular Neurosciences* 41 (2): 101–12.

Gao, Q., B. Yuan, and A. Chess. 2000. “Convergent Projections of Drosophila Olfactory Neurons to Specific Glomeruli in the Antennal Lobe.” *Nature Neuroscience* 3 (8): 780–85.

Hallem, Elissa A., and John R. Carlson. 2006. “Coding of Odors by a Receptor Repertoire.” *Cell* 125 (1): 143–60.

Hallem, Elissa A., Michael G. Ho, and John R. Carlson. 2004. “The Molecular Basis of Odor Coding in the Drosophila Antenna.” *Cell* 117 (7): 965–79.

Hobert, Oliver. 2008. “Regulatory Logic of Neuronal Diversity: Terminal Selector Genes and Selector Motifs.” *Proceedings of the National Academy of Sciences of the United States of America* 105 (51): 20067–71.

Hummel, Thomas, Maria Luisa Vasconcelos, James C. Clemens, Yelena Fishilevich, Leslie B. Vosshall, and S. Lawrence Zipursky. 2003. “Axonal Targeting of Olfactory Receptor Neurons in Drosophila Is Controlled by Dscam.” *Neuron* 37 (2): 221–31.

Jafari, Shadi, Liza Alkhori, Alexander Schleiffer, Anna Brochtrup, Thomas Hummel, and Mattias Alenius. 2012. “Combinatorial Activation and Repression by Seven Transcription Factors Specify Drosophila Odorant Receptor Expression.” *PLoS Biology* 10 (3): e1001280.

Jefferis, Gregory S. X. E., Raj M. Vyas, Daniela Berdnik, Ariane Ramaekers, Reinhard F. Stocker, Nobuaki K. Tanaka, Kei Ito, and Liqun Luo. 2004. “Developmental Origin of Wiring Specificity in the Olfactory System of Drosophila.” *Development* 131 (1): 117–30.

Jefferis, G. S., E. C. Marin, R. F. Stocker, and L. Luo. 2001. “Target Neuron Prespecification in the Olfactory Map of Drosophila.” *Nature* 414 (6860): 204–8.

haveri, Dhanisha, Sumiti Saharan, Anindya Sen, and Veronica Rodrigues. 2004. “Positioning Sensory Terminals in the Olfactory Lobe of Drosophila by Robo Signaling.” *Development* 131 (9): 1903–12.

Joo, William J., Lora B. Sweeney, Liang Liang, and Liqun Luo. 2013. “Linking Cell Fate, Trajectory Choice, and Target Selection: Genetic Analysis of Sema-2b in Olfactory Axon Targeting.” *Neuron* 78 (4): 673–86.

Komiyama, Takaki, John R. Carlson, and Liqun Luo. 2004. “Olfactory Receptor Neuron

Axon Targeting: Intrinsic Transcriptional Control and Hierarchical Interactions." *Nature Neuroscience* 7 (8): 819–25.

Komiyama, Takaki, Wayne A. Johnson, Liqun Luo, and Gregory S. X. E. Jefferis. 2003. "From Lineage to Wiring Specificity. POU Domain Transcription Factors Control Precise Connections of Drosophila Olfactory Projection Neurons." *Cell* 112 (2): 157–67.

Komiyama, Takaki, Lora B. Sweeney, Oren Schuldiner, K. Christopher Garcia, and Liqun Luo. 2007. "Graded Expression of Semaphorin-1a Cell-Autonomously Directs Dendritic Targeting of Olfactory Projection Neurons." *Cell* 128 (2): 399–410.

Kurusu, Mitsuhiko, Amy Cording, Misako Taniguchi, Kaushiki Menon, Emiko Suzuki, and Kai Zinn. 2008. "A Screen of Cell-Surface Molecules Identifies Leucine-Rich Repeat Proteins as Key Mediators of Synaptic Target Selection." *Neuron* 59 (6): 972–85.

Lattemann, Marc, Ariane Zierau, Claus Schulte, Sascha Seidl, Britta Kuhlmann, and Thomas Hummel. 2007. "Semaphorin-1a Controls Receptor Neuron-Specific Axonal Convergence in the Primary Olfactory Center of Drosophila." *Neuron* 53 (2): 169–84.

Mombaerts, Peter. 2004. "Odorant Receptor Gene Choice in Olfactory Sensory Neurons: The One Receptor-One Neuron Hypothesis Revisited." *Current Opinion in Neurobiology* 14 (1): 31–36.

Shanbhag, S. R., B. Müller, and R. A. Steinbrecht. 2000. "Atlas of Olfactory Organs of Drosophila Melanogaster." *Arthropod Structure & Development* 29 (3): 211–29.

Shen, Li, and Mount Sinai. 2013. "GeneOverlap: Test and Visualize Gene Overlaps." *R Package Version* 1 (0).

Stocker, R. F. 1994. "The Organization of the Chemosensory System in Drosophila Melanogaster: A Review." *Cell and Tissue Research* 275 (1): 3–26.

Sweeney, Lora B., Ya-Hui Chou, Zhuhao Wu, William Joo, Takaki Komiyama, Christopher J. Potter, Alex L. Kolodkin, K. Christopher Garcia, and Liqun Luo. 2011. "Secreted Semaphorins from Degenerating Larval OSN Axons Direct Adult Projection Neuron Dendrite Targeting." *Neuron* 72 (5): 734–47.

Thibault, Stephen T., Matthew A. Singer, Wesley Y. Miyazaki, Brett Milash, Nicholas A. Dompe, Carol M. Singh, Ross Buchholz, et al. 2004. "A Complementary Transposon Tool Kit for Drosophila Melanogaster Using P and piggyBac." *Nature Genetics* 36 (3): 283–87.

Thompson, Julie D., Toby J. Gibson, and Des G. Higgins. 2002. "Multiple Sequence Alignment Using ClustalW and ClustalX." *Current Protocols in Bioinformatics / Editoral Board, Andreas D. Baxevanis ... [et Al.]* Chapter 2 (August): Unit 2.3.

Tichy, Andrea L., Anandasankar Ray, and John R. Carlson. 2008. "A New Drosophila POU Gene, pdm3, Acts in Odor Receptor Expression and Axon Targeting of Olfactory

Neurons." *The Journal of Neuroscience: The Official Journal of the Society for Neuroscience* 28 (28): 7121–29.

Turatsinze, Jean-Valery, Morgane Thomas-Chollier, Matthieu Defrance, and Jacques van Helden. 2008. "Using RSAT to Scan Genome Sequences for Transcription Factor Binding Sites and Cis-Regulatory Modules." *Nature Protocols* 3 (10): 1578–88.

Vosshall, L. B., H. Amrein, P. S. Morozov, A. Rzhetsky, and R. Axel. 1999. "A Spatial Map of Olfactory Receptor Expression in the Drosophila Antenna." *Cell* 96 (5): 725–36.

Vosshall, L. B., A. M. Wong, and R. Axel. 2000. "An Olfactory Sensory Map in the Fly Brain." *Cell* 102 (2): 147–59.

Vosshall, Leslie B., and Reinhard F. Stocker. 2007. "Molecular Architecture of Smell and Taste in Drosophila." *Annual Review of Neuroscience* 30: 505–33.

Figure 5.1. Differentially-expressed genes in the *Drosophila* head in POU-domain transcription factor mutants.

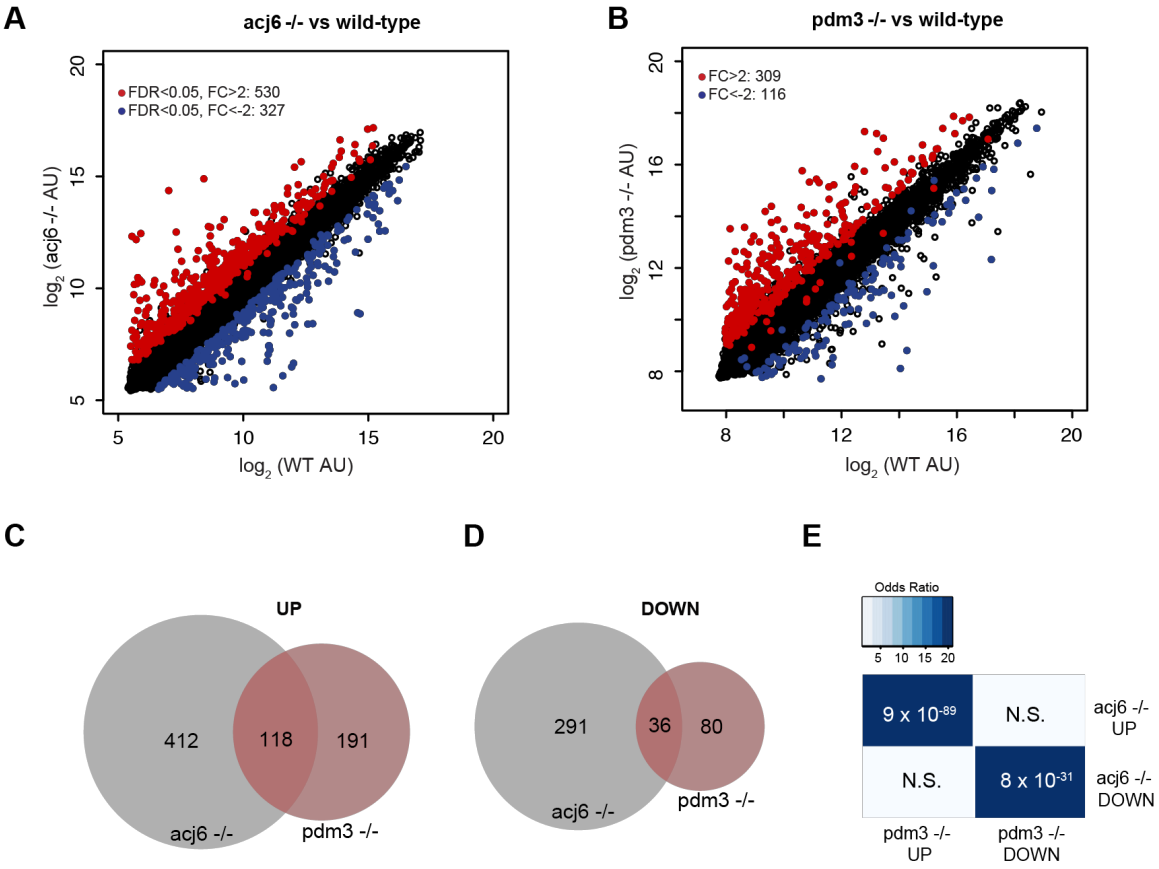

Figure 5.1. Differentially-expressed genes in the *Drosophila* head in POU-domain transcription factor mutants.

(A) Plot highlighting up- and down-regulated genes in *acj6* mutants compared to wild-type. Red and blue dots represent up-regulated genes (Fold-change > 2, FDR< 0.05) and down-regulated genes (Fold-change < -2, FDR< 0.05), respectively.

(B) Plot highlighting up- and down-regulated genes in *pdm3* mutants compared to wild-type. Red and blue dots represent up-regulated genes (Fold-change > 2) and down-regulated genes (Fold-change < -2), respectively.

(C) Venn plot comparing the overlap of up-regulated genes for *acj6* and *pdm3* mutants.
(D) Venn plot comparing the overlap of down-regulated genes for *acj6* and *pdm3* mutants.

(E) Significance of overlap of indicated gene sets (P-value indicated in box; color denotes odds ratio from Fisher's exact test).

Figure 5.2. Characterization of *acj6* and *pdm3* target genes

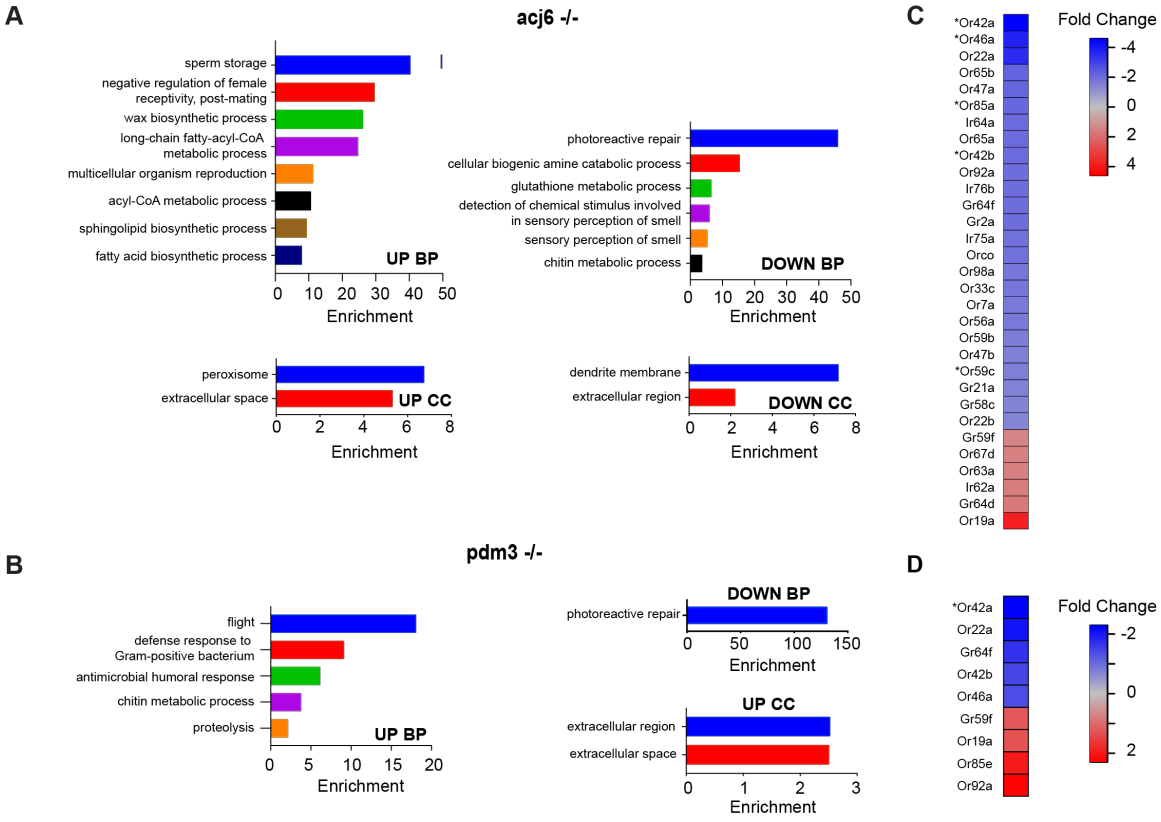

Figure 5.2. Characterization of *acj6* and *pdm3* target genes.

(A) Bar graphs showing fold-enrichment for biological process (BP) and cellular component (CC) GO terms in indicated *acj6* gene lists compared to all genes expressed in the *Drosophila* head ($p<0.05$).

(B) Bar graphs showing fold-enrichment for biological process (BP) and cellular component (CC) GO terms in indicated *pdm3* gene lists compared to all genes expressed in the *Drosophila* head ($p<0.05$).

(C) Heatmap characterizing the expression of chemosensory genes significantly altered in *acj6* mutants . Each column represents the expression of one gene (red= high expression, blue= low expression).

(D) Heatmap characterizing the expression of chemosensory genes significantly altered in *pdm3* mutants . Each column represents the expression of one gene (red= high expression, blue= low expression).

Figure 5.3. Known and putative axon guidance genes regulated by *acj6* and *pdm3.*

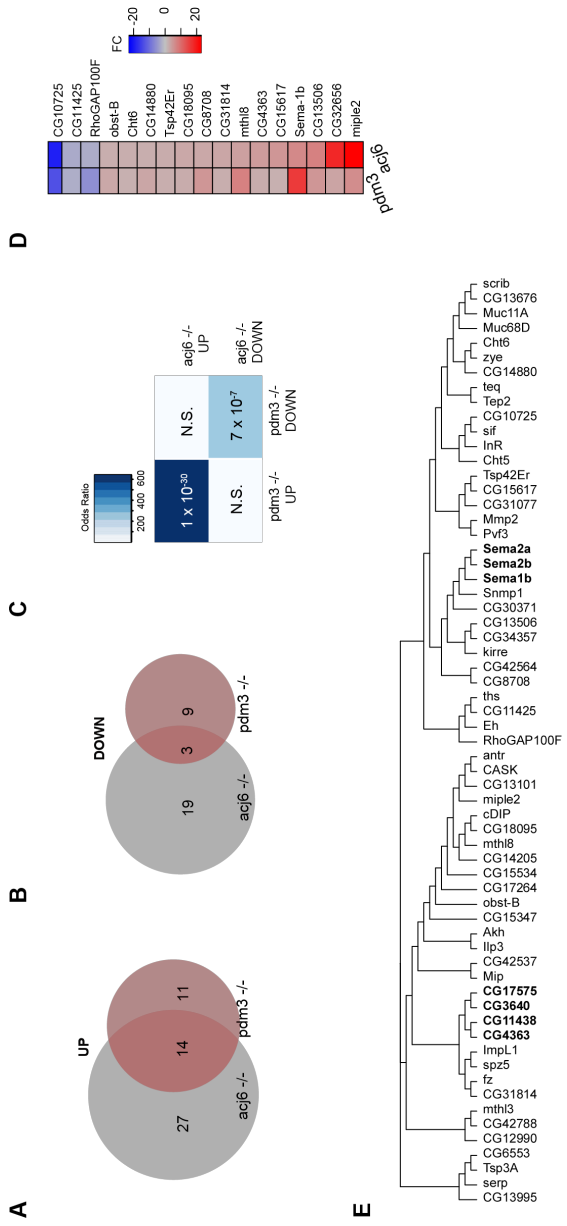

Figure 5.3. Known and putative axon guidance genes regulated by *acj6* and *pdm3.*

(A) Venn plot comparing the overlap of up-regulated axon guidance genes for *acj6* and *pdm3* mutants.

(B) Venn plot comparing the overlap of down-regulated axon guidance genes for *acj6* and *pdm3* mutants.

(C) Significance of overlap of indicated gene sets (P-value indicated in box; color denotes odds ratio from Fisher's exact test).

(D) Heatmap characterizing the expression of axon guidance genes significantly altered in both acj6 and *pdm3* mutants . Each column represents the expression of one gene (red= high expression, blue= low expression).

(E) Phylogenetic tree generated from the peptide sequences of all known and putative axon guidance genes regulated by *acj6*. Highlighted: known semaphorin family of axon guidance genes and an uncharacterized group of genes.

Figure 5.4. *acj6* regulates most semaphorin family members and an uncharacterized group.

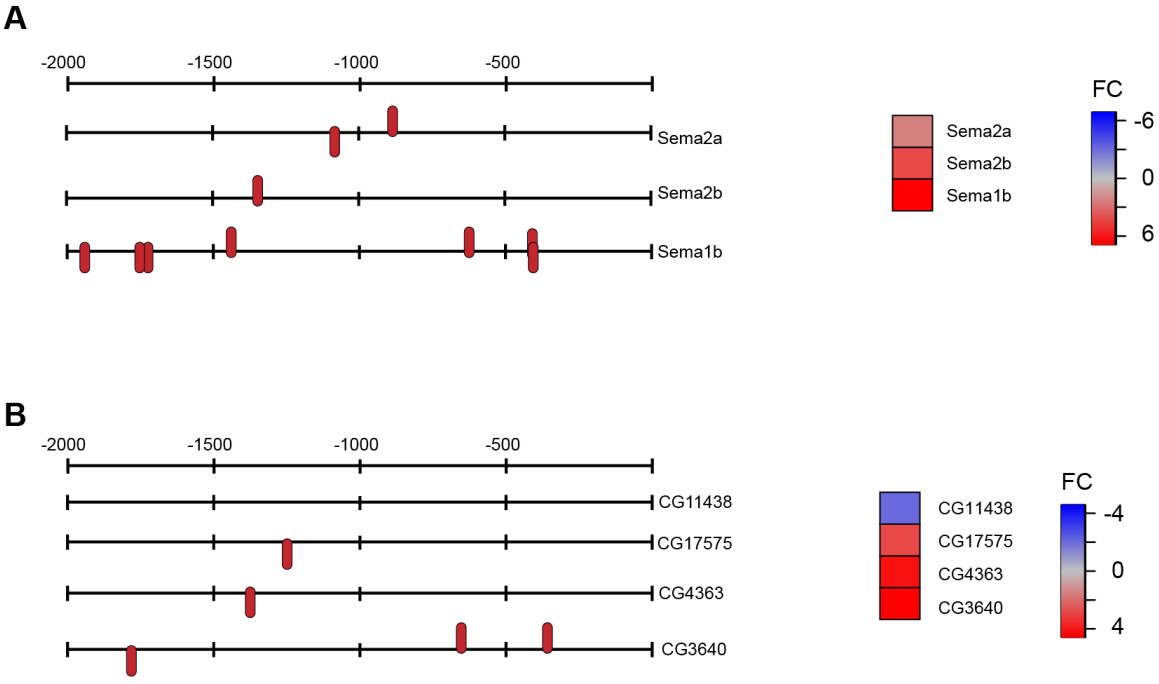

Figure 5.4. *acj6* regulates most semaphorin family members and an uncharacterized group.

(A) Left: Diagram depicting the 2kb sequence upstream of indicated *semaphorin* genes and predicted *acj6* binding sites. Right: Heatmap characterizing the expression of semaphorins significantly altered in acj6 mutants.

(B) Left: Diagram depicting the 2kb sequence upstream of selected uncharacterized genes and predicted *acj6* binding sites. Right: Heatmap characterizing the expression of selected uncharacterized genes significantly altered in acj6 mutants.

Table 5.1 Most genes significantly altered in *acj6* mutants contain at least 1 binding site within 5kb upstream of their TSS.

	Total no. of genes	No. of genes with ≥ acj6 binding site	%
Up-regulated	522	489	93.7
Down-regulated	321	298	92.8
All regulated genes	843	787	93.4

Chapter 6

Concluding remarks and future directions

Short-term odor exposure experiments to identify activity regulated genes offer insight into potential regulators of synaptic plasticity and learning and memory.

Our characterization of the landscape of activity regulated genes (ARGs) in the *Drosophila melanogaster* central nervous system as well as the at the periphery illustrates the remarkable sensitivity that age and stimulus type have on regulation of these genes. We provide several intriguing candidate genes that have potential for involvement in synaptic plasticity and learning and memory. Furthermore, many of our strongest candidates could prove to be valuable tools for neuronal circuit tracing. As others have done with ARGs in mammalian systems, it is possible to isolate and clone the regulatory regions of our ARGs and fuse these sequences to any number of reporter genes in use for this model system. This would provide a valuable opportunity to mark recently active neurons, especially within the visual and olfactory systems. Our top candidates include the *amylase* genes which are strongly induced in response to odor and light in all ages tested. We present several other candidates that may be well-suited for circuit tracing in *Drosophila*.

The up-regulated genes in the antenna could provide valuable markers of active cells within the peripheral nervous system. The transcriptional repressor *hairy* is an intriguing target since we find it reliably induced rapidly in response to both fruit-odors and the repellent DEET. An effective marker for active neurons within the antenna could provide insight into all cells that are affected by DEET exposure, shedding light onto its presently unknown mechanism of action.

We also identified several common genes that are reduced in mRNA abundance following exposure to fruit odors and to DEET. It would be worthwhile to examine which, if any, of these are targets of the antennal ARG *hairy*. THis could provide a mechanism of ARG down-regulation of these genes following brief bouts of odor exposure.

Activity regulated genes are a neuronal-specific subset of immediate early genes (IEGs). The mechanisms by which precise immediate early gene expression programs are regulated are largely uncharacterized. In active neurons, the regulation of ARGs has been linked to both calcium-influx and a rise in cyclic-AMP (cAMP) via the cis-regulatory site known as the cAMP response element (CRE, consensus sequence TGACGTCA) (Montminy et al. 1986; Kaang, Kandel, and Grant 1993; Sheng, McFadden, and Greenberg 1990). The CRE site, found upstream of the transcription start sites of many IEGs, recruits the trans-acting factor CREB (CRE-binding protein) which can be activated after signaling cascades initiated by the calcium and cAMP second messenger molecules (Sheng, McFadden, and Greenberg 1990; Lonze and Ginty 2002). It is postulated that CREB-mediated induction of IEGs in the brain is required for learning and memory, and studies in which overexpression of a dominant-negative CREB isoform leads to learning deficits in *Drosophila* confirm a central role for CREB in long-term memory formation (Perazzona et al. 2004). The connection between CREB-mediated gene expression in *Drosophila* neurons and memory is unknown. Scanning upstream of ARGs identified in our study, we find that many of these do not have a CRE site within 2kb of their transcription start site. The group of genes with the highest CRE site presence is the set of genes induced within 10 minutes of stimulation (UP2). We find just under 7% of genes with a CRE site in this group. We note that this is two-fold more than expected based on the genome-wide frequency of the CRE site upstream of *Drosophila* genes.

It is possible that invertebrates employ a different transcriptional regulators to induce gene expression rapidly following neuronal activation. We provide several enriched motifs present upstream of the transcription start site of many of our various ARGs. Finding unique sequences enriched in different clusters suggests that there may be different transcription factors that mediate precise temporal control of these different gene sets. More work is needed to identify the protein binding partners of these enriched sequences. Such analysis would expand our understanding of how the observed temporal dynamics of gene expression in response to odor and light are tightly controlled.

Our study provides a cursory screen in *Drosophila* larvae for the involvement of our candidate genes in learning and memory. It is possible that a complete screen in adults with mutants and other misexpression variants (flies in which these genes are overexpressed, for example) would expand our understanding of the molecular players involved in processes that follow sensory stimulation, including habituation, synaptic plasticity, and learning and memory.

In this study, we also analyze the striking effect of age on ARG regulation. We provide several promising candidate genes that can be used to examine how altered regulation of these genes leads to age-dependent declines in learning and memory in the *Drosophila* model. This should include investigation into both the set of genes that are no longer induced in older flies (genes induced in juvenile flies and not in middle-aged and old flies) in addition to new genes induced in older flies but not in juveniles. This data set also provides an opportunity to investigate overall genetic changes in the nervous system that accompanies aging. As we did with our comparative analysis between wild type and *Orco*-mutant flies ($\Delta Orco^2$), we can analyze the baseline expression levels in the brain at each timepoint and compare them in a pairwise fashion. This analysis could be used to

ask what are the key molecular differences that are associated with aging? How do these genetic differences antagonize the learning capacity of aging flies? Further exploration on this front would provide beneficial insight into the molecular mechanisms of aging in the adult nervous system.

We characterize a surprising lack of large-scale differences in the brains of wild type flies and those that lack the histone deacetylase HDAC6. Within the relatively small amount of differentially expressed genes, there is an enrichment for activity regulated genes . This suggests that HDAC6, unlike other *Drosophila* histone deacetylases that predominantly reside in the nucleus, may have a more targeted role in gene expression in the brain. Specifically, we hypothesize that HDAC6 has a gene regulatory function within the context of active neurons. It remains to be seen if this role involves shuttling to the nucleus to alter the chromatin landscape of its target genes or if the regulatory action comes by way of HDAC6-led post-translational modifications of other regulators in the cytoplasm. Expansion in our understanding of HDAC6 regulation of ARG expression could provide a mechanistic link between HDAC6 and its known role in memory in the *Drosophila* adult.

Long-term odor exposure reveals unexpected physiological effects in a diverse range of organisms.

In addition to an examination of the genetic effects of short-term olfactory stimulation, we employ high-throughput RNA sequencing analysis to demonstrate the genetic changes associated with long-term odorant exposure. We provide evidence that the volatile odorant diacetyl signals not only through traditional neuronal pathways, but also through inhibition of histone deacetylases (HDACs). The ability of diacetyl to

dramatically alter gene expression, as well as H3K9 acetylation is dependent upon exposure concentration.

We demonstrate that diacetyl exposure alters gene expression in a wide range of organisms, including plants which, of course, lack a nervous system. This bolsters evidence that diacetyl is working in a more conserved manner beyond traditional olfactory signaling. Our analysis of long-term diacetyl exposure highlights two important physiological considerations: safety of continual exposure to small volatiles and potential neuroprotective effects of aroma-based delivery of diacetyl.

First, diacetyl is a chemical highly prevalent in our environment as both a metabolism byproduct of our own microbiome and as an oft-used flavoring agent in foods in our diet. Our finding that this small molecule volatile can reach and alter gene expression in both lung and brain tissue in the mouse model warrants additional investigations. Further work is needed to understand any potential negative effects of this considerable alteration in gene expression. Also, given that volatile chemicals are generally small in size, our findings highlight a need to understand the physiological consequences of persistent exposure to odorants that may be able to reach both our lung and brain tissues. We reason that RNA sequencing experiments provide a valuable output in assessing these consequences.

Second, we show that exposure to diacetyl leads to a slowing of neurodegeneration in a fly model for Huntington's Disease. We postulate that this iss due to specific inhibition of HDAC1 and HDAC3 by diacetyl. Diacetyl, then, could work in a therapeutic capacity as an alternative HDAC inhibitor drug. Future examinations of diacetyl would be required to assess the usefulness of such an aroma-based therapeutic strategy.

Development of the Drosophila olfactory system couples Or gene choice with axon guidance gene expression via POU-domain transcription factors.

While the first chapters explored gene expression following odorant exposure in the fully formed adult olfactory system, the final chapter explores the regulatory principles that guide the development of such an ordered chemosensory system. We characterize the targets of two POU-domain transcription factors *acj6* and *pdm3*. Our whole-genome approach identifies both known and novel chemosensory receptor targets. For *acj6,* we provide evidence that many of these genes are direct targets.

Microarray analysis in the heads of mutants for *acj6* and *pdm3* revealed that both chemosensory receptors and axon guidance genes are targets of these transcription factors. This provides mechanistic support of the long-held hypothesis that these two developmental processes are linked by the same regulatory protein networks. Based on this analysis, the field could benefit from future investigations into the function of these transcription factors. Specifically, sequencing each olfactory sensory neuron (OSN) class individually could uncover the precise suite of genes that coordinate the faithful wiring of OSNs to their cognate second order neurons within their respective glomeruli. Comparative analysis between wild type and the POU transcription factors mutant flies used in this study would allow the exact nature of the cell-specific regulatory function of *acj6* and *pdm3* in axon guidance gene expression to be uncovered.

References

Kaang, B. K., E. R. Kandel, and S. G. Grant. 1993. “Activation of cAMP-Responsive Genes by Stimuli That Produce Long-Term Facilitation in Aplysia Sensory Neurons.” *Neuron* 10 (3): 427–35.

Lonze, Bonnie E., and David D. Ginty. 2002. “Function and Regulation of CREB Family Transcription Factors in the Nervous System.” *Neuron* 35 (4): 605–23.

Montminy, M. R., K. A. Sevarino, J. A. Wagner, G. Mandel, and R. H. Goodman. 1986. “Identification of a Cyclic-AMP-Responsive Element within the Rat Somatostatin Gene.” *Proceedings of the National Academy of Sciences of the United States of America* 83 (18): 6682–86.

Perazzona, Bastianella, Guillaume Isabel, Thomas Preat, and Ronald L. Davis. 2004. “The Role of cAMP Response Element-Binding Protein in Drosophila Long-Term Memory.” *The Journal of Neuroscience: The Official Journal of the Society for Neuroscience* 24 (40): 8823–28.

Sheng, M., G. McFadden, and M. E. Greenberg. 1990. “Membrane Depolarization and Calcium Induce c-Fos Transcription via Phosphorylation of Transcription Factor CREB.” *Neuron* 4 (4): 571–82.